A Study of the Development of Steady and Periodic Unsteady Turbulent Wakes Through Curved Channels at Positive, Zero, and Negative Streamwise Pressure Gradients, Part I

M. T. Schobeiri and J. John
Texas A&M University
College Station, Texas

January 1996

PREFACE TO FINAL REPORT, PART I

The present report is the first of a three-part research report that deals with experimental and theoretical investigations of steady and unsteady wakes and their influence on boundary layer transition. The experimental research was performed in the recently established Turbomachinery Performance and Flow Research Laboratory, a division of the Turbomachinery Laboratory of Texas A&M University.

This part reports on the comprehensive experimental investigations of steady and unsteady wake flows. Based on the results of these investigations, a theoretical framework has been developed that precisely predicts the development and decay of steady and unsteady wake flows through curved and straight channels at positive, zero, and negative pressure gradients. The final report, Part II, describes the theoretical framework where the experimental results from the present report and the literature are compared with theory.

Part III reports the effects of periodic unsteady wake flow and pressure gradient on boundary layer transition along the concave surface of a curved plate. Measurements were done in an unsteady flow research facility using a rotating cascade of rods positioned upstream of the curved plate. Boundary layer measurements using a hot-wire probe were analyzed by ensemble-averaging technique.

M.T. Schobeiri
College Station, Texas
March 1994

ABSTRACT

The turbomachinery wake flow development is largely influenced by streamline curvature and streamwise pressure gradient. The objective of this investigation is to study the development of the wake under the influence of streamline curvature and streamwise pressure gradient. The experimental investigation is carried out in two phases. The first phase involves the study of the wake behind a stationary circular cylinder (steady wake) in curved channels at positive, zero, and negative streamwise pressure gradients. The mean velocity and Reynolds stress components are measured using a X-hot-film probe. The measured quantities obtained in probe coordinates are transformed to a curvilinear coordinate system along the wake centerline and are presented in similarity coordinates. The results of the steady wakes suggest strong asymmetry in velocity and Reynolds stress components. However, the velocity defect profiles in similarity coordinates are almost symmetrical and follow the same distribution as the zero pressure gradient straight wake. The results of Reynolds stress distributions show higher values on the inner side of the wake than the outer side. Other quantities, including the decay of maximum velocity defect, growth of wake width, and wake integral parameters, are also presented for the three different pressure gradient cases of steady wake. The decay rate of velocity defect is fastest for the negative streamwise pressure gradient case and slowest for the positive pressure gradient case. Conversely, the growth of the wake width is fastest for the positive streamwise pressure gradient case and slowest for the negative streamwise pressure gradient. The second phase studies the development of periodic unsteady wakes generated by the circular cylinders of the rotating wake generator in a curved channel at zero streamwise pressure gradient. Instantaneous velocity components of the periodic unsteady wakes, measured with a stationary X-hot-film probe, are analyzed by the phase-averaging techniques. The temporal distribution of velocity and Reynolds stress components obtained in a stationary frame of reference are transformed to a spatial distribution in a relative frame of reference. Profiles of phase-averaged velocity and Reynolds stress distributions in the relative frame of reference and similarity coordinates are presented.

The velocity defect and Reynolds stress distributions agree with the results of the wake development behind a stationary cylinder in the curved channel at zero streamwise pressure gradient. The phase-averaged third-order correlations, presented in the relative frame of reference and similarity coordinates, show pronounced asymmetric features.

ACKNOWLEDGMENT

TABLE OF CONTENTS

LIST OF FIGURES

LIST OF TABLES

NOMENCLATURE

a_{ij} = coefficients of polynomial for sensor j; $j = 1,2$; $i = 0,1,...4$

b = wake width

b_i = coefficients of polynomial; $i = 0,1,...5$

c_i = coefficients of polynomial; $i = 0,1,...5$

C = resultant velocity

C_p = pressure coefficient

C_w = momentum thickness ratio = $2\delta_2/d$

d = diameter of wake generating cylinder (diameter of hot-film sensor in Section 6)

d_i = coefficients of polynomial; $i = 0,1,...5$

e_i = coefficients of polynomial; $i = 0,1,...3$

E_b = anemometer bridge output voltage

E_j = anemometer output voltage of sensor j after temperature compensation; $j = 1,2$

E_{mj} = measured anemometer output voltage of sensor j; $j = 1,2$

f = frequency

H = yaw calibration function in Section 6

H^* = modified yaw calibration function in Section 6

H_{12} = shape factor of wake

k = turbulent kinetic energy

k_j = yaw sensitivity coefficient of sensor j; $j = 1,2$

K = curvature of wake centerline = $1/R$

l = length of hot-wire or hot-film

m = yaw correction parameter

n = exponent in the modified King's law relationship

N = total number of samples per channel of hot-film data for time averaging or total number records for phase-averaging

p = static pressure

p_t = total pressure

p_{in} = inlet static pressure

q = turbulent fluctuation

Q = any arbitrary instantaneous quantity

$<Q>$= ensemble average or phase-average

$\bar{Q}$ = time average

$\tilde{Q}$ = periodic component

r = radial position of probe from the center of curvature of the convex wall

r_i = radius of curvature of convex wall = 500 mm

R = radius of curvature of wake centerline

R_{uv} = correlation coefficient

Re_d = Reynolds number based on the diameter of wake generating cylinder and the average velocity at the wake generating section

t = time

T = period of wake passing

T_a = temperature of fluid

T_c = temperature of fluid at calibration

T_s = operating temperature of sensor

T_u = turbulence intensity

U = velocity component in the streamwise (ξ_1) direction of curvilinear coordinates

U_p = hypothetical potential velocity distribution of streamwise component of velocity

U_r = velocity component in the streamwise (ξ_{1r}) direction of curvilinear coordinate system in relative frame of reference

U_{1m} = maximum velocity defect

U_{1mr}= maximum velocity defect in relative spatial coordinate

V = velocity component in the transverse (ξ_2) direction of curvilinear coordinates

V_N = velocity component normal to sensor

V_r = velocity component in the transverse (ξ_{2r}) direction of curvilinear coordinate system in relative frame of reference

V_T = velocity component tangential to sensor

V_x = velocity component along x-direction

V_y = velocity component along y-direction

V_{ej} = effective velocity of sensor j; $j = 1,2$

V_{in} = average velocity at the wake generating section

V_{xp} = hypothetical potential velocity component along x-direction

α = angle between resultant velocity vector and x-axis

α_e = effective angle

α_s = angle between sensor wire and x-axis

α_{id} = yaw calibration function defined in Section 6

β = angular position of the wake generating cylinder from the horizontal

γ = integral of the Gaussian curve $\gamma = \int_0^{\infty} e^{-\zeta^2} d\zeta = \dfrac{\sqrt{\pi}}{2}$

δ_1 = displacement thickness

δ_2 = momentum thickness

Δp = differential pressure across the calibration nozzle

ΔQ = uncertainty in quantity Q; $Q = V$, V_e, α_{id} or H^*

Δt = time step of data acquisition

$\Delta \alpha$ = difference between actual and calculated α

ε_V = percentage deviation of V

ε_{Vx} = percentage deviation of V_x

ε_{Vy} = percentage deviation of V_y

ζ = nondimensional coordinate = ξ_2/b

θ = angular position of the probe location from the inlet

ν = kinematic viscosity of air

$\vec{\xi}$ = absolute spatial vector

$\vec{\xi}_r$ = relative spatial vector

ξ_1 = streamwise direction of curvilinear coordinates

ξ_2 = transverse direction of curvilinear coordinates

ξ_{1r} = streamwise direction of curvilinear coordinates in relative frame of reference

ξ_{2r} = transverse direction of curvilinear coordinates in relative frame of reference

ρ = density of air

$\vec{\chi}$ = spatial vector along the rotational direction of wake generator

ϑ = angle between probe and curvilinear coordinates

φ_1 = nondimensional velocity defect $\varphi_1 = \bar{U}_1/\bar{U}_{1m}$

Ω = vorticity

Subscripts

a = actual

c = calculated

in = inlet velocity

max = maximum

o = location of maximum velocity defect = location of center of wake

r = relative frame of reference

Ref = reference state

x = x-direction

y = y-direction

Superscripts

___ = time averaged value

~ = periodic value

1. INTRODUCTION

The wake flow constitutes a special case of free turbulent flows with a broad range of general scientific and engineering applications. In turbomachinery aerodynamics and heat transfer the periodic unsteady wakes generated by the preceding row of blades influence the boundary layer development and, consequently, the heat transfer characteristics of the blades downstream of the wake. Because of its significant impact on the turbomachinery efficiency and performance, the wake development associated with the inherent unsteadiness induced by mutual interaction between stator and rotor has recently attracted the interest of the scientific and engineering community, resulting in many publications in the turbomachinery performance area. As extensively discussed by Schobeiri (1992), the major part of the research work performed in the above areas deals with the effects of the periodic unsteady wakes on various turbomachinery performance aspects previously mentioned. Despite these efforts, little attention has been paid to the wake development phenomenon under turbomachinery flow conditions.

The streamline curvature significantly influences the properties of turbulent flows as demonstrated by Wattendorf (1935) in his study of turbulent flows through curved channels and by Lumley and Margolis (1963) in their study of the curved turbulent mixing layer. The wake development under turbomachinery flow conditions is subjected to pressure gradient and curvature effects. The laws governing the decay of wake centerline defect velocity and the development of the wake width can be different from the development of a plane wake under zero pressure gradient. The curvature and pressure gradient have significant effects on the mean velocities and turbulent properties of the wake. Most of the research conducted on wakes deals with two-dimensional plane turbulent wakes under zero pressure gradient. However, results of the plane turbulent wakes cannot be directly applied to turbomachinery flow situation where pressure gradient and curvature effects are present. This situation is the motivation for conducting a systematic investigation of the wake development under turbomachinery flow conditions.

Experimental investigation of the wake development through actual turbomachines

requires complicated instrumentation and measurement techniques and a test facility with large financial investments. A unique experimental facility designed and built by Schobeiri et al. (1992) at the Turbomachinery Performance Laboratory of Texas A&M University enables the simulation of the blade passage of a turbomachinery cascade, where positive, zero, and negative pressure gradients can be established. A circular cylinder simulates the wake of a cascade. The use of a cylinder instead of a blade cascade is appropriate, as shown by Reichardt (1950), Pfeil and Pache (1977), Pfeil and Schröder (1981), Pfeil et al. (1983), Doorly (1985), and Liu & Rodi (1991), since the turbulence characteristics of the cylinder wake flows for the Reynolds stress components are similar to those of rotor blade wakes. This is particularly true for downstream distances $x/d > 80$. The present investigation uses a circular cylinder under simulated turbomachinery flow conditions that provides a basic understanding of the phenomenon of wake development subjected to curvature and pressure gradients.

2. LITERATURE REVIEW

A review of the classical and current research on plane turbulent wakes is first presented and is followed by a literature review on the effect of curvature on turbulent flows and wakes. Finally, the periodic unsteady wakes are reviewed.

The two-dimensional wakes were first theoretically and experimentally investigated by Schlichting (1930, 1979). Applying Prandtl's mixing length hypothesis and assuming a mixing length proportional to wake width Schlichting derived expressions for wake width and defect velocity. The theoretical expressions showed excellent agreement against the measurements performed in the wake of a circular cylinder.

Reichardt (1942) succeeded in explaining free turbulent flows based on an inductive theory of turbulence as opposed to the deductive theory of turbulence where a suitable assumption like the Prandtl's mixing length hypothesis is necessary for the unknown relation between the turbulent shear stress and mean motion. After examining the large number of data on free turbulent flows, which he supplemented with his own experiments, he discovered that the velocity profiles under consideration could be represented by Gauss's function or its integral, the error function.

Townsend (1947, 1949a,b) investigated the far wakes of circular cylinders with measurements for mean velocity distribution, the distribution of the three components of turbulence, correlation derivatives in downstream direction, viscous dissipation, energy diffusion, Reynolds shear stress, and intermittency factors. An analysis of the energy of mean and turbulent motion showed that the complete dynamic similarity in the wake, if ever attained, occurs beyond 1,000 diameters downstream of the wake generating cylinder. The observations revealed that the wake flow was intermittently turbulent except the fully turbulent core near the wake center. Making the usual boundary layer approximations and assuming that local isotropy exists, a turbulent energy balance was also presented. It should be mentioned that Townsend's data on the distribution of transverse fluctuation velocity differed from the later measurements reported by Eifler (1975), Fabris (1979), and many others, where a minima were observed at the wake center.

Roshko (1953) studied wake development behind circular cylinders using spectrum and statistical measurements at Reynolds numbers (Re) ranging from 40 to 10,000. The Reynolds number range of periodic vortex is divided into two distinct sub ranges joined by a transition range. Regular vortex streets are formed in the stable range (40 < Re <150) and periodic vortex shedding is accompanied by turbulent fluctuation in the irregular range (300 < Re <10,000). Free vortices decay by viscous diffusion in the stable range, while in the irregular range the diffusion is turbulent and the wakes become fully turbulent in 40 to 50 cylinder diameters. Also, the Strouhal number, a measure of the vortex shedding frequency, is found to be rapidly rising in the stable range and is practically constant in the irregular range.

Hill et al. (1963) investigated the effect of pressure gradients on the decay of the wakes. The measurement of the mean velocity distribution of the wake through a two-dimensional diffuser section with variable divergence angle showed that the wake can grow instead of decay. This can lead to stagnation flow at the wake center at large adverse pressure gradients. Employing a momentum integral equation and eddy viscosity proportional to the product of local free-stream velocity and momentum thickness, expressions were derived for estimating the decay of wake centerline velocity and growth of wake width. A criterion for the limiting value of pressure gradient to prevent the growth of defect velocity was also obtained.

Gartshore (1967) experimentally and theoretically examined two nearly self-preserving wakes subjected to adverse pressure gradient, the pressure gradient being adjusted to give a constant ratio between maximum wake defect velocity and local free-stream velocity. A comparison of data for longitudinal and lateral turbulence intensity and shear stress distributions with Townsend's (1956) data for the small-deficit zero pressure gradient wake showed that the effect of pressure gradient was to have slightly lower turbulence intensities and significantly lower shear stresses with all quantities being nondimensionalized by a local velocity scale.

Uberoi and Freymuth (1969) measured the one-dimensional spectra of turbulent wakes behind circular cylinders for downstream positions between 50-800 cylinder diameters and for Reynolds number between 320-95000. The spectra of large scale

turbulence are found to be anisotropic and dynamically similar. A formula is proposed to describe the spectra over the entire wave number range and for all Reynolds numbers.

Eifler (1975) and Pfeil and Eifler (1975 a,b) theoretically and experimentally investigated the development of wake for zero pressure gradient for a wide range of downstream locations and different cylinder diameters. Extending Reichardt's inductive approach on free turbulence theory, they obtained theoretical expression for the Reynolds shear stress. The theoretical expression for the Reynolds shear stress is in excellent agreement with Eifler's (1975) measurements.

Fabris (1979, 1983) measured the far wake of a circular cylinder using a four-wire probe to obtain instantaneous values of three components velocity and temperature. The wake generating cylinder is heated slightly to allow conditional sampling techniques using the temperature as a tracer to distinguish between the turbulent (heated) and potential (cold) intermittent fluid. The conventional and conditional averages are presented for velocities, temperature, turbulent fluctuations, and second- and third-order correlations. The conditional averages are calculated in turbulent zone, potential zone, and the upstream and downstream interfaces of the turbulent zone.

Cantwell and Coles (1983) investigated the transport processes in the near wake of a circular cylinder in the first eight diameters of the wake and at a Reynolds number 140,000 using a X-wire probe and flying-hot-wire techniques. The ensemble averages of data at constant phases of the vortex shedding yielded a sequence of pictures of the instantaneous mean flow field, with the vortices frozen as they would be in a photograph. In addition to globally averaged data for velocity and turbulent stress, results are presented for averages at constant phase for velocity, intermittency, vorticity, turbulent stress, and turbulent energy production. The kinematics of vortex formation process is described in terms of the formation and evolution of saddle points between vortices in the first few diameters of the near wake.

All the investigations reviewed so far are for symmetric wakes where the curvature is absent. Wattendorf (1935) investigated the effect of curvature on two-dimensional fully developed turbulent flow. He measured the mean velocity and pressure distributions in two channels of different curvature radius and found that velocity

distributions are strongly influenced by curvature.

Görtler (1940) has shown that longitudinal vortices are generated by instability with respect to three-dimensional disturbances in boundary layer flows along concave walls. The effect is absent on convex walls. The result is to move the transition point toward the leading edge of the concave wall boundary layer.

Eskinazi and Yeh(1956) studied fully developed turbulent flow in a curved channel between two concentric circular walls by measuring mean velocity, static pressure, turbulent intensities, shear stresses, and one-dimensional spectra. They showed that the turbulence structure was dependent on the distribution of the angular momentum. The turbulence was suppressed near the convex wall where the gradient of the angular momentum was positive and promoted near the concave wall where the gradient of angular momentum was negative. This is similar to the Rayleigh's criterion for centrifugal instability for an inviscid, irrotational curved flow where the radial equilibrium of the fluid element is stable if the radial gradient of angular momentum is positive and unstable if the radial gradient of the angular momentum is negative.

Margolis and Lumley (1965) investigated the curved mixing layer produced by a two-dimensional jet of air issued into a curved channel with part of the channel entrance open to the atmosphere. They measured the mean velocity, turbulence intensity, shear correlation, and one-dimensional streamwise energy spectra of two dynamically different flows obtained by placing the jet next to the convex or concave wall. When the jet was placed next to the convex wall of the channel, the angular momentum gradient was negative and the flow was unstable. When the jet was placed next to the concave wall of the channel, the angular momentum gradient was positive and the flow was stable. The results also showed self preservation for the mean velocity distribution.

Turbomachinery boundary layers and wakes are two important cases of turbulent flow with streamline curvature. Their characteristics are the most influential factors on the performance of machines. Raj and Lakshminarayana (1973) investigated the near and far wake characteristics of a cascade of airfoils for three different incidence angles. The measurements of mean velocity, turbulence intensity, and Reynolds stress showed asymmetric distribution, and the decay of the wake defect was found strongly dependent

on the downstream variation of wake edge velocity. Also presented are semi-theoretical expressions for the wake profile, decay of the defect velocity, turbulence intensity and Reynolds stress.

The sensitivity of the flow to the curvature and pressure gradient can best be realized from the study by Schobeiri (1976, 1979) involving viscous flows with low Reynolds numbers in symmetric convex and concave channels. The investigation shows that the flow through the symmetric channel with convex wall is more sensitive, with respect to flow separation, to adverse pressure gradient than the flow through a channel with concave walls. Other investigations by Schobeiri (1980, 1990) in asymmetric channels show that the flow tends to separate on the convex wall than on the concave wall in the presence of adverse pressure gradient.

Bradshaw (1973) reviewed earlier work on the effect of streamline curvature on turbulent flow. Castro and Bradshaw (1976) studied the turbulence structure of a highly curved mixing layer bounding a normally impinging plane jet with an irrotational core. The measurement of Reynolds stress and other turbulence quantities showed a decrease in the region of stabilizing curvature. Muck et al. (1985) and Hoffmann et al. (1985), in their experiments on boundary layers on convex and concave surfaces, observed that convex (stabilizing) curvature tends to attenuate the preexisting turbulence while the concave (destabilizing) curvature results in the generation of Taylor-Görtler vortices.

Koyama (1983) studied the curvature effect on the mean velocity and turbulent stress in the initial developing part of a cylinder wake developing in a curved channel without streamwise pressure gradient. When the wake generating cylinder is located normal to the streamline curvature (spanwise), he observed asymmetry about the wake centerline in the mean velocity and turbulent intensity profiles owing to the destabilizing effects on the inner side of the wake and stabilizing effects on the outer side.

Savill (1983) and recently Nakayama (1987) investigated the effects of pressure gradient and curvature on wakes. Savill investigated a fully developed cylinder wake that is abruptly turned 90° by means of a back plate so that the wake is subjected to strong curvature and streamwise pressure gradient. The data for mean velocity and turbulent stress revealed the strong influence of curvature on the wake. The turbulent

stress fields are found complex owing to the coexistence of the stabilized and destabilized regions across the wake and strong interaction between them. Nakayama (1987) carried out a systematic study of the effect of mild pressure gradient and mild streamline curvature on a small-deficit wake. The wake was subjected to mild curvature and mild pressure gradient by deflecting it by an airfoil like thin plate placed at small angles in the external flow. The qualitative separation between the effects of the curvature and pressure gradient is achieved by placing the thin plate at positive and negative angles to the free-stream direction. Despite the governing mild pressure gradient and curvature, the measured data suggests a strong sensitivity of turbulence quantities, especially the Reynolds shear stress, to the curvature and pressure gradient.

The study of the wake characteristics by Ramjee and Neelakandan (1989) involved a rectangular cylinder wake in both the straight and curved channels up to a downstream location of 160 cylinder heights. The sensitivity of wake flow to the curvature is evident from the pronounced changes in the maximum defect velocity and Reynolds stress intensities in the downstream side between the straight and curved wakes. Larger maximum defect velocity and asymmetry of the mean velocity profile were quite evident in the curved duct case. The lateral fluctuations are found to be more sensitive to curvature than the streamwise fluctuations. Of all the Reynolds stresses, shear stress exhibited pronounced changes with downstream distance bringing out the strongest sensitivity to the streamline curvature.

In turbomachines, unsteady wakes impinging on the blade surface have significant influence on boundary layer development and heat transfer rate to the blades. Raj and Lakshminarayana (1976) analytically and experimentally investigated the characteristics of three-dimensional turbulent wakes of a turbomachinery rotor. Measurements of mean velocities, turbulence intensities, and Reynolds stresses were carried out using a triple sensor hot-wire probe in a stationary system at various axial and radial locations downstream of the rotor. Semi-theoretical expressions for the decay rate of the defect velocity, turbulence intensity, and Reynolds stresses with downstream distance of the rotor are derived. A comparison with an isolated airfoil and cascade data suggests that the decay of the rotor wake was faster than the cascade or an isolated airfoil wake.

Other investigations on rotor wakes include measurements by Evans (1975) using X-hot-wire probe and Lakshminarayana and Poncet (1974) using a triple sensor hot-wire probe. Ravindranath and Laksminarayana (1979, 1980) also investigated the relative flow behind blade cascades using rotating probes.

Recently, rotating wake generators have been used to simulate the unsteady flow as reported by Pfeil and Schröder (1981), Schröder (1985), Doorly and Oldfield (1985), and O'Brien and Capp (1989). Pfeil and Schröder (1981) and Schröder (1985) studied the unsteady wake development downstream of rotating cylinders within a straight channel. The data for velocity and turbulent stresses measured in the absolute frame of reference were transformed to a relative frame of reference. From these data they could describe the relative wake defect by the theory of free turbulence established by Reichardt (1942) and extended by Pfeil and Eifler (1975).

Doorly and Oldfield (1985) employed a rotating bar wake generator consisting of bars mounted on the rim of a large diameter disk. The test section consisted a row of blades in a cascade. Their study revealed that wakes undergo massive distortion due to high velocity gradients in the rotor blade passages. There is also a very high rate of transient heat transfer because of the production of a boundary layer patch on the suction surface and subsequent sweeping along the blade surface.

O'Brien and Capp (1989) investigated the mean velocity and turbulence statistics downstream of a rotating spoked-wheel wake generator located in an annular passage at three Reynolds numbers and three wake passing frequencies. Phase-averaged measurements obtained in the stationary frame of reference showed that the mean axial velocities are independent of Reynolds and bar passing Strouhal numbers. Phase-averaged Reynolds stresses were consistent with related cylinder wake measurements but were higher than corresponding measurements of Reynolds stresses obtained in large scale research turbomachines.

Wake-induced unsteady flow using rotating wake generators have been studied in many other experiments, e.g., in a transitional turbine blade boundary layer by Ashworth, LaGraff and Schultz (1989), in a compressor cascade boundary layer by Dong and Cumpsty (1989 a,b), in a flat plate transitional boundary layer by Liu and

Rodi (1991), in a linear turbine cascade by Liu and Rodi (1992), and in a flat plate boundary layer at different pressure gradients by Orth (1992). Morehouse and Simoneau (1986), O'Brien et al. (1986), and O'Brien (1988) investigated the effect of unsteady wakes generated by a rotating spoked-wheel wake generator on heat transfer in the stagnation region of a cylinder.

The investigations discussed above have significantly contributed to better understanding of the wake flow under different boundary conditions. However, several fundamental questions are still unanswered. Further, the existing data on the direct influence of curvature and pressure gradient on wake development are limited. Therefore, a comprehensive experimental investigation is needed to study the steady and periodic unsteady wake development through curved channels under positive, zero, and negative streamwise pressure gradients.

3. OBJECTIVES

The objective of this investigation is to study the development of steady and unsteady wakes in a curved channel at different streamwise pressure gradients. The wakes are generated by circular cylinders. The steady wake generated by a stationary cylinder is investigated for positive, zero, and negative streamwise pressure gradients, while the unsteady wake generated by the rotating wake generator is investigated for zero streamwise pressure gradient. An X-hot-film probe takes the measurements. The components of the velocity and the Reynolds stress in the radial and tangential directions (probe coordinate), obtained with a X-hot-film probe, are transformed to a curvilinear coordinate system along the wake centerline. The mean and turbulence quantities of unsteady wakes are studied using ensemble averaging techniques. The unsteady wake quantities obtained in a stationary frame of reference are transformed to a relative frame of reference.

The mean velocity and Reynolds stress distributions in similarity coordinates are compared against the plane wake data. The decay rate of wake defect velocity and growth of wake width are determined. The integral quantities, momentum thickness and product $\bar{U}_{1m}b$, are also found. The data obtained from this study provides a good understanding of the effect of curvature and pressure gradient on the wake development, which is extremely useful in understanding turbomachinery wake flows.

Another part of this research program implemented instrumentation and data acquisition for the newly built test facility. An accurate method of calibrating X-hot-film probe was also implemented.

4. THE EXPERIMENTAL TEST FACILITY

Figure 1 shows the complete layout of the test facility, which consists of a large centrifugal fan, a settling chamber, a nozzle, a wake generator, a curved channel test section, and an exit duct. The components are discussed in the following sections. A more detailed description of the test facility is given by Schobeiri (1988), Pardivala (1991), and Schobeiri and Pardivala (1992).

4.1. Fan and Inlet Duct Assembly

The centrifugal fan is driven by a 112 kW (150 hp) 3-phase a.c. motor running at its rated speed of 1785 rpm, which is reduced to the fan speed by a belt pulley transmission with a ratio of 190/330. At the test section the above motor speed results in a mean velocity of 36 m/s and a maximum Reynolds number (based on the test section height) of 8.0×10^5. Variation of the flow velocity and thus the Reynolds number can be achieved by operating a throttle at the fan exit or varying the fan speed. For the present investigations, the throttle was adjusted to give a mean velocity of about 20 m/s just upstream of the wake generator. This corresponds to a Reynolds number of 2600 based on the wake generating cylinder diameter of 1.984 mm. The flow entering the fan passes through a 50-mm thick fiber glass filter, that can filter particles of up to 5 μm.

Since the fan exit is at a higher level than the centerline of the test facility, a set of transition ducts followed by 3.25 m of straight piping, with a diameter of 500-mm, are used to smoothly channel the flow from the fan exit to the diffuser inlet. The first transition duct is S-shaped with a cross-section of 615 mm x 690 mm, which corresponds to the cross-section of the fan exit. This duct has two sections separated by a 100-mm rubber connector. The rubber connector isolates the test facility from the vibrations of the fan and is the first of a series of steps that ensure smooth operation of the facility. The second transition duct connects the rectangular cross-sectioned S-shaped duct to the circular cross-sectioned straight pipe. The straight pipe
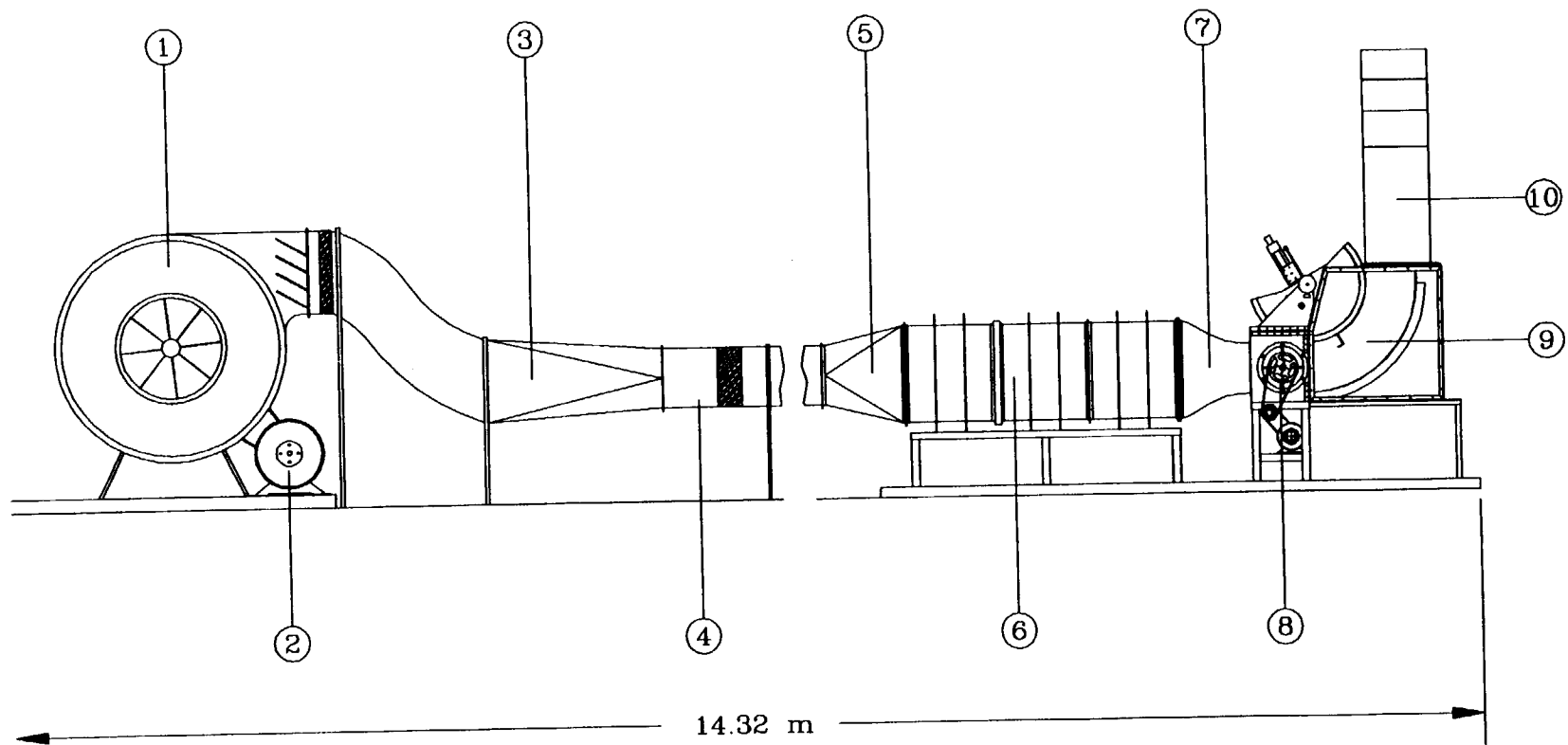
Fig. 1 Overall layout of the test facility. 1-fan; 2-motor; 3-transition duct; 4-straight pipe; 5-diffuser; 6-settling chamber; 7-nozzle; 8-wake generator; 9-test section; 10-exit duct

is made of two sections for easy assembly and passes through the wall of the laboratory. The first section of the straight pipe has another 200-mm rubber connector to further isolate the test facility from the upstream vibrations. A small step introduced between the two sections of the straight pipe provides sudden flow contraction and relaxation, which results in better mixing and a more uniform velocity profile downstream. Trost (1975) and Schobeiri (1979) used a similar contraction. Tests with a Prandtl probe in the final section of the pipe confirm the existence of a fully-developed turbulent velocity profile upstream of the diffuser inlet. The Prandtl probe, permanently located in the straight pipe upstream of the diffuser, senses any variation in the mean velocity resulting from fluctuations in the fan speed due to unsteadiness in the line voltage.

4.2. Diffuser, Settling Chamber and Nozzle Assembly

A 600-mm long short diffuser with an area ratio of 1:5, designed on the optimum design criteria (see Schobeiri, 1979), is located downstream of the straight pipe and decelerates the flow before it enters the settling chamber. The settling chamber is made of three sections each of 750-mm length and a cross-section of 1200 mm x 820 mm. Four screens and one honeycomb flow straightener control the flow uniformity and turbulence level within the settling chamber. The screens are made of stainless steel and have different mesh sizes and wire diameters. The first screen, placed at the diffuser exit, reduces the scale of the vortices generated by the diffuser vanes. A 50-mm wide honeycomb flow straightener with a 6-mm cell size is located between the first two settling chamber sections. Directly downstream of the honeycomb is the second screen. This honeycomb-screen combination results in a much lower exit turbulence level than a honeycomb alone, since the large scale jets exiting from the honeycomb cells are broken into smaller scale eddies (see Blair et al., 1981). The third and fourth screens are located downstream of the second and third settling chamber sections. This diffuser-settling chamber configuration with four screens results in a free-stream turbulence intensity of 1.2% at the inlet of the test section. Table 1 list the specifications of the screens. Downstream of the settling chamber is a nozzle with an

area ratio 4:1 that accelerates the flow to the required velocity before it enters the wake generator. The nozzle establishes a smooth transition of the flow from the settling chamber to the wake generator.

Table 1 Details of the screen configuration

Number of Screens	Mesh Size (per 25.4 mm)	Open Area (%)	Turbulence Intensity (%)
4	Screen 1: 20 x 20 Screen 2: 20 x 20 Screen 3: 30 x 30 Screen 4: 30 x 30	67 67 65 65	1.2

4.3. Wake Generator for Simulation of Unsteady Inlet Flow

The wake generator (see Figs. 2 and 3) simulates the unsteady inlet flow and the flow pattern downstream of a rotor row. Figure 3 shows a cross-section of the wake generator where a series of circular cylinders can be arranged circumferentially on two parallel rotating disks. The disks are covered by two stationary circular disks connected with the shafts (see Fig. 3) to avoid an undesirable inception of secondary shear flow generated by the rotating disks. The diameter and number of cylinders can be varied to simulate the wake width and spacing that stems from the trailing edge of rotor blades. The minimum cylinder diameter with this configuration is 2-mm while the maximum diameter is 5-mm. The number of cylinders may vary between 1 and 30. The present investigation uses a cylinder of diameter 1.984-mm for both steady and unsteady wakes. For the three pressure gradient cases of steady wake, the wake generator is kept stationary with a single circular cylinder of diameter 1.984-mm kept at mid-height of the channel and a distance 67-mm upstream of the entrance to the curved test section. Three circular cylinders of 1.984-mm diameter each, fixed at equal angle on the rotating disk, are used for the unsteady pressure gradient case. Figure 2 shows the rotating disks driven by a frequency controlled electric motor with a belt transmission with maximum
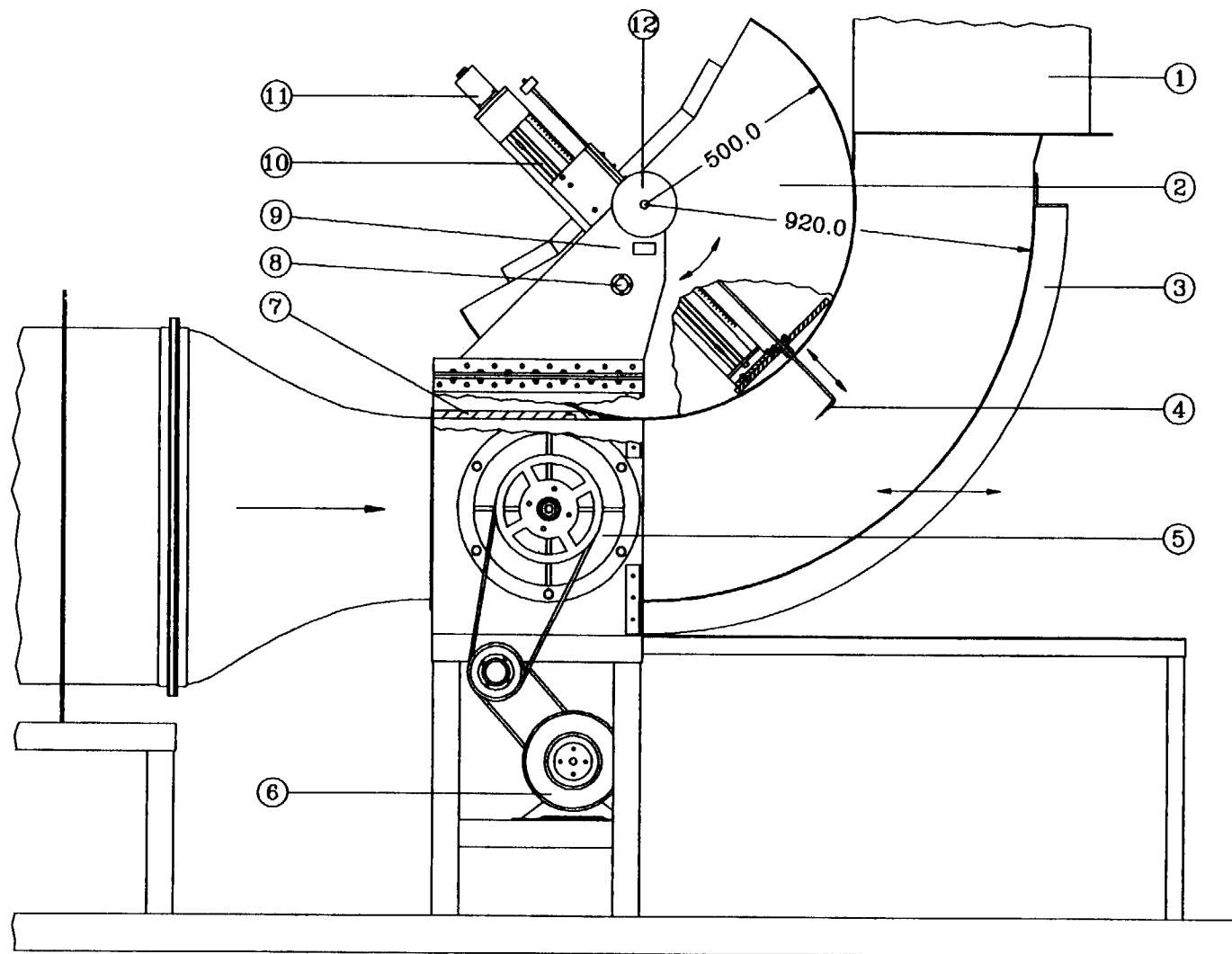
Fig. 2 Test section. 1-exit duct; 2-convex wall assembly; 3-concave wall; 4-probe; 5-wake generator; 6-motor; 7-top wall; 8-safety pin; 9-rotary vernier; 10-traversing system; 11-stepper motor; 12-encoder; 13-locking wheel
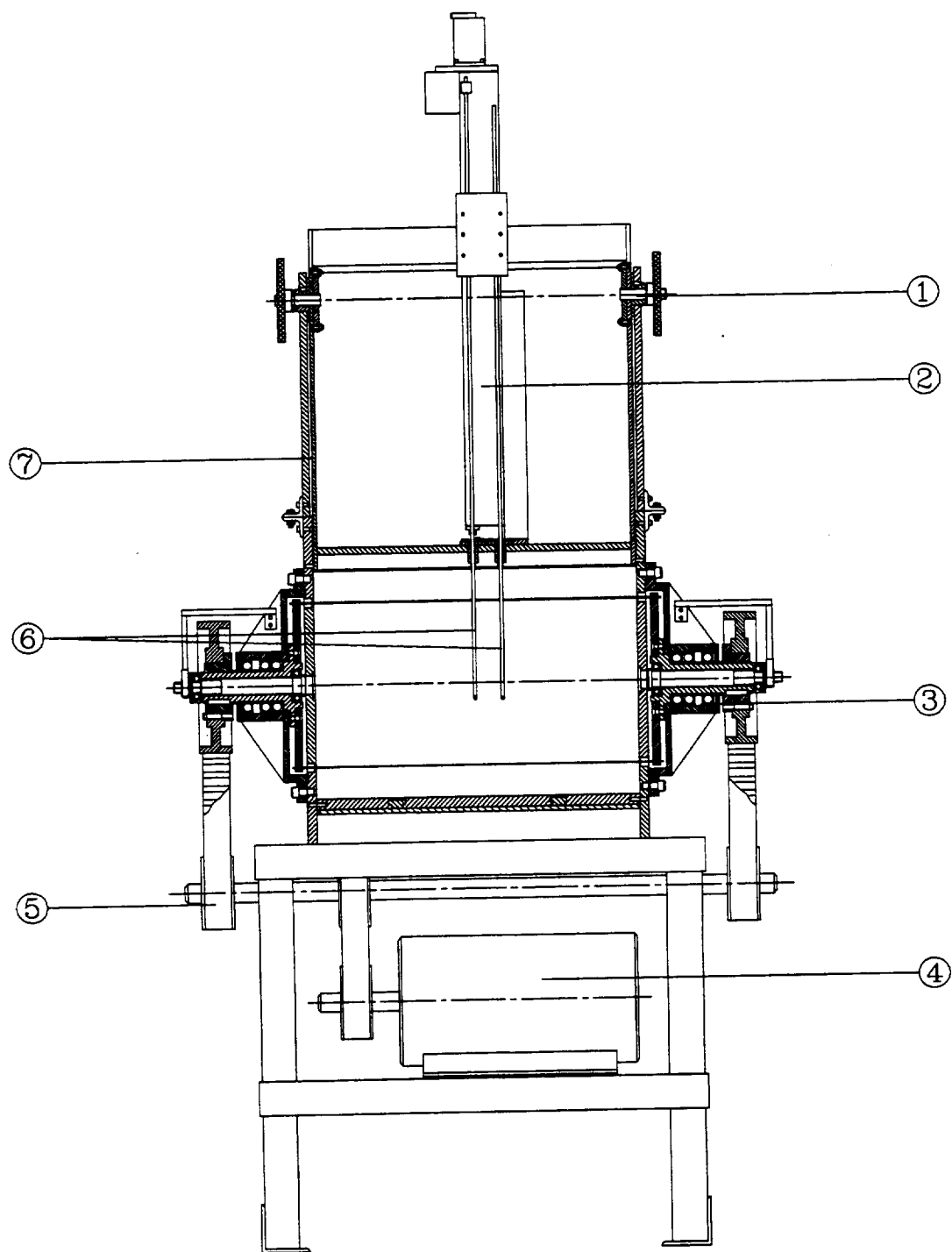
Fig. 3 Section of convex wall assembly and wake generator. 1-locking wheel assembly; 2-probe traversing assembly; 3-wake generator; 4-motor; 5-driving system for wake generator; 6-probes; 7-convex wall assembly

power of 7.45 kW (10 hp) and maximum rotational speed of 1750 rpm. A fiber-optic sensor provides the input to the frequency controller that generates the signal to monitor the angular frequency of the wake generator. The sensor also generates the signal for external triggering of the analog to digital (A/D) conversion board needed for phase-averaged measurement.

4.4. Test Section for Simulation of Curvature Effect

The test section in Fig. 2 is located downstream of the wake generator and consists of a convex top wall, a concave bottom wall, and two vertical plexiglass side walls. The probe traversing system is mounted within the convex wall assembly. Details of this system are discussed in the following section. The concave bottom wall slides horizontally within two T-slots in the bottom wall of the wake generator. This allows the creation of adverse or favorable streamwise pressure gradients within the test section. Table 2 summarizes the geometry of the test section for the four cases investigated in the present study. The fourth column of the table gives the area ratio

Table 2 Details of the test section and the wake generating cylinder used

Test cases for wake development	Test section inlet area (mm x mm)	Test section outlet area (mm x mm)	Area ratio	Cylinder dia. (mm)	No. of Cylinders
steady, zero pressure gradient	420 x 593	420 x 593	1.0	1.984	1
steady, positive pressure gradient	420 x 593	547 x 593	0.7	1.984	1
steady, negative pressure gradient	420 x 593	295 x 593	1.3	1.984	1
unsteady, zero pressure gradient	420 x 593	420 x 593	1.0	1.984	3

of the inlet to outlet of the curved test section. The two curved walls have static

pressure ports mounted flush with the surface at regular arc lengths of 50-mm. The static pressure ports are connected to a manometer bank for visualization purposes. The test section allows integration of test objects such as a curved plate, a cylinder, or a turbine cascade for boundary layer and heat transfer investigations.

4.5. Probe Traversing System

Besides simulating convex curvature, the convex wall assembly also allows precise radial and circumferential traversing of the probes. Figure 2 shows the mounting of the traversing system within the convex wall assembly (details are shown in Fig. 3). The traversing system is vertically mounted on the base plate of the convex wall assembly and consists of a 152.4-mm slider that moves within a dovetail guide. A lead screw with a maximum traversing length of 610.0-mm, connected to a d.c. stepper motor, provides the required drive for the slider. It receives signals from a computer driven by a FORTRAN code with an arbitrary traversing schedule as an input, which turns the lead screw by the exact number of pulses required. An optical encoder connected to the traversing system provides continuous feedback to the stepper motor for accurate positioning of the probes. The system can traverse in small steps with a resolution of 2.5 μm. Both software and mechanical stops prevent the probes from traversing beyond the desired limits.

The slider of the traversing system allows the simultaneous positioning of two probes (Fig. 3). The first probe is a hot-wire or hot-film probe (single hot-film, x-film) while the second probe is a total pressure probe (Kiel probe). Angular (streamwise) positioning of the probes is achieved by rotating the entire convex wall assembly about its center of curvature. A rotary vernier mounted on one of the triangular supporting walls allows precise angular positioning of the probes.

5. INSTRUMENTATION AND DATA ACQUISITION

Digital data acquisition and analysis have been used throughout this study. The test facility was instrumented for fully automated data acquisition. The following sections describe the instrumentation, data acquisition procedure, and calibration of sensors.

5.1. Instrumentation of the Test Facility

Figure 4 shows a schematic layout of the test facility instrumentation. The data acquisition system is controlled by a 386SX, 16 mHz personal computer with a math coprocessor, a 210 Mb hard disk, a 1.2 Mb floppy drive, and a 120 Mb tape backup system. A 12-bit A/D (analog to digital conversion) board is installed in one of the expansion slots of the computer. The board has 16 channels and a data transfer rate of 1 mHz throughput rate. The voltage range of -10 V to +10 V is selected for the A/D board input. The first eight channels of the A/D board have simultaneous sample and hold circuits. This is particularly important for measuring Reynolds shear stress, as the voltages from the two sensors of the X-probe can be obtained without any time delay between them.

A 3-channel, constant temperature anemometer (TSI, IFA 100) system obtains the mean velocity and turbulent stress components. Each channel of the anemometer system has a signal conditioner with variable low and high pass filters, dc-offset, and adjustable gain. The offset and gain are adjusted to obtain maximum resolution and signal to noise ratio. Based on numerous spectral measurements within the wake, the low pass filter of the signal conditioner is set at 20 kHz. The hot-film probes are operated at 1.5 overheat ratios and 250°C sensor operating temperature. All measurements in the present study are made with platinum hot-film sensors with 25-μm diameters. Preliminary measurements are made using a standard single-film probe (TSI 1210-10) and the two component measurements are made using a specially designed X-film probe (TSI 1241-XX-10). The X-film probe allows the sensors to remain along the axis of the probe support. The first channel of the anemometer is connected to a single-film

21
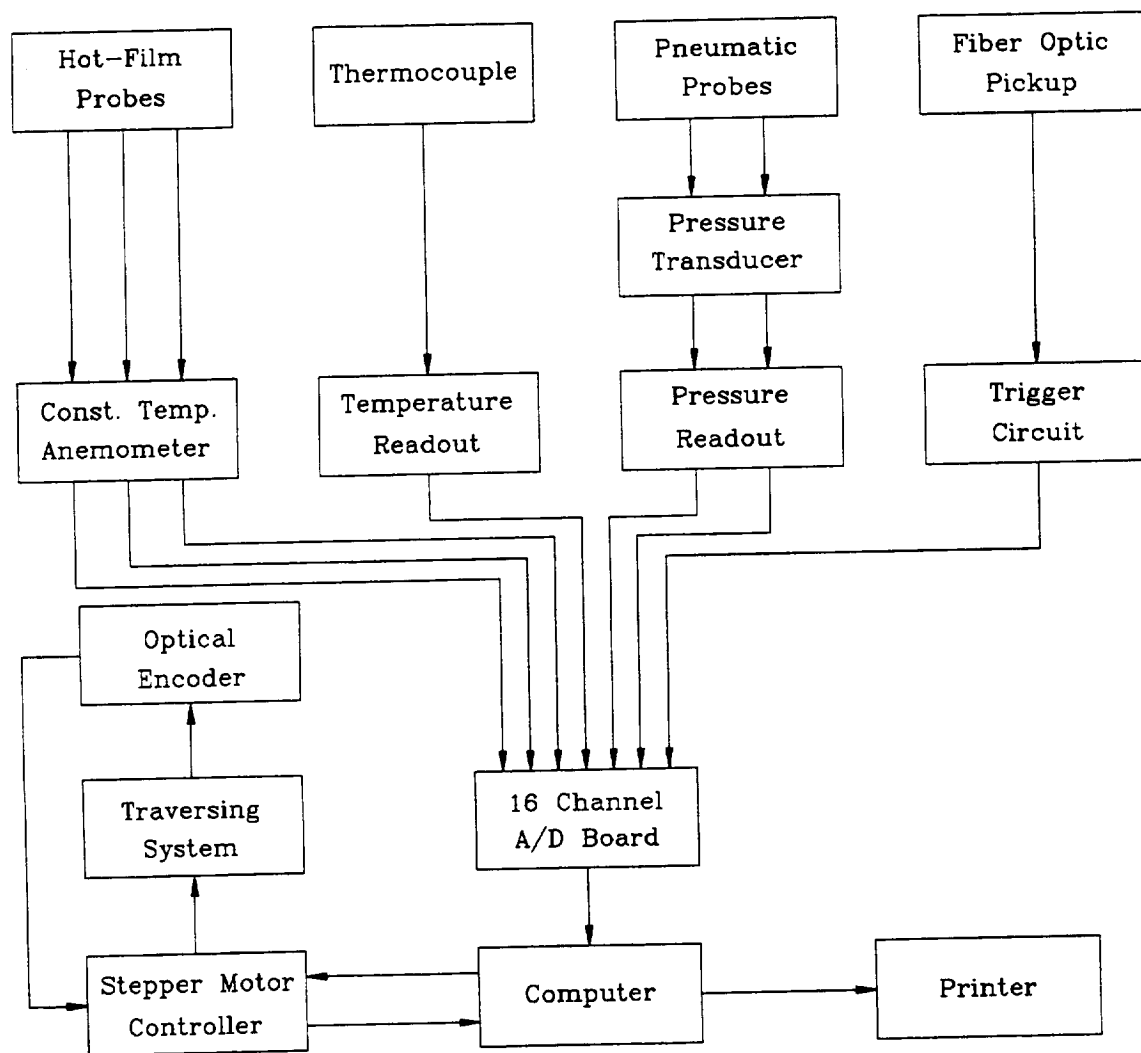
Fig. 4 Schematic view of the test facility instrumentation

probe and the second and third channels are connected to a X-film probe. The anemometer output is connected to the first channel of the A/D board when the single-film probe is used. For measurements using X-film probes, the two anemometer outputs are connected to the first two channels of the A/D board from which the data is sampled by the computer.

Two high precision differential pressure transducers (MKS 220CD, Range: 0-10 mm Hg and 0-100 mm Hg) with a 2-channel digital readout are connected to the fourth and fifth channels of the A/D board. The pressure transducers are of capacitance type and have 0-10 V analog outputs. A Prandtl probe (pitot-static probe), placed upstream of the diffuser, connects to one of the pressure transducers and monitors reference velocity at a fixed location. The second pressure transducer measures the total pressure from a Kiel probe (United Sensor) positioned at the same radial and streamwise location as the X-probe. The third channel of the A/D board connects to a thermocouple with a digital readout. The temperature readout has a 4-20 mA current output which is converted to voltage output before transferring to the A/D board input channel. The thermocouple is placed just downstream of the test section to constantly monitor the flow temperature.

A high response, reflective type fiber-optic proximity sensor (ATC 7062A) located close to the pulley of the wake generator generates once in a revolution signal. The signal is generated when a piece of reflective tape fixed on the pulley comes across the proximity sensor. The signal generated from the fiber optic sensor is converted to 0-5 V level and transferred to the Schmitt-trigger inputs of two monostable multivibrator circuits with adjustable output pulse width. The output of the first monostable multivibrator circuit is adjusted to 900-μs for the high pulse and transferred to the eighth channel of the A/D board for rpm measurement. The rpm is measured by sampling the voltage at the eighth channel of the A/D board and calculating elapsed time between successive high pulses. This method of measuring rpm is highly accurate and calibration is not needed. The output of the second monostable multivibrator is adjusted to 1 μs high pulse and externally triggers the A/D board for phase averaged measurements for the periodic unsteady wakes. A photoelectric proximity sensor with a digital readout displays the rpm of the centrifugal fan.

A stepper motor driven traversing system (Velmex Unislide) with micro motion capability and optical encoder feedback allowed accurate positioning of the probes. The stepper motor drive was actuated by a stepper motor controller (Whedco) that also receives the feedback from the optical encoder. The personal computer communicates with the stepper motor controller through the RS232 serial interface. Fortran subroutines were written for this communication.

5.2. Data Acquisition Procedure

As previously stated, the data acquisition system is fully automated. All computer programs are written in Microsoft FORTRAN and access the A/D board driver routines written in assembly language. Before actual data acquisition, a program runs that continuously monitors and displays the pressure, temperature, anemometer voltages, and rpm to ensure that the instrument settings and output cable connections are correct. The files COORD.DAT and CP.DAT contain the radial coordinates for a complete traverse. The overtravel limits and the current probe position are edited before starting the actual data acquisition. Given the probe coordinates to be traversed as an input, the probes are positioned automatically. The optical encoder feedback ensures accurate positioning of the probes. The computer then samples the voltages from the differential pressure transducer and thermocouple, calculates the mean pressure and temperature on line, and stores them in a data file. For unsteady wakes, the output from the fiber-optic sensor circuit is sampled to obtain the rpm which is stored along with the pressure and temperature. The voltages from the constant temperature anemometer are then sampled and stored. The anemometer outputs are sampled at a rate of 2 kHz with 32768 samples per channel taken. These numbers are chosen based on results of preliminary tests conducted by varying the sampling rate from 0.5 kHz to 5 kHz with number of samples ranging from 8000 to 64000. In the case of unsteady wakes, 2048 samples per channel were taken during one revolution and the data was acquired for a total of 500 revolutions. Once data is acquired at a location and stored in its individual data file, the probe moves to a new location given in the coordinate data file (COORD.DAT).

Data acquisition is started for the new location after a specified delay. The process is repeated until data is acquired for all locations specified in the coordinate file. The programs AUTO.FOR, XAUTO.FOR, and UXACQUIR.FOR acquire data employing single-film probe, X-film probe, and unsteady measurements using X-film probe, respectively.

The frequency spectra are measured to find the desired cut off frequency of the low pass filter of the anemometer system. One-dimensional frequency spectra are obtained from a single sensor hot-film probe by performing a Fast Fourier Transform (FFT) on 1024 points using the WAVEPAK FFT system available at the Turbomachinery Laboratory. Final smooth frequency spectra are then obtained by averaging the results of 150 such FFTs. Figures 5-7 show the spectra obtained at the inlet ($\theta = 0°$) for the three different pressure gradients. Spectra are obtained at three radial locations for each pressure gradient case . The location corresponding to the dotted line spectrum is in the potential flow region outside the wake. The thick solid line corresponds to a location almost near the center of the wake and the thin solid line corresponds to a location slightly away from the center of the wake. The peaks observed in the solid line spectra clearly indicate the Kármán vortex shedding with a Strouhal Number S ($S = f.d/V_{in}$) equal to 0.21, which matches with the data of Roshko (1956). Here, f denotes the vortex shedding frequency in hz and V_{in} is the average velocity just upstream of the wake generating cylinder. The vortex shedding frequency is slightly higher in Fig. 5 than in Figs. 6 and 7, since the spectra for that case are taken at a slightly higher velocity.

5.3 Calibration of Sensors

Sensor calibration is a prime requirement for an accurate measurement of a physical quantity. The most preferable method to calibrate a channel is to directly measure the full-channel response using an external reference that produces a known result. That way, all the components along the signal path are calibrated together as opposed to separate calibration of transducer, A/D board, etc. The calibration involves fitting the
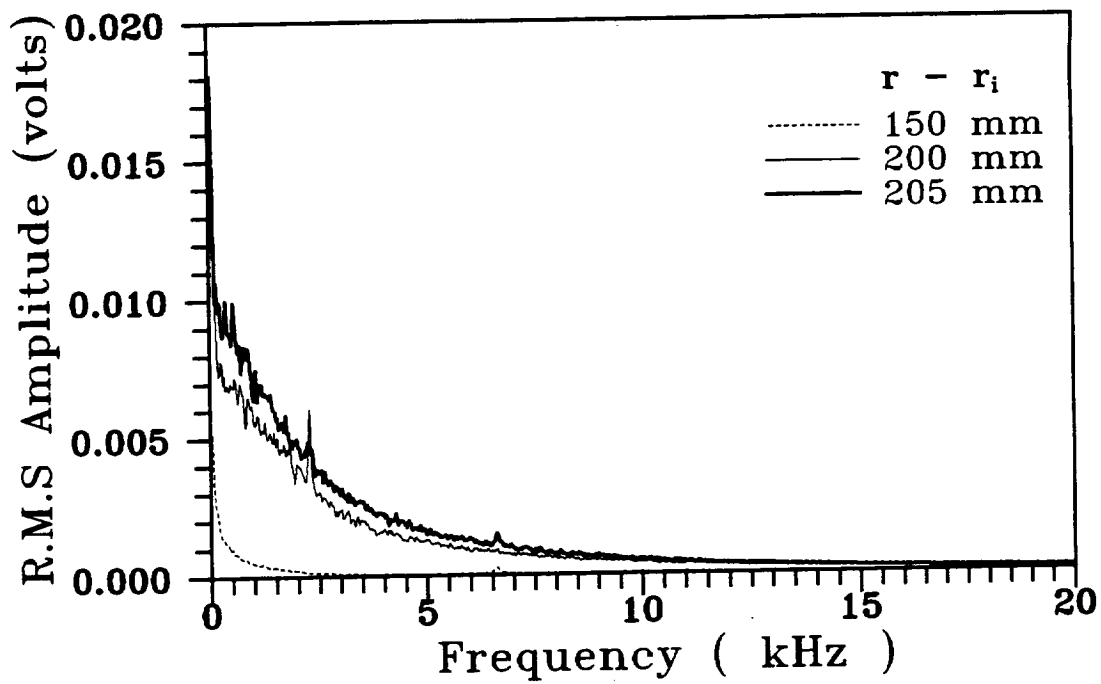
Fig. 5 Frequency spectra at different radial locations for zero streamwise pressure gradient at $\theta = 0°$, $V_{in} = 21.5$ m/s
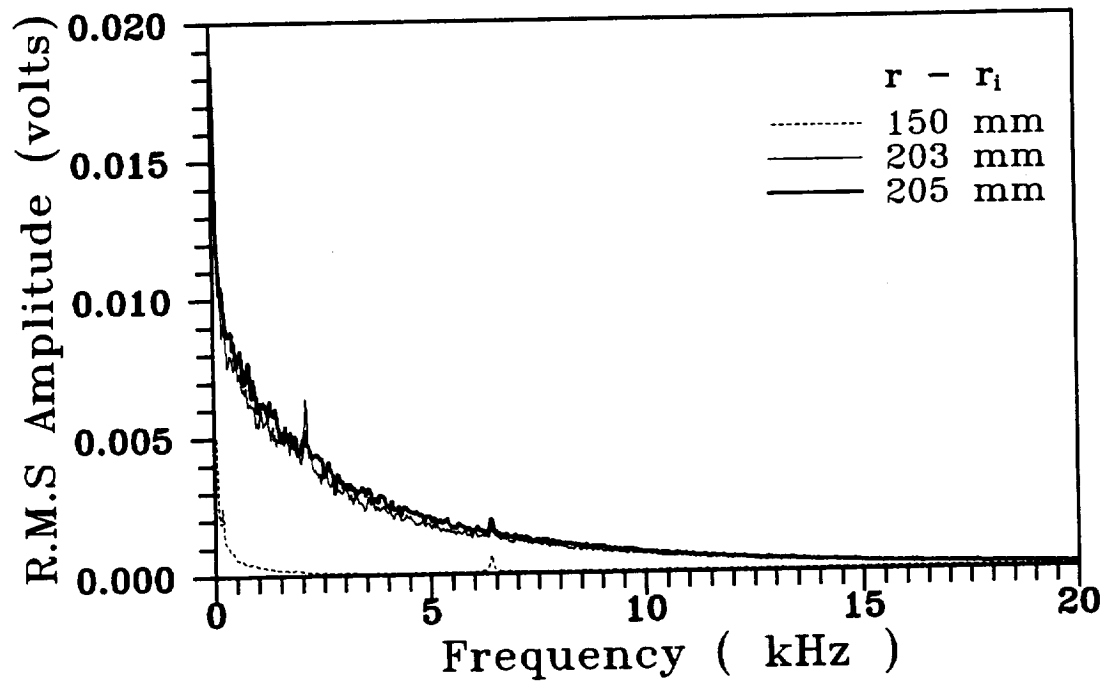
Fig. 6 Frequency spectra at different radial locations for positive streamwise pressure gradient at $\theta = 0°$, $V_{in} = 20$ m/s
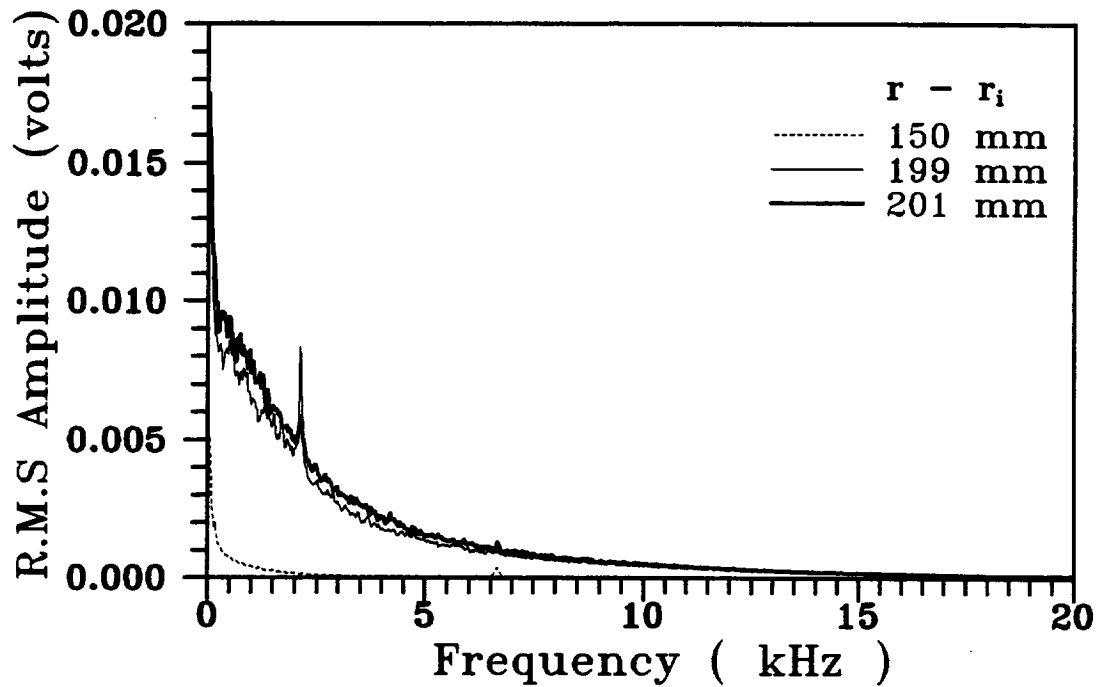
Fig. 7 Frequency spectra at different radial locations for negative streamwise pressure gradient at θ = 0°, V_{in} = 20 m/s

time averaged voltages calculated from sampled data of the A/D board channel against known mechanical quantities such as temperature, pressure, flow velocity, flow angle, etc. The Fortran program CAL.FOR (Appendix B) is a general purpose routine for calibrating a sensor. The pressure transducer is calibrated using a dead weight tester and the thermocouple is calibrated using a thermocouple calibrator. The analog outputs from the instruments are connected to the A/D board and sampled by the computer. Polynomial fits, obtained through a least squares technique, are used to fit the recorded time averaged output voltages with the actual readings obtained from the dead weight tester and the thermocouple calibrator. The calibration coefficients are then stored in appropriate data files on the computer. The hot-film sensors are calibrated frequently in a low turbulence, uniform flow, open jet calibrating facility. A more detailed description of the calibration of the single-film and X-film sensors is given in the next section.

6. CALIBRATION OF HOT-FILM PROBES

The present study of the wake development in curved channels involves measurements of the instantaneous two-dimensional velocity field using a X-hot-film probe. High quality experimental measurements using X-probe require accurate calibration procedures. The present investigation used a simple and accurate method to calibrate X-probes in incompressible flow (John and Schobeiri (1993)). The yaw response of the hot-film X-probe was investigated for different velocities and found to be strongly velocity dependent at low velocities. A simple relation corrected the variation of yaw response at low velocities. The calibration method used in the present investigation is described in this section. It should be mentioned that this section uses no separate nomenclature to distinguish between instantaneous and time averaged quantities, since the equations are the same in both cases. All equations use time averaged velocities and voltages to obtain the calibration coefficients.

6.1. Review of Existing Methods of Calibration

X-probes are widely used for measuring the two components of flow velocity. Various methods interpret the signals from the two sensor probes and almost all methods relate the output voltage to the effective cooling velocity V_e. The effective velocity is related to the actual flow velocity C in different forms. Hinze (1959) and Champagne et al. (1967) introduced the most accurate representation of the directional response of a hot-wire or hot-film:

$$V_e^2 = V_N^2 + k^2 V_T^2 \qquad (6.1)$$

This equation considers the cooling due to both normal and tangential velocity components. Webster (1962) experimentally found the values of k for various l/d ratios for a single hot-wire sensor. Jorgensen (1971) investigated the dependence of k on the yaw angle and found that the value of k varies with the yaw angle. Bradshaw (1971) introduced a calibration method based on an effective angle defined as:

$$V_e = C\cos\alpha_e \qquad\qquad (6.2)$$

Brunn et al. (1990) used a conventional calibration method with a constant k-factor in Eq. (6.1) and compared it with Bradshaw's method, which is based on Eq. (6.2). As a result, Brunn showed that the conventional method based on Eq. (6.1) gives the smallest error over the complete angle range.

Lekakis (1988) obtained the k values at a given velocity from a yaw calibration. He found that a constant value for k, determined by a least square-fit of all k values, provides a good representation of the probe angular response. In a similar way, he learned the value of k for different velocities. Using the above k values, Lekakis developed an analytical method for calculating the velocity and its components.

The use of constant k at a given velocity, which is common to the previously described methods, introduces significant errors particularly at higher yaw angles. Schröder (1985) employed a simple calibration method by introducing an ideal flow angle for which k was equal to zero and applied the method to X-hot-wire probes. A yaw calibration covering the entire angle range was done at a single velocity. Compared to constant k-factor based methods, the method by Schröder was more accurate to a wide range of yaw angles ($-40° < \alpha < 40°$). A more detailed description of this method is given later.

Another alternative to reduce calibration errors is to use a full-range velocity-angle calibration technique in conjunction with look-up tables. Such a calibration technique was first introduced by Willmarth and Bogar (1977). Johnson and Eckelmann (1984), Lueptow et al. (1988), and Browne et al. (1989) further developed and modified it. However, the generation of such tables from a full-range velocity-angle calibration, requires a significant amount of calibration time and effort. Furthermore, setting up the above tables into a corresponding data reduction and analysis program requires excessive computational overhead, particularly concerning unsteady flow measurements.

The calibration method in the present study is based on the ideal flow angle previously mentioned. A correction procedure introduced for the accurate measurement of lower velocities significantly improves the accuracy of the velocity components. The

calibration technique is applicable to X-hot-wire and hot- film probes. However, a hot-film probe performed the measurements in the present investigation.

6.2. Description of Calibration Facility

The calibration was done in a uniform low-turbulence jet issuing from an axisymmetric nozzle with an area ratio of 16. Figure 8 shows a schematic of the calibration facility. Compressed air from an air supply passes through a pressure regulator, filter, and a flow control valve and enters a settling chamber and pipe consisting of three segments with a 150-mm diameter. The nozzle, with an outlet diameter of 38.1-mm, is attached to the exit of the pipe. Figure 9 shows a cross sectional view of the nozzle. The nozzle is made from aluminum block machined in an n.c. machine. The inside contour of the nozzle is given by a third-order polynomial with the inlet and exit of the contour parallel to the axis of the nozzle. The inside of the nozzle is finished smooth by polishing. Screens located between flanges of pipe sections reduce the turbulence level, which is about 0.35% at the measuring location (0.4 diameter from the exit plane of the nozzle and within the potential core of the jet). A high precision differential pressure transducer measures the pressure drop across the nozzle and a thermocouple located upstream of the nozzle measures the air temperature. Calibration measurements were done with a X-hot-film probe connected to the two channels of a TSI IFA100 constant temperature anemometer system. The diameter of the platinum X-hot-film sensor (TSI 1241-XX-10) is 25-µm with the two sensors separated by a distance of approximately 1-mm. The hot-film sensors are made of fine quartz rods with platinum film on the outer surface. Plating on the ends of the rod isolate the active sensing length and provide a contact material for mounting the sensors to support needles. The active sensing length of the film sensor is 0.5-mm. The sensors were operated at an overheat ratio of 1.5. The analog signals from the pressure transducer, thermocouple, and hot-film anemometer were transferred to the input channels of an A/D board plugged into the expansion slot of a personal computer, which is used for data acquisition and analysis. The data acquisition program XCAL.FOR is
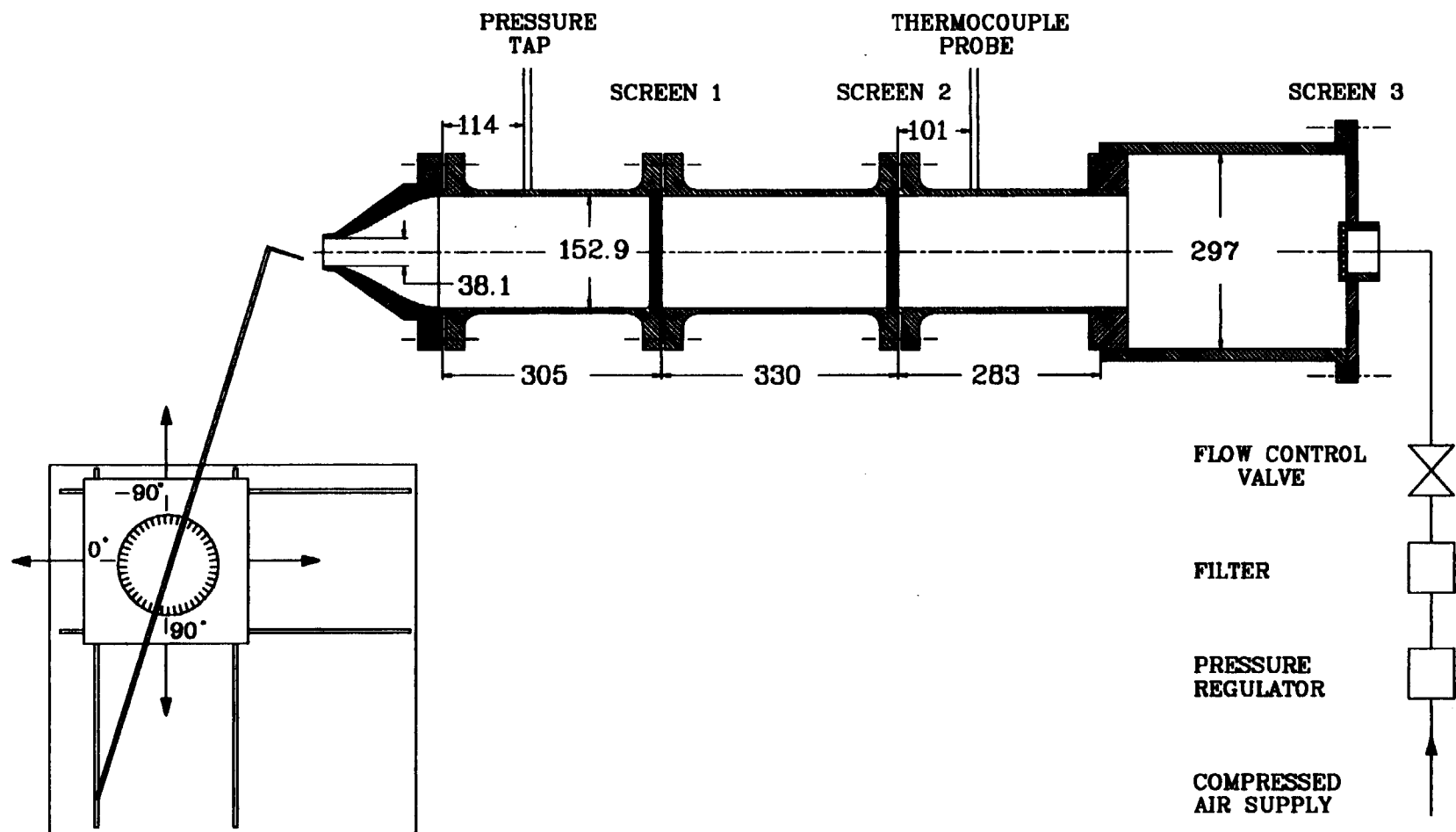
Fig. 8 Calibration set-up for hot-film calibration
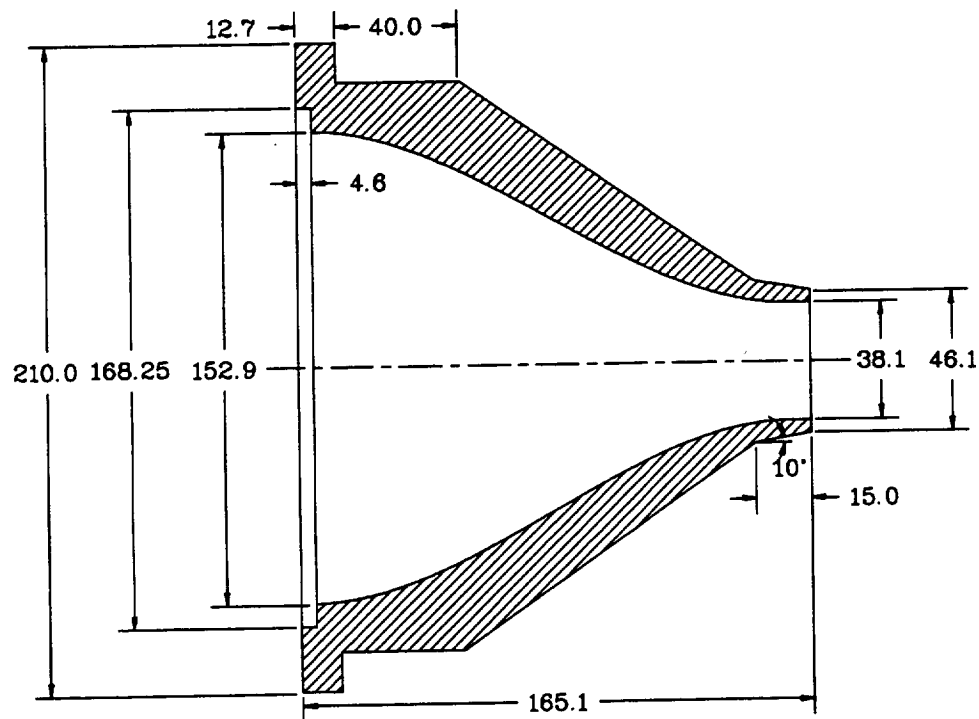
Fig. 9 Section of the nozzle used for calibrating hot-film probes

used for calibrating the X-probes.

Figure 10 shows the probe geometry, the flow velocity C, and direction α, as well as the components V_x and V_y. Each sensor of the X-hot-film probe under investigation had an angle $\alpha_s = 45°$ to the X-axis. The components of velocity C along and perpendicular to the probe axis are V_x and V_y, respectively.

6.3. Description of Calibration Technique

This section gives a brief description of the calibration technique for a single freestream velocity (John and Schobeiri, 1993). It is followed by a description of the calibration procedure, a discussion on calibration uncertainty, and the yaw angle correction at different velocities.
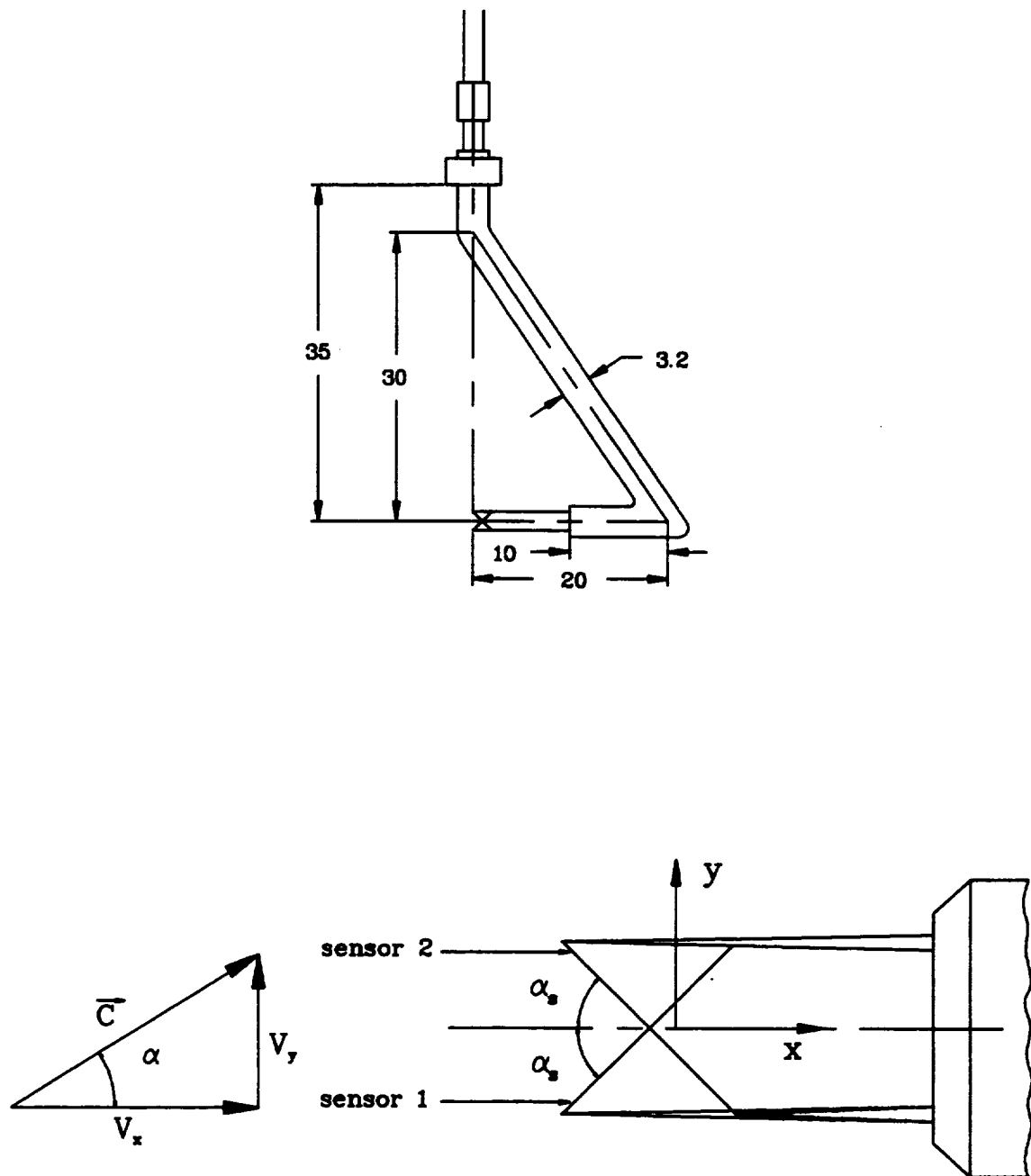
Fig. 10 Probe geometry and flow coordinates of the X-hot-film probe

6.3.1. Calibration at Single Freestream Velocity, Equations

The effective cooling velocity V_{ej} is approximated as a fourth-order polynomial function of the anemometer output voltage E_j.

$$V_{ej} = a_{0j} + a_{1j}E_j + a_{2j}E_j^2 + a_{3j}E_j^3 + a_{4j}E_j^4$$ (6.3)

where the coefficients a_{ij} are obtained by a least-squares fit. The angle response equations for sensor 1 and 2 are derived from Eq. (6.1).

$$V_{e1}^2 = C^2[\sin^2(\alpha_s + \alpha) + k_1^2\cos^2(\alpha_s + \alpha)]$$ (6.4)

$$V_{e2}^2 = C^2[\sin^2(\alpha_s - \alpha) + k_2^2\cos^2(\alpha_s - \alpha)]$$ (6.5)

V_{e1} and V_{e2} are the effective cooling velocities and k_1 and k_2 are the yaw coefficients for sensor 1 and 2. As previously mentioned, Schröder (1985) defined an ideal angle α_{id} for which k_j is equal to zero. Applying this definition to Eqs. (6.4) and (6.5) leads to

$$\alpha_{id} = \tan^{-1}\left(\frac{V_{e1} - V_{e2}}{V_{e1} + V_{e2}}\tan\alpha_s\right)$$ (6.6)

For probes with $\alpha_s = 45°$, Eq. (6.6) can be written as:

$$\alpha_{id} = \tan^{-1}\left(\frac{V_{e1}}{V_{e2}}\right) - 45$$ (6.7)

Schröder also introduced a nondimensional parameter H that relates the effective cooling velocities to the actual velocity. It is defined by:

$$H = \frac{C^2}{V_{e1}^2 + V_{e2}^2}$$ (6.8)

The yaw angle calibration finds the values of α_{id} and H for various α. H and α are represented by a fifth-order polynomial function of α_{id} by a least-squares fit, i.e.,

$$H = b_0 + b_1\alpha_{id} + b_2\alpha_{id}^2 + b_3\alpha_{id}^3 + b_4\alpha_{id}^4 + b_5\alpha_{id}^5 \tag{6.9}$$

$$\alpha = c_0 + c_1\alpha_{id} + c_2\alpha_{id}^2 + c_3\alpha_{id}^3 + c_4\alpha_{id}^4 + c_5\alpha_{id}^5 \tag{6.10}$$

To increase the curve fit accuracy, a new function H^* defined by

$$H^* = \frac{C\cos\alpha}{\sqrt{V_{e1}^2 + V_{e2}^2}} \tag{6.11}$$

is introduced. Similar to H, the new function H^* is also represented by a fifth order polynomial function of α_{id}, i.e.,

$$H^* = d_0 + d_1\alpha_{id} + d_2\alpha_{id}^2 + d_3\alpha_{id}^3 + d_4\alpha_{id}^4 + d_5\alpha_{id}^5 \tag{6.12}$$

Figure 11 shows the variation of α with α_{id}. The values of H and H^* are plotted against α_{id} in Fig. 12. The solid lines in Figs. 11 and 12 show the fifth-order polynomial curve fit. As seen in Fig. 12, the function H^* gave lower scatter of data points compared to the function H. Figure 11 shows that the differences between α_{id} and α are very high at higher absolute values of α.

6.3.2. Calibration Procedure

The velocity calibration to obtain the coefficients of Eq. (6.3) for each sensor is done by keeping the sensors normal to the flow and varying the velocity C. When the sensor is normal to the flow, the effective cooling velocity V_{ej} equals the flow velocity C. Measurements are taken for about 30 velocities in the selected velocity range. The velocity C, obtained from the pressure drop across the nozzle, is approximated (isentropic flow assumption) by $C = (2\Delta P/\rho)^{1/2} (1-(d_2/d_1)^4)^{-1/2}$ where ΔP is the pressure
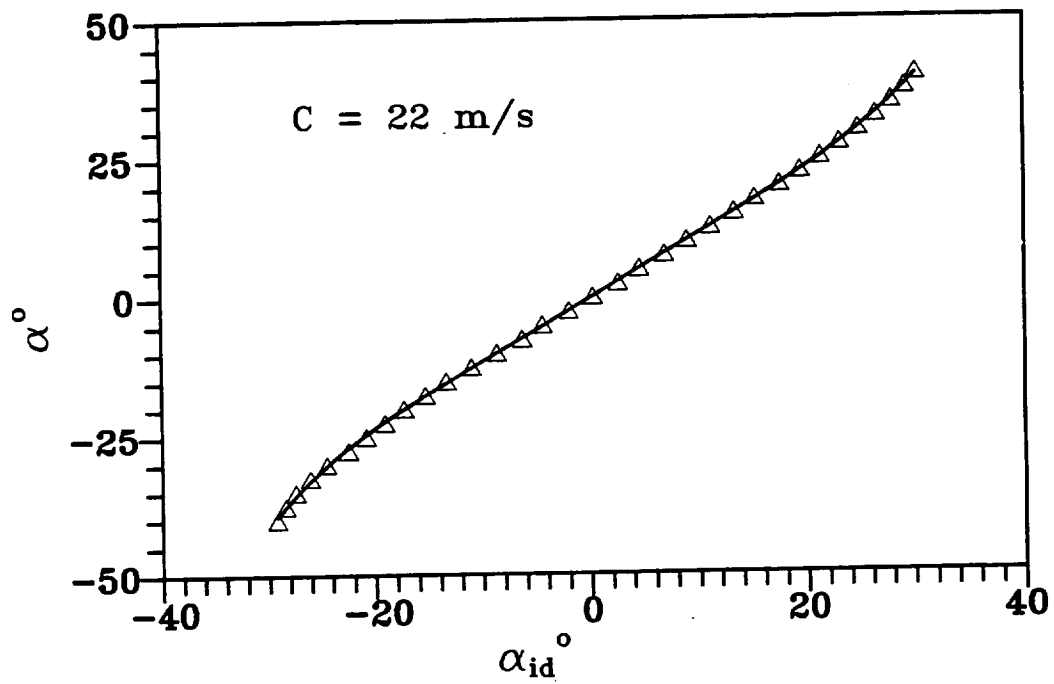
Fig. 11 Variation of α with α_{id} obtained from yaw calibration at 22 m/s
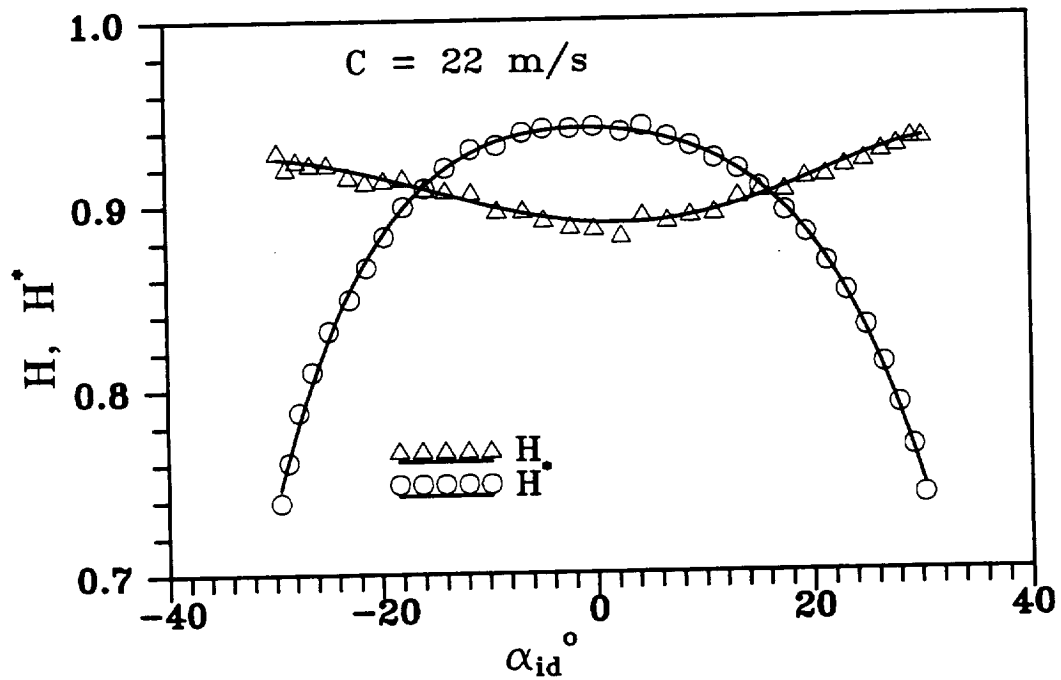
Fig. 12 Variation of H and H^* with α_{id} obtained from yaw calibration at 22 m/s

drop across the nozzle, ρ is the density of the fluid, and d_2/d_1 is the diameter ratio of the nozzle exit to the nozzle inlet. The above equation is arrived at by applying continuity and Bernoulli's equations for incompressible flow through the nozzle. The velocity, obtained from the pressure drop across the nozzle and using a pitot probe at a location 0.3 to 0.5 diameters from the exit plane of the nozzle and inside the potential core of the jet, showed close agreement.

The yaw angle calibration is carried out for α from $-40°$ to $40°$ at every $2.5°$ interval keeping the velocity C constant. The function α_{id} and H^* are calculated from Eqs. (6.7) and (6.11). The coefficients c_i in Eq. (6.10) and d_i in Eq. (6.12) are found by a least-squares fit of α_{id} against α and H^*, respectively. The values of α_{id} and H^* are found to have good reproducibility. As compared to α_{id} and H^*, the coefficients of velocity calibration in Eq. (6.3) can drift and so frequent calibration is essential. It is always preferable to do the calibration in the test section where actual measurements are carried out. Often the specific geometry of the test section and the probes, as in the present study, makes it impossible to yaw the probe to the extent to make the sensors normal to flow. However, the velocity calibration can be done simultaneously for both sensors at any angle α, provided c_i and d_i are already found from yaw angle calibration and the velocity C is known and can be varied. For a known angle α, α_{id} is obtained from Eq. (6.10) using the Newton-Raphson method. The corresponding value of H^* is determined using Eq. (6.12). The effective cooling velocities are obtained from the following relations derived from Eqs. (6.7) and (6.11).

$$V_{e1} = \frac{C \cos\alpha \ \tan(\alpha_{id}+45)}{H^* \sqrt{1+\tan^2(\alpha_{id}+45)}} \qquad (6.13)$$

$$V_{e2} = \frac{C \cos\alpha}{H^* \sqrt{1+\tan^2(\alpha_{id}+45)}} \qquad (6.14)$$

Figure 13 shows velocity calibrations with $\alpha = -45°$, $0°$, and $+45°$. The flow velocity C is normal to sensors 1 and 2 when α is $+45°$ and $-45°$, respectively. The two

calibration curves for each sensor are almost identical, which proves the validity of the above-mentioned calibration procedure.

Three separate programs generate the calibration coefficients from the raw digitized data obtained by executing the program XCAL.FOR. The program XCALP.FOR generates the coefficients in Eq. (6.3) from the raw data obtained by the velocity calibration keeping the sensor normal to the flow velocity. XCALF.FOR obtains the yaw calibration coefficients in Eqs. (6.10) and (6.12). The program VEFF.FOR generates the coefficients in Eq. (6.3) from the raw data obtained by the velocity calibration when the sensors are not normal to the flow. The above-mentioned programs are in Appendix B.

6.3.3 Calibration Uncertainty

The calibration uncertainties of the various quantities are estimated according to the method suggested by Yavuzkurt (1984) and is based on the uncertainty analysis by Moffat (1982). Table 3 shows the uncertainties for four different velocities. The main contribution to the uncertainty comes from the differential pressure transducer which has an uncertainty of $\pm$ 0.6 Pa. However, significantly lower uncertainties can be achieved by using transducers or manometers with lower uncertainties.

6.3.4. Yaw Calibration at Different Velocities and Yaw Angle Correction

A yaw angle calibration is carried out at different velocities to investigate the effect of velocity on the yaw response. The results are plotted in Fig. 14. Note that the value of α_{id} varies with α and velocity C. For a given α, the variation of α_{id} increases with decreasing velocity. The above variation is also higher at a higher absolute value of α. This can be explained in terms of the k-factors of each sensor. A preliminary investigation showed that for a given α, the k remains almost constant for velocities above 17 m/s and for $-20^\circ < \alpha < +20^\circ$. Lekakis et al. (1989) found that k is constant for flow velocities higher than approximately 15 - 20 m/s. The relation between α_{id} and
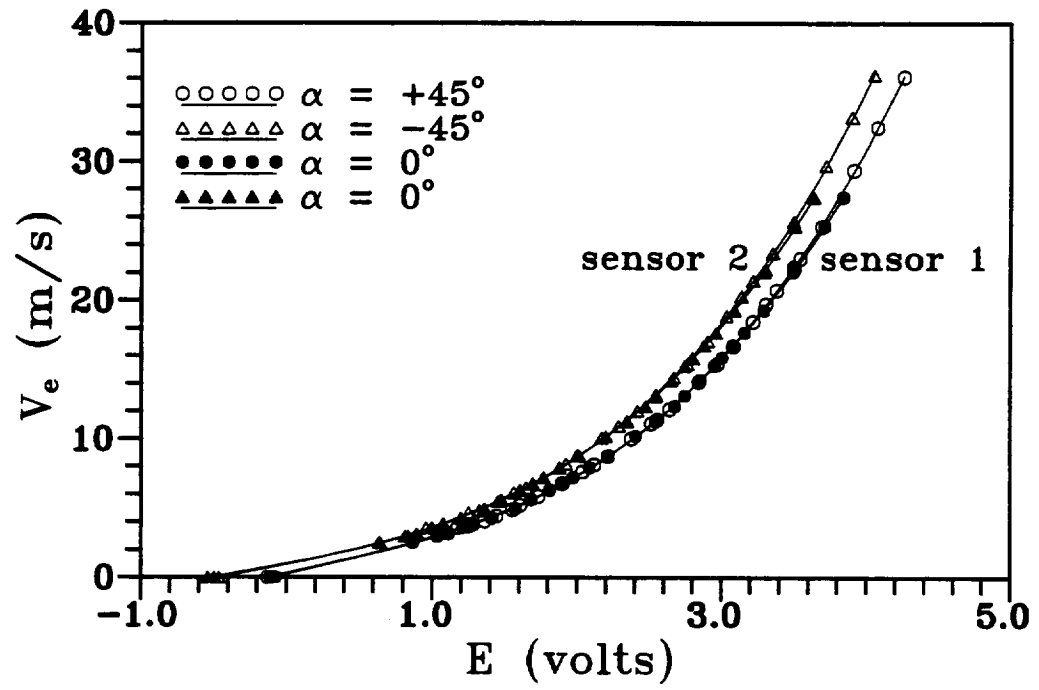
Fig. 13 Effective velocities of sensors 1 and 2
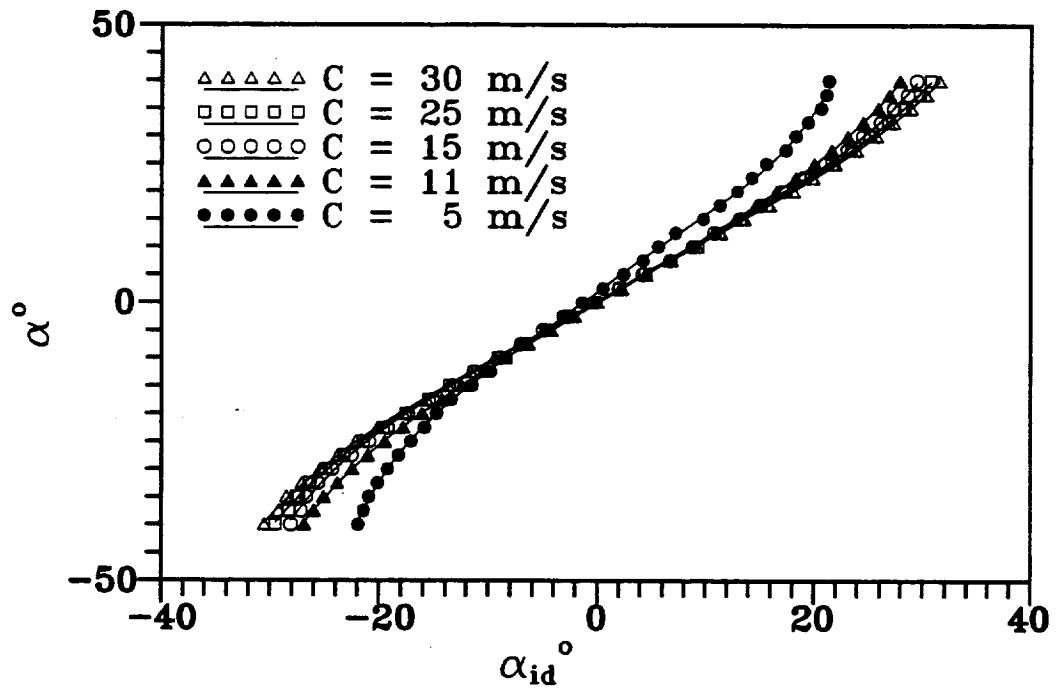
Fig. 14 Distribution of α_{id} Vs α for different velocities

Table 3 Calibration uncertainties

C m/s	$\Delta C/C$ %	$\Delta V_e/V_e$ %	$\Delta\alpha_{id}/\alpha_{id}$ %	$\Delta H^r/H^r$ %
5	2.00	2.30	3.30	2.95
10	0.50	1.30	1.80	1.28
20	0.10	1.22	1.71	1.09
30	0.06	1.20	1.70	1.07

k_1 and k_2 can be obtained from Eqs. (6.4), (6.5) and (6.7), i.e.,

$$\tan(\alpha_{id}+45) = \sqrt{\frac{\sin^2(45+\alpha)+k_1^2\cos^2(45+\alpha)}{\sin^2(45-\alpha)+k_2^2\cos^2(45-\alpha)}} \qquad (6.15)$$

Since k_1 and k_2 are functions of C and α, the left-hand side of Eq. (6.15) depends on C for a particular α. Based on the assumption of a power law relationship between Eq. (6.15) and C, Eq. (6.16) can be derived to compensate for the deviation of α_{id}. When using the result of yaw angle calibration at a velocity above 20 m/s to any other velocity below 15 m/s, α_{id} was corrected using the following relation.

$$\frac{\tan(\alpha_{id_{Ref}}+45)}{\tan(\alpha_{id}+45)} = \left(\frac{C_{Ref}}{C}\right)^m \qquad (6.16)$$

The subscript Ref denotes the quantities at the reference velocity at which the yaw angle calibration is carried out. The power m is a function of α and can be least-square-fitted by a third-order polynomial as shown in Fig. 15. i.e.,

$$m = e_0 + e_1\alpha + e_2\alpha^2 + e_3\alpha^3 \tag{6.17}$$

Figure 15 was arrived at using a reference velocity yaw angle calibration at 22 m/s and two other calibrations at 5 m/s and 10 m/s.

6.4. Reduction Method

This section briefly describes the steps to calculate the velocity components from the voltage outputs of the two sensors obtained during an actual measurement. The first step is to compensate the anemometer output voltage E_{mj} of each sensor for the change in fluid temperature. An equation for temperature compensation is obtained from the modified form of King's law, $E_b^2 = (A + B*C^n)(T_s - T_a)$. As shown by Lekakis (1988), the temperature dependency of the constants A and B can be neglected for a hot-film sensor of 25 μm diameter at velocities above 1 m/s. This leads to a temperature compensation formula given by

$$E_j = E_{mj}\sqrt{\frac{T_s - T_a}{T_s - T_c}} \tag{6.18}$$

where T_s, T_c, and T_a are the sensor operating temperature, calibration temperature, and the temperature of fluid during actual measurement, respectively. As a second step, the instantaneous effective velocities V_{e1} and V_{e2} are calculated from instantaneous temperature-compensated voltages using Eq. (6.3). The instantaneous value of α_{id} is obtained from V_{e1} and V_{e2} using Eq. (6.7) while α and H' are calculated using Eqs. (6.10) and (6.12). The magnitude of instantaneous velocity C is determined using Eq. (6.11). Its components V_x and V_y are calculated from its magnitude and direction α. If the velocity C is below 15 m/s, α_{id} is corrected by Eq. (6.16) using the yaw correction parameter m obtained from Eq. (6.17). From the new α_{id}, instantaneous values of α, H', and C are computed again using Eqs. (6.10), (6.12), and (6.11), respectively. The
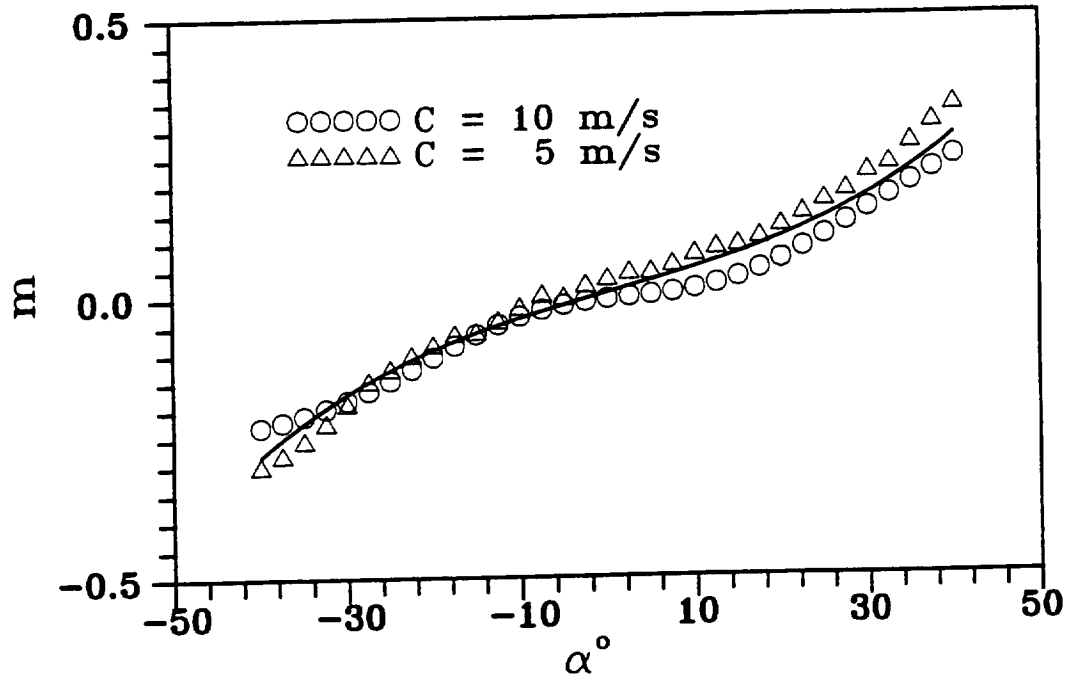
Fig. 15 Variation of yaw correction parameter _m_ with α

instantaneous velocity components V_x and V_y are calculated as before.

6.5. Correction Results, Comparison

This section compares the results of the single velocity calibration without the yaw correction to those with the yaw correction. After the calibration was complete, 50 new sets of data independent from that of calibration were taken in the same calibration jet covering a velocity range of 10 - 30 m/s and angle $-30° < α < +30°$. The actual values of C, V_x, and V_y are obtained from the measured pressure drop across the nozzle, temperature of air, and α read from the vernier of the rotary table. The absolute percentage deviation between actual and calculated C is given by

$$\varepsilon_C = \frac{|C_a - C_c|}{C_a} \times 100 \qquad (6.19)$$

where C_a and C_c are actual and calculated values of C. Similarly, percentage deviations of V_x and V_y, denoted by ε_{V_x} and ε_{V_y}, are computed. $\Delta\alpha$ denotes the absolute difference between actual and calculated α.

Table 4 shows the maximum deviations of C, V_x, V_y and α when the yaw angle calibration at 22 m/s is used. These deviations were expected from the results plotted in Fig. 14. At the velocity of 10 m/s, $\Delta\alpha_{max}$ is higher compared to deviations pertaining to the velocity range of 20 - 30 m/s. The above high angle deviations result in significant error for velocity, particularly for the y-direction component. Table 5 gives the results for the velocity 10 m/s when the yaw correction is applied. The error decreases significantly and the deviations are of the same order as those in the 20 - 30 m/s range. The calibration method presented here is faster, easier to implement, and requires fewer steps when compared to full velocity yaw angle calibration methods.

Table 4 Maximum deviation between actual and calculated values of velocities and angle for the case without yaw angle correction

Angle α o	Velocity C m/s	ε_{Cmax} %	$\varepsilon_{Vx,max}$ %	$\varepsilon_{Vy,max}$ %	$\Delta\alpha_{max}$ o
-20 - +20	20 - 30	1.3	1.2	3.0	.5
±20 - ±30	20 - 30	2.0	2.7	3.8	.9
-20 - +20	10	1.3	1.5	8.0	1.9
±20 - ±30	10	1.1	3.9	10.0	3.5

Table 5 **Maximum deviation between actual and calculated values of velocities**
and angle for the case with yaw angle correction

Angle α o	Velocity C m/s	ε_{Cmax} %	$\varepsilon_{Vx,max}$ %	$\varepsilon_{Vy,max}$ %	$\Delta\alpha_{max}$ o
-20 - +20	10	1.25	1.27	3.0	.74
±20 - ±30	10	1.0	1.7	3.6	1.1

6.6. Calibration of Single Sensor Hot-film Probes

All the preliminary and spectral measurements are performed with single sensor hot-film probes. The calibration of the single sensor hot-film probe is accomplished by keeping the hot-film sensor normal to the flow velocity and taking about 20-30 readings of (E, C) in the selected velocity range. A fourth-order polynomial function of the anemometer output voltage E accurately represents the flow velocity C. The coefficients of the polynomial are obtained by a least-squares fit. The program CTAN.FOR (Appendix B) processes the data acquired during the calibration of the single sensor probes by using the program ADRDTR.FOR (which generates the calibration coefficients and writes to the CTA.CAL file). In actual measurements, if the temperature of the flow differs from the calibration temperature, the measured anemometer voltage E_m is temperature compensated using Eq. (6.18) to obtain E.

7. DATA REDUCTION AND ANALYSIS

As previously mentioned, digital data acquisition acquired the data. The digitized data at each location, stored in individual files, are processed to obtain the mean velocity and Reynolds stress components. The velocity and Reynolds stress components obtained in probe coordinates are transformed to an appropriately chosen curvilinear coordinate system. This section presents the equations and the methods employed for data reduction and analysis.

7.1. Data Reduction for Steady Wakes

For data reduction and analysis, the characteristic response of X-film probe is stored as calibration coefficients. As explained in Section 6, the instantaneous velocity components are calculated from the temperature compensated instantaneous voltages using the calibration coefficients. The velocity components are obtained in the probe coordinates that, in the present measurements, coincide with the radial and tangential directions to the convex wall. V_x and V_y denote the instantaneous velocity components in the tangential and radial directions, respectively. The radial velocity V_y is positive if its direction is toward the convex wall. The instantaneous velocity components can be represented in the following form.

$$V_x = \bar{V}_x + v_x \quad ; \quad V_y = \bar{V}_y + v_y \tag{7.1}$$

$\bar{V}_x$ and $\bar{V}_y$ are the mean (time averaged) velocity components in the x and y directions (tangential and radial directions), respectively. The turbulent fluctuation components are denoted by v_x and v_y. The mean velocity components, also known as time average or global mean, are given by

$$\bar{V}_x = \frac{1}{N} \sum_{j=1}^{N} V_{x_j} \tag{7.2}$$

$$\bar{V}_y = \frac{1}{N} \sum_{j=1}^{N} V_{y_j} \tag{7.3}$$

where N (=32768) is the total number of samples per sensor of the X-film probe at one probe location. At the sampling rate of 2 kHz, used in the investigation of steady wakes, 32768 samples per sensor provided good convergence for the mean velocities and Reynolds stresses. The mean square values of the components of turbulent velocity fluctuations are obtained from the instantaneous and mean velocities as

$$\overline{v_x^2} = \frac{1}{N} \sum_{j=1}^{N} (V_{x_j} - \bar{V}_x)^2 \tag{7.4}$$

$$\overline{v_y^2} = \frac{1}{N} \sum_{j=1}^{N} (V_{y_j} - \bar{V}_y)^2 \tag{7.5}$$

and the percentage turbulence intensity is

$$T_u = \frac{\sqrt{\overline{v_x^2}}}{\bar{V}_x} \times 100 = \frac{1}{\bar{V}_x} \sqrt{\frac{1}{N} \sum_{j=1}^{N} (V_{x_j} - \bar{V}_x)^2} \times 100 \tag{7.6}$$

The Reynolds shear stress is calculated by

$$\overline{v_x v_y} = \frac{1}{N} \sum_{j=1}^{N} (V_{x_j} - \bar{V}_x)(V_{y_j} - \bar{V}_y) \tag{7.7}$$

The program BXPRO.FOR reduces the digitized data and calculates the mean velocity and turbulent stress components in the probe coordinates.

7.2. Data Analysis for Steady Wakes

The measurements made in the probe coordinates (x,y) shown in Fig. 16 give the tangential velocity component $\bar{V}_x$ and the radial velocity component $\bar{V}_y$. To compare with the plane wake data, the results must be represented in a curvilinear coordinate system $(\xi_1\text{-}\xi_2)$, where ξ_1 is the direction along a streamline near the center of wake and ξ_2 the direction normal to it. The maximum inclination between these two orthogonal coordinate systems was less than $7.5°$. Therefore, the distance taken radially from the wake center to a measuring point was approximated as ξ_2 and for all the measuring points at an angular position θ, the ξ_1 coordinate was assumed constant. The errors due to this approximation will be small considering that for most streamwise locations the inclination between the two coordinate systems was less than $4°$.

Equations (7.10)-(7.14) give the equations for transforming the time averaged velocity and turbulent stresses calculated in the (x,y)-coordinate to the curvilinear coordinate system $(\xi_1\text{-}\xi_2)$. The instantaneous velocity components in $(\xi_1\text{-}\xi_2)$ can represent the instantaneous velocity components in the (x,y)-coordinates, i.e.,

$$U = V_x\cos\vartheta + V_y\sin\vartheta \qquad (7.8)$$

$$V = V_y\cos\vartheta - V_x\sin\vartheta \qquad (7.9)$$

where ϑ is the angle between the ξ_1 and x-direction, and U and V are the velocities in the ξ_1 and ξ_2 directions, respectively. Also, the mean velocity components in the $(\xi_1\text{-}\xi_2)$-coordinates are obtained from the mean velocities in the (x,y)-coordinates by:

$$\bar{U} = \bar{V}_x\cos\vartheta + \bar{V}_y\sin\vartheta \qquad (7.10)$$

$$\bar{V} = \bar{V}_y\cos\vartheta - \bar{V}_x\sin\vartheta \qquad (7.11)$$

where $\bar{U}$ and $\bar{V}$ are the mean velocities in the ξ_1 and ξ_2 directions, respectively. Subtracting the mean velocity value from the instantaneous one gives the fluctuating
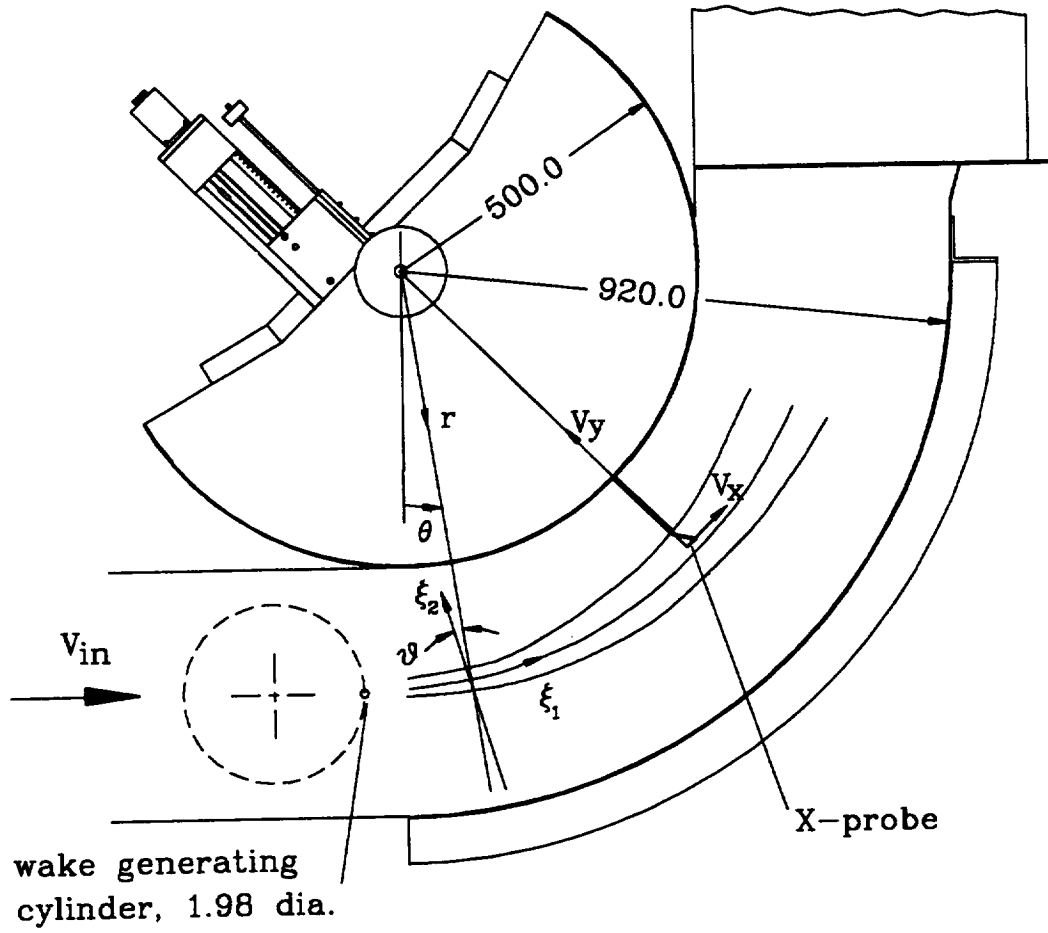
Fig. 16 Representation of probe coordinate and curvilinear coordinate systems

velocity ($u = U - \bar{U}$, $v_x = V_x - \bar{V}_x$, etc.). The mean Reynolds stress components in the $(\xi_1 - \xi_2)$-coordinates are obtained by time-averaging the product of the fluctuating velocities and are given by:

$$\overline{u^2} = \overline{v_x^2}\cos^2\vartheta + \overline{v_y^2}\sin^2\vartheta + \overline{v_x v_y}\sin2\vartheta \qquad (7.12)$$

$$\overline{v^2} = \overline{v_x^2}\sin^2\vartheta + \overline{v_y^2}\cos^2\vartheta - \overline{v_x v_y}\sin2\vartheta \qquad (7.13)$$

$$\overline{uv} = (\overline{v_x^2} - \overline{v_y^2})\frac{sin2\vartheta}{2} + \overline{v_x v_y}cos2\vartheta \qquad (7.14)$$

The procedure for finding the mean velocity defect $\overline{U_1}$, the location of maximum wake velocity defect, and the edges of the wake are illustrated with the measurements at a 35° angular position for the zero pressure gradient case. A hypothetical potential velocity distribution for $\overline{V_{xp}}$ is found in the wake by fitting the mean velocity $\overline{V_x}$ in the region outside the wake with a suitable curve on both sides. The example in Fig. 17 shows that the outside region of the wake for finding the hypothetical potential velocity distribution was chosen between $110 < r-r_i < 150$-mm on the convex wall side and between $235 < r-r_i < 285$-mm on the concave wall side. A least-squares fit by a third degree polynomial was employed to find the potential velocity distribution. Nakayama (1987) used a straight line fit to find the potential velocity distribution in the study of wake subjected to mild curvature. For the present case, a straight line fit through the mean velocity data outside the wake was inaccurate for determining the potential velocity in the wake for all streamwise locations. In general, a least-squares fit by a third degree polynomial accurately represents the potential velocity distribution. A comparison of the above potential velocity distribution against the velocity distribution obtained by measurements at selected streamwise locations without the wake generating rod, also supported the choice of third degree polynomial. This is clearly displayed in Fig. 18, where the $\overline{V_x}$ data without the wake generation is plotted along with the wake velocity data at an angular position of 35°. Curves 3 and 4 in Fig. 18 represent the hypothetical potential velocity distribution plotted by fitting the outside wake velocity data obtained with the wake generating cylinder by first and third degree polynomials, respectively. As seen, the hypothetical potential velocity distribution obtained by a third degree polynomial fit agrees with the velocity distribution obtained without the wake generating cylinder. Also, the potential velocity obtained without the wake generating cylinder agrees with free vortex distribution $r\overline{V_x}$ = constant.

The wake velocity data and hypothetical potential velocity distribution determine
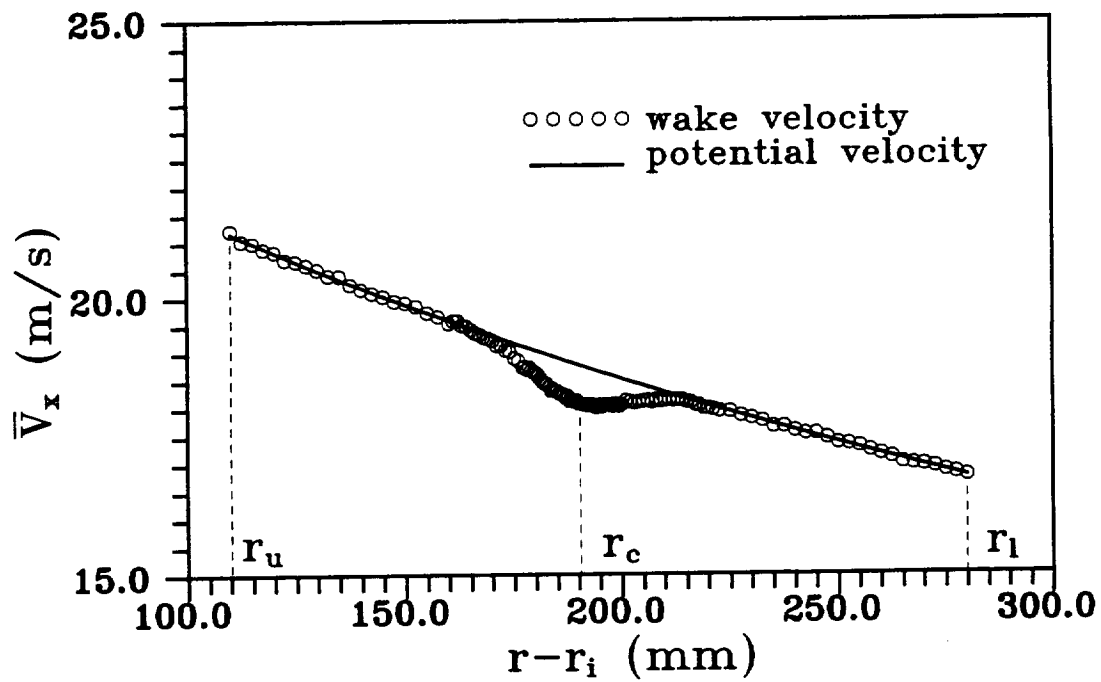
Fig. 17 Mean velocity profile at an angular position of 35°
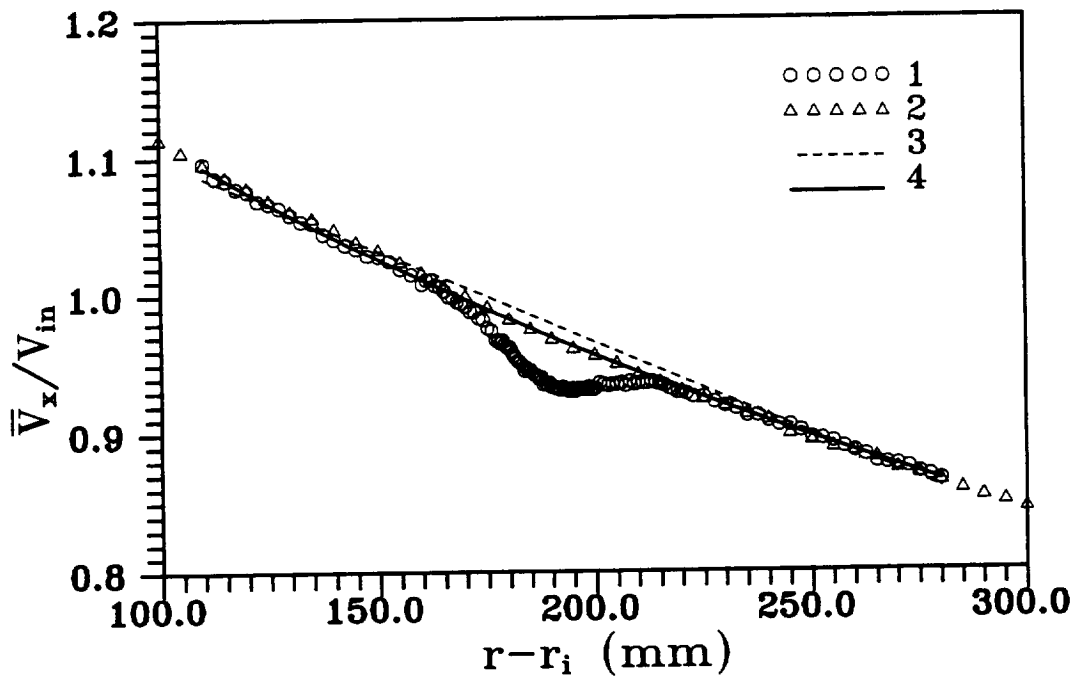
Fig. 18 Nondimensional velocity profile at an angular position of 35°. (1-wake velocity; 2-velocity without wake; 3-potential velocity using linear fit; 4-potential velocity using third degree polynomial)

the velocity defect distribution. To accurately obtain the location of the maximum velocity defect, a smoothed cubic spline function is used to fit the tangential component of the velocity defect $\bar{V}_{xl}$ ($\bar{V}_{xl} = \bar{V}_{xp} - \bar{V}_x$). The wake edges were determined by an integral method developed by the principal investigator and was similar to the one used by Schobeiri et al. (1992) in the investigation of boundary layers on convex and concave walls. The method involves numerical integration of defect velocity and potential velocity profiles. Refer to Fig. 17 for an explanation of the method. The tangential component of wake velocity $\bar{V}_x$ is curve fitted by a cubic spline function with no smoothing. The area under the hypothetical potential velocity distribution between a starting point r_l on one side of the wake and the location of the maximum velocity defect r_c was found by numerical integration. The area under the tangential component of wake velocity was subtracted from the above area to find the area under the wake velocity defect (denoted by A). The numerical integration continued by incrementing the starting point in small steps, going toward the center of the wake, and calculating the area A_i under the velocity defect profile between the new starting point and the point of the maximum wake velocity defect. The wake edge is located when the percentage deviation between A and A_i exceeds a specified value from 0.5% to 1%. The other wake edge is located by repeating the steps using r_l as the starting point and moving toward the center of the wake. The wake edge locations are sensitive to the initial selection of the potential region used to find the hypothetical potential velocity distribution. However, the integral parameters, momentum thickness and wake width (defined later) are much less sensitive to the wake edge locations, especially if the wake edge locations are in the potential flow region. The tangential component r.m.s velocity distribution, which was found to be less sensitive to the choice of potential flow region, provides an alternative to the mean velocity distribution for finding the wake edges. The r.m.s velocity distribution used the integral method applied for the mean velocity distribution to find the wake edges. The hypothetical potential distribution of the r.m.s velocity in the wake was found by a linear fit of the r.m.s velocity data outside the wake region. Determination of the wake edges from r.m.s velocity provides advantage

for far wakes where the velocity defect can be very small. When the values of momentum thickness obtained by using the wake edges from the mean velocity and r.m.s velocity distribution differed more than 1.5%, the initial choice for the potential flow region for finding the hypothetical potential velocity distribution was changed. The procedure was repeated until the deviation was within 1.5%.

As mentioned before, the velocity components in the probe coordinates (x,y) must be transformed to the curvilinear coordinate system (ξ_1,ξ_2). To find the angle ϑ, required for the above transformation, the location of the maximum velocity defect was found at every streamwise location. The location of the maximum velocity defect will also be called as the wake center. Curve fitting the locations of maximum wake defect by a least-squares fit determined the trajectory of the path of the wake center. The angle ϑ between the wake centerline and probe in the x direction was found at each measuring station along the wake centerline. The angle ϑ calculated in this manner varied with the type of curve fit used for the path of the wake centerline. The angle ϑ closely agreed with the velocity vector angle α ($\alpha = \tan^{-1}(\bar{V}_y/\bar{V}_x)$) for most streamwise locations at the location of maximum wake velocity defect. At the streamwise locations where ϑ was different from α, the difference was less than $1°$. It was possible to get close agreement between α and ϑ even in these locations, if the degree of the polynomial curve fit for the wake center path differed from the one used for other locations. Considering the uncertainty in locating the wake center and calculating the velocity components using the X-film probe, it can be assumed that the flow angle α at the wake center is equal to ϑ. In other words, the velocity vector is tangent to the wake centerline at the location of maximum velocity defect. Therefore, the wake centerline is a streamline with $\xi_2 = 0$ in the curvilinear coordinate system.

The components of mean velocity and Reynolds stresses in curvilinear coordinate system are calculated from Eqs. (7.10)-(7.14). The velocity defect distribution, maximum value of velocity defect, and location of the maximum velocity defect are calculated for the streamwise component $\bar{U}$. Figure 19 shows the schematic diagram of the velocity defect distribution for the streamwise velocity. The velocity defect

component in the streamwise direction $\bar{U}_1$, defined as $\bar{U}_1 = \bar{U}_p - \bar{U}$, is calculated in a manner identical to the determination of the tangential velocity defect component. Here, $\bar{U}_p$ represents the hypothetical potential velocity distribution obtained by curve fitting $\bar{U}$ velocity outside the wake. The location of the maximum velocity defect obtained from $\bar{U}$ was almost the same as the one obtained from $\bar{V}_x$.

The maximum velocity defect $\bar{U}_{1m}$ is used as the velocity scale to nondimensionalize the mean velocity defect, normal velocity $\bar{V}$, and Reynolds shear stress. Many researchers have used $(U_\infty (d/(x - x_o))^{-0.5})$ as the velocity scale for plane turbulent wakes at zero pressure gradient, since the maximum velocity defect decay is proportional to it in plane turbulent wakes. The notation x stands for the downstream distance from the wake generating cylinder, x_o for the virtual origin of the wake, and $\bar{U}_\infty$ for the freestream velocity. The literature reports values ranging from 40 to 100 cylinder diameters for x_o. The length scale to nondimensionalize ξ_2 is the wake width b defined by

$$ b = \frac{1}{\bar{U}_{1m}} \int_{-\infty}^{+\infty} \bar{U}_1 d\xi_2 \qquad (7.15) $$

Note that many researchers used different definitions for b. Some researchers used the width measured between the edges of the wake and the width measured at half height of the velocity defect profile. The b in this study differs from the b used by Eifler (1975) by a constant factor.

A characteristic quantity used in the study of wakes is momentum thickness δ_2. The momentum thickness, representing the momentum deficit due to the wake, is given by

$$ \delta_2 = \frac{1}{\bar{U}_{po}^2} \int_{-\infty}^{+\infty} \bar{U} (\bar{U}_p - \bar{U}) d\xi_2 \qquad (7.16) $$

The momentum thickness δ_2 should be constant for far wakes at zero pressure gradient.
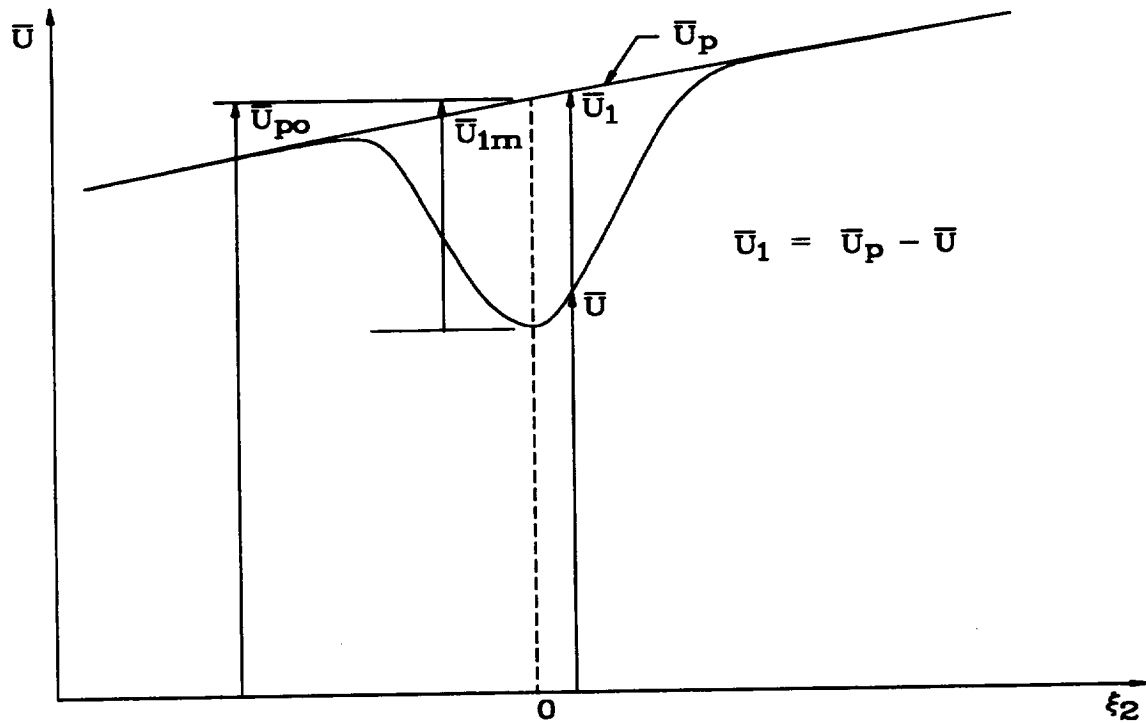
Fig. 19 Representation of streamwise component of velocity, velocity defect, and potential velocity distribution

The values of b and δ_2 were found by numerical integration.

7.3. Data Reduction and Analysis for the Unsteady Wakes

The wake quantities behind the moving cylinders of the rotating wake generator are computed by phase averaging techniques. This section presents the complete details of the data reduction and analysis used for unsteady wakes.

7.3.1. Wake Development in the Relative Rotating Frame of Reference

A stationary X-hot-film probe measured the wake development from the moving

54

cylinders. The moving wakes generated by the rotating wake generator periodically cross the stationary X-probe. The X-probe measures the velocity components in probe coordinates (x,y) and absolute (stationary) frame of reference. The wake development behind the moving cylinder must be established in a frame of reference relative to the moving cylinder. Also, the velocity components must be expressed in a curvilinear coordinate system along the wake centerline. Figure 20 shows the kinematics of the wake development in the relative flow behind the cylinder. The wake generator is rotating in a counterclockwise direction with a peripheral velocity U_t for the wake generating cylinder. The wake pattern at a certain instant is shown by the dotted line. At the same instant the wake generating cylinder makes an angle β with respect to the horizontal. The angle β is a function of time and is represented by $\beta = \beta_o + (t_o - t)\omega$. Here, ω is the angular velocity, t_o is the time when the wake center is at the probe location, and β_o is the angular position at time t_o. The X-probe located at an angular position θ measures the velocity components in the probe coordinates (x,y). The relative spatial vector $\vec{\xi}_r$ is given by

$$\vec{\xi}_r = \vec{\xi} - \vec{\chi}$$

where $\vec{\xi}$ is the absolute spatial vector and $\vec{\chi}$ $(d\vec{\chi} = \vec{U}_t dt)$ is the spatial vector along the peripheral velocity. Decomposition of $d\vec{\xi}_r$ in the x and y directions gives the components of relative spatial vector in probe coordinates, i.e.,

$$d\xi_{rx} = d\xi_x + U_t \sin(\beta - \theta) dt$$

$$d\xi_{ry} = d\xi_y - U_t \cos(\beta - \theta) dt$$

ξ_x and ξ_y are the components of absolute spatial vector in the x and y directions, respectively. The relative spatial vector components in the probe coordinates are transformed to the curvilinear coordinate system defined along and perpendicular to the trajectory of the wake centerline. The relative spatial components in the curvilinear
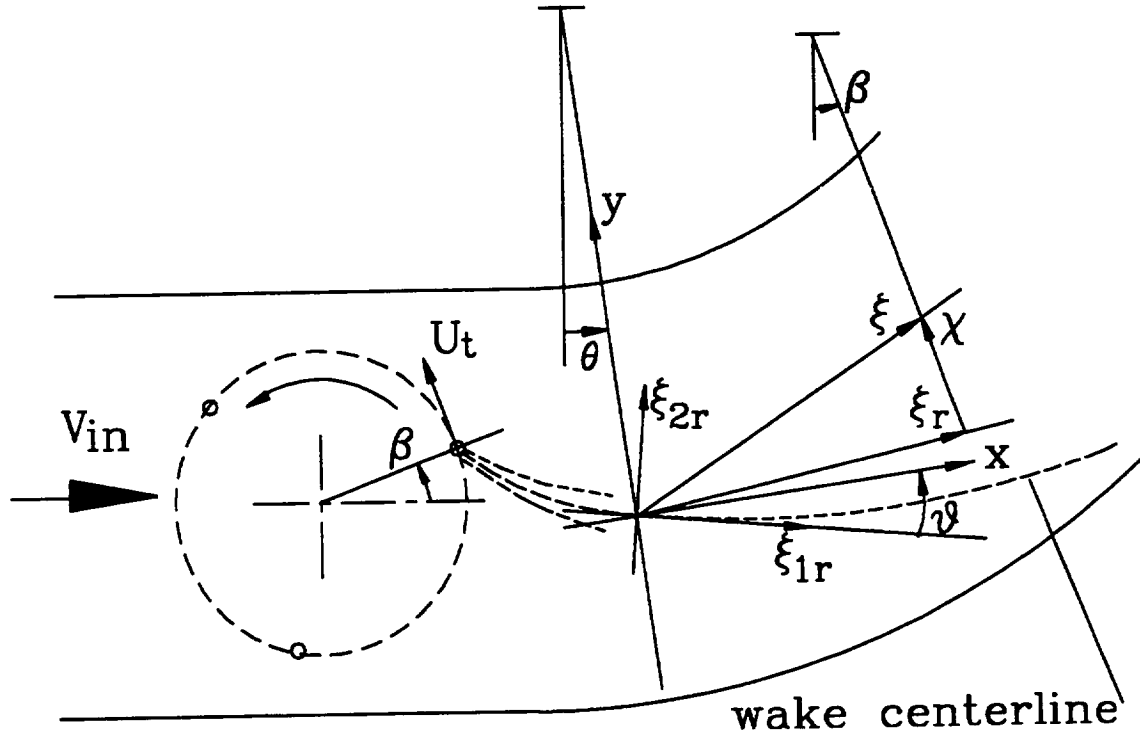
Fig. 20 Representation of curvilinear coordinate system for unsteady wakes

coordinate system are given by

$$d\xi_{1r} = d\xi_{rx}\cos\vartheta - d\xi_{ry}\sin\vartheta$$

$$d\xi_{2r} = d\xi_{ry}\cos\vartheta + d\xi_{rx}\sin\vartheta$$

where ϑ is the angle between the probe coordinate and curvilinear coordinate system. Substituting $d\xi_{rx}$ and $d\xi_{ry}$ in the above equations gives:

$$d\xi_{1r} = d\xi_{x}\cos\vartheta - d\xi_{y}\sin\vartheta + U_{t}\sin(\beta-\theta+\vartheta)dt$$

$$d\xi_{2r} = d\xi_{y}\cos\vartheta + d\xi_{x}\sin\vartheta - U_{t}\cos(\beta-\theta+\vartheta)dt$$

Dividing the above two equations by dt gives the velocity components in the curvilinear coordinate system and relative frame of reference, i.e.,

$$U_r = V_x \cos\vartheta - V_y \sin\vartheta + U_t \sin(\beta-\theta+\vartheta) \qquad (7.17)$$

$$V_r = V_y \cos\vartheta + V_x \sin\vartheta - U_t \cos(\beta-\theta+\vartheta) \qquad (7.18)$$

where V_x and V_y are the absolute velocity components in the x and y directions, respectively.

7.3.2. Data Reduction by Ensemble Averaging

As mentioned in Section 5, the data acquisition was triggered by a once-per-revolution signal from a fiber-optic proximity sensor. The data was reduced by ensemble averaging (also referred as phase averaging) method. During one revolution of the wake generator, a total of 2048 instantaneous voltage samples were taken for each channel of hot-film system. The above number was chosen to resolve the periodic wake with sufficient points. The hot-film voltages were sampled for 500 revolutions to obtain convergence for the phase averaged quantities. Since the wake generator had three rods, 500 revolutions of the wake generator produced 1500 primary periodic wakes.

An instantaneous measured quantity of the periodic wake can be considered as a combination of time averaged component, periodic component, and a random fluctuation component. Applying this definition to an arbitrary instantaneous quantity Q, it can be written as

$$Q = \bar{Q} + \tilde{Q} + q$$

where $\bar{Q}$ is the time averaged value, $\tilde{Q}$ is the periodic component, and q is the random fluctuation component. The sum of the time averaged component and the periodic component gives the ensemble average $<Q>$.

$$<Q> = \bar{Q} + \tilde{Q}$$

The ensemble average, also known as phase average or mean at constant phase, is calculated by

$$<Q_i(t_i)> = \frac{1}{N} \sum_{j=1}^{N} Q_{ij}(t_i)$$

where $i = 1,2,...m$, $t_i = (i-1)\Delta t$, m (=2048) is the number of samples of the quantity Q acquired during one revolution, Δt is the time interval between two samples where the reciprocal is equal to sampling frequency, and N (=500) is the total number of records of m samples. Figure 21 shows a typical example of instantaneous, time averaged, ensemble averaged, periodic, and random fluctuation component of tangential velocity. The curves shown are obtained from actual measurements of the periodic wakes from a stationary X-film probe. The period of wake generation T is obtained from the reciprocal of wake passing frequency. The two wakes seen in the curves represent primary and secondary wakes. The primary wakes are generated during the upward movement of cylinders and the secondary wakes are generated during the downward movement of cylinders.

The ensemble averages for V_x, V_y, U_r, and V_r are obtained by replacing Q with the corresponding velocity components. The ensemble averaged velocity components in the probe coordinate and absolute frame of reference are given by

$$<V_{x_i}(t_i)> = \frac{1}{N} \sum_{j=1}^{N} V_{x_v}(t_i) \qquad ; <V_{y_i}(t_i)> = \frac{1}{N} \sum_{j=1}^{N} V_{y_v}(t_i) \qquad (7.19)$$

and the ensemble averaged velocity components in the curvilinear coordinate system and relative frame of reference are calculated by

$$<U_{r_i}(t_i)> = \frac{1}{N} \sum_{j=1}^{N} U_{r_v}(t_i) \qquad ; <V_{r_i}(t_i)> = \frac{1}{N} \sum_{j=1}^{N} V_{r_v}(t_i) \qquad (7.20)$$

The ensemble averaged Reynolds normal stresses are obtained by ensemble averaging mean square value of the turbulent fluctuations, i.e.,
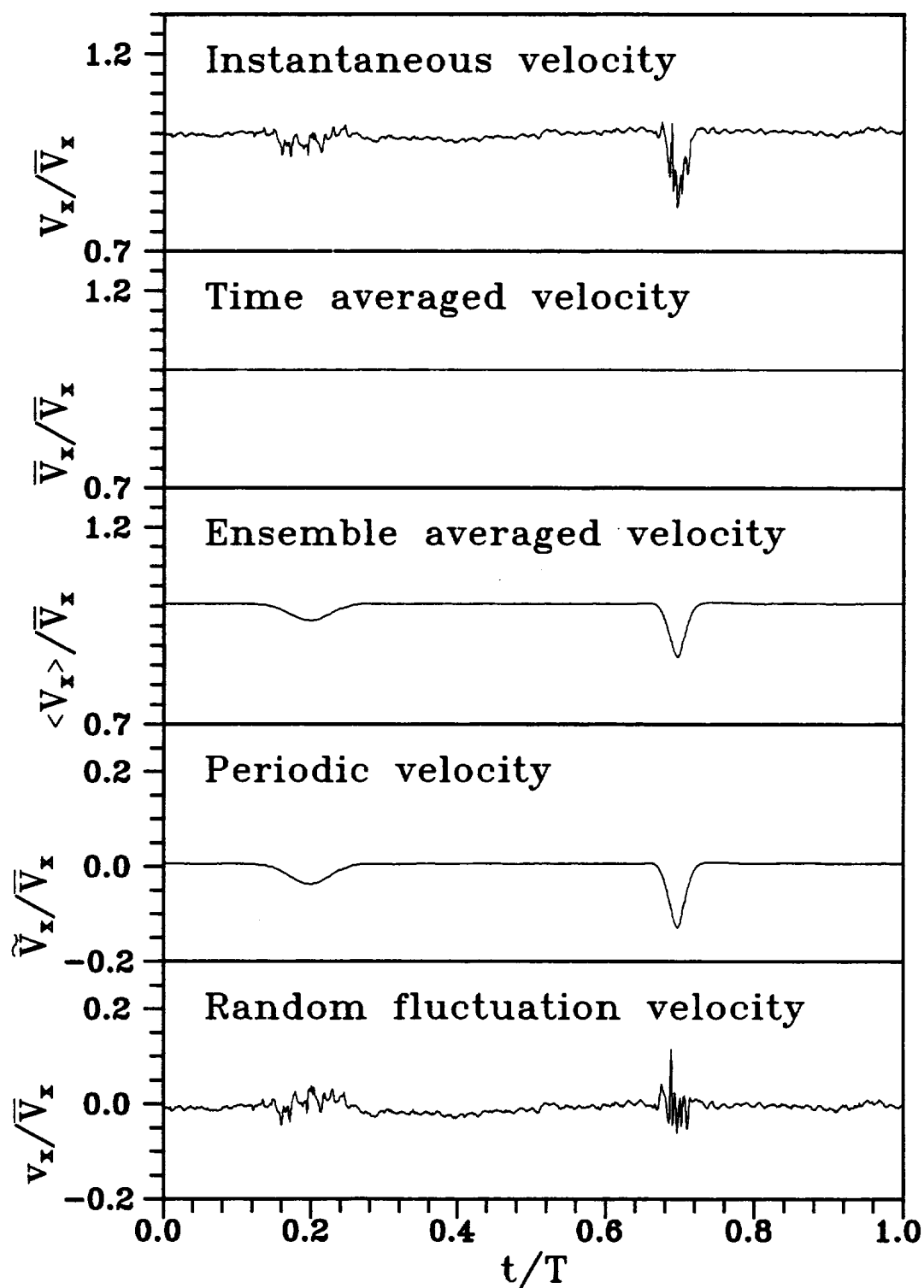
Fig. 21 Exemplary presentation of the normalized tangential component of velocity for different type of averaging

$$<v_{x_i}^2(t_i)> = \frac{1}{N} \sum_{j=1}^{N} (V_{x_{ji}}(t_i) - <V_{x_i}(t_i)>)^2 \qquad (7.21)$$

$$<v_{y_i}^2(t_i)> = \frac{1}{N} \sum_{j=1}^{N} (V_{y_{ji}}(t_i) - <V_{y_i}(t_i)>)^2 \qquad (7.22)$$

$$<u_{r_i}^2(t_i)> = \frac{1}{N} \sum_{j=1}^{N} (U_{r_{ji}}(t_i) - <U_{r_i}(t_i)>)^2 \qquad (7.23)$$

$$<v_{r_i}^2(t_i)> = \frac{1}{N} \sum_{j=1}^{N} (V_{r_{ji}}(t_i) - <V_{r_i}(t_i)>)^2 \qquad (7.24)$$

Similarly, the ensemble average of Reynolds shear stress is calculated by

$$<v_{x_i}v_{y_i}(t_i)> = \frac{1}{N} \sum_{j=1}^{N} [(V_{x_{ji}}(t_i) - <V_{x_i}(t_i)>) (V_{y_{ji}}(t_i) - <V_{y_i}(t_i)>)] \qquad (7.25)$$

$$<u_{r_i}v_{r_i}(t_i)> = \frac{1}{N} \sum_{j=1}^{N} [(U_{r_{ji}}(t_i) - <U_{r_i}(t_i)>) (V_{r_{ji}}(t_i) - <V_{r_i}(t_i)>)] \qquad (7.26)$$

The subscript r denotes the relative frame of reference.

7.3.3. Data Analysis

Data analysis for the periodic unsteady wakes involves the transformation of the velocity components in probe coordinates to the curvilinear coordinate system and relative frame of reference. This transformation was done on instantaneous velocity components using Eqs. (7.17) and (7.18). The ensemble averaged velocity and Reynolds stress components were found from Eqs. (7.19)-(7.26).

The transformation from the probe coordinates to the curvilinear coordinate system requires the angle ϑ. Accurate determination of the angle ϑ from the trajectory of wake centerline requires measurements at many locations. However, this angle can be obtained by applying the stationary wake results. For stationary wakes, it was observed that the velocity vector at the location of maximum defect was tangential to the trajectory of the wake centerline. Assuming this observation is true for unsteady wakes, the angle ϑ can be determined as the angle between the probe axis x and the mean relative velocity vector at the location of maximum velocity defect. The location of maximum velocity defect was found for the resultant relative velocity C_r

$(C_r^2 = U_r^2 + V_r^2)$. The locations of maximum velocity defect obtained from the resultant velocity C_r and streamwise velocity U_r were found to be the same. The procedure for finding the maximum velocity defect, location of maximum velocity defect, and the edges of the wake was identical to that of steady wake.

The ensemble averaged quantities in the relative frame of reference, obtained as a function of time, can be represented as a function of spatial coordinate ξ_{2r}. The spatial coordinate ξ_{2r} is calculated by assuming that the wake passes the measuring location at the same velocity as the peripheral velocity U_r. The direction of U_t is assumed constant during the interval when the wake passes the measuring location and is taken as the direction corresponding to the time t_o at which the wake center coincides with the measuring location. This leads to an expression for ξ_{2r} given by

$$\xi_{2r} = U_t(t_o - t)\cos(\beta - \theta + \vartheta) \qquad (7.27)$$

In Eq. (7.27), $U_t\cos(\beta - \theta + \vartheta)$ represents the component of U_t along the ξ_{2r}. The wake width b, similar to the case of steady wake, is obtained by numerical integration and defined by

$$b = \frac{1}{U_{1mr}}\int_{-\infty}^{+\infty} <U_{1r}> d\xi_{2r} \qquad (7.28)$$

8. PRESENTATION AND DISCUSSION OF RESULTS

This section presents the wake measurement results. All measurements were carried out for an average inlet velocity of about 20 m/s. The wake development behind a stationary cylinder at zero, positive, and negative pressure gradients are discussed first. Profiles of mean velocity and Reynolds stresses are obtained in similarity coordinates. These results are analyzed and compared with reference to the symmetrical plane turbulent wakes. Finally, the results of the wake development behind the cylinders of a rotating wake generator are discussed.

8.1. Wake Development at Zero Pressure Gradient

An X-hot-film probe measured the wake behind a 1.984-mm diameter stationary cylinder, located at mid-height of the wake generating section. The curved channel test section had an inlet to exit area ratio of 1. The wake profiles were obtained at fifteen angular positions (also called streamwise positions) from $\theta = 0°$ to $70°$ in $5°$ intervals. The first measuring station $\theta = 0°$ corresponds to the inlet of the curved test section and is at a distance of 67-mm downstream of the wake generating cylinder.

8.1.1. Path of Wake Center, Curvature of the Path of Wake Center, and Development of the Wake

The wake center, defined as the location of the maximum velocity defect, is found by the methods described in Section 7. The wake center path represents the ξ_I direction for the previously defined curvilinear coordinate system. Figure 22(a) shows the radial distance from the convex wall to the wake center, denoted by r-r_i, at various streamwise positions. Figure 22(b) shows the local curvature of the wake centerline. As the wake propagates through the channel, the trajectory of the wake center gradually moves toward the convex wall up to a streamwise location of $\xi_1/d = 240$, and from there onward it moves away from the convex wall. The maximum inclination between the
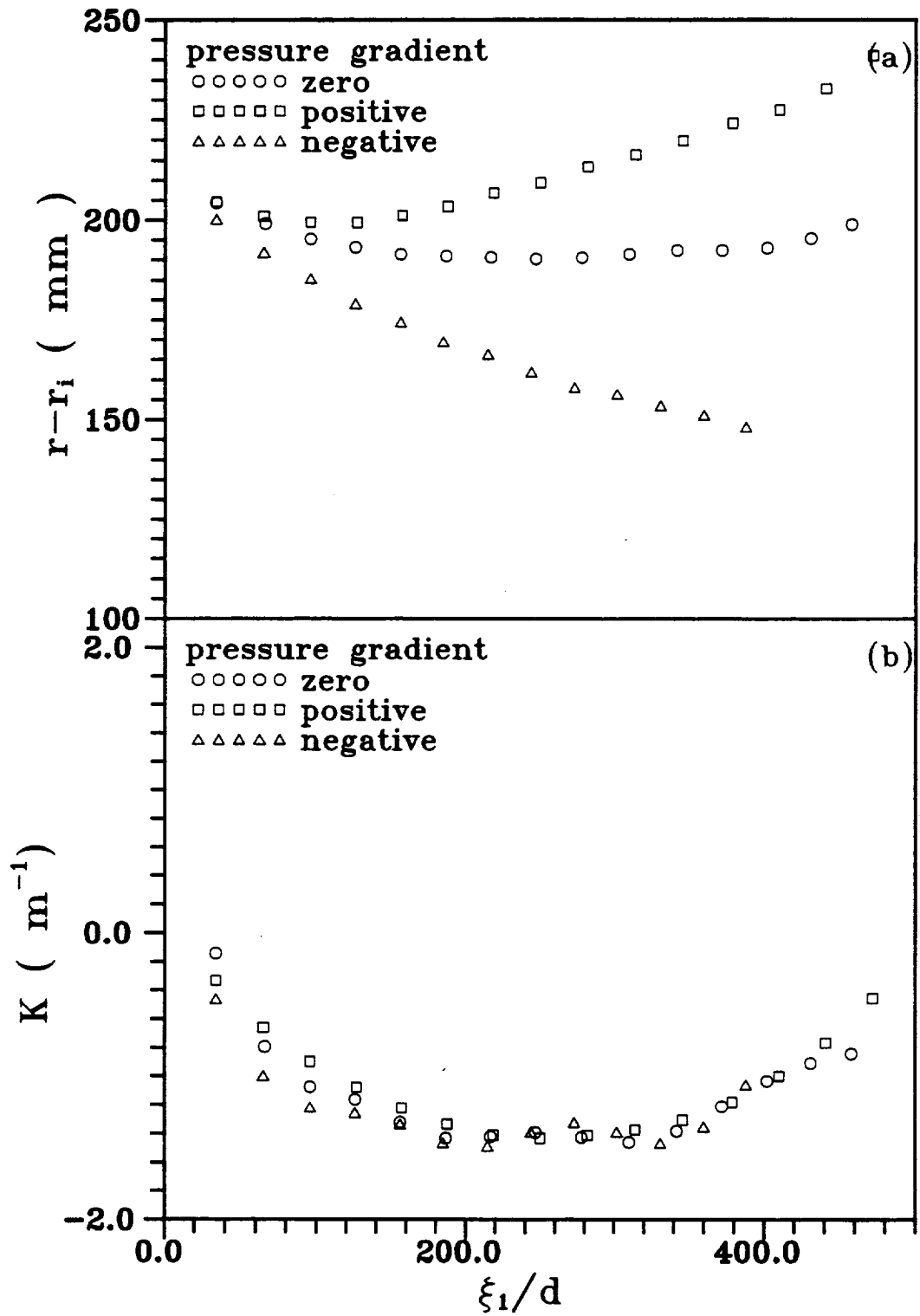
Fig. 22 Radial position (a) and local curvature (b) of wake center at different streamwise positions

trajectory of the wake center and the tangential direction x is less than $5°$. The local curvature of the wake centerline shown in Fig. 22(b) is calculated from the first and second derivative of the polynomial fit through the wake center at different streamwise position. The negative value of K suggests that the curvature of the wake centerline is concave in the positive ξ_2 direction.

Figure 23(a) shows the decay of maximum velocity defect normalized by the potential velocity at wake center $\bar{U}_{po}$. The solid line represents a power law fit with $\bar{U}_{1m}/\bar{U}_{po} \sim (\xi_1/d)^{-0.71}$. For comparison, a zero pressure gradient straight wake follows $\bar{U}_{1m}/\bar{U}_\infty \sim (x/d)^{-0.5}$ for near wake ($x/d < 100$), and $\bar{U}_{1m}/\bar{U}_\infty \sim (x/d+x_o/d)^{-0.5}$ for far wake ($x/d > 100$). Here, U_∞ is the free-stream velocity and x_o is the virtual origin of the wake. The value of x_o reported by different researchers varies from 40 to $100d$. Obviously, the decay of wake centerline velocity defect for the present curved wake is faster than the straight wake. Figure 23(b) shows the wake width b nondimensionalized by the diameter of the wake generating rod as a function of ξ_1/d. The solid line is the power law fit with $b/d \sim (\xi_1/d)^{0.74}$. b/d is proportional to $(x/d)^{0.5}$ for near wake and $(x/d+x_o/d)^{0.5}$ for far wake for a zero pressure gradient straight wake. Therefore, the spreading rate of b in the curved wake is higher than the straight wake. The difference in the absolute value of powers (-0.71 and 0.74) for wake width and velocity defect may be due either to the uncertainty involved in finding $\bar{U}_{1m}$ and b or to the mild pressure gradient.

Figure 24(a) shows the hypothetical potential velocity at wake center nondimensionalized by the freestream velocity just upstream of the wake generating rod as a function of ξ_1/d. The hypothetical potential velocity distribution along the wake centerline can give some indication of the streamwise pressure gradient along the wake centerline. An increasing potential velocity along the wake centerline suggests a negative pressure gradient and vice versa. An approximately constant value of potential velocity confirms a near zero pressure gradient along the streamwise direction. Figure 24(b) shows the pressure coefficient C_p ($C_p = (p-p_{in})/\frac{1}{2}\rho V_{in}^2$) at the wake center for various streamwise locations. Here, p denotes static pressure at the wake center and
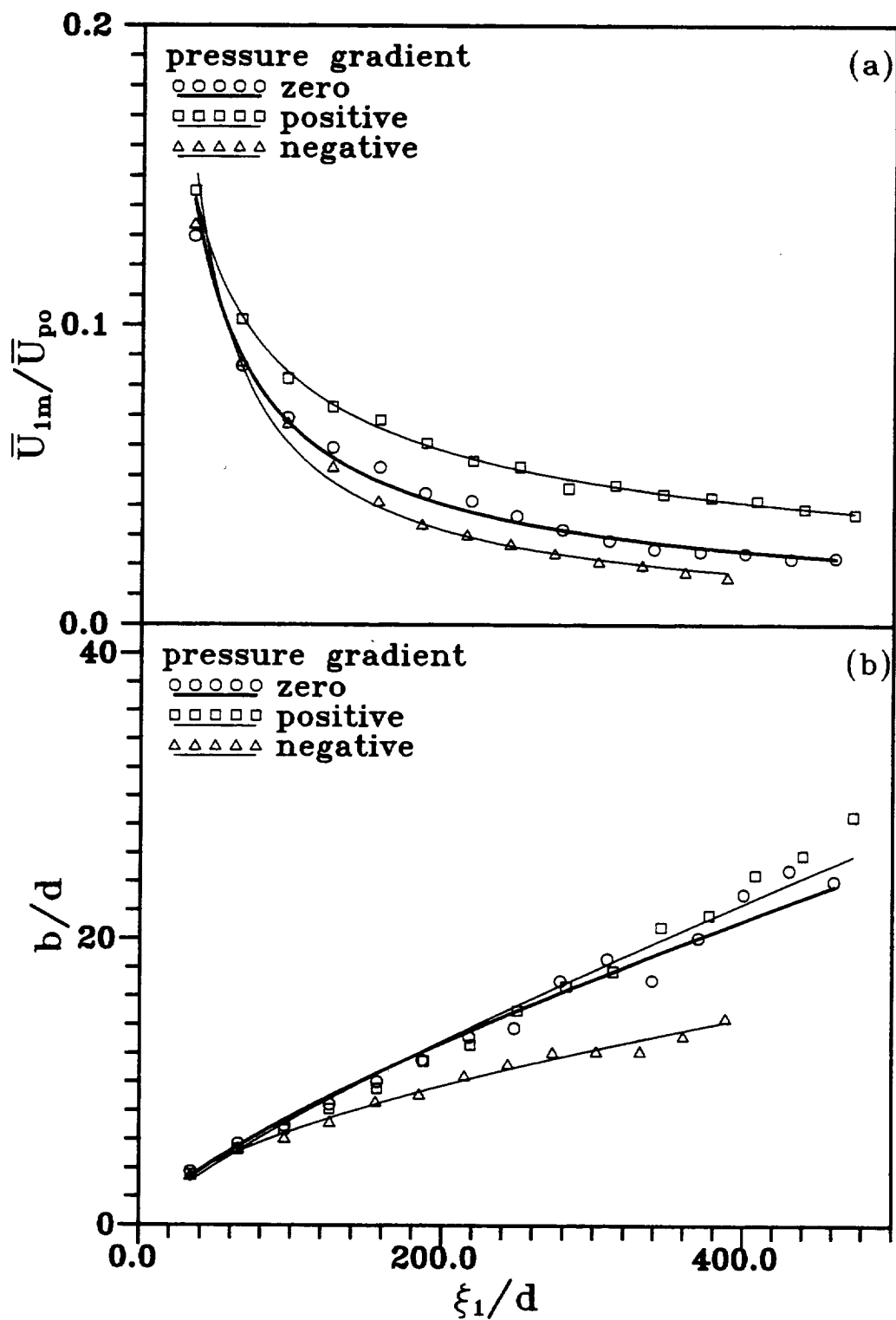
Fig. 23 Decay of maximum velocity defect (a) and growth of wake width (b) as a function of streamwise position
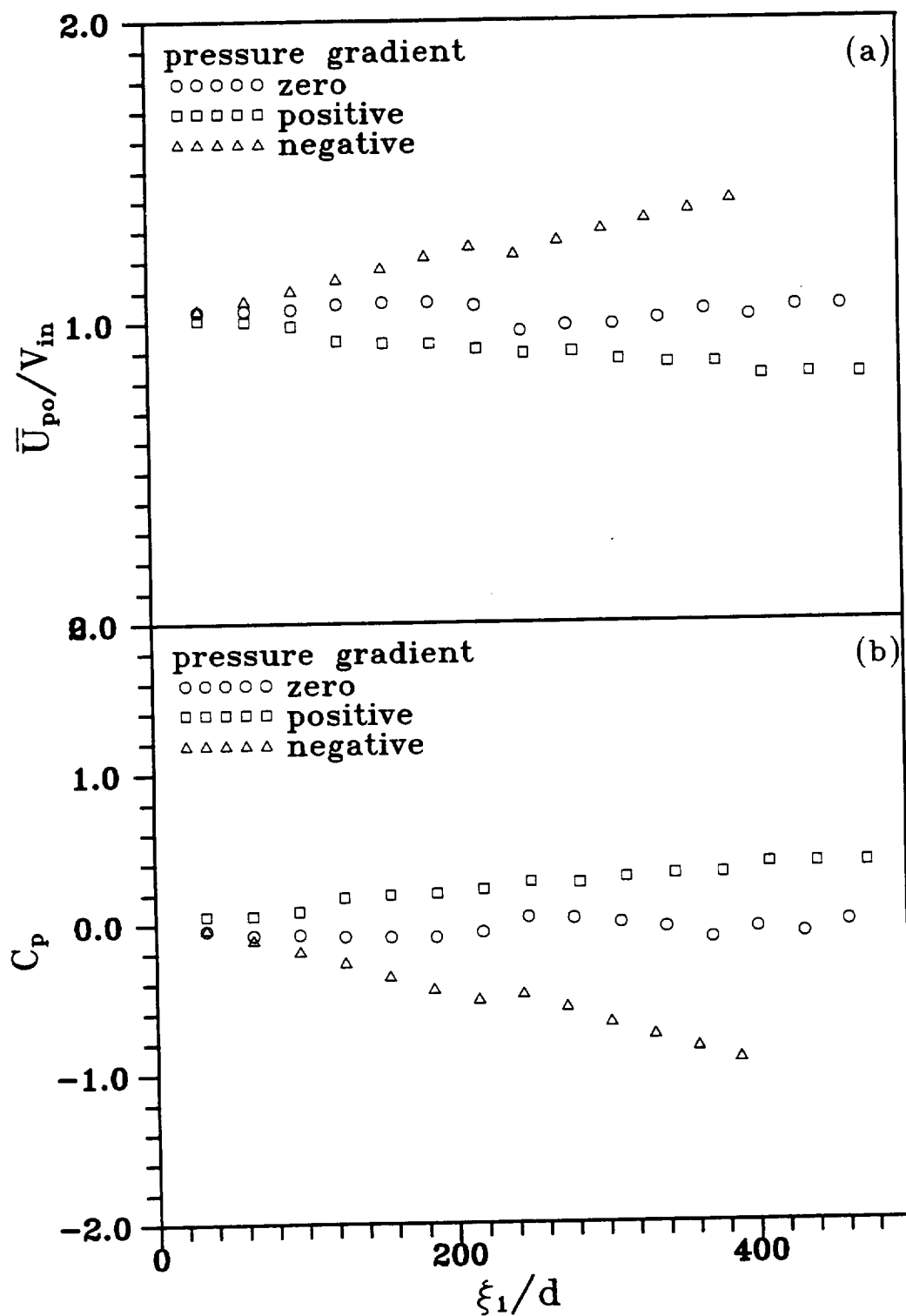
Fig. 24 Variation of potential velocity (a) and pressure coefficient (b) at the wake center as a function of streamwise position

p_{in} denotes static pressure at the straight section upstream of the wake generating cylinder. The static pressure p at the wake center is calculated from the total pressure p_t at the wake center measured using the Kiel probe and the velocity obtained from the X-film probe (i.e., $p = p_t - \frac{1}{2}\rho(\overline{U}^2 + \overline{V}^2 + \overline{u'^2} + \overline{v'^2})$). As seen in Fig. 24(b), the pressure

coefficient is approximately constant, which confirms the zero pressure gradient. Figure 25(a) shows the momentum thickness ratio C_w, defined as $C_w = 2\delta_2/d$. The solid line in Fig. 25(a), obtained from Eq. (8.8), agrees with the data obtained by numerical integration. The momentum thickness ratio is the same as the drag coefficient for the zero pressure gradient straight wake case. The nearly constant value of C_w clearly shows the absence of any significant streamwise pressure gradient. Another useful quantity in the study of wakes is the shape factor $H_{12} = \delta_1/\delta_2$. Here, δ_1 is the wake displacement thickness given by

$$\delta_1 = \frac{1}{\overline{U}_{po}} \int_{-\infty}^{+\infty} (\overline{U}_p - \overline{U}) d\xi_2 \qquad (8.1)$$

and δ_2 is the previously defined momentum thickness. The von Kármán momentum integral equation interrelates the shape factor, momentum thickness, and streamwise distribution of potential velocity. As shown by Raj and Laksminarayana (1973), the shape factor of a cascade wake can be related to the shape factor at the trailing edge of the blade. The momentum thickness can be predicted if the shape factor and streamwise distribution of potential velocity are known. Figure 25(b) shows the shape factor variation with downstream distance from the wake generating cylinder. The shape factor first decreases and then approaches a nearly constant value in the far wake. The limiting value of the shape factor for far wakes can be found at $\overline{U}_{1m}/\overline{U}_{po} \rightarrow 0$, i.e., $\lim_{\xi_2/d \to \infty} H_{12} = \lim_{\overline{U}_{1m}/\overline{U}_{po} \to 0} H_{12}$. Expressions for momentum thickness and shape factor are obtained in the following derivations.

$$\delta_2 = \frac{1}{\overline{U}_{po}^2} \int_{-\infty}^{+\infty} \overline{U} (\overline{U}_p - \overline{U}) d\xi_2 = \frac{1}{\overline{U}_{po}^2} \int_{-\infty}^{+\infty} (\overline{U}_p - \overline{U}_1) \overline{U}_1 d\xi_2 \qquad (8.2)$$
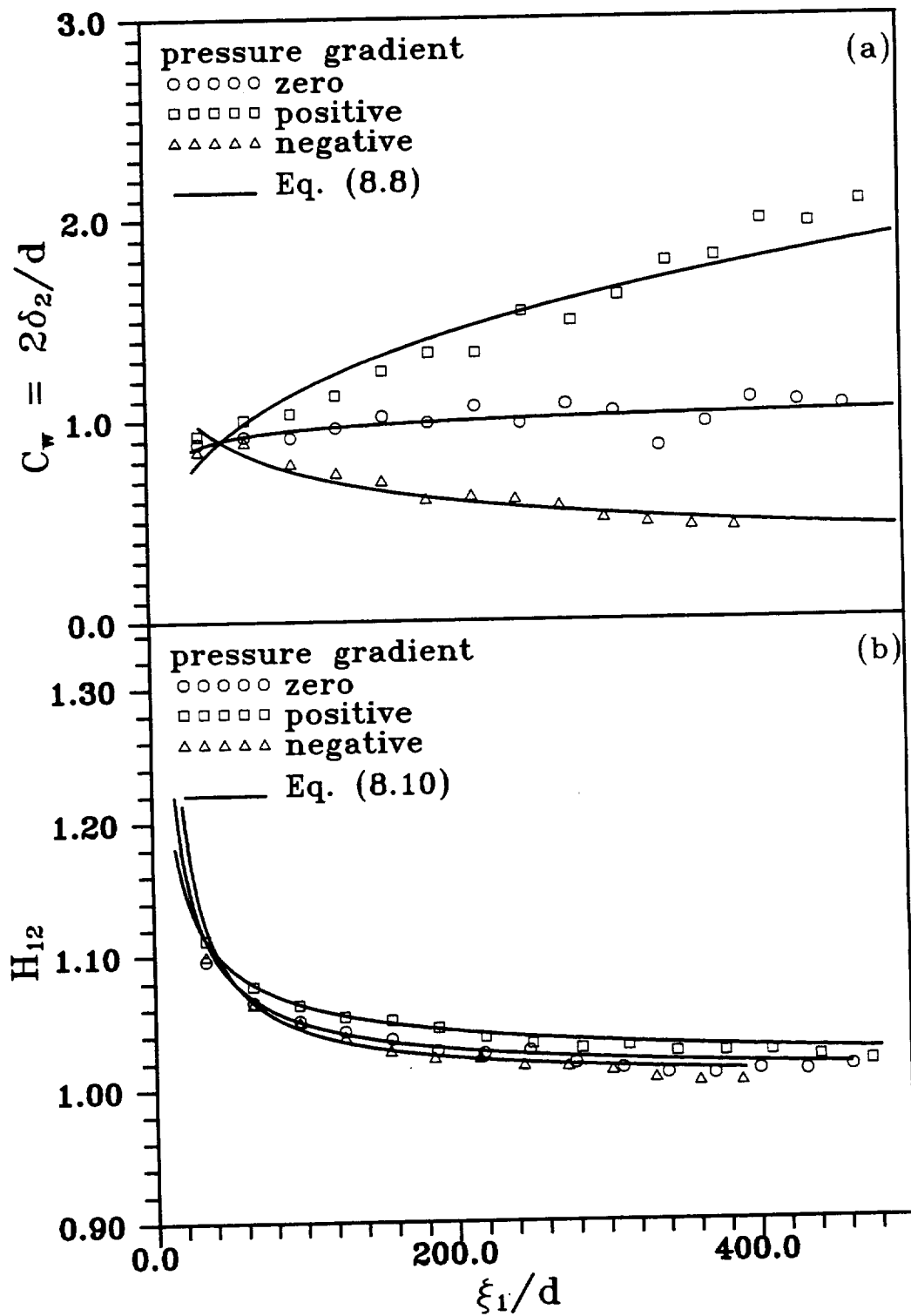
Fig. 25 Momentum thickness ratio (a) and shape factor (b) at different streamwise positions

Schobeiri (1992) showed that the expression $\bar{U}_p = \bar{U}_{po}(1-\frac{\xi_2}{R})$ can approximate the potential velocity distribution. This expression is obtained from the equation of motion for fully inviscid flow employing some simplified assumptions. The inviscid flow equation yields $\bar{U}_p = \bar{U}_{po}(1+\xi_2/R)^{-1}$. Expanding $(1+\xi_2/R)^{-1}$ by Taylor series and neglecting the higher order terms, the potential velocity becomes $\bar{U}_p = \bar{U}_{po}(1-\frac{\xi_2}{R})$.

Substituting the expression for potential velocity, the momentum thickness becomes:

$$\delta_2 = \frac{1}{\bar{U}_{po}^2}\int_{-\infty}^{+\infty}(\bar{U}_p\bar{U}_1 - \bar{U}_1^2)d\xi_2 = \frac{1}{\bar{U}_{po}^2}\int_{-\infty}^{+\infty}(\bar{U}_{po}(1-\frac{\xi_2}{R})\bar{U}_1 - \bar{U}_1^2)d\xi_2 \quad (8.3)$$

$$\delta_2 = \frac{1}{\bar{U}_{po}}\int_{-\infty}^{+\infty}\bar{U}_1 d\xi_2 + \frac{1}{\bar{U}_{po}R}\int_{-\infty}^{+\infty}\xi_2\bar{U}_1 d\xi_2 - \frac{1}{\bar{U}_{po}^2}\int_{-\infty}^{+\infty}\bar{U}_1^2 d\xi_2 \quad (8.4)$$

Normalizing $\bar{U}_1$ by $\bar{U}_{1m}$ and replacing $\bar{U}_1/\bar{U}_{1m} = e^{-(2\gamma\zeta)^2}$ (see section 8.1.2.) the momentum thickness can be written as:

$$\delta_2 = b\frac{\bar{U}_{1m}}{\bar{U}_{po}}\int_{-\infty}^{+\infty}e^{-(2\gamma\zeta)^2}d\zeta + \frac{b^2}{R}\frac{\bar{U}_{1m}}{\bar{U}_{po}}\int_{-\infty}^{+\infty}\zeta e^{-(2\gamma\zeta)^2}d\zeta - b\frac{\bar{U}_{1m}^2}{\bar{U}_{po}^2}\int_{-\infty}^{+\infty}e^{-8(\gamma\zeta)^2}d\zeta \quad (8.5)$$

The integral in the second term is zero. Thus, the equation for momentum thickness reduces to :

$$\delta_2 = b\frac{\bar{U}_{1m}}{\bar{U}_{po}}\int_{-\infty}^{+\infty}e^{-(2\gamma\zeta)^2}d\zeta - b\frac{\bar{U}_{1m}^2}{\bar{U}_{po}^2}\int_{-\infty}^{+\infty}e^{-8(\gamma\zeta)^2}d\zeta \quad (8.6)$$

$$\delta_2 = b\frac{\bar{U}_{1m}}{\bar{U}_{po}}(1-\frac{1}{\sqrt{2}}\frac{\bar{U}_{1m}}{\bar{U}_{po}}) \quad (8.7)$$

The momentum thickness ratio C_w can be written as:

$$C_w = 2\frac{b}{d}\frac{\bar{U}_{1m}}{\bar{U}_{po}}(1-\frac{1}{\sqrt{2}}\frac{\bar{U}_{1m}}{\bar{U}_{po}}) \quad (8.8)$$

The shape factor can be obtained by taking the ratio of δ_1 over δ_2, i.e.,

$$H_{12} = \frac{\delta_1}{\delta_2} = \frac{b\dfrac{\bar{U}_{1m}}{\bar{U}_{po}}\displaystyle\int_{-\infty}^{+\infty}e^{-(2\gamma\zeta)^2}d\zeta}{b\dfrac{\bar{U}_{1m}}{\bar{U}_{po}}\displaystyle\int_{-\infty}^{+\infty}e^{-(2\gamma\zeta)^2}d\zeta - b\dfrac{\bar{U}_{1m}^2}{\bar{U}_{po}^2}\displaystyle\int_{-\infty}^{+\infty}e^{-8(\gamma\zeta)^2}d\zeta}$$ (8.9)

$$H_{12} = \frac{\delta_1}{\delta_2} = \frac{\displaystyle\int_{-\infty}^{+\infty}e^{-(2\gamma\zeta)^2}d\zeta}{\displaystyle\int_{-\infty}^{+\infty}e^{-(2\gamma\zeta)^2}d\zeta - \dfrac{\bar{U}_{1m}}{\bar{U}_{po}}\displaystyle\int_{-\infty}^{+\infty}e^{-8(\gamma\zeta)^2}d\zeta} = \frac{1}{1-\dfrac{1}{\sqrt{2}}\dfrac{\bar{U}_{1m}}{\bar{U}_{po}}}$$ (8.10)

$$\lim_{\xi_1/d\to\infty} H_{12} = \underset{\bar{U}_{1m}/\bar{U}_{po}\to 0}{Lim}\ H_{12} = 1$$ (8.11)

This shows that the shape factor approaches unity for small defect wakes ($H_{12} \approx 1$ for $\bar{U}_{1m}/\bar{U}_{po} \ll 1$). This is clearly the trend in Fig. 25(b). The solid line, obtained from the theoretical model represented by Eq. (8.10), is in close agreement with the values obtained from mean velocity data by numerical integration. Figure 26 shows the product $\bar{U}_{1m}b$ at various streamwise locations. The product $\bar{U}_{1m}b$, which is constant for zero pressure gradient straight wake, remains approximately constant for the curved wake. Table 6 (Appendix A) gives the values of maximum velocity defect, wake width, potential velocity at wake center, and average velocity upstream of the cylinder at various downstream locations.

8.1.2. Mean Velocity Distribution

Figure 27 shows plots of streamwise component of velocity as a function of the transverse distance for six streamwise locations. The velocity distributions for other streamwise locations are similar to the asymmetric distribution shown in Fig. 27 with a higher velocity at the positive side of ξ_2. The transverse location $\xi_2 = 0$ corresponds
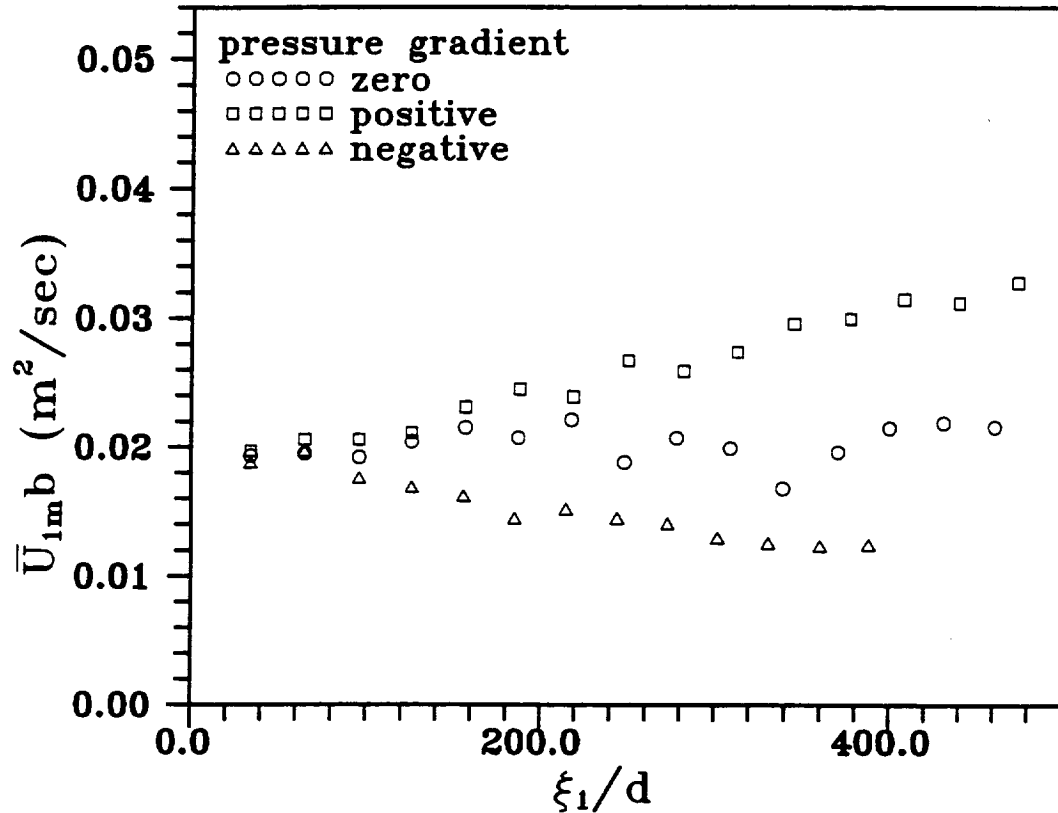
Fig. 26 Integral parameter $U_{1m}b$ as a function of streamwise position

to the wake center while a point with a higher value of ξ_2 corresponds to a location closer to the convex wall. The velocity distribution is asymmetric with respect to the wake center with a higher value on the positive side of ξ_2. The wake velocity defect decreases and the wake width increases with downstream location. A close examination of the velocity data points outside the wake and at $\xi_2 > 0$ for the initial three streamwise locations reveals an increasing potential velocity with increasing downstream distance. This increase in the potential velocity at the outer half of the wake, which is due to the turning of flow from a straight section to the curved channel, is dominant up to the streamwise location $\xi_1/d = 96$.

Figures 28-30(a) show the transverse distribution of mean velocity defect for different streamwise locations. The mean velocity defect is normalized by its maximum

Fig. 27 Transverse distribution of streamwise component of velocity at different streamwise positions and under zero streamwise pressure gradient

value and the transverse distance by the wake width b. The purpose of normalizing the transverse distance with length scale b and the velocity defect with velocity scale $\bar{U}_{1m}$ is to check the existence of similarity for mean velocity defect profiles. Figures 28-30(a) also show the existence of similarity for mean velocity defect profiles. The solid line represents Eifler's (1975) results for straight wake given by the function φ_1,

$$\varphi_1 = \bar{U}_1/\bar{U}_{1m} = e^{-(2\gamma\zeta)^2}, \text{ where } \gamma = \int_0^\infty e^{-\zeta^2}d\zeta = \frac{\sqrt{\pi}}{2} = 0.886 \text{ and } \zeta = \frac{\xi_2}{b}. \text{ The mean}$$

velocity defect profiles are symmetric and almost identical to those of a straight wake except that they are slightly wider on the inner side (concave side of the trajectory of the wake centerline) of the wake. This small deviation from the straight wake data is more clear at farther streamwise locations. It may be considered that the effect of curvature on the mean velocity defect distribution is small. The high scatter of the normalized velocity defect at higher downstream locations is because the maximum velocity defect is very small at these locations.

Figures 30(b)-32 show the transverse distribution of normalized transverse (normal) velocity $\bar{V} / \bar{U}_{1m}$ for various streamwise locations. The transverse distribution at the measurement locations shown in Fig. 30(b) is similar to the straight wake results, where the distribution is antisymmetric with a minimum at $\zeta > 0$, a maximum at $\zeta < 0$, and zero transverse velocity at the center. The $\bar{V} / \bar{U}_{1m}$ distribution for straight wake approaches zero at the edges. The transverse distribution in Figs. 31 and 32 can be considered as a superposition of the distribution at zero pressure gradient straight wake on a normalized hypothetical potential distribution of V. The hypothetical potential distribution will be dictated by the streamwise pressure gradient and streamline curvature. The analytical equation for the transverse velocity distribution obtained from the continuity equation is shown by Schobeiri et al. (1993). It should be noted that many relevant papers on wakes, including those dealing with symmetrical wakes, have not reported the transverse velocity distribution. This may be due to very high scatter in experimental data. The consistent trend in the distribution transverse velocity for the present measurements shows the reliability of the data. The distribution of velocity at
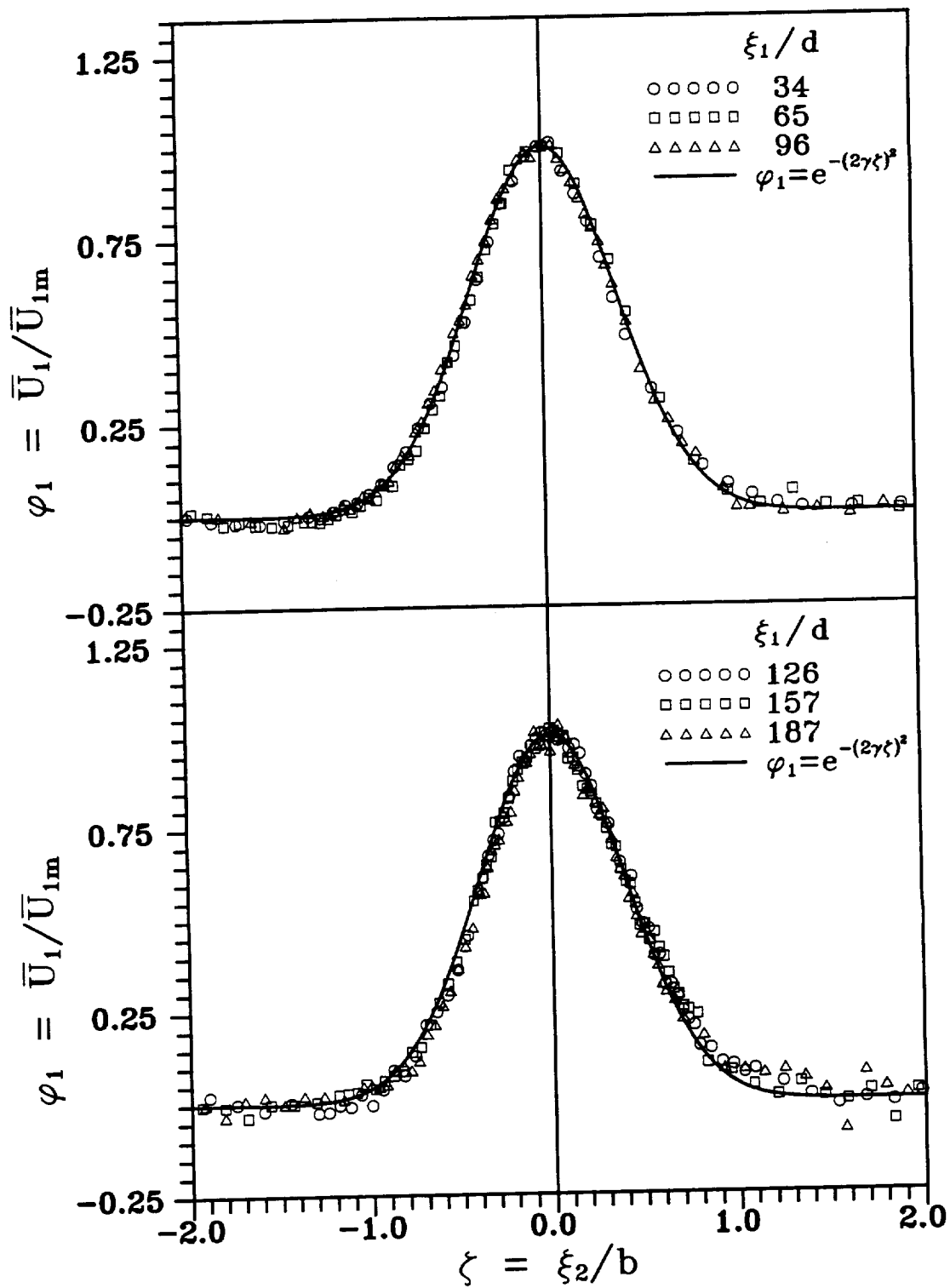
Fig. 28 Transverse distribution of velocity defect at different streamwise positions and under zero streamwise pressure gradient, ξ_1/d = 34 to 187

Fig. 29 Transverse distribution of velocity defect at different streamwise positions and under zero streamwise pressure gradient, ξ_1/d = 218 to 370

(a)

$\dfrac{\xi_1}{d}$

○ ○ ○ ○ ○ 400
□ □ □ □ □ 431
△ △ △ △ △ 461
——— $\varphi_1 = e^{-(2\gamma\zeta)^2}$

1.25

0.75

0.25

$\varphi_1 = \bar{U}_1/\bar{U}_{1m}$

-0.25

(b)

$\dfrac{\xi_1}{d}$

○ ○ ○ ○ ○ 34
□ □ □ □ □ 65
△ △ △ △ △ 96

0.25

0.00

-0.25

$\bar{V}/\bar{U}_{1m}$

-2.0   -1.0   0.0   1.0   2.0

$\zeta = \xi_2/b$
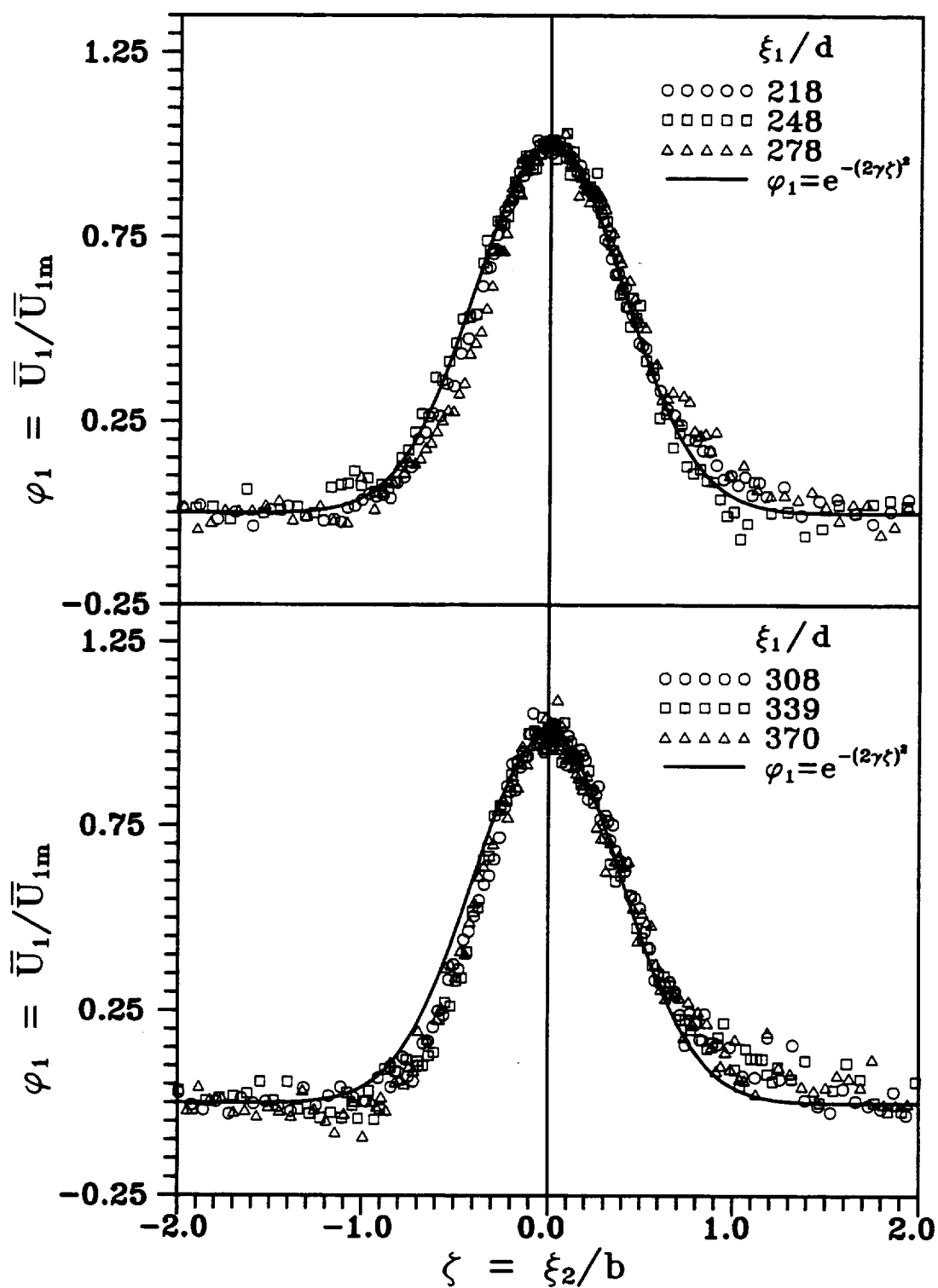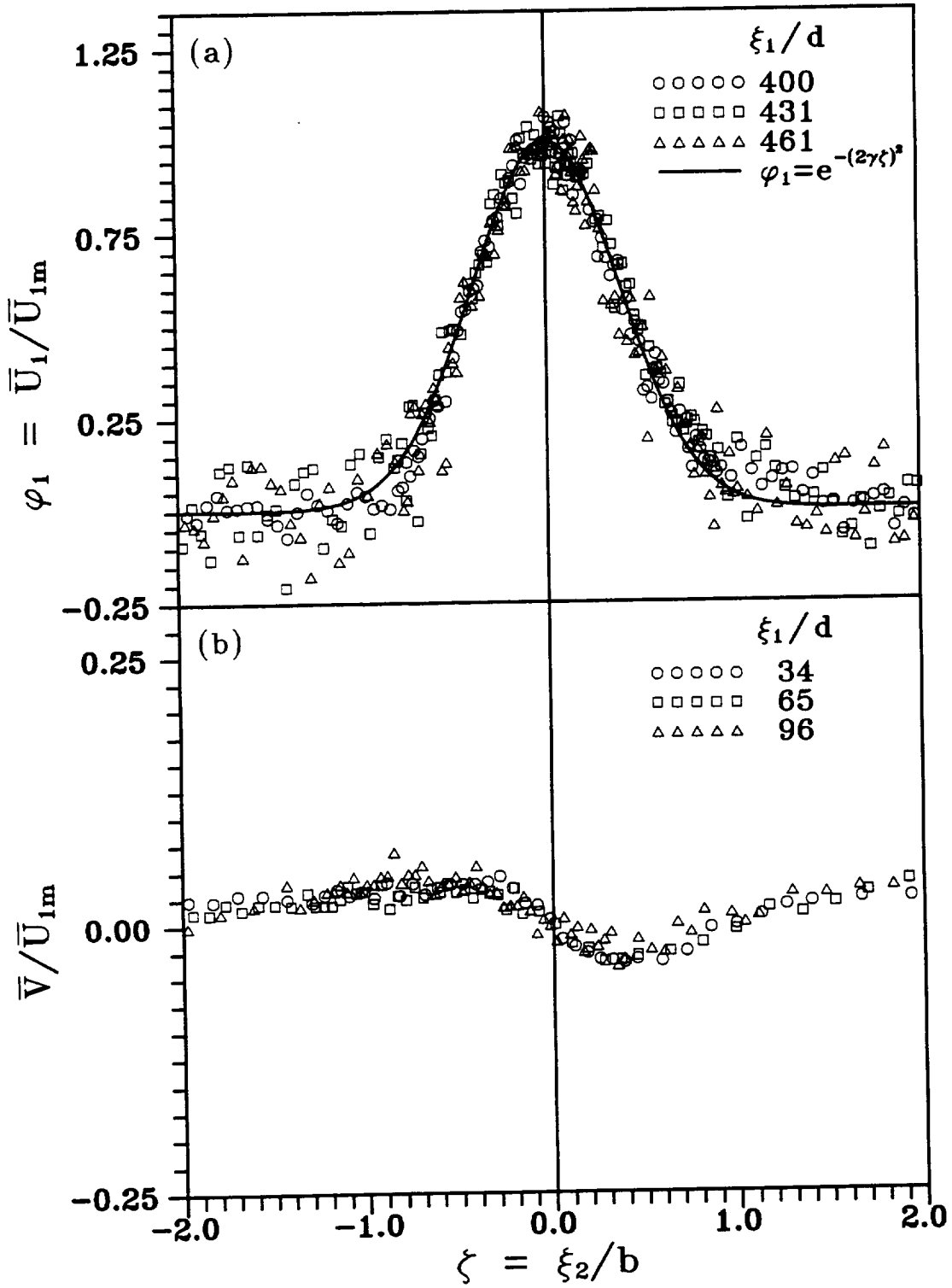
Fig. 30 Transverse distributions of velocity defect (a) and normal velocity (b) at zero streamwise pressure gradient, (a) ξ_1/d = 400 to 461, (b) ξ_1/d = 34 to 96
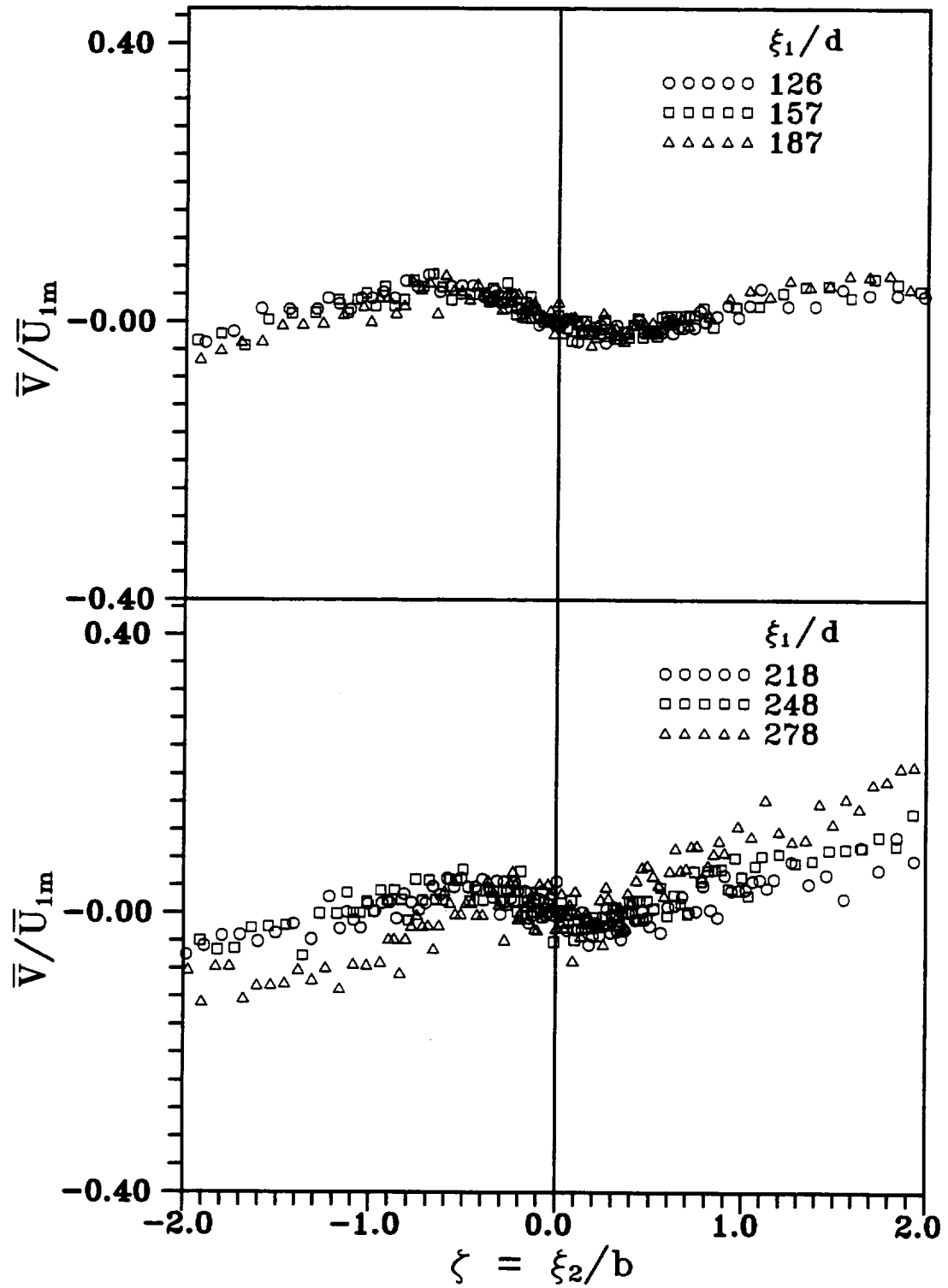
Fig. 31 Transverse distributions of normal velocity at different streamwise positions and under zero streamwise pressure gradient, ξ_1/d = 126 to 278
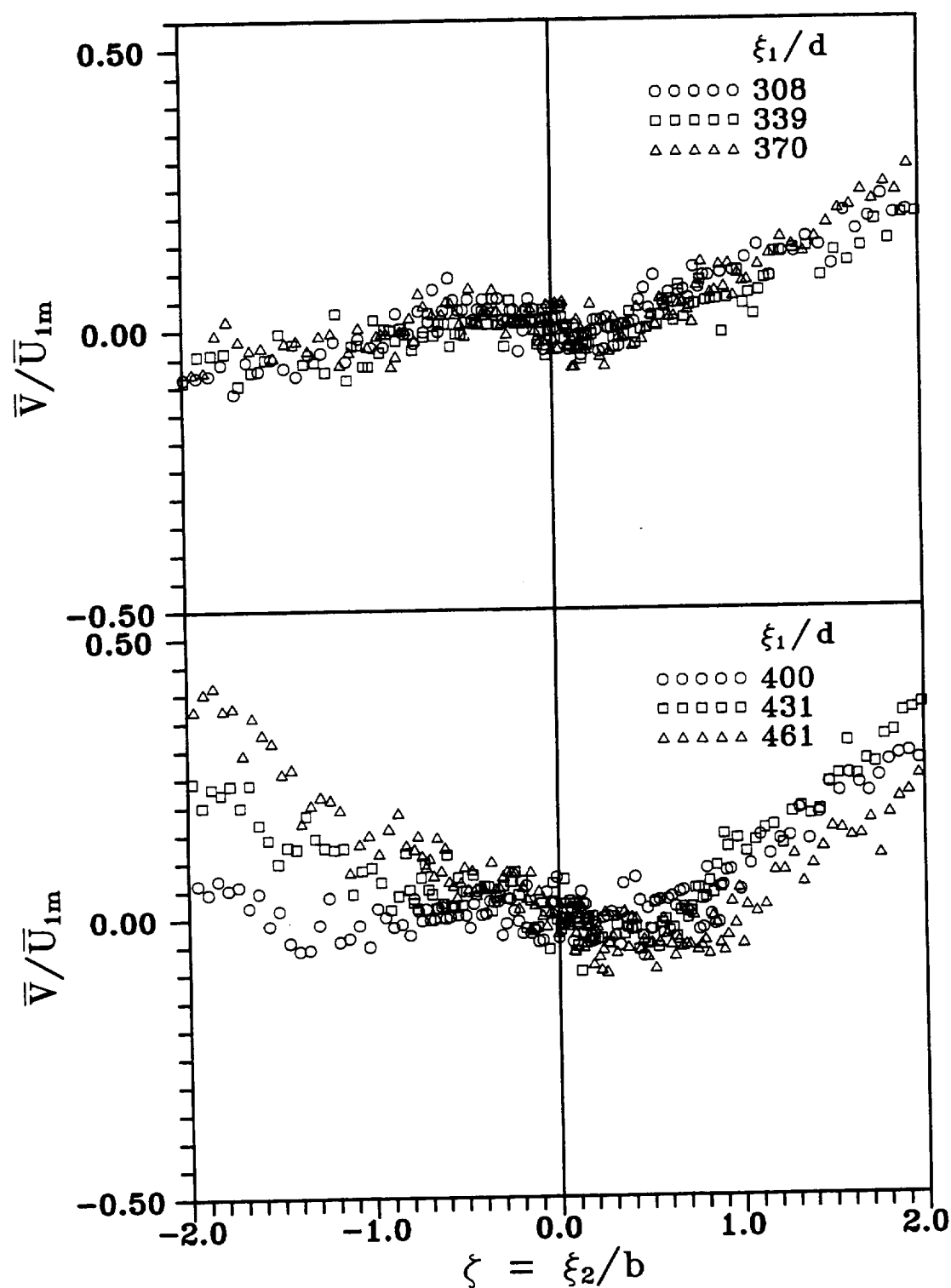
Fig. 32 Transverse distributions of normal velocity at different streamwise positions and under zero streamwise pressure gradient, ξ_1/d = 308 to 461

the last three downstream locations in Fig. 32 is different from the other locations because the changes in the potential velocity distribution of $\bar{V}$. Many factors affect the hypothetical potential distribution of velocities. The flow pattern will change as the flow enters the straight exit duct from the curved channel. Also, the downstream of the exit duct has a 90° bend. The boundary layer growth on the concave wall, convex wall, and side walls has some effect on the velocity distribution. The flow may not be strictly two-dimensional due to secondary flows that can occur in curved channels whose height and width are of the same order of magnitude. All these factors can influence the hypothetical velocity distribution in the curved test section.

8.1.3. Reynolds Stresses

Figures 33-40 show the transverse distribution of the normalized Reynolds stresses. The Reynolds normal stresses are normalized with respect to its value at the wake center. Table 6 (Appendix A) gives the values of Reynolds normal stresses at the wake center at different downstream locations. Figures 33-35(a) show the normalized Reynolds stress component in the streamwise direction. In comparison with straight wake data, the present results exhibit an asymmetric feature due to the curvature of the wake path. In a straight wake, the streamwise component of Reynolds stress is symmetric with respect to the wake center with a maximum on each side of the wake center and a minimum at the wake center. The asymmetry of the Reynolds stresses in the present data is due to the asymmetric velocity distribution of $\bar{U}$ generated by the curvature. Generally, a positive velocity gradient in the radial direction suppresses the turbulence in a curved shear flow. However, a negative velocity gradient in the radial direction promotes the turbulence. This is analogous to the radial equilibrium of a fluid element in an inviscid, irrotational curved flow where the flow is stable if the radial gradient of angular momentum is positive and unstable if the radial gradient of angular momentum is negative. The radius of curvature of the wake centerline in Fig. 22(b) is positive in the negative ξ_2 direction. For measurements at all streamwise locations, the gradient of streamwise velocity in the positive radial direction is negative on the inner
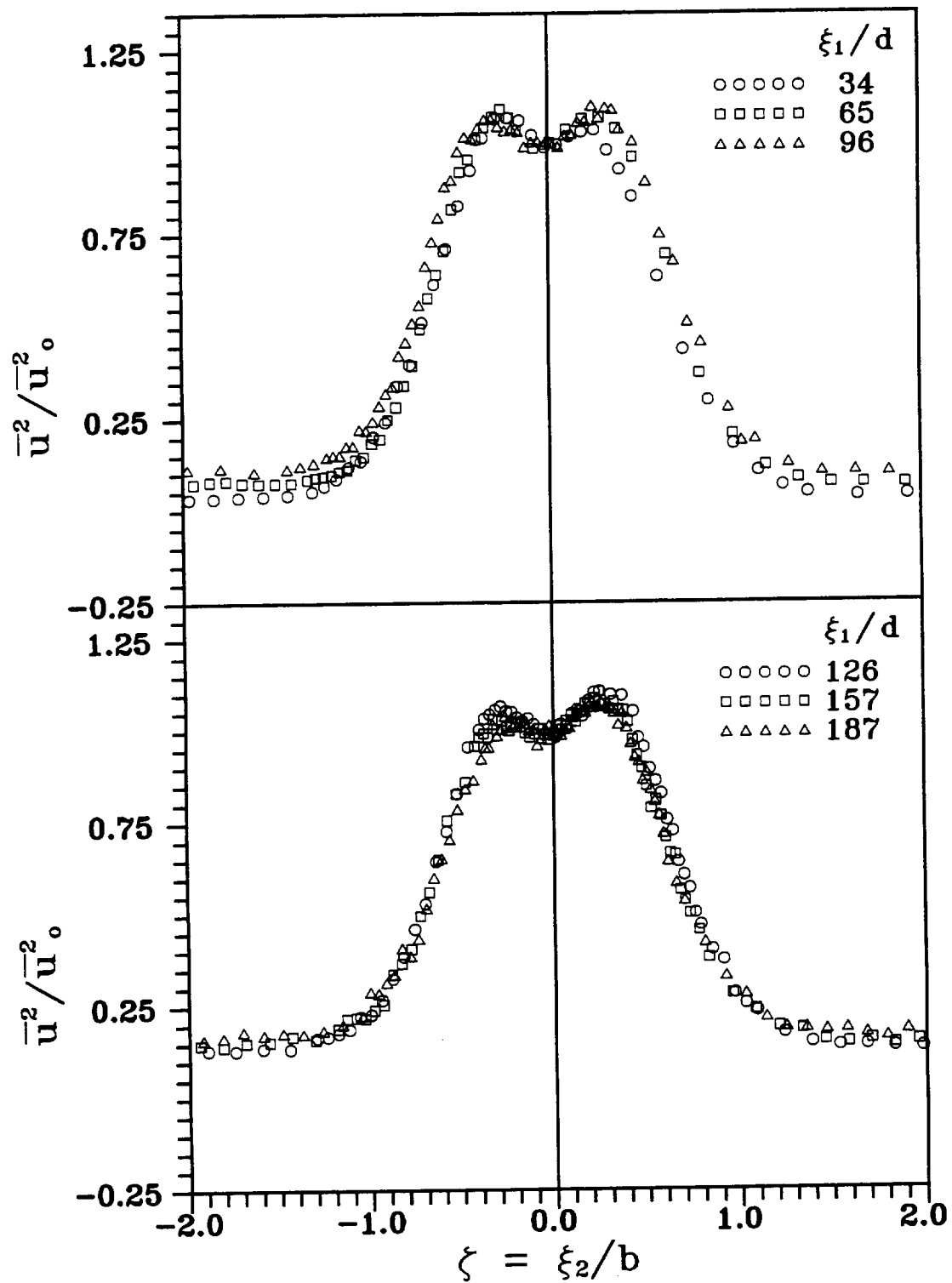
Fig. 33 Transverse distribution of streamwise component of Reynolds normal stress at different streamwise positions and under zero streamwise pressure gradient, ξ_1/d = 34 to 187

Fig. 34 Transverse distribution of streamwise component of Reynolds normal stress at different streamwise positions and under zero streamwise pressure gradient, ξ_1/d = 218 to 370
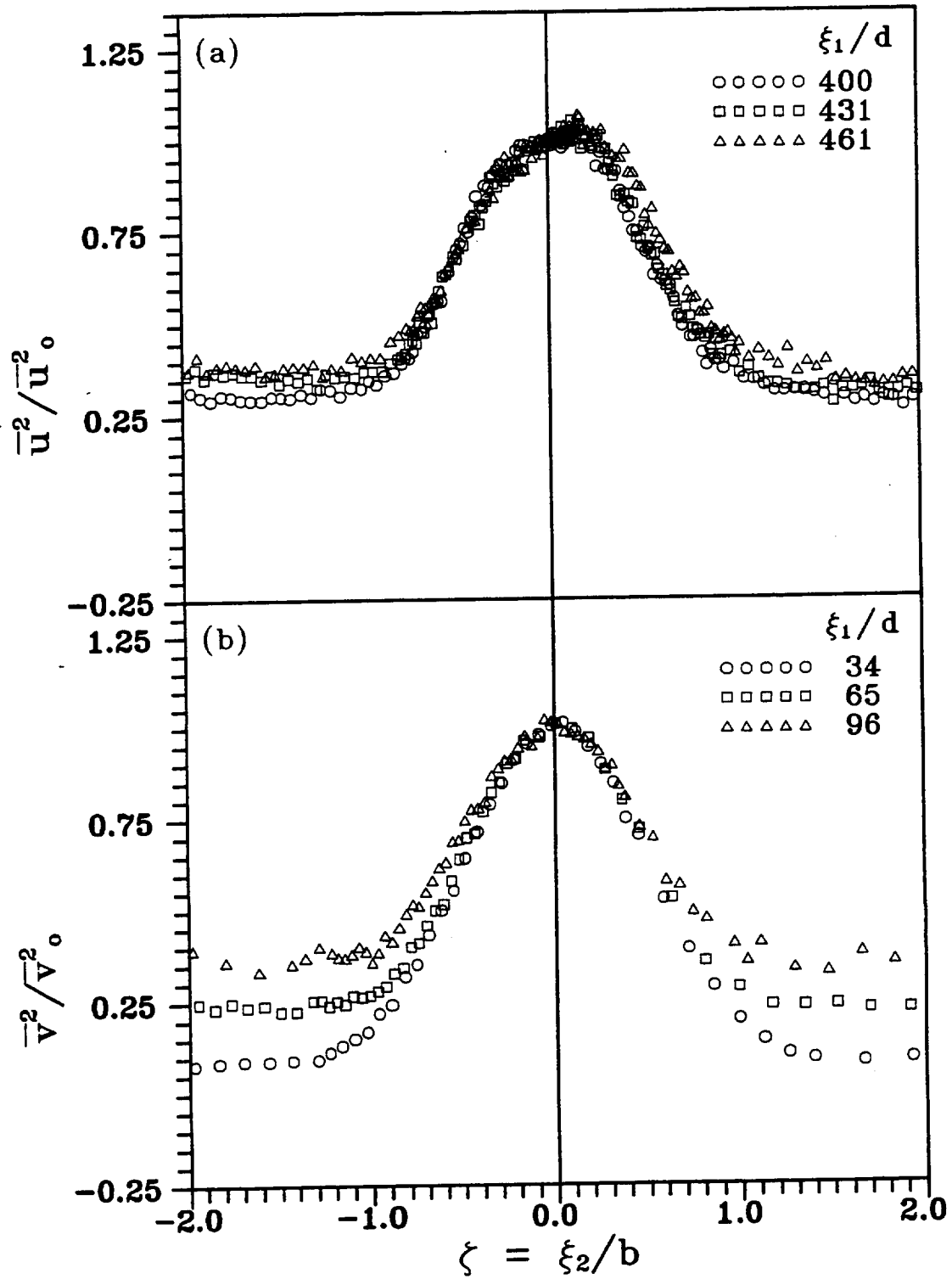
Fig. 35 Transverse distributions of streamwise (a) and normal (b) components of Reynolds normal stress at different streamwise positions and under zero streamwise pressure gradient, (a) ξ_1/d = 400 to 461, (b) ξ_1/d = 34 to 96
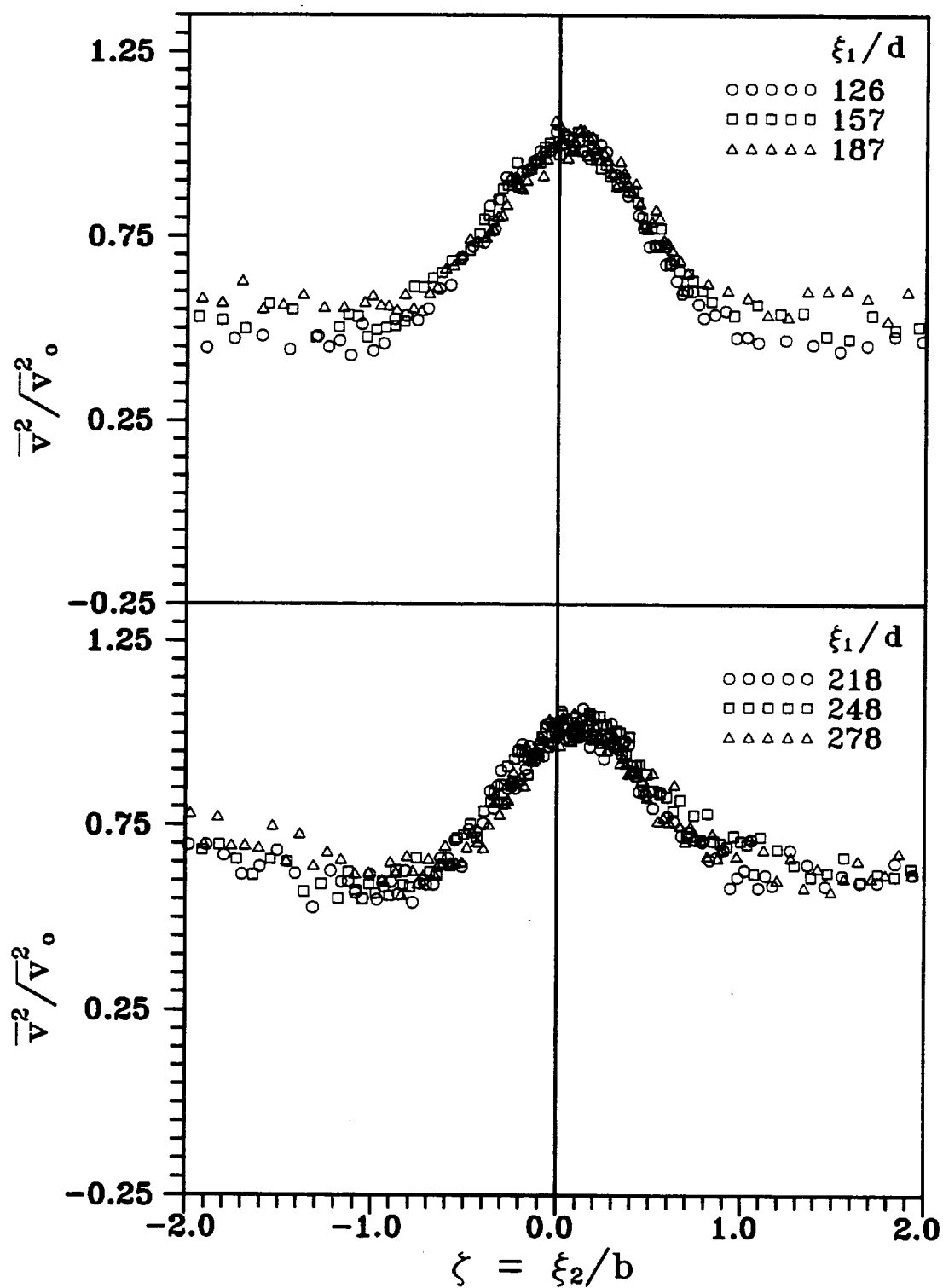
Fig. 36 Transverse distribution of normal component of Reynolds normal stress at different streamwise positions and under zero streamwise pressure gradient, ξ_1/d = 126 to 278
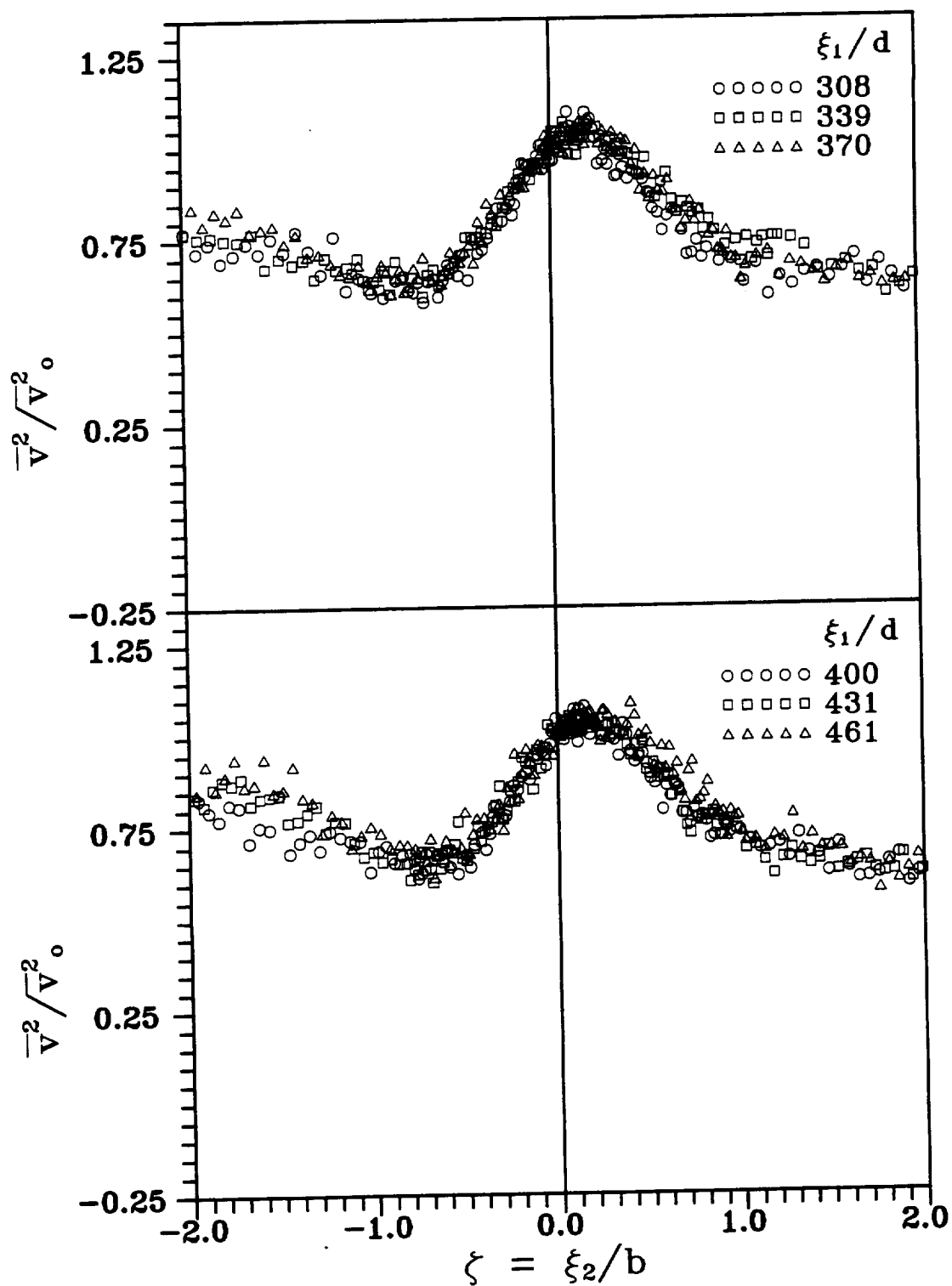
Fig. 37 Transverse distribution of normal component of Reynolds normal stress at different streamwise positions and under zero streamwise pressure gradient, ξ_1/d = 308 to 461
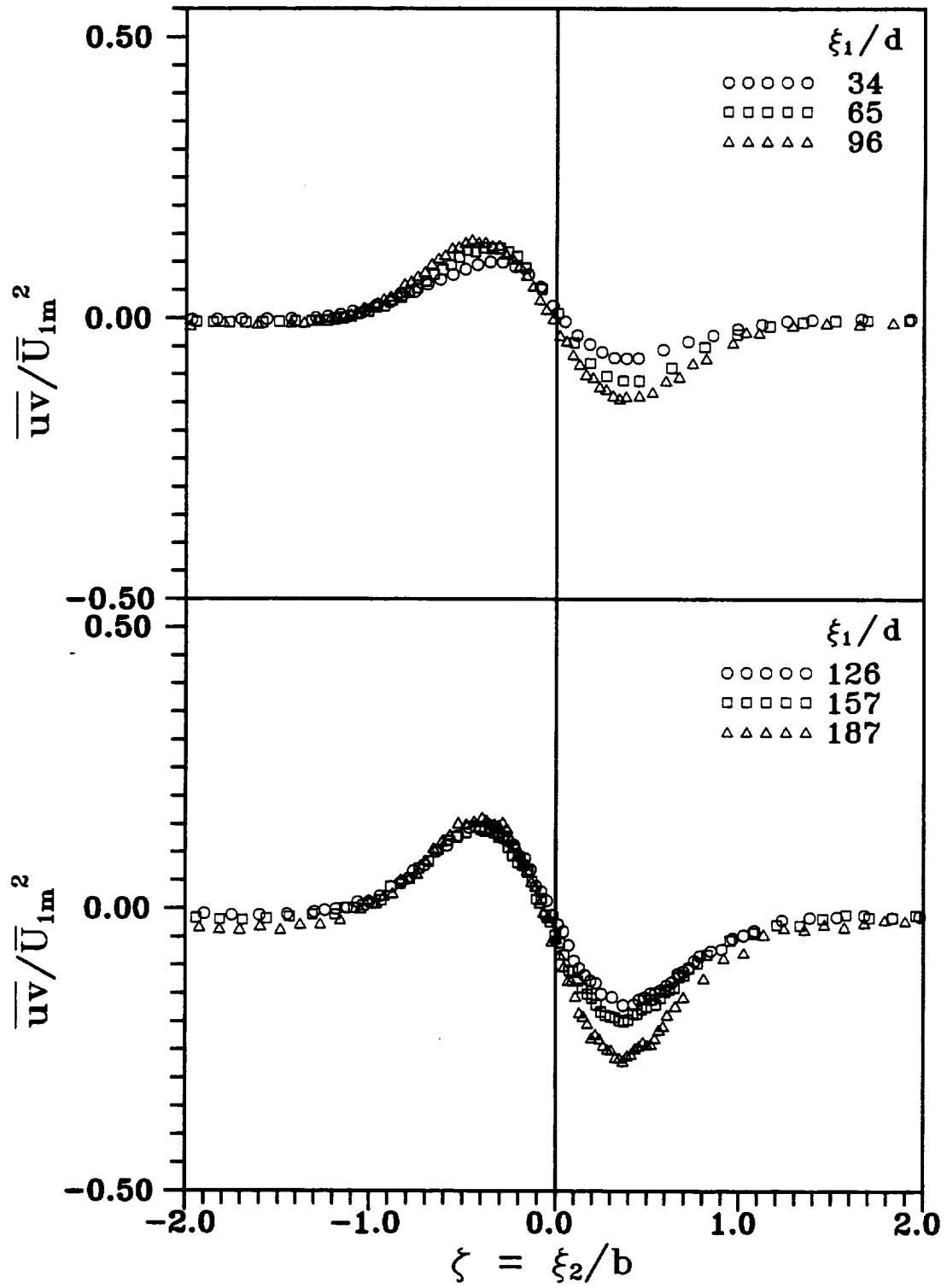
Fig. 38 Transverse distribution of Reynolds shear stress at different streamwise positions and under zero streamwise pressure gradient, ξ_1/d = 34 to 187
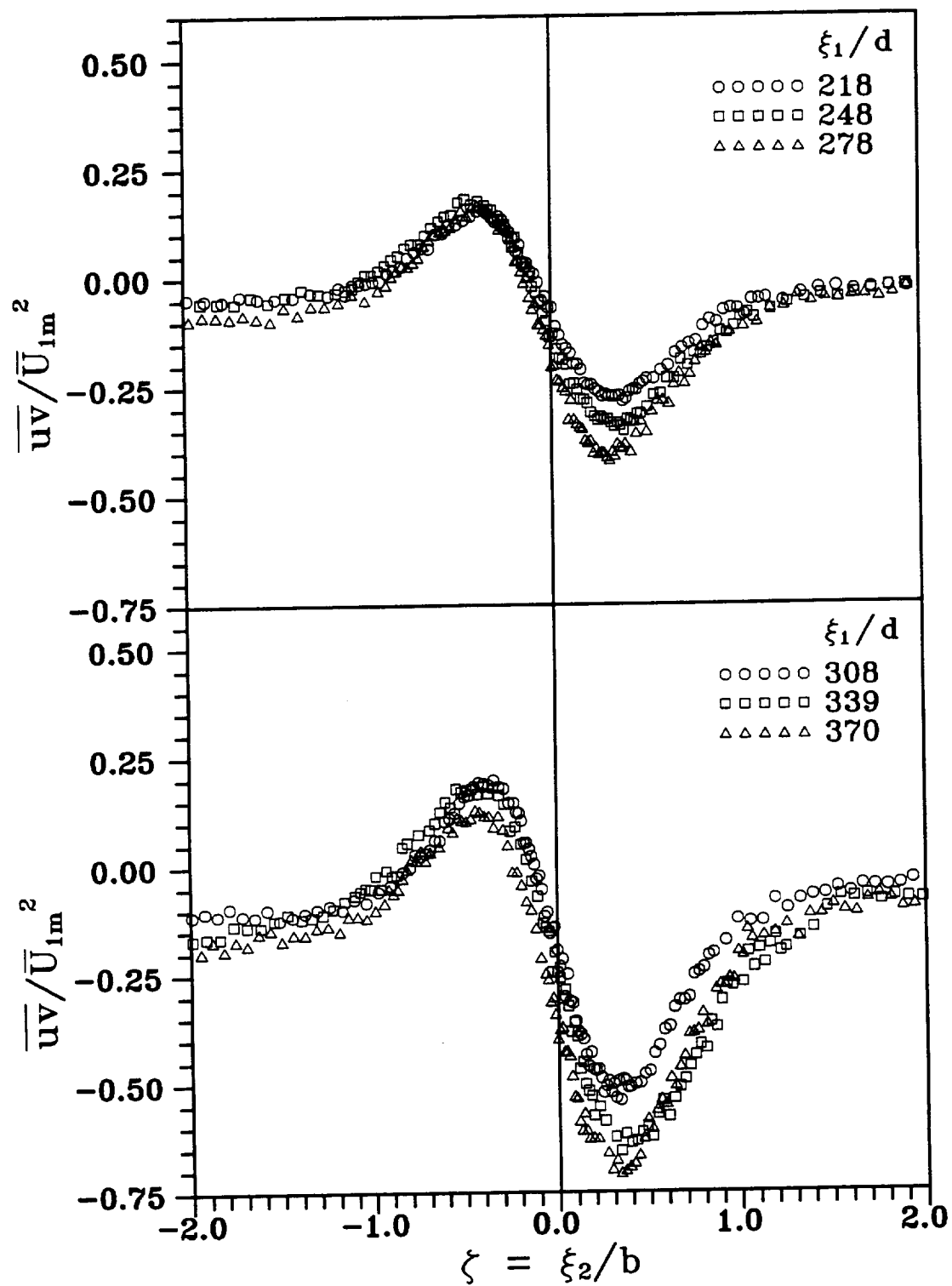
Fig. 39 Transverse distribution of Reynolds shear stress at different streamwise positions and under zero streamwise pressure gradient, ξ_1/d = 218 to 370
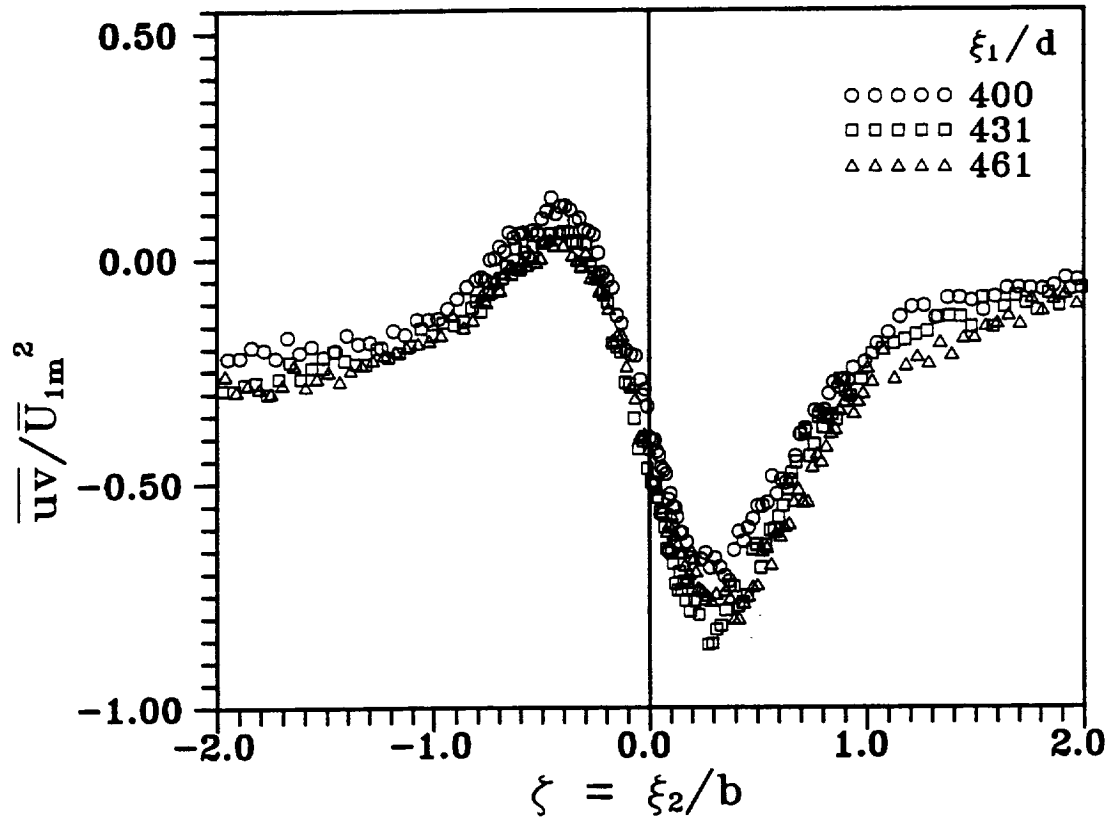
Fig. 40 Transverse distribution of Reynolds shear stress at different streamwise positions and under zero streamwise pressure gradient, ξ_1/d = 400 to 461

half (concave side of the trajectory of wake centerline, i.e., $\xi_2 > 0$) of the wake. Opposed to this, the gradient of streamwise velocity in the positive radial direction is positive in the outer half (convex side of the trajectory of the wake centerline, i.e., $\xi_2 < 0$) of the wake. Therefore, the turbulent stresses of the wake should be higher on the inner half than the outer half. This is the case for all measurement locations except the first measurement location. The asymmetric nature of the streamwise component of Reynolds stress is qualitatively similar to the results obtained by Koyama (1983) and Nakayama (1987). It may be observed that the asymmetry of the streamwise component of Reynolds stress increases with the downstream location.

The deviationary behavior in the asymmetric nature of the turbulent stresses at the

first measurement location may be due to the streamwise pressure gradient generated as the flow enters the curved channel from the straight section. The velocity distribution should be uniform upstream of the wake generating rod. At the inlet of the curved channel, the flow accelerates near the convex wall and decelerates near the concave wall. This is evident from the plots in Fig. 27 of the streamwise component of velocity at the first three measurement locations. Therefore, the streamwise pressure gradient at the inlet region of the curved channel varies across the channel, although the streamwise pressure gradient is almost zero along the center region of the wake. The effect of this varying pressure gradient on Reynolds stresses is opposite to the curvature effect here.

Figures 35(b)-37 show the transverse distribution of the transverse component of Reynolds stresses. Similar to the streamwise component, the maximum value of transverse component of Reynolds stress occurs at the inner half of the wake. The asymmetry of the transverse component of Reynolds stress is more than that of the streamwise component. In other words, the transverse component of Reynolds normal stress exhibits more distortion from the symmetrical straight wake results. Note that the two maxima observed in the straight wake data are not seen in the present data for the curved wake.

Figures 38-40 show the transverse distributions of Reynolds shear stress at various streamwise locations. The Reynolds shear stress is nondimensionalized by the square of the maximum velocity defect. The Reynolds shear stress distribution for the straight wake case is antisymmetric about the wake center. For the present curved wake case, the Reynolds shear stress distribution shows a strong asymmetry due to the curvature. The nature of curvature of the wake centerline and the gradient of streamwise velocity in the transverse direction suggest a higher value of Reynolds shear stress on the inner half of the wake. This is observed at every streamwise location except the very first measurement location, where, as previously explained, the pressure gradient dominates over the curvature effect. It appears that the Reynolds shear stress distribution in the outer half of the wake is closer to a self preservation state than that in the inner half of the wake. The Reynolds shear stress at the center of the wake is not zero, although the

transverse gradient of streamwise velocity is zero at the wake center. Raj and Lakshminarayana (1973) also observed nonzero value of Reynolds shear stress at the wake center.

The Reynolds shear stress in the hypothetical potential flow outside the wake is not exactly equal to zero due to the turbulence existing in that region. Measurements at selected streamwise locations without wake show a transverse gradient of $\overline{uv}$ with a negative value near the concave wall and a positive value near the convex wall. The radial position where $\overline{uv} = 0$ is located between the convex wall and mean radius of the channel. For example, at the streamwise position $\theta = 0^\circ$, $\overline{uv}$ was zero at $r - r_i = $ 120-mm. Wattendorf (1935) and Eskinazi and Yeh (1956) observed similar distributions of Reynolds shear stress in turbulent flows in curved channels. The normalized Reynolds shear stress distributions in Figs. 38-40 have nonzero values outside the wake. The $\overline{uv}$ outside the wake also has higher absolute value near the concave side of the wall ($\xi_2 < 0$).

8.1.4. Vorticity, Correlation Coefficient, and Turbulent Kinetic Energy

A transport equation for mean vorticity Ω, relating the gradient of mean vorticity to a second order derivative of Reynolds shear stress, can be obtained from the momentum equation. The mean vorticity Ω ($\Omega = \frac{R}{R+\xi_2}(\frac{\partial \overline{V}}{\partial \xi_1} - \frac{\overline{U}}{R}) - \frac{\partial \overline{U}}{\partial \xi_2}$) can be approximated to $-\frac{\overline{U}}{R+\xi_2} - \frac{\partial \overline{U}}{\partial \xi_2}$, by order-of-magnitude assumptions. Figure 41 shows the transverse distribution of normalized vorticity for streamwise locations from $\xi_1/d = $ 34 to 244. The mean vorticity is normalized with $\overline{U}_{1m}/b$. Similar to the straight wake results, the mean vorticity profiles for the present case are almost antisymmetric with respect to the wake center. Therefore, the effect of curvature on mean vorticity profiles is considered small. The near zero value of vorticity in the region outside the wake suggests that the mean flow is mostly irrotational in that region. The determination of

vorticity involves calculating the transverse gradient of velocity by numerical method from the cubic spline-fitted data of streamwise velocity, and is highly sensitive to the scatter in mean velocity data. This is the reason for high scatter in the mean vorticity data observed in the furthest downstream locations shown in Fig. 41.

The correlation between streamwise and transverse fluctuations, which is also a measure of the degree of anisotropy of the flow, is represented by the correlation coefficient R_{uv} and defined as $R_{uv} = \overline{uv}/\sqrt{\overline{u^2}}\,\sqrt{\overline{v^2}}$. The correlation coefficient will be zero for isotropic turbulence. Figures 42 and 43 show the transverse distribution of the correlation coefficient at different streamwise locations. The distribution of the correlation coefficient is asymmetric with higher absolute values at the inner half of the wake. The maximum absolute value of the correlation coefficient at the inner half of the wake remains constant from $\xi_1/d = 96$ onwards. However, the maximum absolute value of the correlation coefficient at the outer half of the wake decreases with downstream distance and reaches close to zero at $\xi_1/d = 461$.

The information on turbulent kinetic energy k, $k = \frac{1}{2}(\overline{u^2}+\overline{v^2}+\overline{w^2})$, is useful in turbulence modeling. Here, w stands for the component of fluctuation velocity perpendicular to the ξ_1-ξ_2 plane. An estimate of the turbulent kinetic energy can be obtained from $k = \frac{3}{4}(\overline{u^2}+\overline{v^2})$, which is obtained from the assumption $\overline{w^2} = \frac{1}{2}(\overline{u^2}+\overline{v^2})$.

Figure 44 shows the transverse distribution of turbulent kinetic energy normalized by the square of the mean velocity defect. The turbulent kinetic energy distribution is asymmetric with respect to the wake center with higher values at the inner half of the wake. The normalized turbulent kinetic energy increases with downstream location because the turbulent kinetic energy decays at a slower rate than the mean velocity defect.

8.2. Wake Development at Positive Pressure Gradient

An X-hot-film probe measured the wake behind a 1.984-mm diameter stationary cylinder, with the cylinder located at mid height of the wake generating section. The
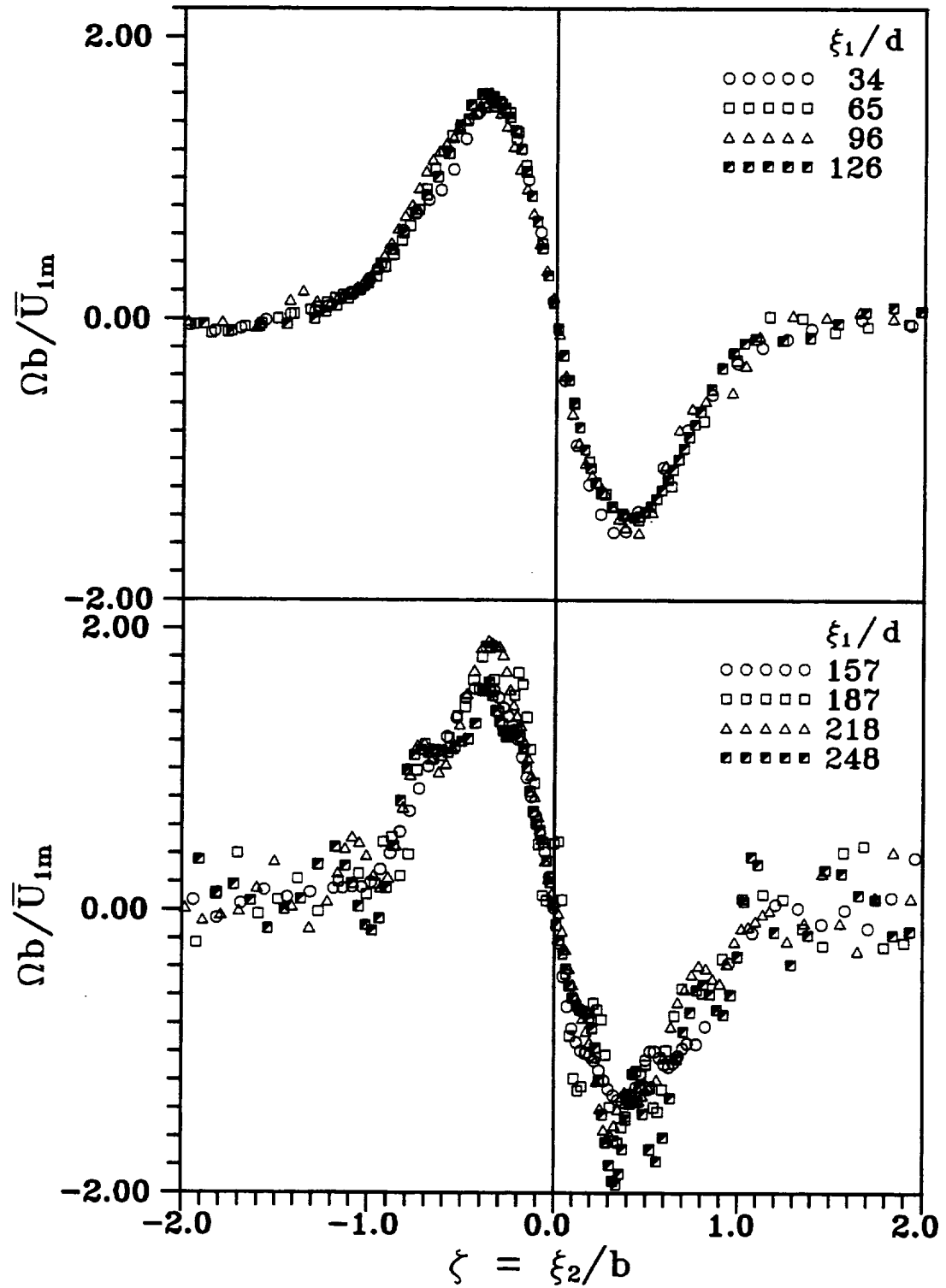
Fig. 41 Transverse distribution of mean vorticity at different streamwise positions and under zero streamwise pressure gradient

Fig. 42 Transverse distribution of correlation coefficient at different streamwise positions and under zero streamwise pressure gradient, ξ_1/d = 34 to 248
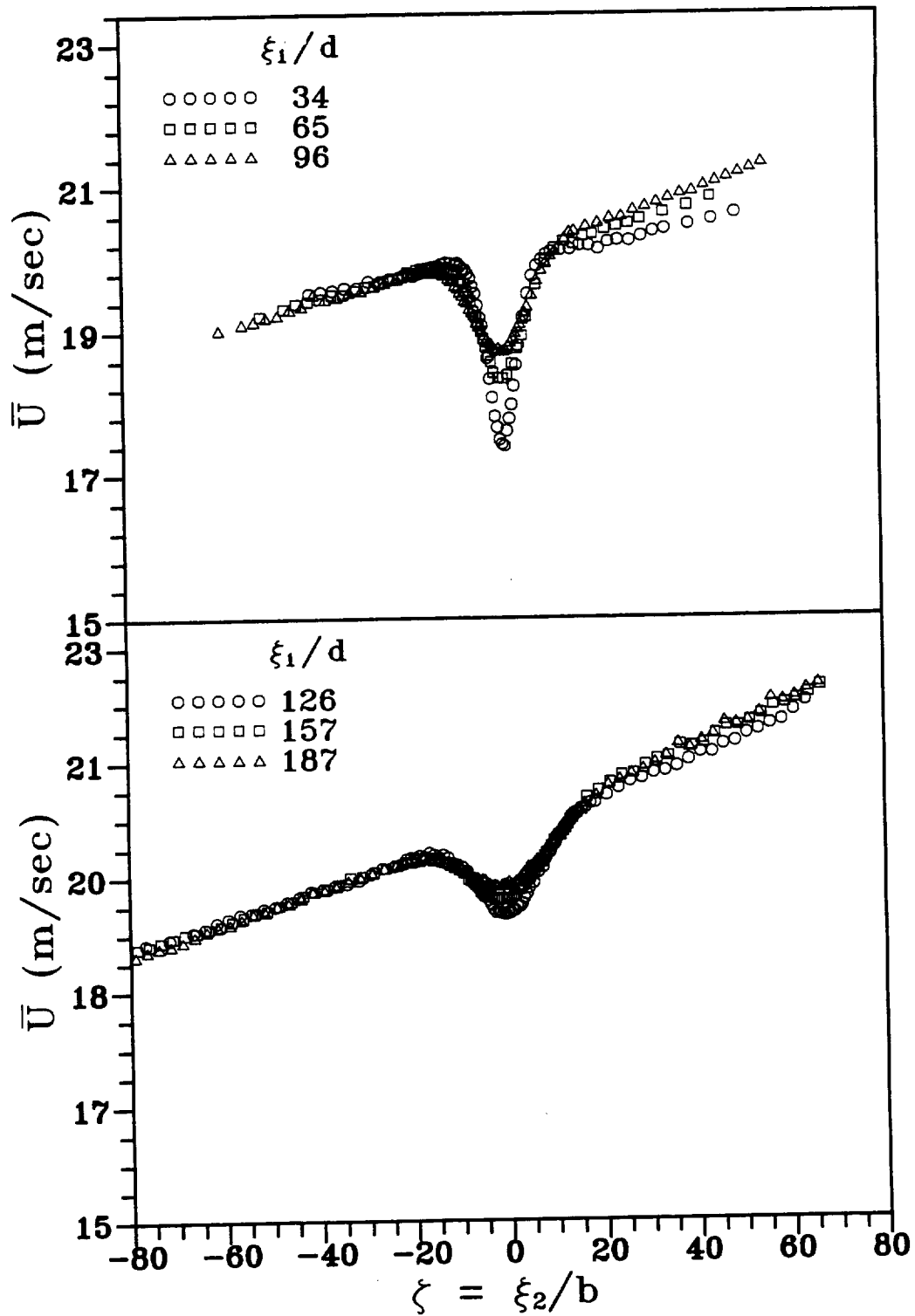
Fig. 43 Transverse distribution of correlation coefficient at different streamwise positions and under zero streamwise pressure gradient, ξ_1/d = 278 to 461

curved channel test section has a 0.7 inlet to exit area ratio. The wake profiles were obtained at fifteen angular positions from $\theta = 0°$ to $70°$ in $5°$ intervals. The first measuring station $\theta = 0°$ corresponds to the inlet of the curved test section and is 67-mm downstream of the wake generating cylinder.

8.2.1. Path of Wake Center, Curvature of the Path of Wake Center, and Development of the Wake

The wake center path representing the ξ_1 direction for the curvilinear coordinate system was determined similar to that with zero pressure gradient wake. Figure 22(a) shows the radial distance from the convex wall to the wake center, denoted by r-r_i, at various streamwise positions. As the wake propagates through the channel, the trajectory of the wake center gradually moves toward the convex wall up to a downstream location $\xi_1/d = 100$, and from there onwards it moves away from the convex wall. The maximum inclination between the trajectory of the wake center and the tangential direction x is less than $7.5°$. Figure 22(b) shows the local curvature of the wake centerline. The changes in the local radius of curvature are similar to that in the zero pressure gradient wake. As previously mentioned, the negative value of K suggests that the curvature of the wake centerline is concave in the positive ξ_2 direction.

Figure 23(a) gives the decay of maximum velocity defect normalized by potential velocity at the wake center $\bar{U}_{po}$. The solid line represents a power law fit with $\bar{U}_{1m}/\bar{U}_{po} \sim (\xi_1/d)^{-0.51}$. Therefore, the decay rate of maximum velocity defect in the positive pressure gradient curved channel is slower than the zero pressure gradient curved channel. Figure 23(b) shows the wake width b nondimensionalized by the diameter of the wake generating rod as a function of ξ_1/d. The solid line is the power law fit with $b/d \sim (\xi_1/d)^{0.81}$. Therefore, the spreading rate of b in the positive pressure gradient curved wake is higher than in the zero pressure gradient curved wake.

Figure 24(a) presents the distribution of the hypothetical potential velocity at the wake center nondimensionalized by the freestream velocity just upstream of the wake generating rod as a function of ξ_1/d. The decreasing hypothetical potential velocity
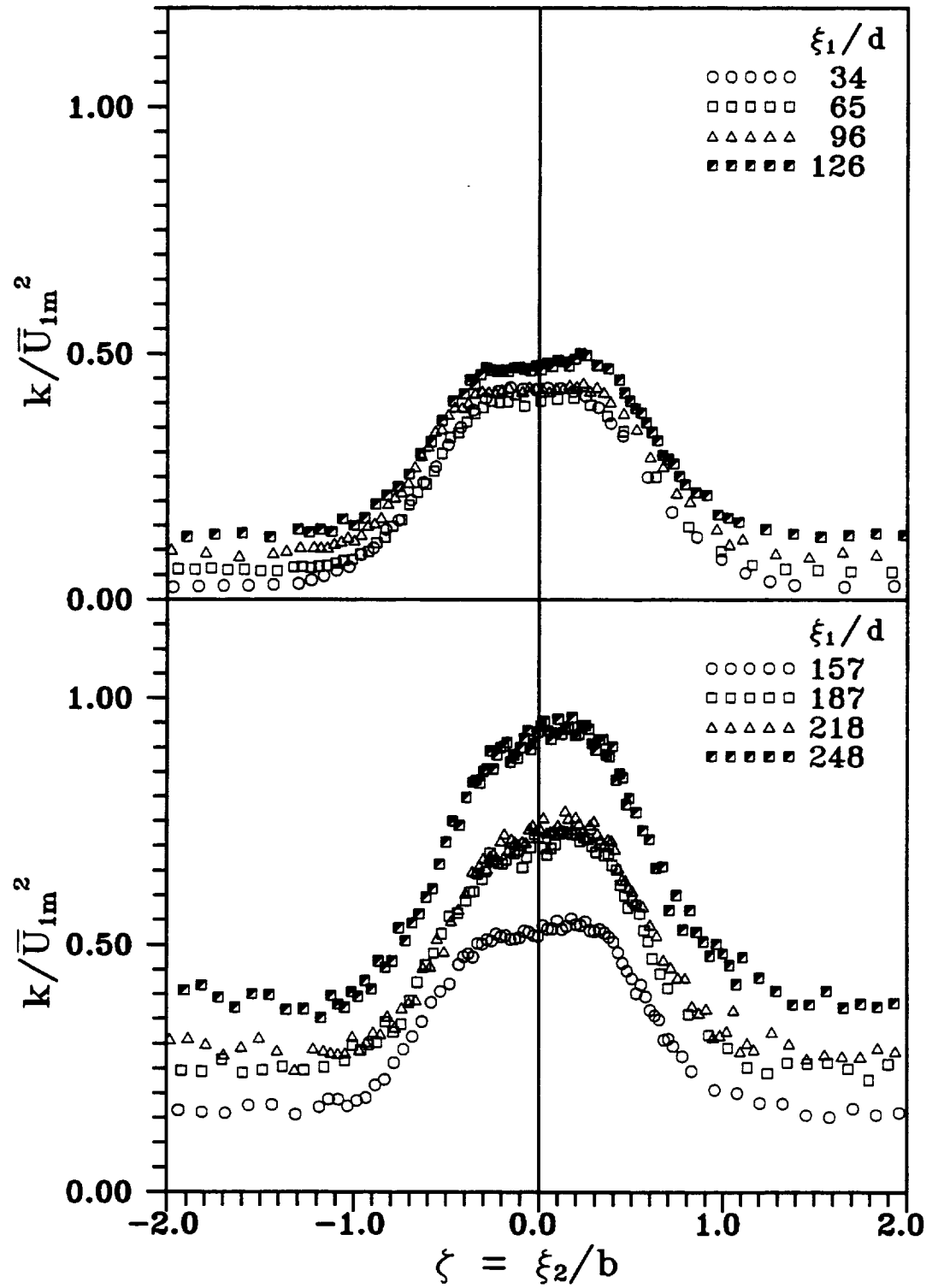
Fig. 44 Transverse distribution of turbulent kinetic energy at different streamwise positions and under zero streamwise pressure gradient

distribution along the wake centerline is due to the diverging channel that creates the positive streamwise pressure gradient. Figure 24(b) shows the pressure coefficient C_p ($C_p = (p - p_{in})/\frac{1}{2}\rho V_{in}^2$) at the wake center at various streamwise locations. The pressure coefficient is calculated by method explained in section 8.1.1. As seen in Fig. 24(b), the pressure coefficient increases with downstream distance, which confirms the positive pressure gradient. Also, the momentum thickness ratio C_w, plotted in Fig. 25(a), increases with the downstream location. The solid line in Fig. 25(a), obtained from Eq. (8.8), agrees with those values from the velocity profile using numerical integration. Figure 25(b) shows the variation of shape factor H_{12} with downstream distance from the wake generating cylinder. Similar to the zero pressure gradient straight wake, the shape factor approaches unity for far wakes. The rate at which the shape factor approaches unity is slightly smaller for the positive pressure gradient wake than the zero pressure gradient wake. The solid line in Fig. 25(b), obtained from the theoretical model represented by Eq. (8.10), is in close agreement with the values from the mean velocity data by numerical integration. Figure 26 shows the product $\overline{U}_{1m}b$ at various streamwise locations. As seen from Fig. 26, the product $\overline{U}_{1m}b$ increases with downstream location.

Table 7 (Appendix A) gives the values of maximum velocity defect, wake width, potential velocity at the wake center, and average velocity upstream of the cylinder at various downstream locations.

8.2.2. Mean Velocity Distribution

Figure 45 shows the streamwise component of velocity as a function of the transverse distance for six streamwise locations. The velocity distributions for other streamwise locations are similar to the asymmetric distribution in Fig. 45 with a higher velocity at the positive side of ξ_2. The velocity distribution in Fig. 45 is asymmetric with respect to the wake center with a higher value on the positive side of ξ_2. The wake velocity defect decreases and the wake width increases with downstream location. A close examination of the velocity data points outside the wake for the initial three

streamwise locations reveals a nonuniform decrease in potential velocity across the channel. This nonuniform decrease in potential velocity across the channel, due to the turning of flow from a straight section to the curved channel, occurs up to the streamwise location $\xi_1/d = 96$.

Figures 46-48(a) are the plots of the transverse distribution of the mean velocity defect in similarity coordinates. The solid line represents Eifler's (1975) results for straight wake given by the function φ_1, $\varphi_1 = \bar{U}_1/\bar{U}_{1m} = e^{-(2)(\zeta)^2}$. The mean velocity defect profiles are symmetric and almost identical to the straight wake except that they are slightly wider on the inner side of the wake. This small deviation from the straight wake data is clearer at higher streamwise locations. It may be considered that the effect of curvature on the mean velocity defect distribution is small.

Figures 48(b)-50 show plots of the transverse distribution of normalized transverse velocity $\bar{V} / \bar{U}_{1m}$ for various streamwise locations. The transverse distribution at the first measurement location in Fig. 48(b) is similar to the straight wake results, where the transverse velocity at the wake edges approaches zero. The transverse velocity distribution shown at other locations can be considered as a superposition of the distribution at zero pressure gradient straight wake on a normalized hypothetical potential distribution of transverse component of velocity. The streamwise pressure gradient and streamline curvature dictate the profile of the hypothetical potential distribution of $\bar{V}$. The hypothetical potential distribution of $\bar{V}$ in the wake region is almost linear with a positive slope up to a streamwise location $\xi_1/d = 400$. As explained for the zero pressure gradient case, the hypothetical potential distribution at the last three measurement locations is affected by different factors that cause the transverse velocity distribution at these location to differ from the distribution at other locations.

8.2.3. Reynolds Stresses

Figures 51-58 show the transverse distribution of the normalized Reynolds stresses.
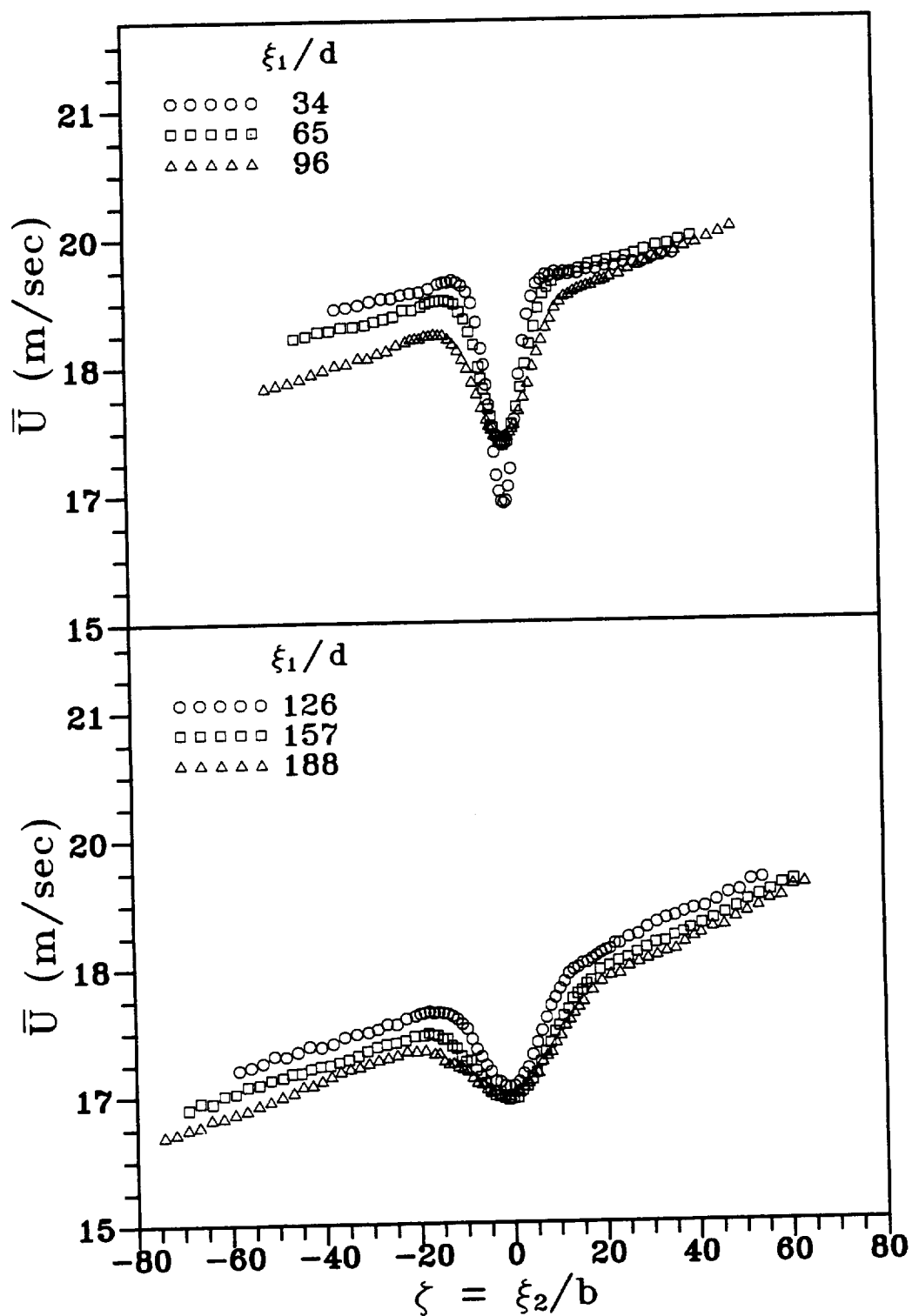
Fig. 45 Transverse distribution of streamwise component of velocity at different streamwise positions and under positive streamwise pressure gradient
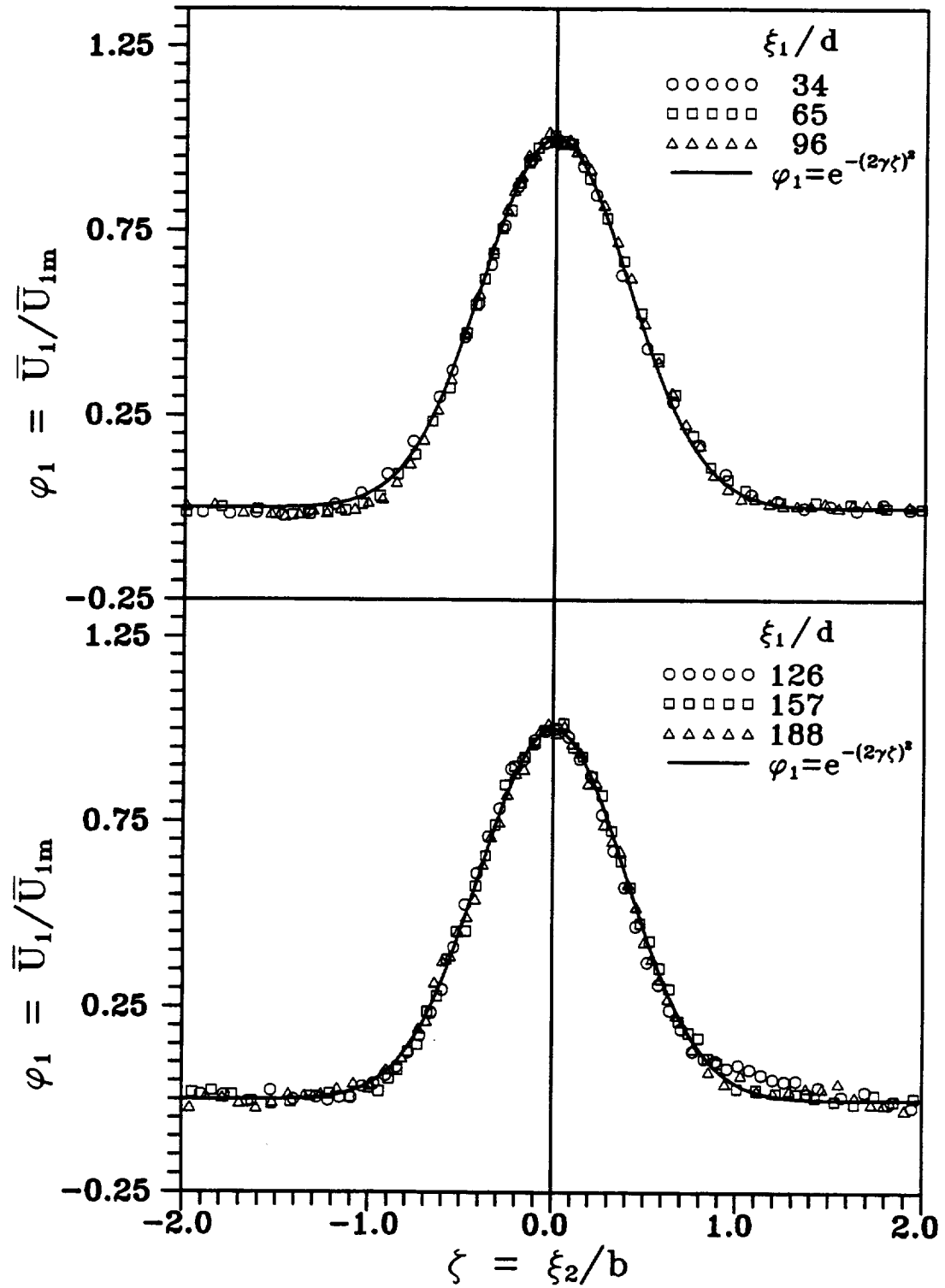
Fig. 46 Transverse distribution of velocity defect at different streamwise positions and under positive streamwise pressure gradient, ξ_1/d = 34 to 188
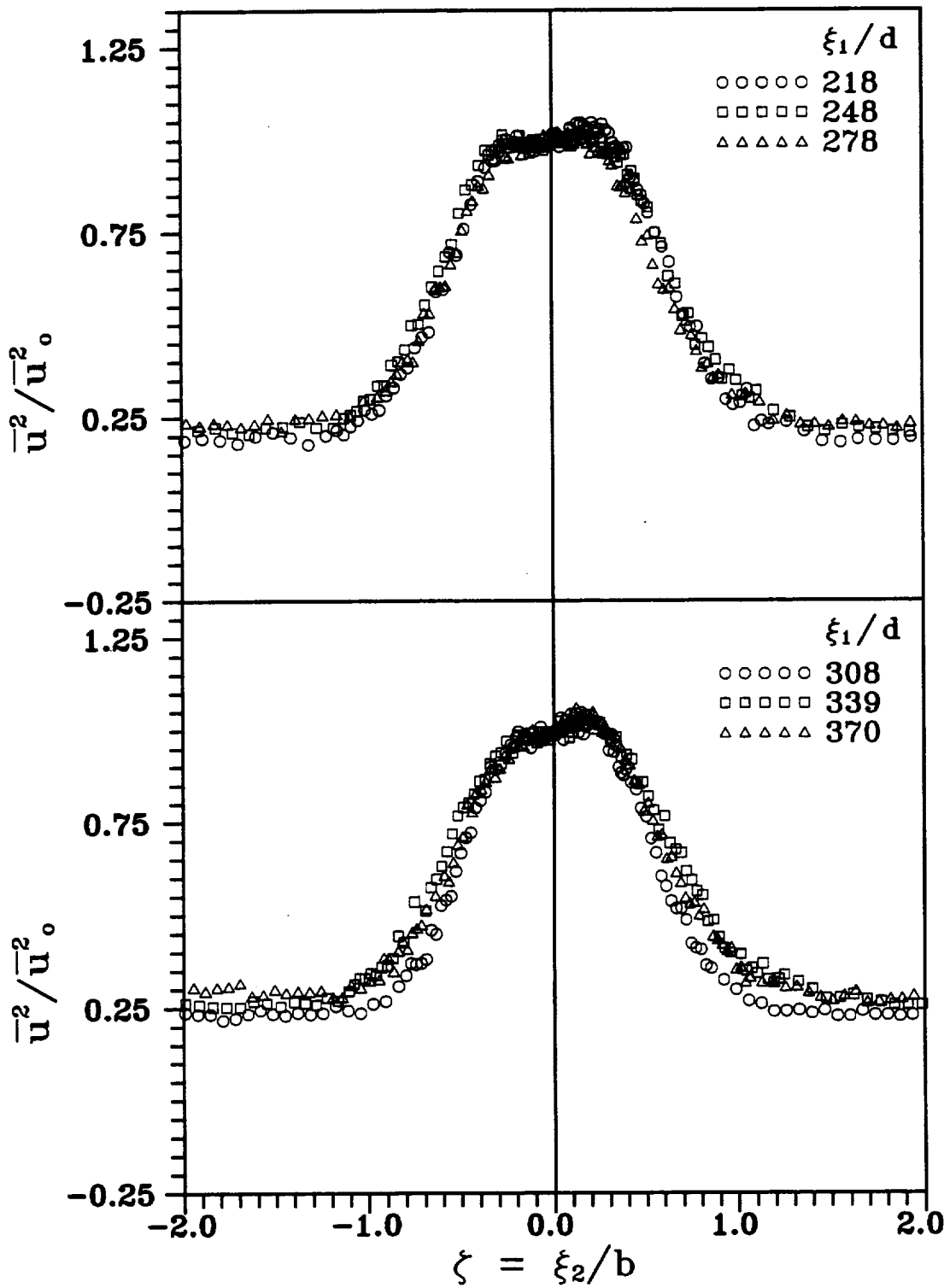
Fig. 47 Transverse distribution of velocity defect at different streamwise positions and under positive streamwise pressure gradient, ξ_1/d = 219 to 377
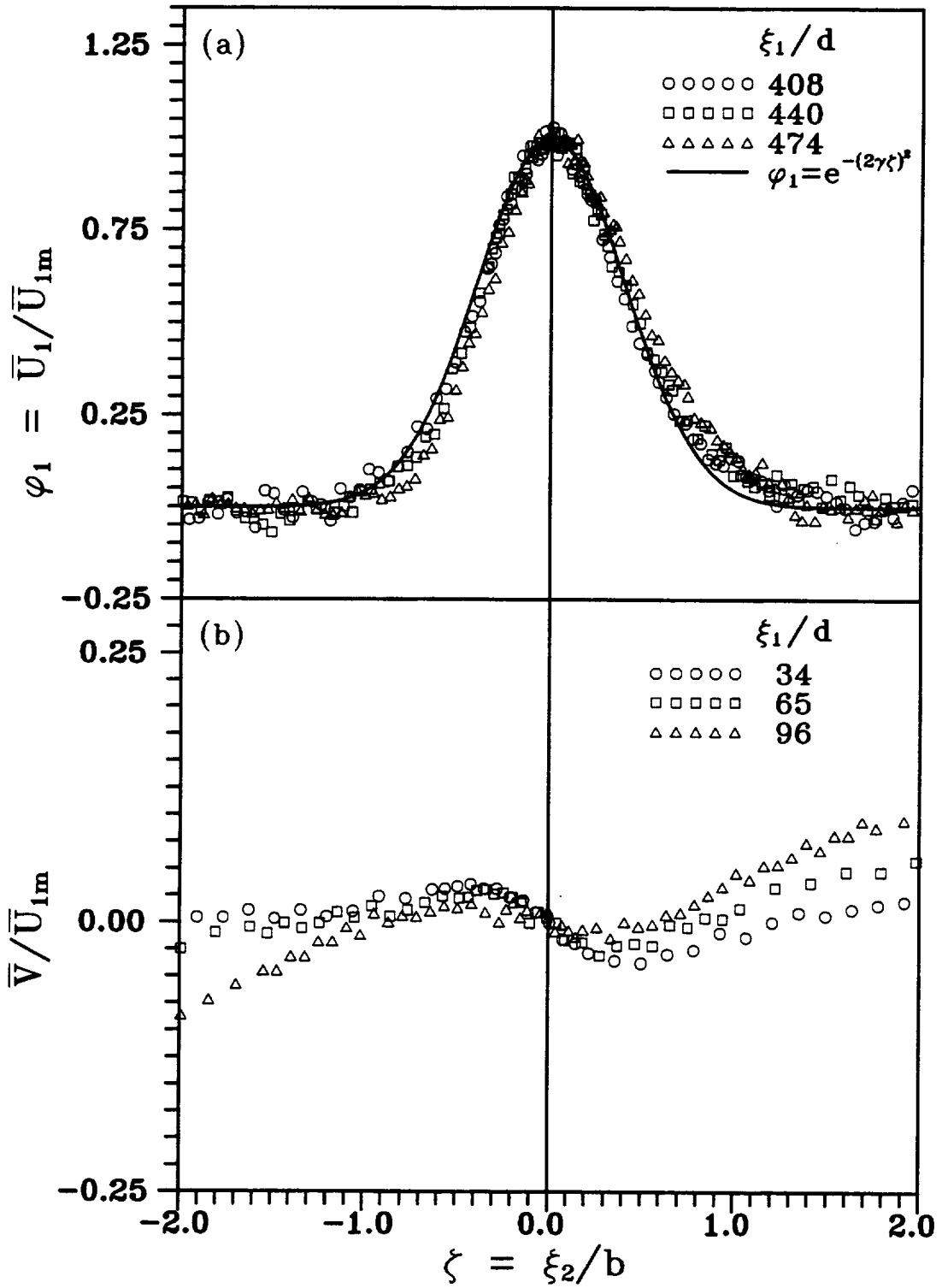
Fig. 48 Transverse distributions of velocity defect (a) and normal velocity (b) at positive streamwise pressure gradient, (a) ξ_1/d = 408 to 474, (b) ξ_1/d = 34 to 96
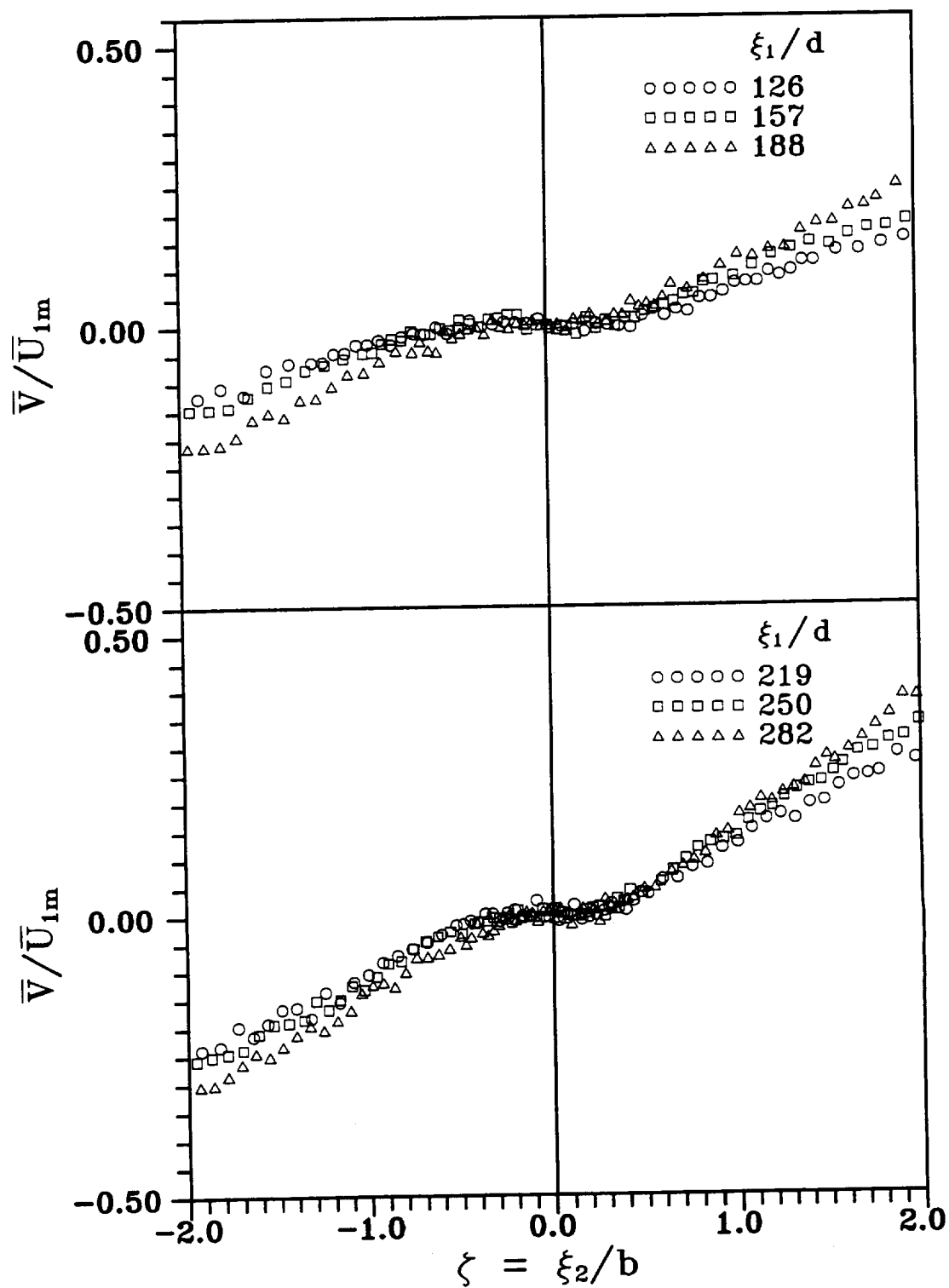
Fig. 49 Transverse distributions of normal velocity at different streamwise positions and under positive streamwise pressure gradient, ξ_1/d = 126 to 282
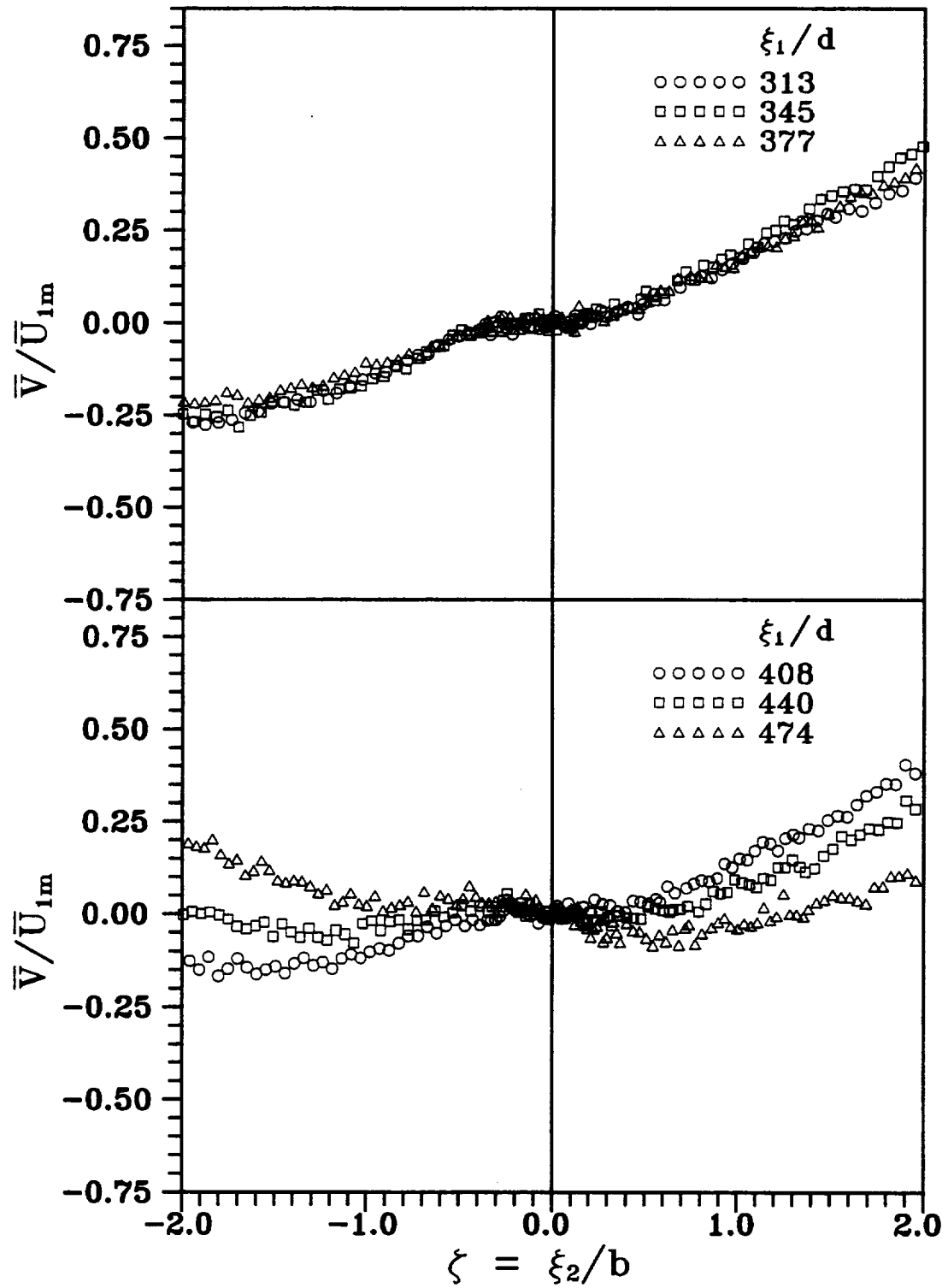
Fig. 50 Transverse distributions of normal velocity at different streamwise positions and under positive streamwise pressure gradient, ξ_1/d = 313 to 474

The Reynolds normal stresses are normalized with respect to its value at the wake center. Table 7 (Appendix A) gives the values of Reynolds normal stresses at the wake center at different downstream locations. The normalized Reynolds stress component in the streamwise direction are shown in Figs. 51-53(a). In comparison with straight wake data, the present result exhibits an asymmetric feature due to the curvature of the wake path. The radius of curvature of the wake centerline, shown in Fig. 22(b), is positive in the negative ξ_2 direction. For the measurements at all streamwise locations, the gradient of streamwise velocity in the positive radial direction is negative on the inner half of the wake. As opposed to this, the gradient of streamwise velocity in the positive radial direction is positive in the outer half of the wake. Therefore, the turbulent stresses should be higher on the inner half of the wake than in the outer half of the wake. This is the case for all measurement locations except for the first two measurement locations. As explained for the zero pressure gradient curved wake, this may be due to the varying streamwise pressure gradient existing at the inlet of the curved channel. The asymmetric nature of the streamwise component of Reynolds stress is qualitatively similar to the results obtained for the zero pressure gradient curved wake. In the positive pressure gradient case, the asymmetry of the streamwise component of Reynolds stress also increases with the downstream location.

Figure 53(b)-55 show the transverse distribution of the transverse component of Reynolds stresses. Similar to the streamwise component, the maximum value of the transverse component of Reynolds stress occurs at the inner half of the wake. The asymmetry of the transverse component of Reynolds stress is more than the streamwise component.

The transverse distribution of Reynolds shear stress at various streamwise location are plotted in Figs. 56-58. The Reynolds shear stress is nondimensionalized by the square of the maximum velocity defect. The Reynolds shear stress distribution shows the strong asymmetry due to the curvature. The nature of curvature of the wake centerline and the gradient of streamwise velocity suggest a higher value of Reynolds shear stress on the inner half of the wake. This is observed at every streamwise location except for the first two measurement locations, where, as previously explained,
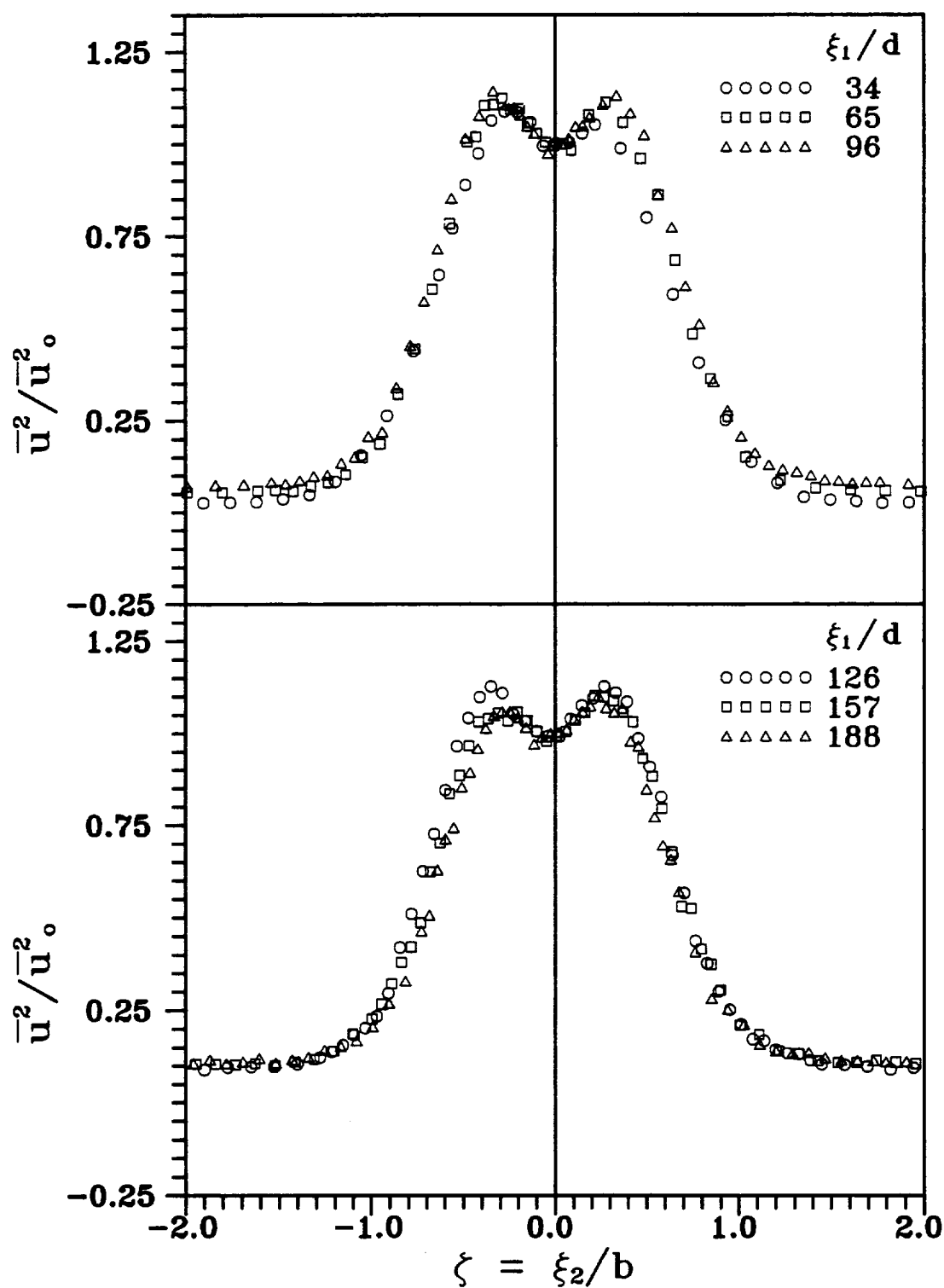
Fig. 51 Transverse distribution of streamwise component of Reynolds normal stress at different streamwise positions and under positive streamwise pressure gradient, ξ_1/d = 34 to 188

Fig. 52 Transverse distribution of streamwise component of Reynolds normal stress at different streamwise positions and under positive streamwise pressure gradient, ξ_1/d = 219 to 377
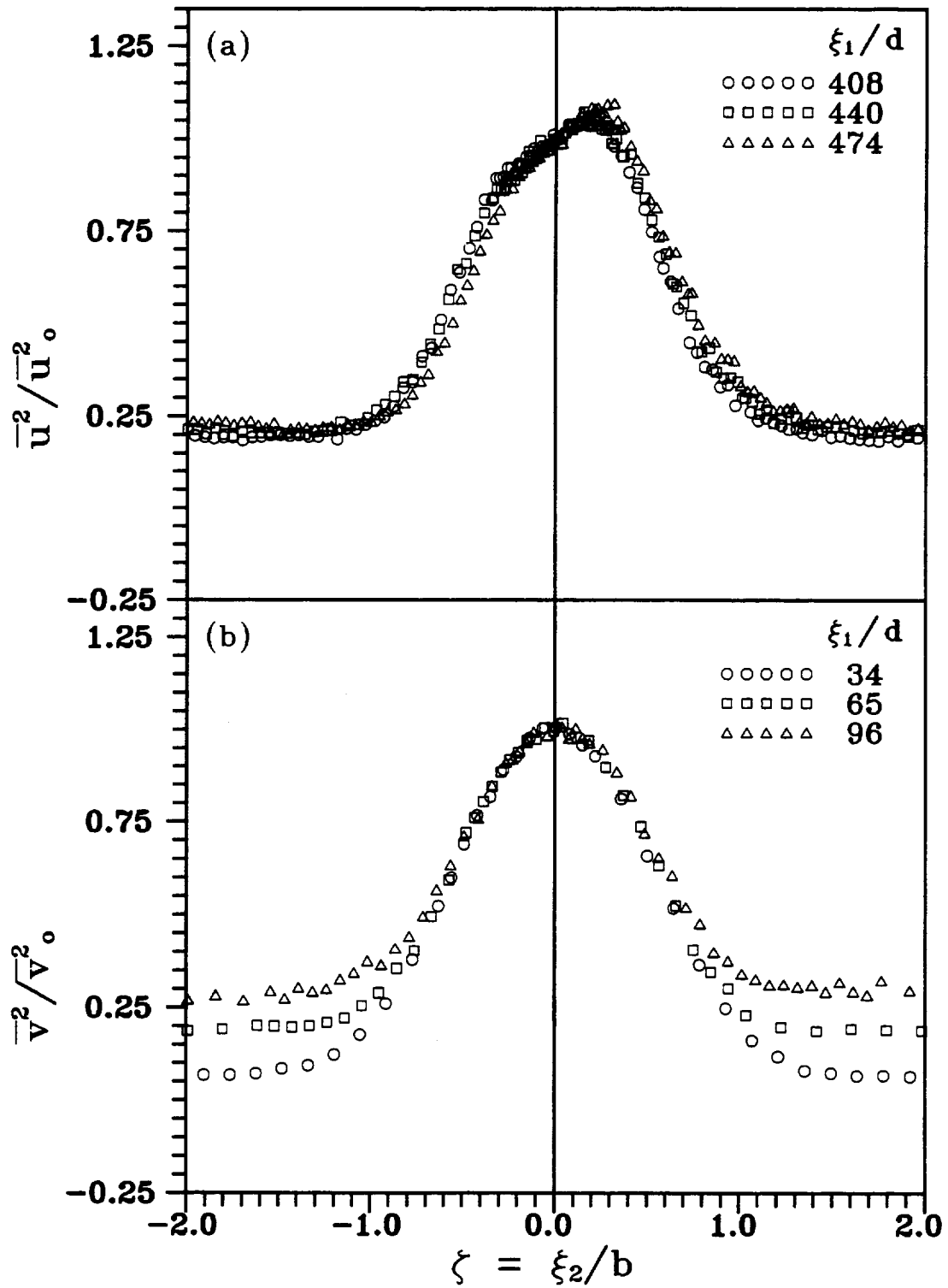
Fig. 53 Transverse distributions of streamwise (a) and normal(b) components of Reynolds normal stress at positive streamwise pressure gradient, (a) ξ_1/d = 408 to 474, (b) ξ_1/d = 34 to 96
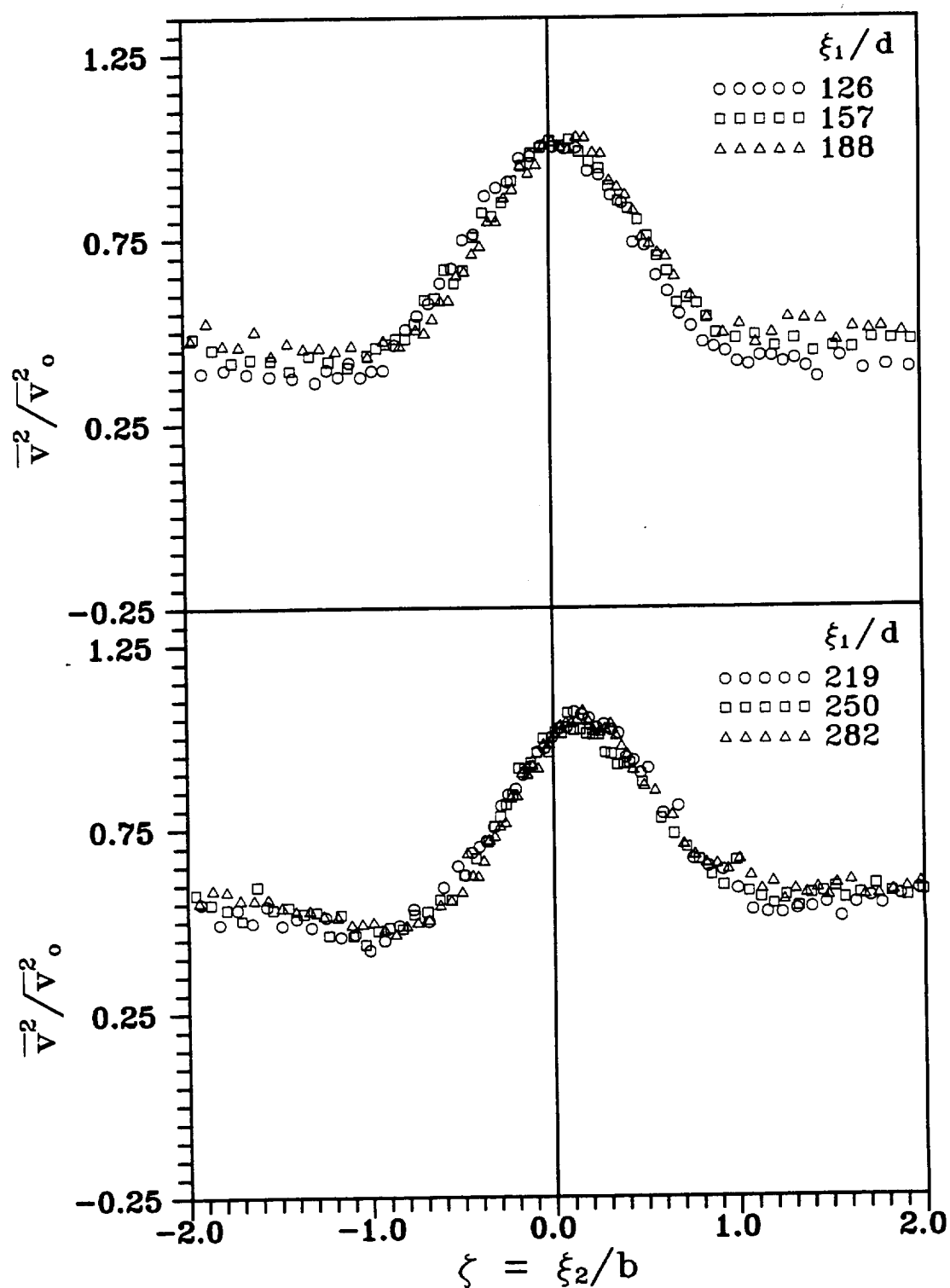
Fig. 54 Transverse distribution of normal component of Reynolds normal stress at different streamwise positions and under positive streamwise pressure gradient, ξ_1/d = 126 to 282
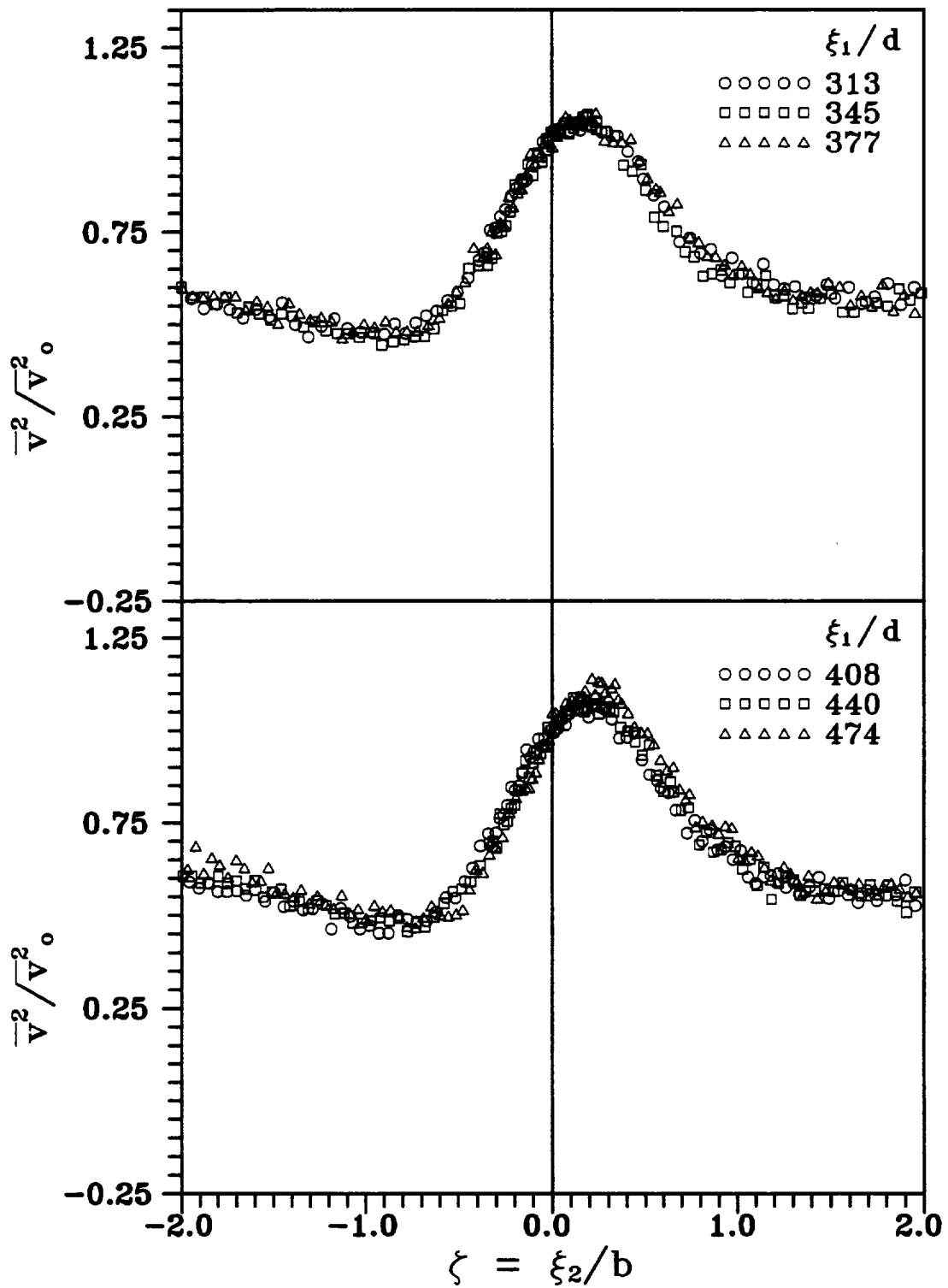
Fig. 55 Transverse distribution of normal component of Reynolds normal stress at different streamwise positions and under positive streamwise pressure gradient, ξ_1/d = 313 to 474
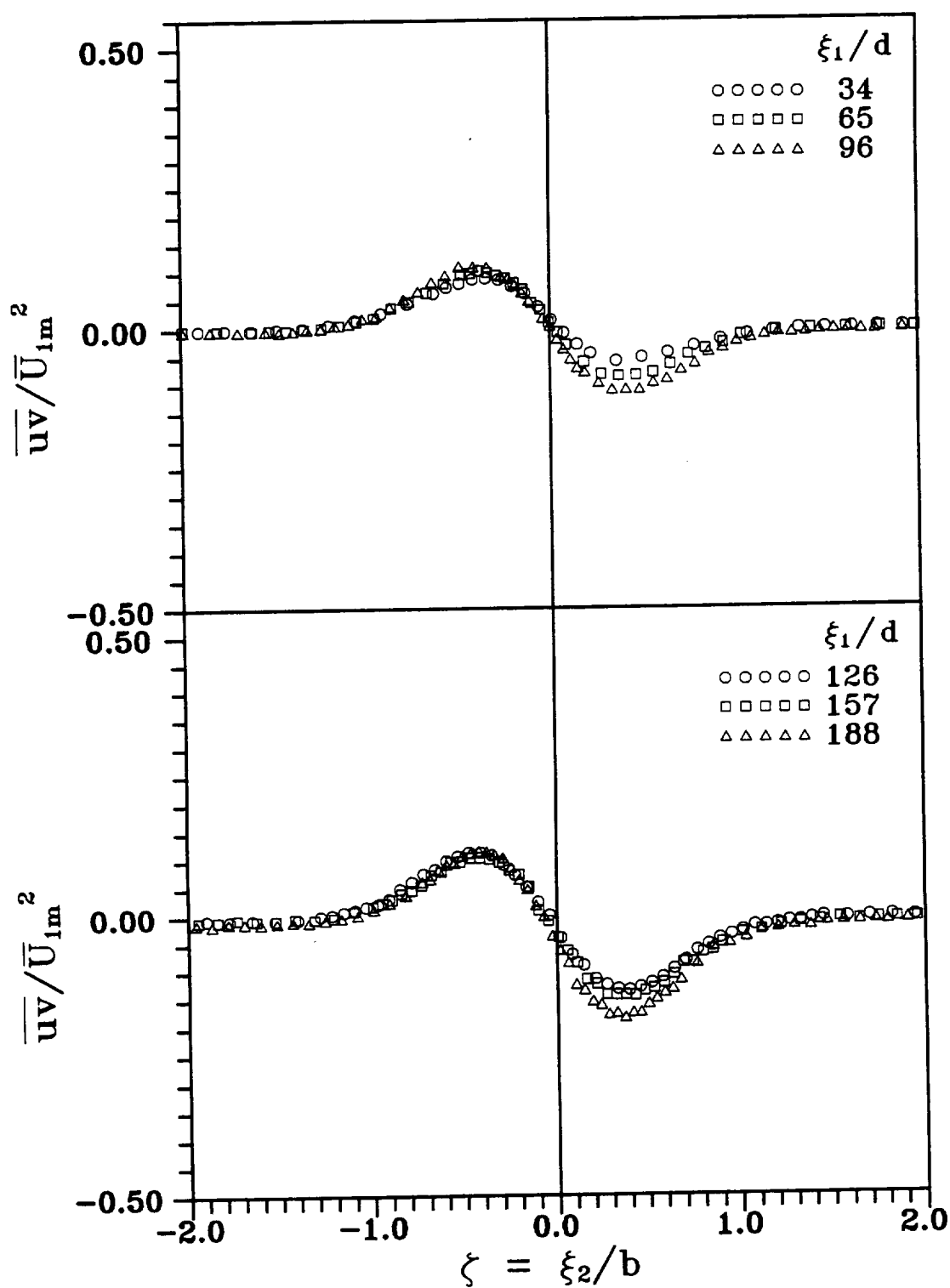
Fig. 56 Transverse distribution of Reynolds shear stress at different streamwise positions and under positive streamwise pressure gradient, ξ_1/d = 34 to 188
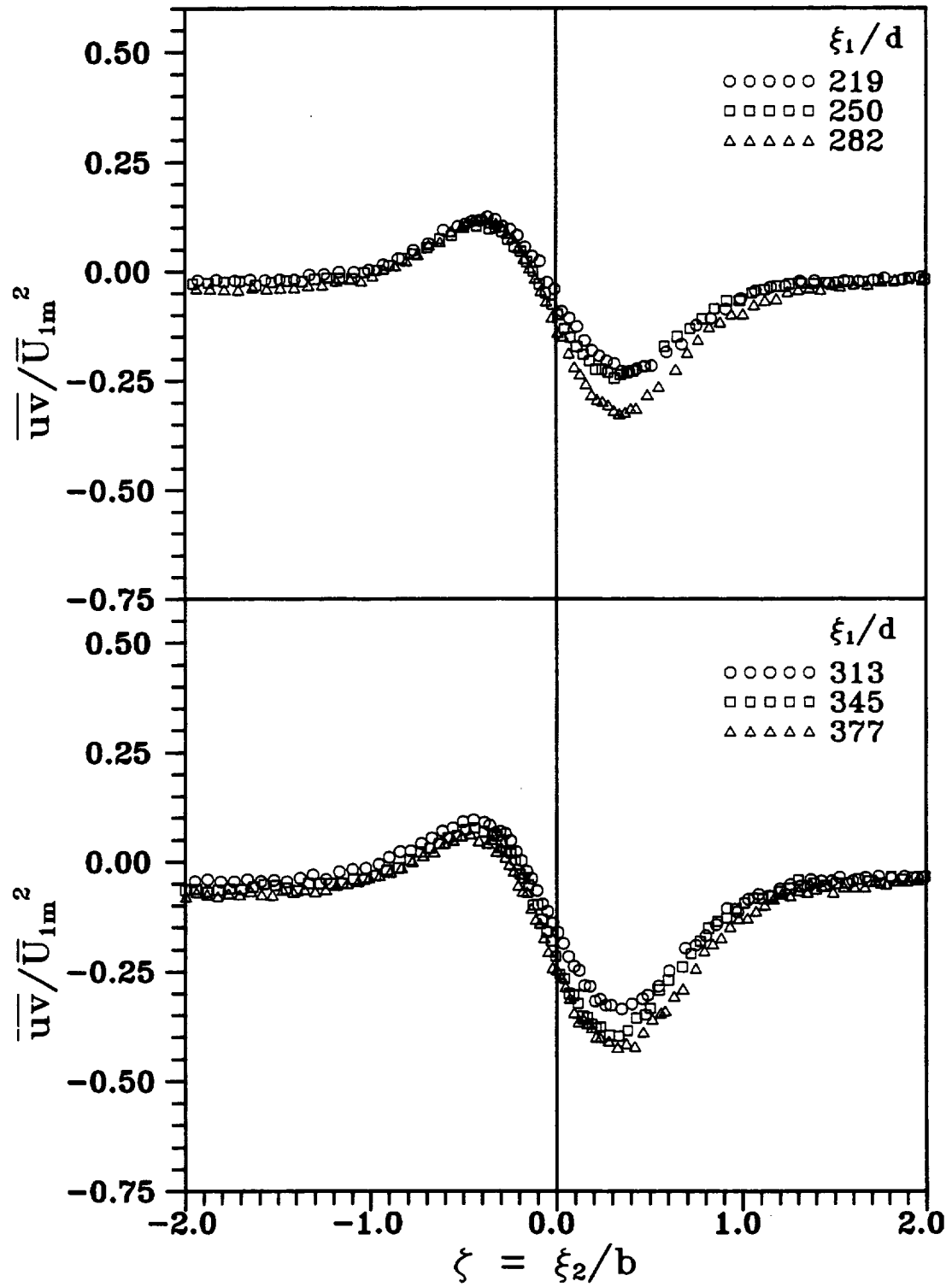
Fig. 57 Transverse distribution of Reynolds shear stress at different streamwise positions and under positive streamwise pressure gradient, ξ_1/d = 219 to 377
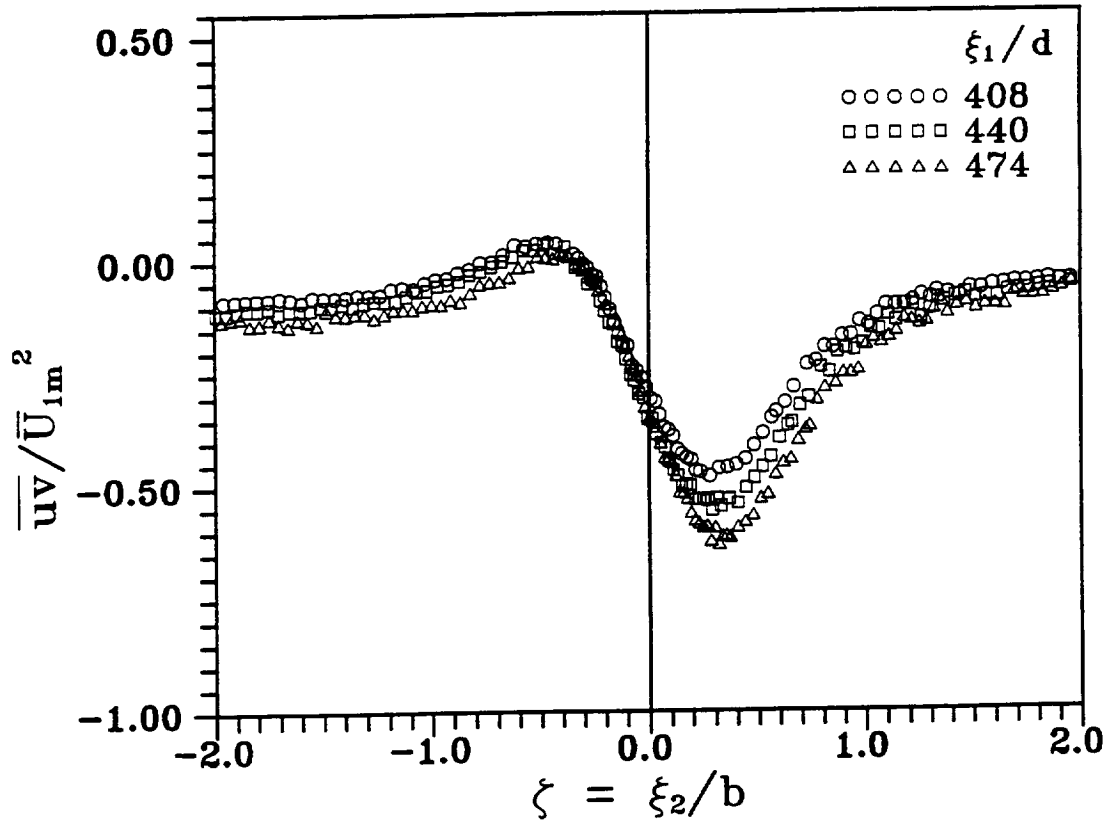
Fig. 58 Transverse distribution of Reynolds shear stress at different streamwise positions and under positive streamwise pressure gradient, ξ_1/d = 408 to 474

the pressure gradient dominates over the curvature effect. It appears that the Reynolds shear stress distribution in the outer half of the wake is closer to a self preservation state than the inner half of the wake. The Reynolds shear stress is not equal to zero either at the center or outside the edges of the wake.

8.2.4. Vorticity, Correlation Coefficient, and Turbulent Kinetic Energy

Figure 59 shows the transverse distributions of normalized vorticity for streamwise locations from ξ_1/d = 34 to 250. The mean vorticity is normalized by $\overline{U}_{1m}/b$. Similar to the results of zero pressure gradient straight and curved wakes, the mean vorticity

profiles for the present case are almost antisymmetric with respect to the wake center. Therefore, the effect of curvature and pressure gradient on mean vorticity profiles in Fig. 59 can be considered small. The near zero value of vorticity in the region outside the wake suggests that the mean flow is mostly irrotational in that region. As mentioned in section 8.1.4, the calculation of vorticity involves the determination of transverse gradient of velocity, which introduces scatter in the value of vorticity particularly at farther downstream locations.

Figures 60 and 61 show the transverse distribution of the correlation coefficient at different streamwise locations. The distribution of correlation coefficient is asymmetric with higher absolute values at the inner half of the wake. The maximum absolute value of correlation coefficient at the inner half of the wake remains constant from $\xi_1/d = 126$ onwards. However, the maximum absolute value of correlation coefficient at the outer half of the wake decreases with downstream distance and reaches close to zero at $\xi_1/d = 474$. The value of correlation coefficient at the outer half of the wake for the positive pressure gradient is approximately the same as the value for the zero pressure gradient curved wake. However, for the inner half of the wake, the absolute value of the correlation coefficient has slightly higher value at positive pressure gradient than at zero pressure gradient, especially at higher downstream locations.

Figure 62 shows the transverse distribution of turbulent kinetic energy normalized by the square of mean velocity defect. The turbulent kinetic energy distribution is asymmetric with respect to the wake center with higher values at the inner half of the wake. The normalized turbulent kinetic energy increases with downstream location. This is because the turbulent kinetic energy decays at a slower rate than the mean velocity defect. At a particular streamwise location, the normalized kinetic energy has a lower value at positive pressure gradient than at zero pressure gradient.

8.3. Wake Development at Negative Pressure Gradient

An X-hot-film probe measured the wake behind a stationary cylinder of 1.984-mm diameter with the cylinder located at mid height of the wake generating section. The

Fig. 59 Transverse distribution of mean vorticity at different streamwise positions and under positive streamwise pressure gradient

Fig. 60 Transverse distribution of correlation coefficient at different streamwise positions and under positive streamwise pressure gradient, ξ_1/d = 34 to 250
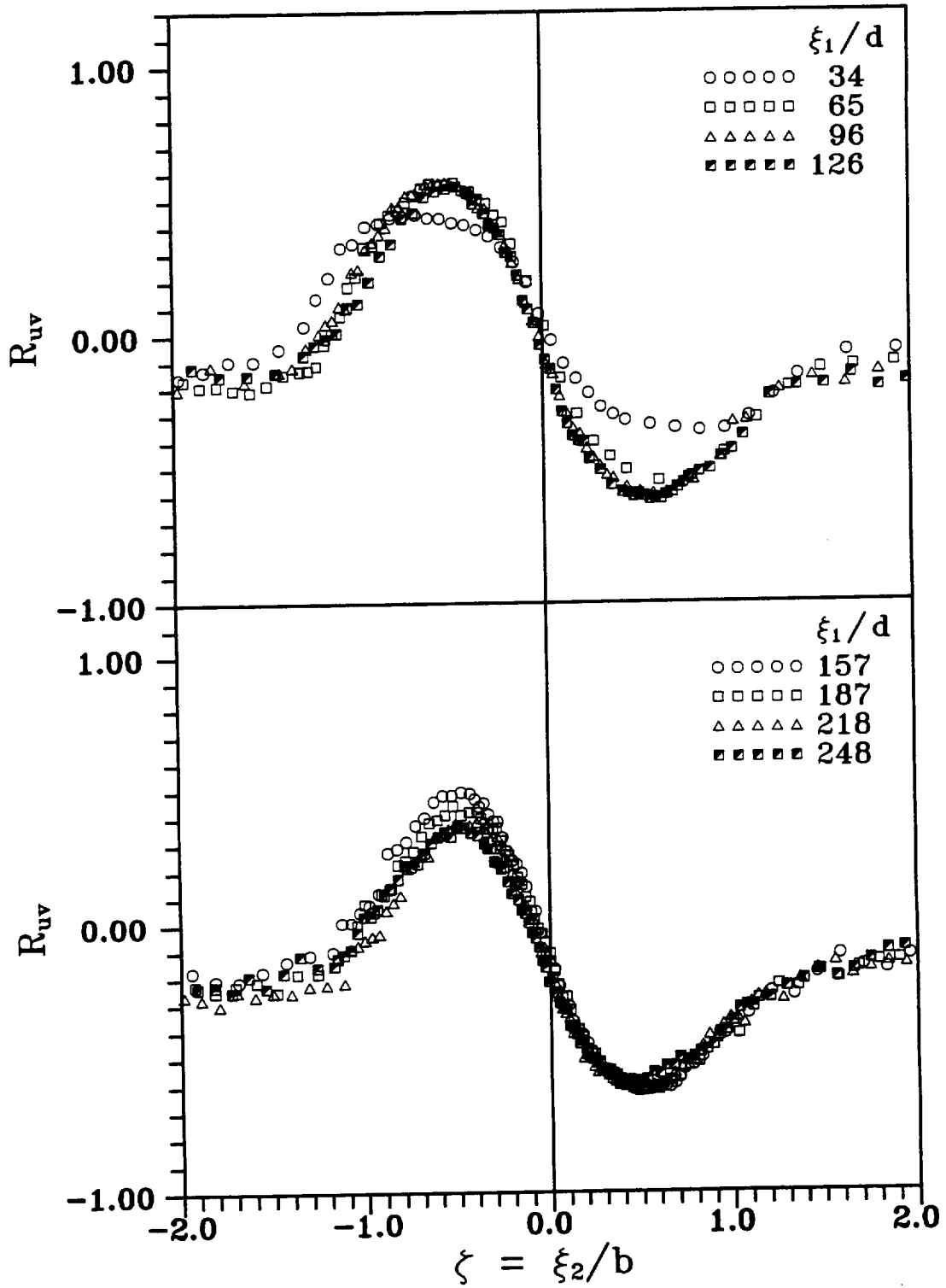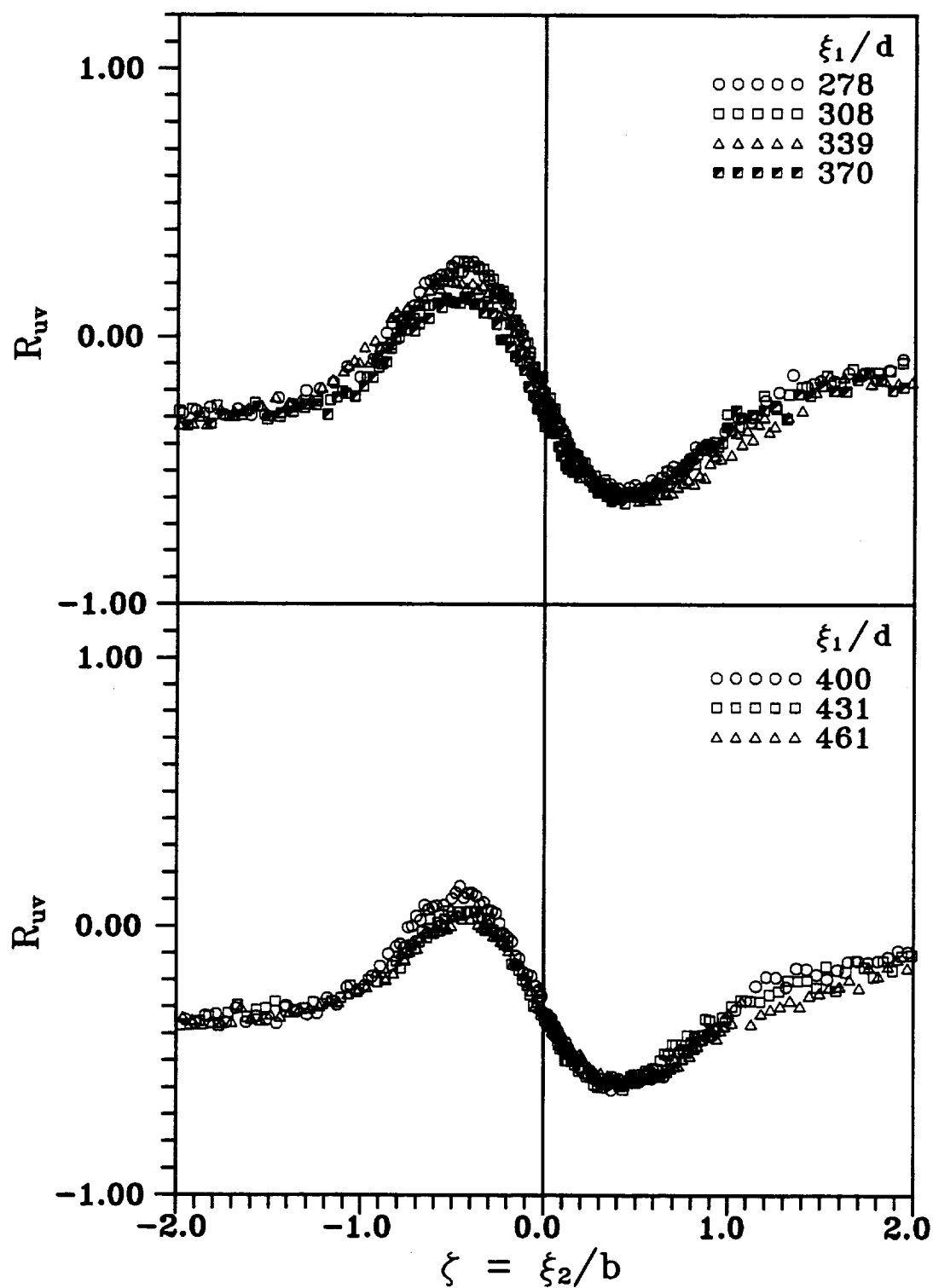
Fig. 61 Transverse distribution of correlation coefficient at different streamwise positions and under positive streamwise pressure gradient, ξ_1/d = 282 to 474

curved channel test section had an inlet to exit area ratio of 1.3. The wake profiles were obtained in 5° intervals at thirteen angular positions from $\theta = 0°$ to $60°$. Measurements at angular positions beyond $60°$ were not carried out since the ratio of velocity defect to potential velocity was very small. The first measuring station $\theta = 0°$ is at a distance of 67-mm downstream of the wake generating cylinder.

8.3.1. Path of Wake Center, Curvature of the Path of Wake Center, and Development of the Wake

Figure 22(a) shows the radial distance from the convex wall to the wake center, denoted by r-r_i, at various streamwise positions. As the wake propagates through the channel, the trajectory of the wake center gradually moves toward the convex wall for all the measurement locations used for the negative pressure gradient case. The maximum inclination between the trajectory of the wake center and the tangential direction x was less than $7.3°$. Figure 22(b) shows the local curvature of the wake centerline. The changes in the local radius of curvature are almost similar to the zero pressure gradient wake. As mentioned before, the negative value of K indicates that the curvature of the wake centerline is concave in the positive ξ_2 direction.

Figure 23(a) shows the decay of maximum velocity defect normalized by the potential velocity at wake center $\bar{U}_{po}$. The solid line represent a power law fit with $\bar{U}_{1m}/\bar{U}_{po} \sim (\xi_1/d)^{-0.90}$. Therefore, the decay rate of maximum velocity defect in the negative pressure gradient curved channel is faster than the zero pressure gradient curved channel. Figure 23(b) shows the wake width b nondimensionalized by the diameter of the wake generating rod as a function of ξ_1/d with the solid line being the power law fit with $b/d \sim (\xi_1/d)^{0.57}$. Therefore, the spreading rate of b in the negative pressure gradient curved wake is lower than that in the zero pressure gradient curved wake.

Figure 24(a) shows the distribution of hypothetical potential velocity at the wake center nondimensionalized by the freestream velocity just upstream of the wake generating rod as a function of ξ_1/d. Of course, the increasing hypothetical potential

Fig. 62 Transverse distribution of turbulent kinetic energy at different streamwise positions and under positive streamwise pressure gradient

velocity distribution along the wake centerline is due to the converging channel creating the required negative streamwise pressure gradient. Figure 24(b) shows the pressure coefficient C_p ($C_p = (p - p_{in})/\frac{1}{2}\rho V_{in}^2$) at the wake center at various streamwise locations.

The pressure coefficient, calculated by the method explained in section 8.1.1, decreases with downstream distance, which confirms the negative pressure gradient. Also, the momentum thickness ratio C_w plotted in Fig. 25(a) decreases with the downstream location. The solid line in Fig. 25(a) is obtained from Eq. (8.8) and agrees with the values obtained from the velocity profile using numerical integration. Figure 25(b) shows the variation of shape factor H_{12} with downstream distance from the wake generating cylinder. Similar to the zero pressure gradient straight wake, the shape factor approaches unity for far wakes. The rate at which the shape factor approaches unity is slightly higher for negative pressure gradient wake than that for zero pressure gradient wake. The solid line in Fig. 25(b) is obtained from the theoretical model represented by Eq. (8.10), and is in close agreement with the values obtained from the mean velocity data by numerical integration. Figure 26 shows the product $\overline{U}_{1m}b$ decreasing with downstream location at various streamwise locations. The values of maximum velocity defect, wake width, potential velocity at wake center, and average velocity upstream of the cylinder at various downstream locations are given in Table 8 (Appendix A).

The wake development in the curved channel at the three streamwise pressure gradients can be characterized with respect to the following wake quantities. The decay of the velocity defect normalized by potential velocity at the wake center is fastest with negative pressure gradient and slowest with the positive pressure gradient. Also, the growth of the wake width is fastest at the positive pressure gradient and slowest at the negative pressure gradient. The momentum thickness ratio as a function of the streamwise distance remains approximately constant at zero pressure gradient, increases at positive pressure gradient, and decreases at negative pressure gradient. The shape factor for all three pressure gradients decreases with streamwise distance and approaches to unity for far wakes. At a particular streamwise location, the shape factor has the

highest value at positive pressure gradient and the lowest value at negative pressure gradient. The product $\bar{U}_{1m}b$ as a function of streamwise location, while remaining approximately constant at zero pressure gradient, increases at positive pressure gradient and decreases at negative pressure gradient.

8.3.2. Mean Velocity Distribution

Figure 63 shows the plots of streamwise component of velocity as a function of the transverse distance for six streamwise locations. The velocity distributions for other streamwise locations are similar to the asymmetric distribution in Fig. 63 with a higher velocity at the positive side of ξ_2. The velocity distribution is asymmetric with respect to the wake center with a higher value on the positive side of ξ_2. As seen from Fig. 63, the wake velocity defect decreases and the wake width increases with downstream location. A close examination of the velocity data points outside the wake for two initial streamwise locations reveals that the increase in potential velocity is not uniform across the channel. This nonuniform increase in potential velocity across the channel, which is due to turning of the flow from a straight section to a curved channel, is dominant up to the streamwise location $\xi_1/d = 65$.

Figures 64 and 65 show the transverse distribution of the mean velocity defect in similarity coordinates. The solid line represents the results for straight wake by Eifler (1975) given by the function φ_1, $\varphi_1 = \bar{U}_1/\bar{U}_{1m} = e^{-(2\eta\zeta)^2}$. The mean velocity defect profiles are symmetric and almost identical to the straight wake, except that they are slightly wider on the inner side of the wake. This small deviation from the straight wake data is clearer at higher streamwise locations and near the edges of the wake. In general, it may be considered that the effect of curvature on the mean velocity defect distribution is small. The high scatter of normalized velocity defect at higher downstream locations is because the maximum velocity defect is very small at these locations.

Figures 66 and 67 show the plots of the transverse distribution of normalized
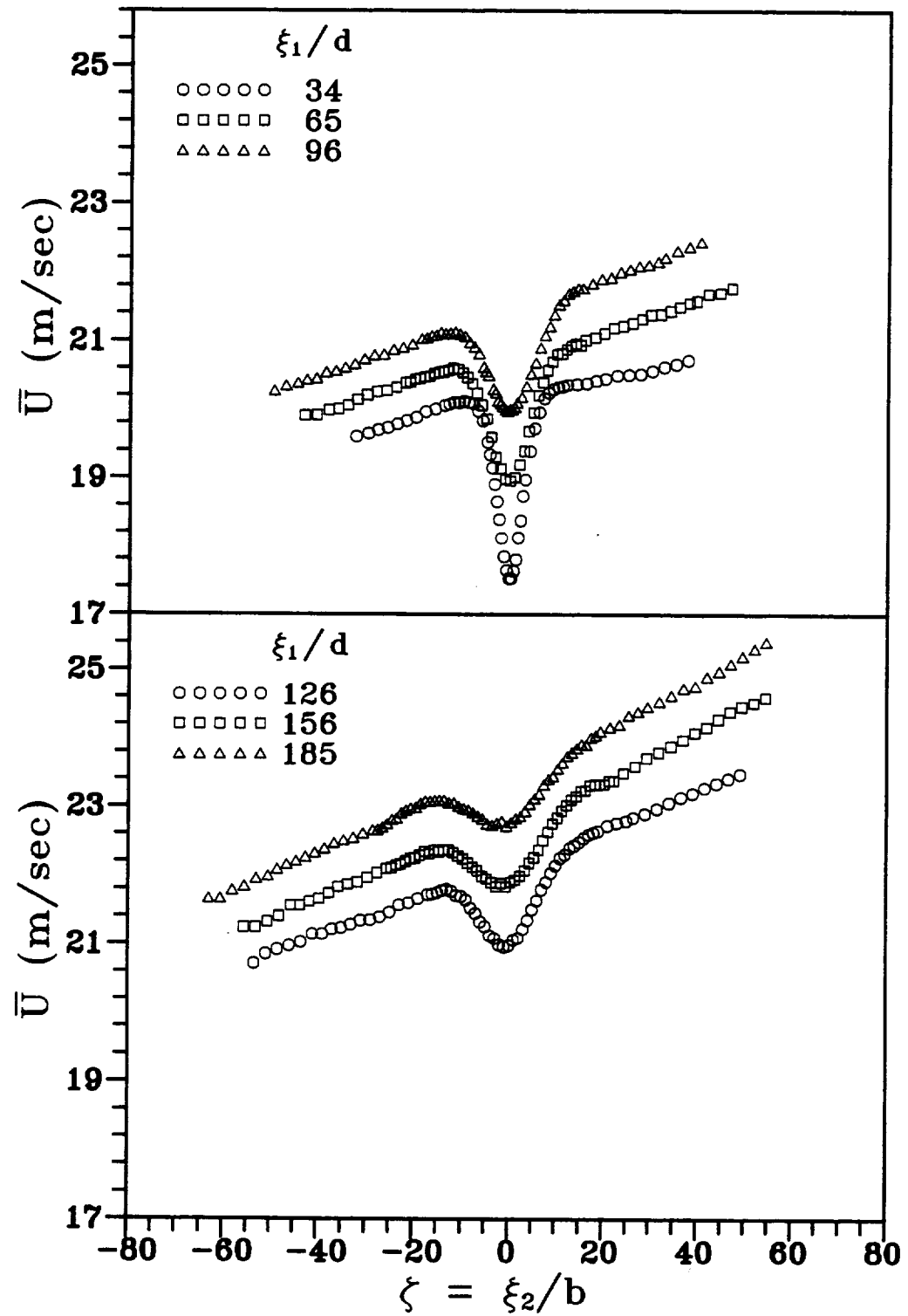
Fig. 63 Transverse distribution of streamwise component of velocity at different streamwise positions and under negative streamwise pressure gradient
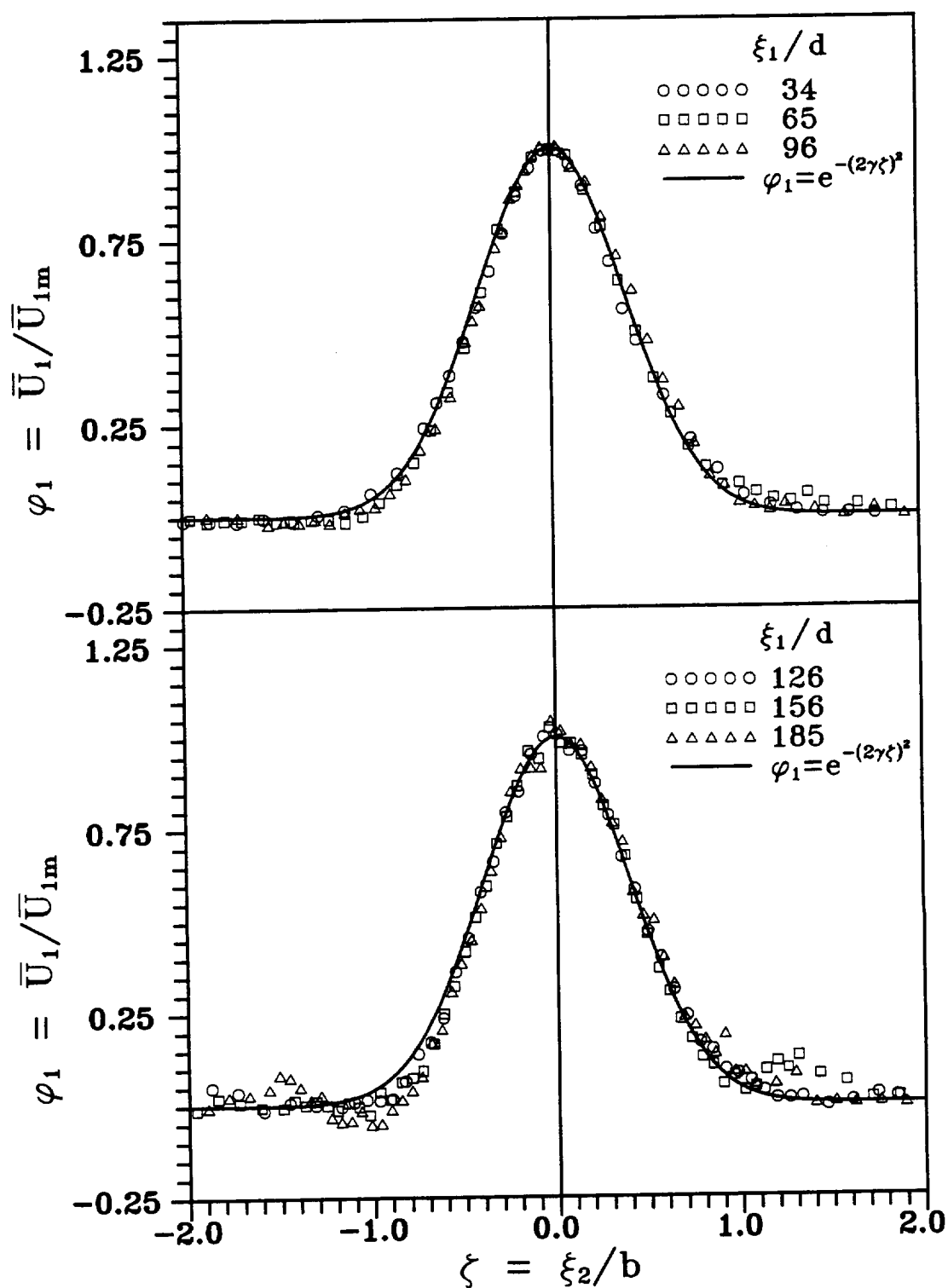
Fig. 64 Transverse distribution of velocity defect at different streamwise positions and under negative streamwise pressure gradient, ξ_1/d = 34 to 185
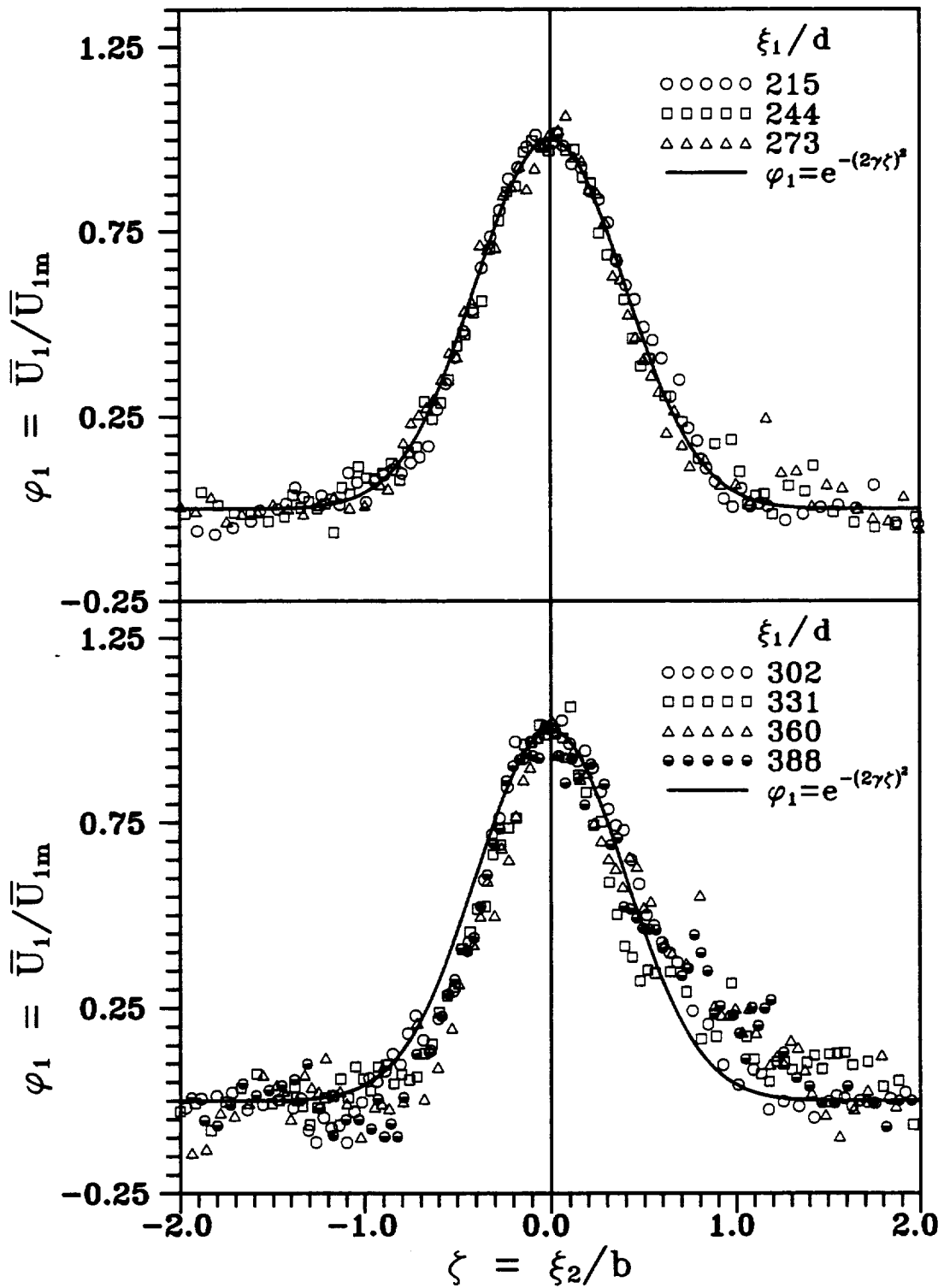
Fig. 65 Transverse distribution of velocity defect at different streamwise positions and under negative streamwise pressure gradient, ξ_1/d = 215 to 388
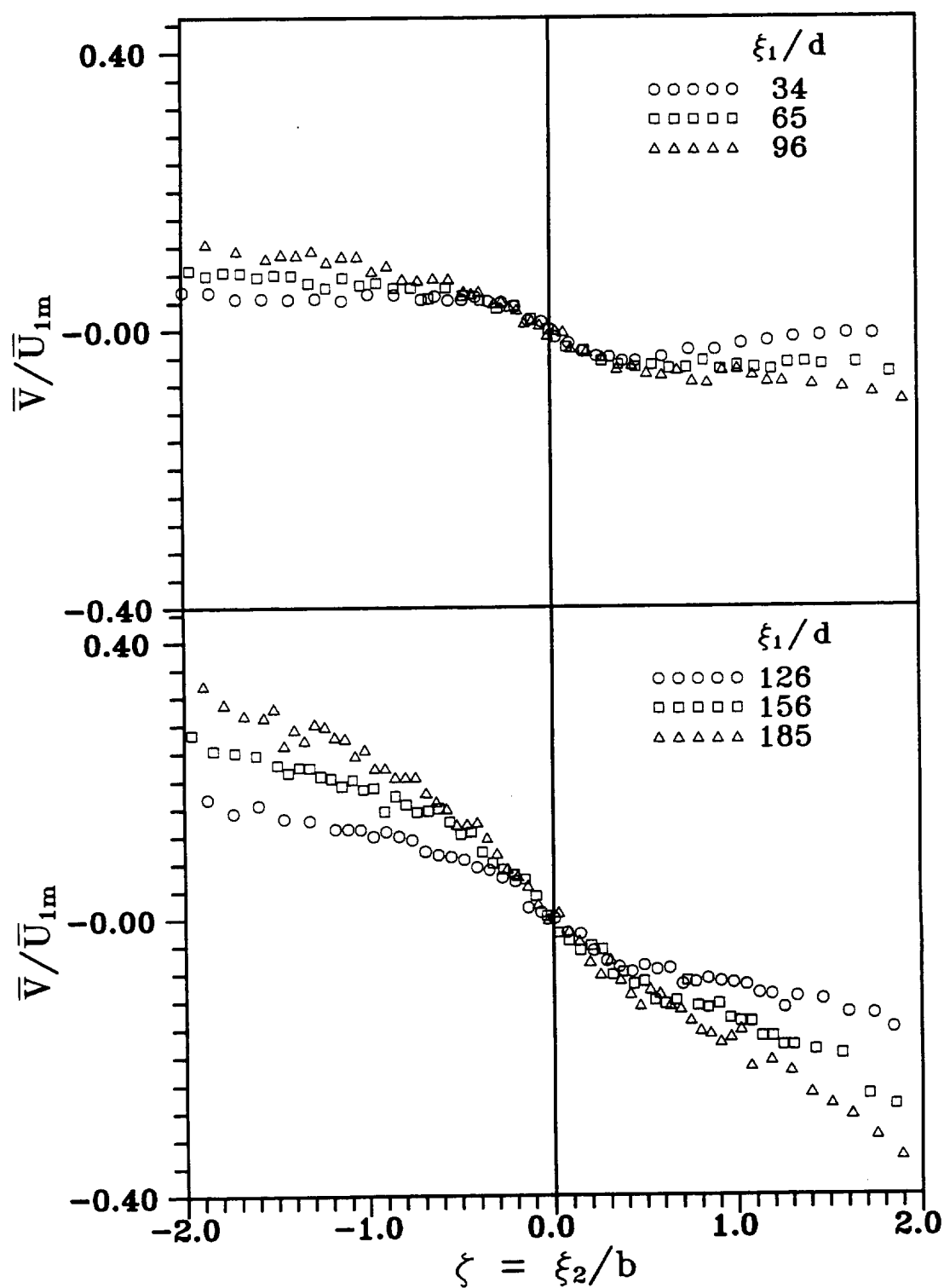
Fig. 66 Transverse distributions of normal velocity at different streamwise positions and under negative streamwise pressure gradient, ξ_1/d = 34 to 185
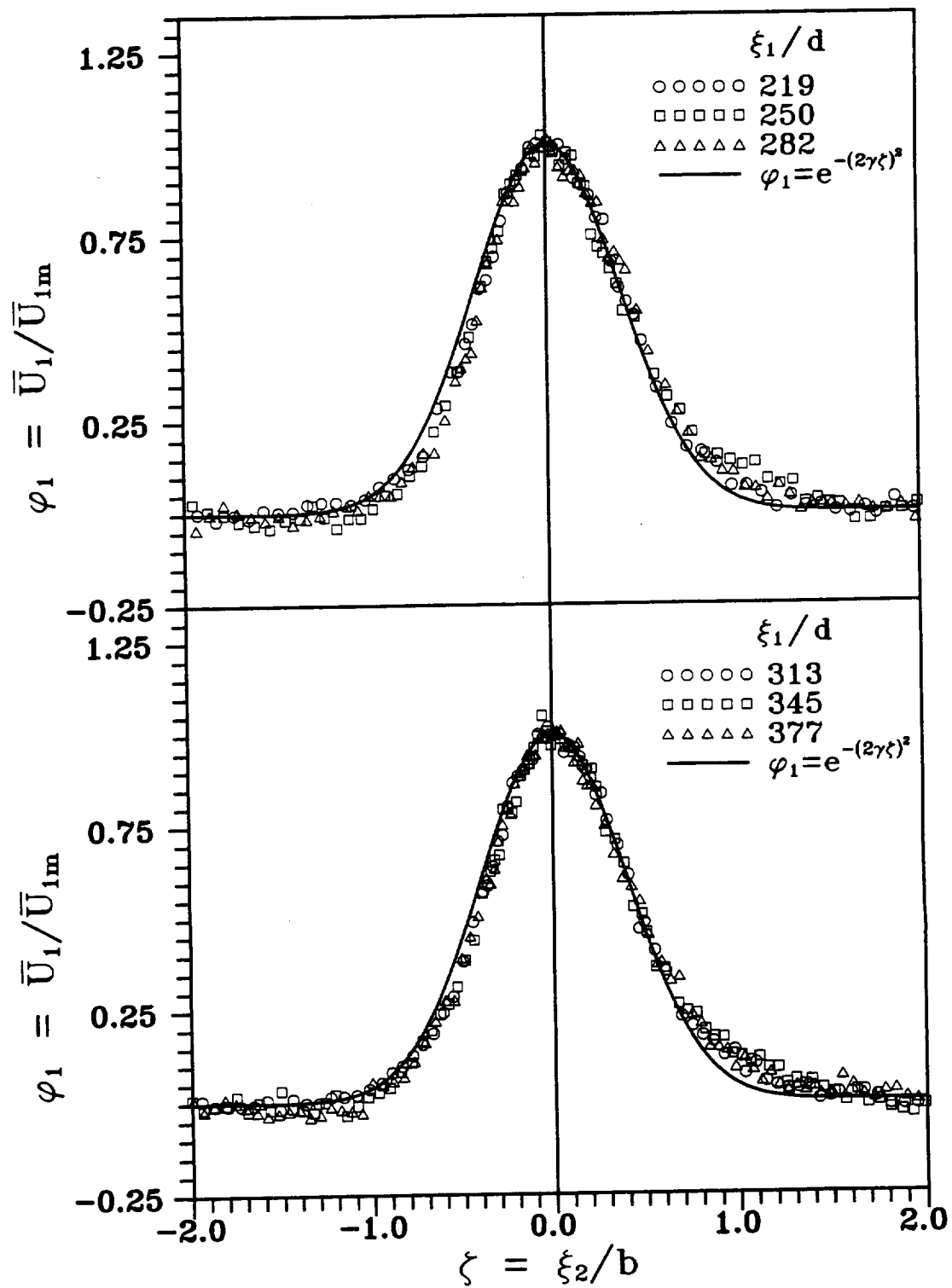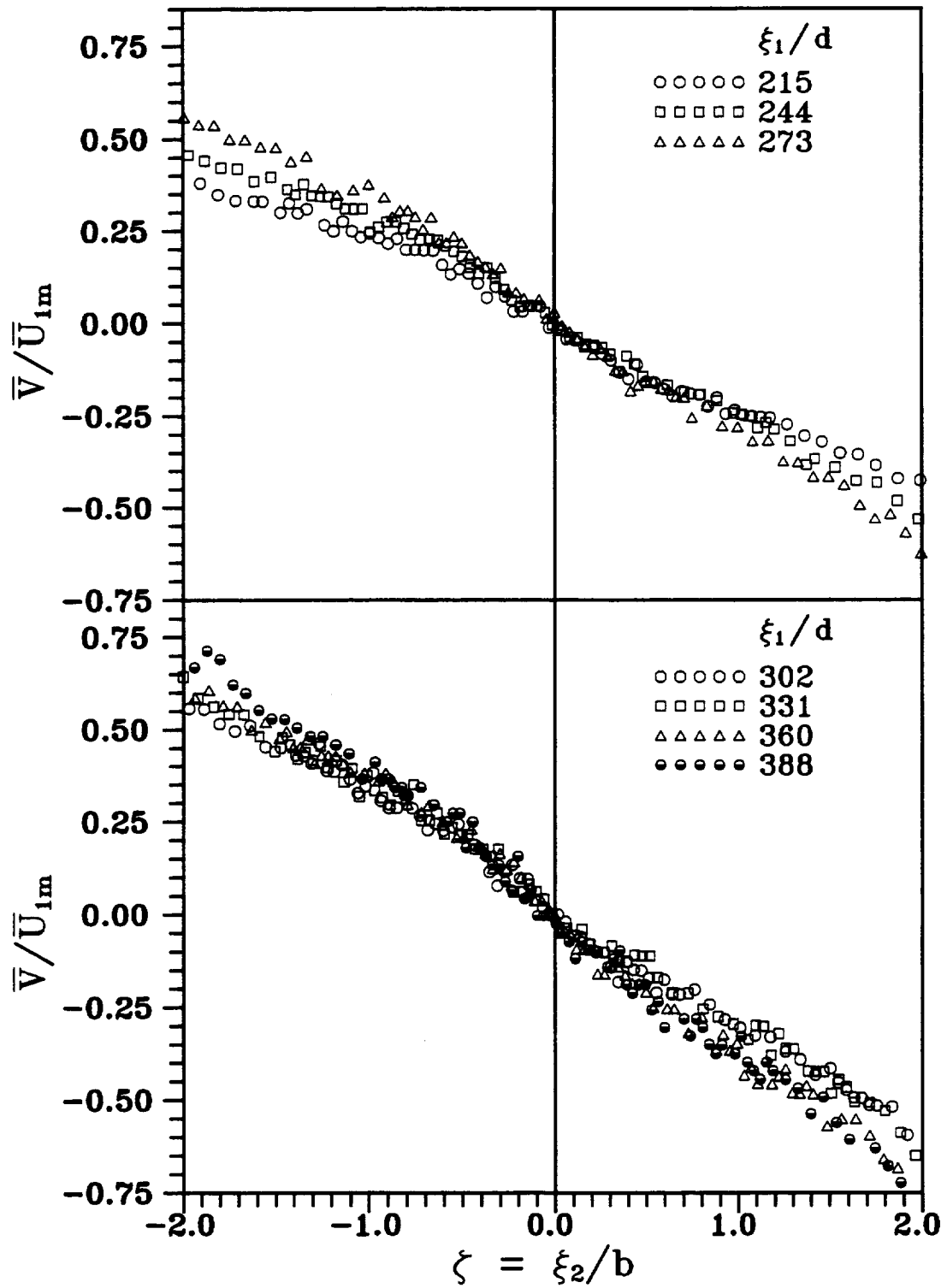
Fig. 67 Transverse distributions of normal velocity at different streamwise positions and under negative streamwise pressure gradient, ξ_1/d = 215 to 388

transverse velocity $\bar{V} / \bar{U}_{1m}$ for various streamwise locations. The transverse velocity distribution can be considered as a superposition of its distribution at zero pressure gradient straight wake on a normalized hypothetical potential distribution of transverse velocity. The profile of the hypothetical potential distribution of $\bar{V}$ will be dictated by the streamwise pressure gradient and streamline curvature. The hypothetical potential distribution of $\bar{V}$ in the wake region is almost linear with a negative slope.

8.3.3. Reynolds Stresses

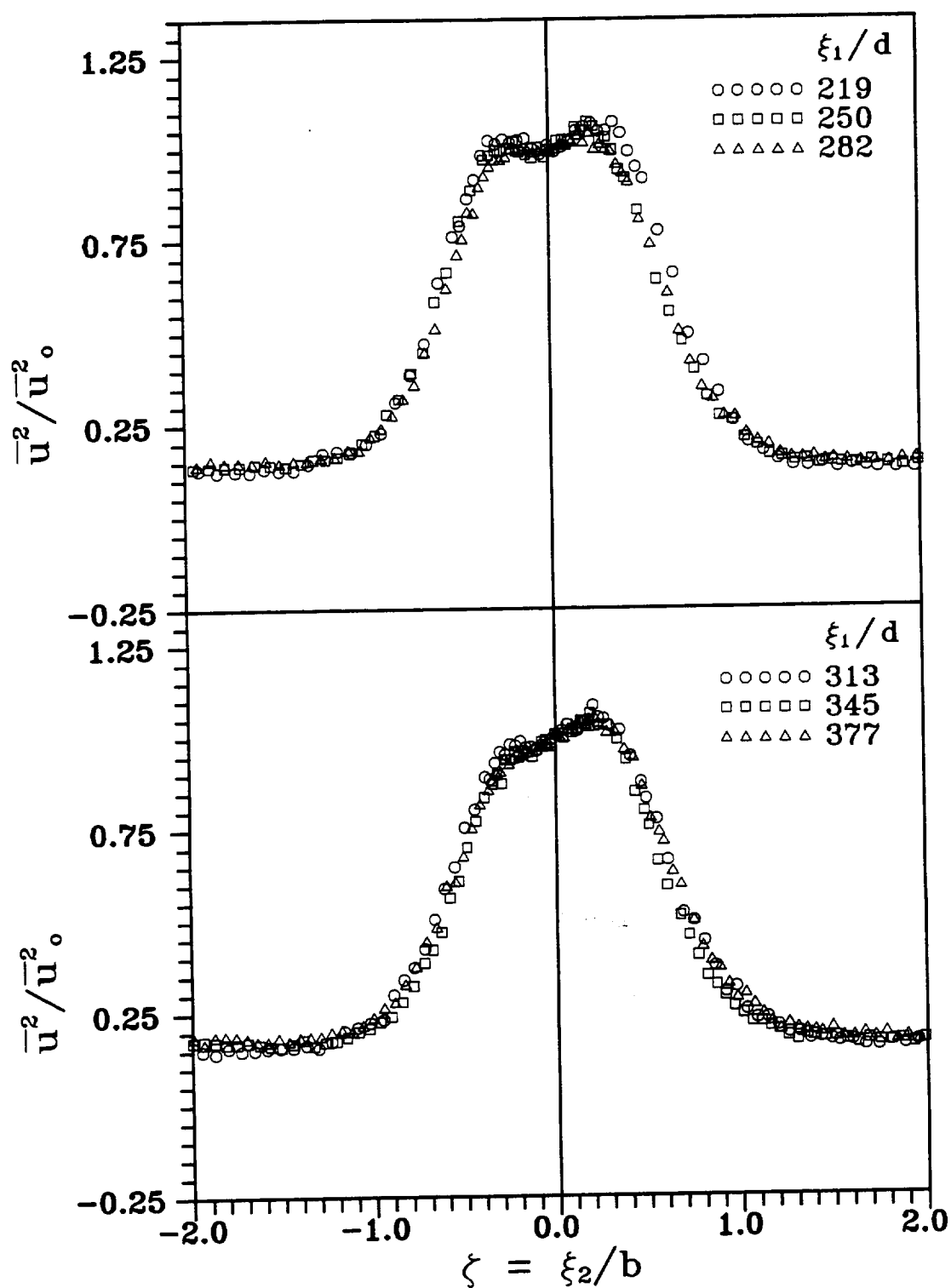The transverse distributions of the normalized Reynolds stresses are shown in Figs. 68-73. The Reynolds normal stresses are normalized with respect to its value at the wake center. Table 8 (Appendix A) gives the values of Reynolds normal stresses at the wake center at different downstream locations. The normalized Reynolds stress component in the streamwise direction is shown in Figs. 68-69. Comparing the straight wake data with the present results exhibits an asymmetric feature due to the curvature of the wake path. The radius of curvature of the wake centerline, shown in Fig. 22(b), is positive in the negative ξ_2 direction. For the measurements at all streamwise locations, the gradient of streamwise velocity in the positive radial direction is negative on the inner half of the wake. In contrast, the gradient of streamwise velocity in the positive radial direction is positive in the outer half of the wake. Therefore, the turbulent stresses should be higher on the inner half of the wake than the outer half of the wake. This is the case for all measurement locations except for the first two measurement locations. As explained for the zero pressure gradient curved wake, this may be due to the different streamwise pressure gradient existing at the inlet of the curved channel. The asymmetric nature of the streamwise component of Reynolds stress is qualitatively similar to the results obtained for the zero pressure gradient curved wake. In the negative pressure gradient case, the asymmetry of the streamwise component of Reynolds stress also increases with the downstream location. However, the asymmetry of the streamwise component appears to be smaller than those in the zero
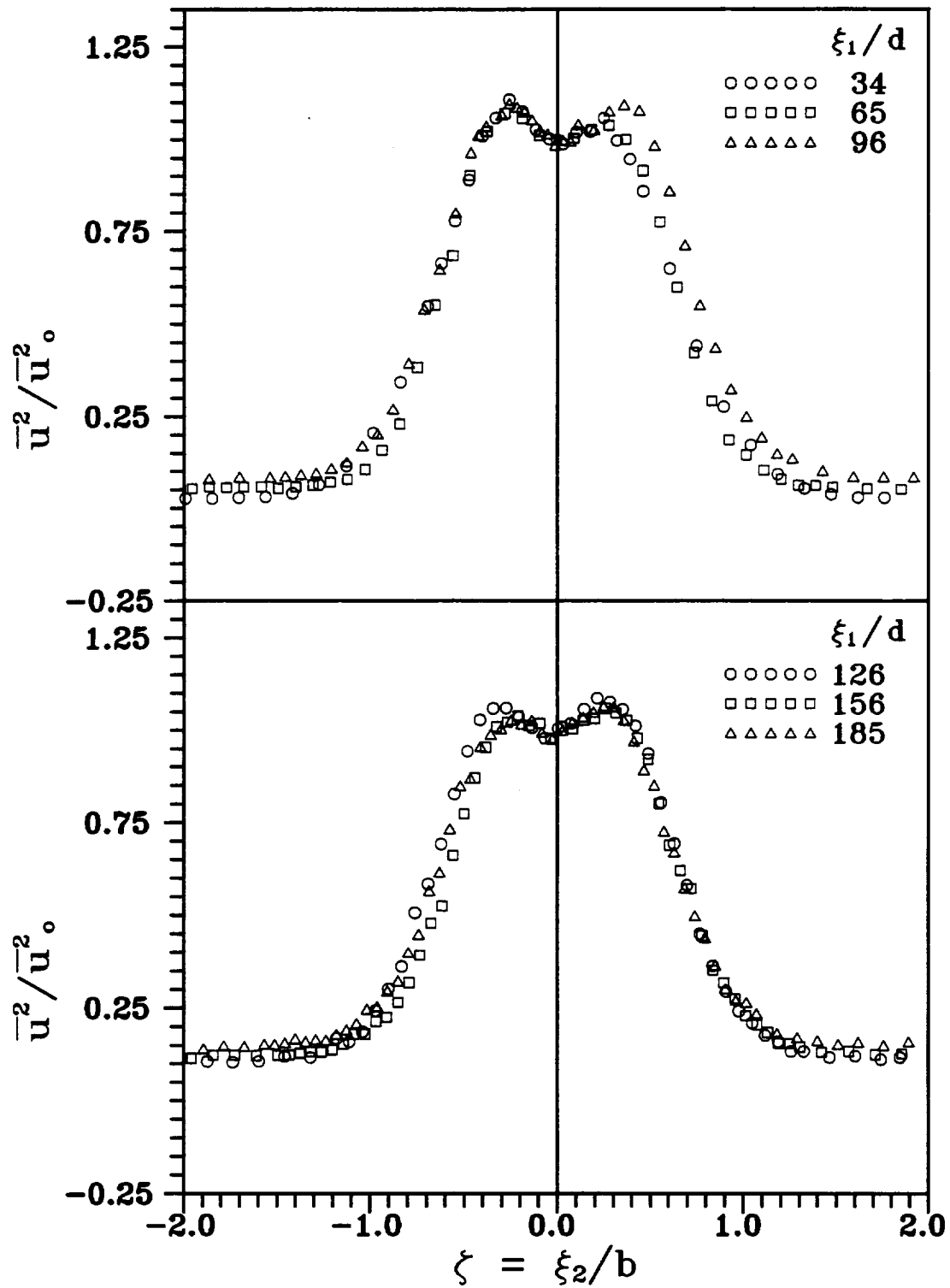
Fig. 68 Transverse distribution of streamwise component of Reynolds normal stress at different streamwise positions and under negative streamwise pressure gradient, ξ_1/d = 34 to 185
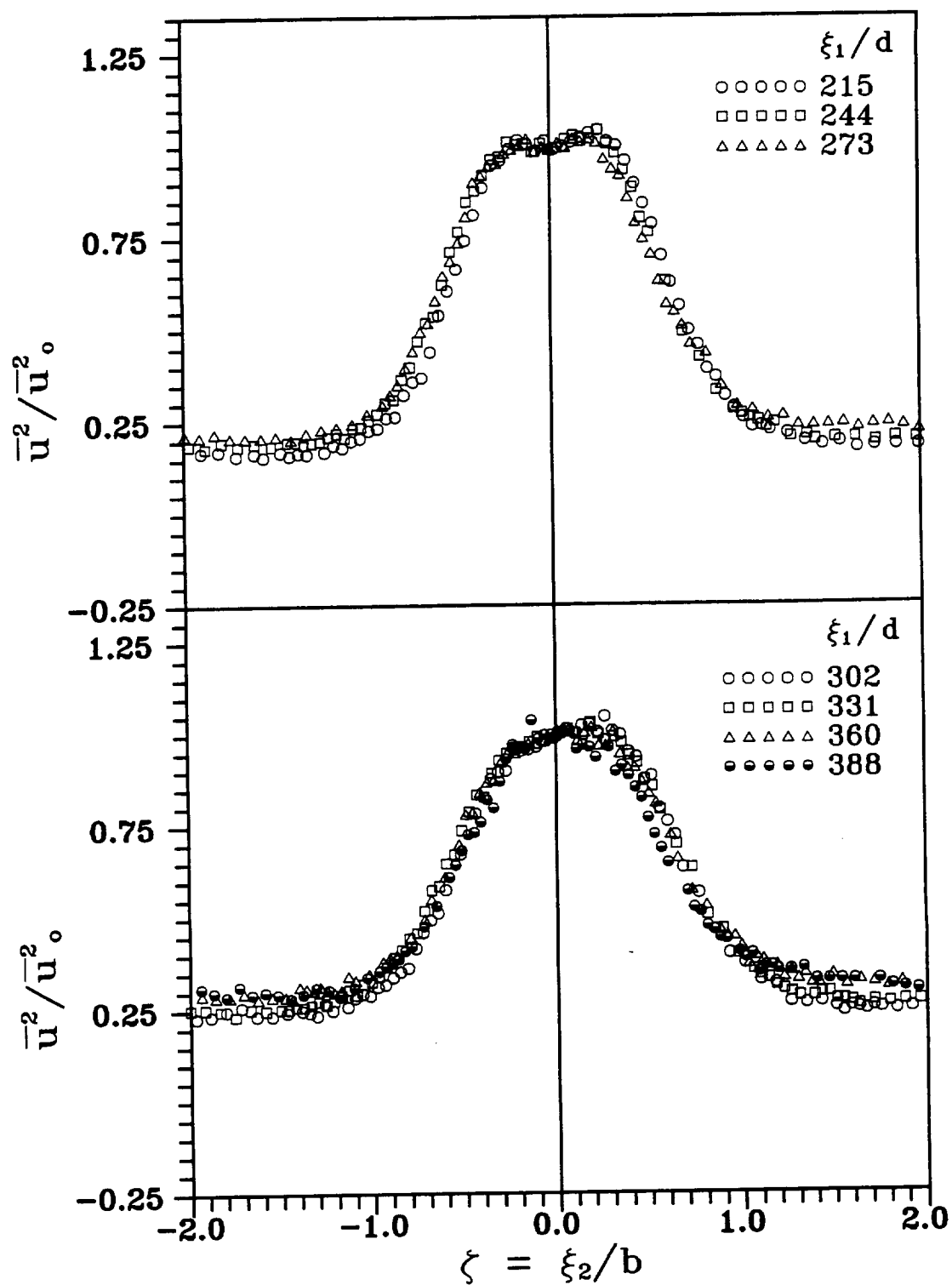
Fig. 69 Transverse distribution of streamwise component of Reynolds normal stress at different streamwise positions and under negative streamwise pressure gradient, ξ_1/d = 215 to 388
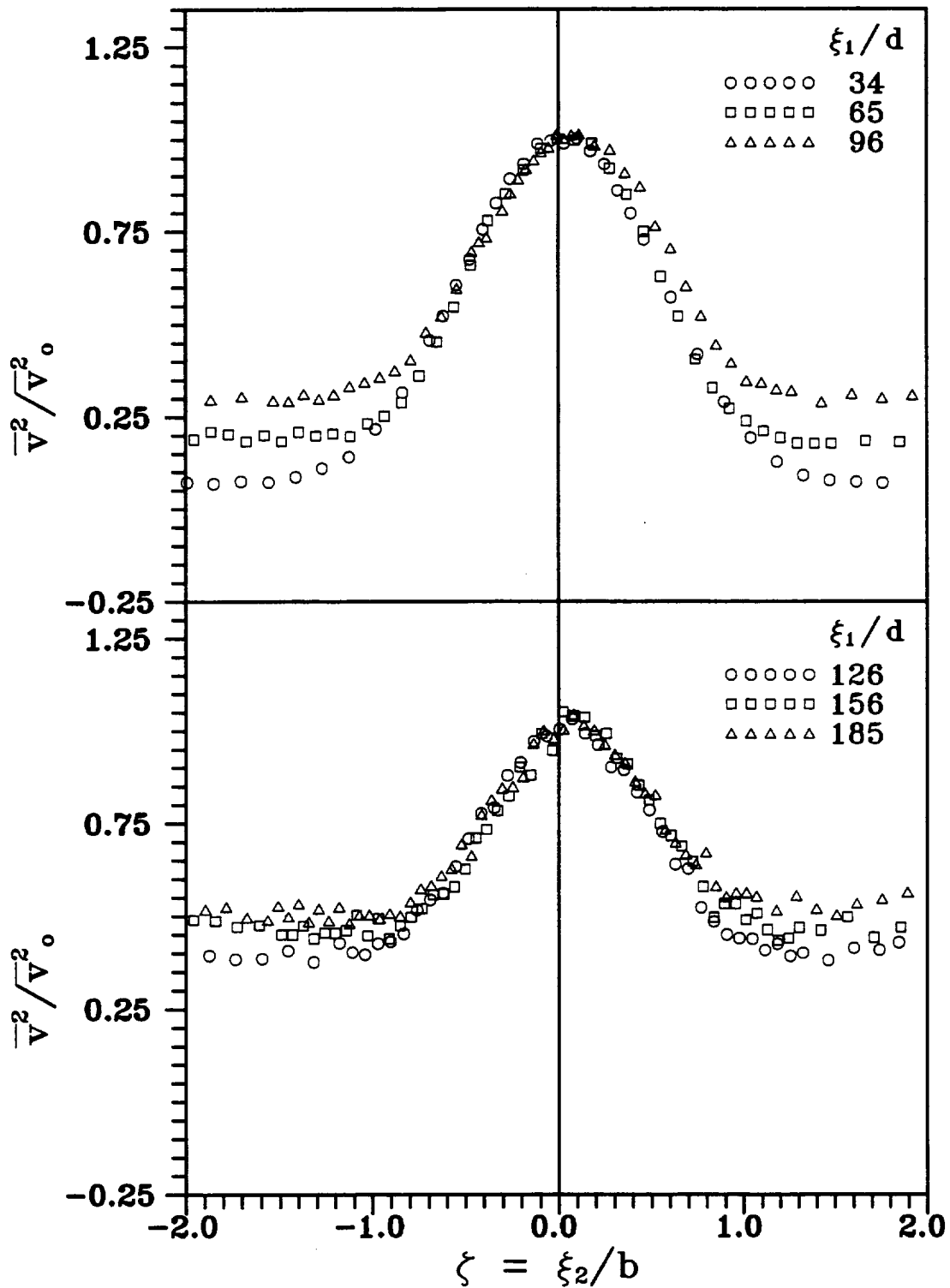
Fig. 70 Transverse distribution of normal component of Reynolds normal stress at different streamwise positions and under negative streamwise pressure gradient, ξ_1/d = 34 to 185
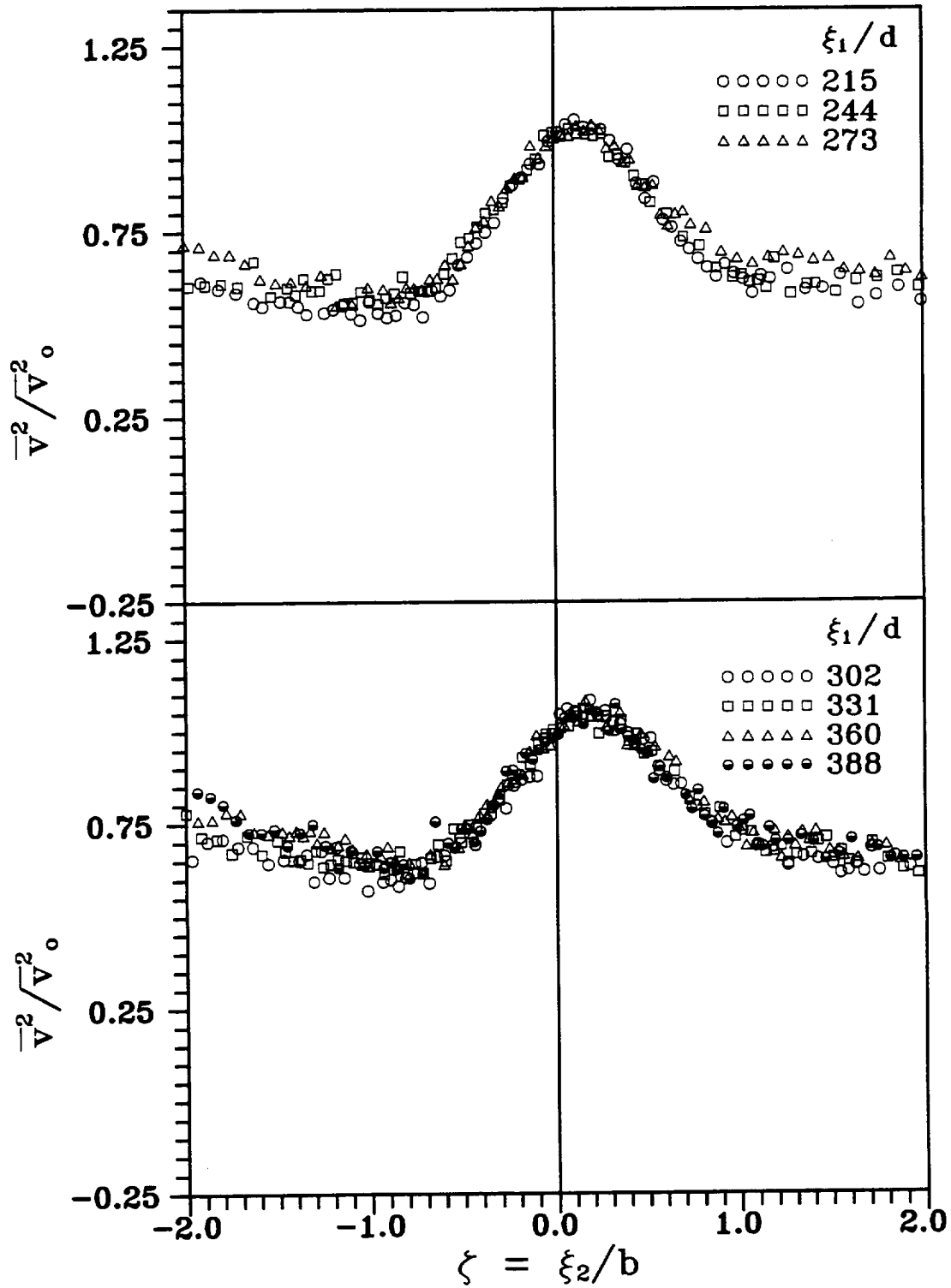
Fig. 71 Transverse distribution of normal component of Reynolds normal stress at different streamwise positions and under negative streamwise pressure gradient, ξ_1/d = 215 to 388
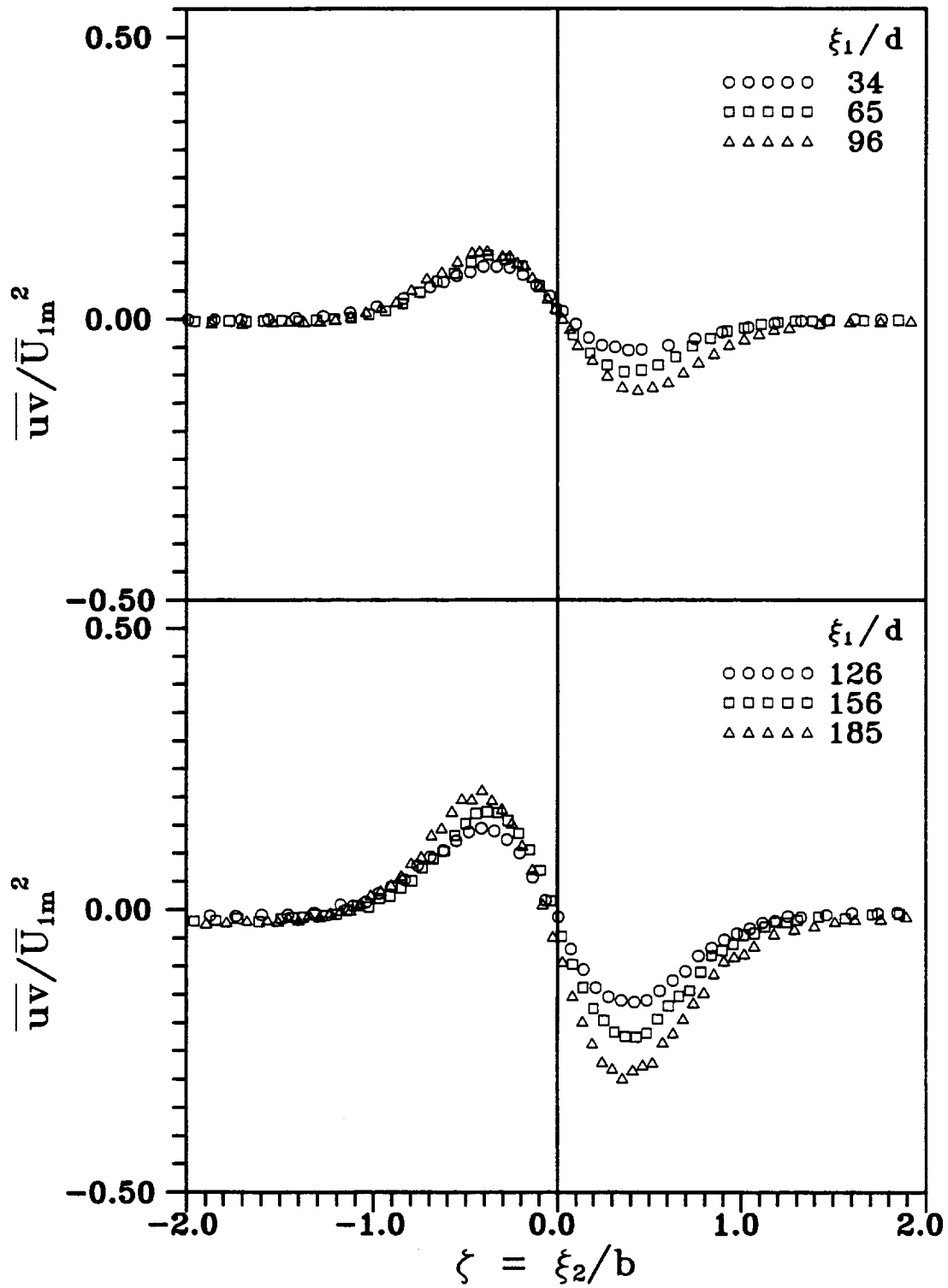
Fig. 72 Transverse distribution of Reynolds shear stress at different streamwise positions and under negative streamwise pressure gradient, ξ_1/d = 34 to 185
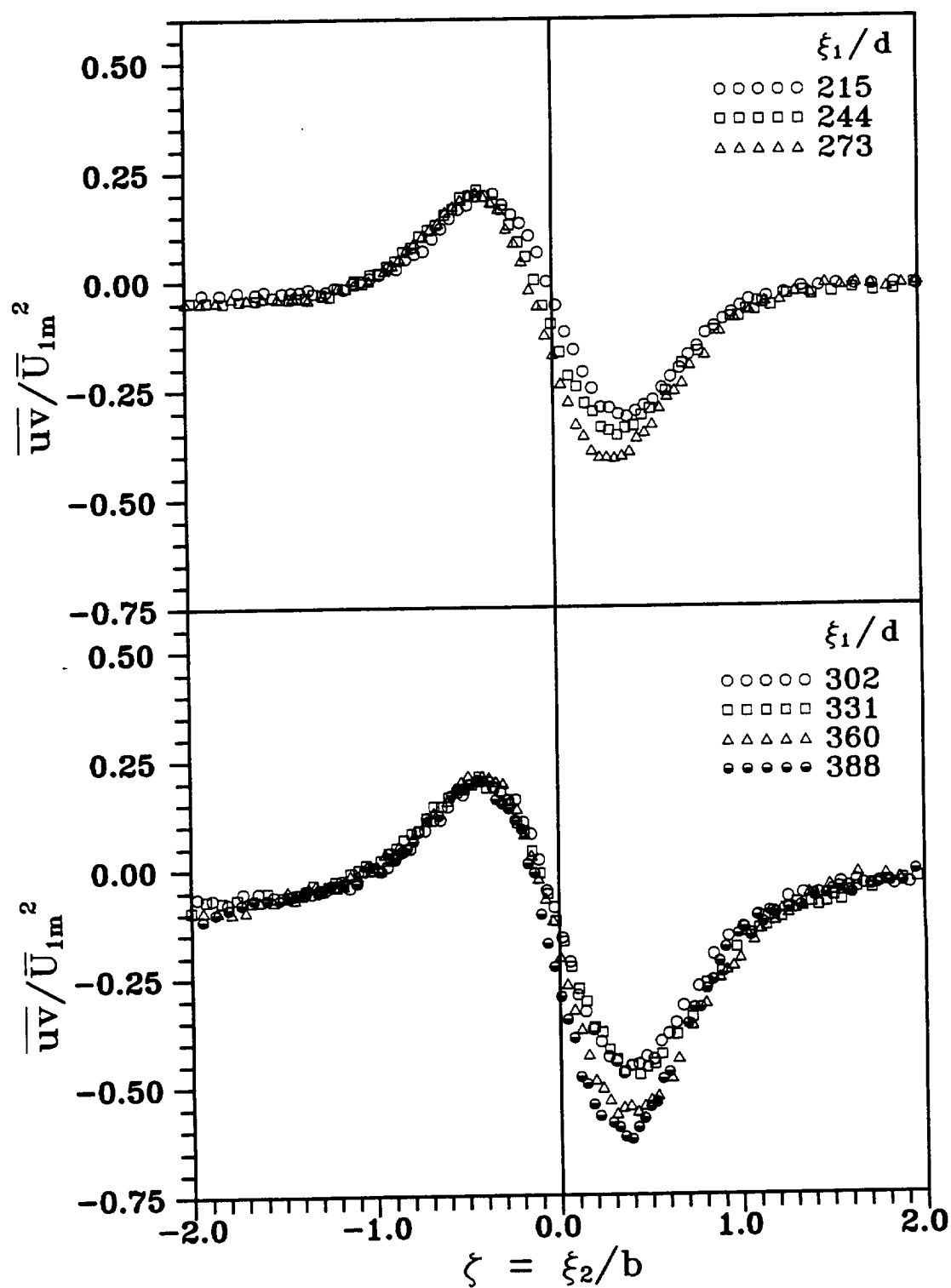
Fig. 73 Transverse distribution of Reynolds shear stress at different streamwise positions and under negative streamwise pressure gradient, ξ_1/d = 215 to 388

or positive pressure gradient cases.

Figures 70 and 71 show the transverse distribution of the transverse component of Reynolds stresses. Similar to the streamwise component, the maximum value of the transverse component of Reynolds stress occurs at the inner half of the wake. The asymmetry of the transverse component of Reynolds stress is more than the streamwise component.

Figures 72 and 73 show plots of the transverse distribution of Reynolds shear stress at various streamwise locations. The Reynolds shear stress is nondimensionalized by the square of the maximum velocity defect. The Reynolds shear stress distribution shows the strong asymmetry due to the curvature. The nature of curvature of the wake centerline and the gradient of streamwise velocity suggest a higher value of Reynolds shear stress on the inner half of the wake. This is observed at every streamwise location except the very first two measurement locations where, as previously explained, the pressure gradient dominates over the curvature effect. As with the zero and positive pressure gradient curved wake, the Reynolds shear stress distribution in the outer half of the wake is closer to a self preservation state than the inner half of the wake. The Reynolds shear stress is not equal to zero either at the center or at the outside edges of the wake.

Figure 74 shows an overall comparison of the maximum and minimum values of the Reynolds shear stress for all three pressure gradients as a function of the downstream distance. The symbol $\overline{uv}_m$ stands for the maximum value of Reynolds shear stress at the outer half of the wake and minimum value of Reynolds shear stress at the inner half of the wake. The Reynolds shear stress, nondimensionalized with the square of the average velocity upstream of the wake generating cylinder, is shown in Fig. 74(a). Figure 74(b) shows the Reynolds shear stress normalized with the square of the maximum velocity defect. The filled symbols represent the maximum value of Reynolds shear stress that occurs at the outer half of the wake. The open symbols represent the minimum value of Reynolds shear stress that occurs at the inner half of the wake. The absolute values of the maximum and minimum Reynolds shear stress should be the same for a straight wake. Figure 74 shows that the absolute value of the
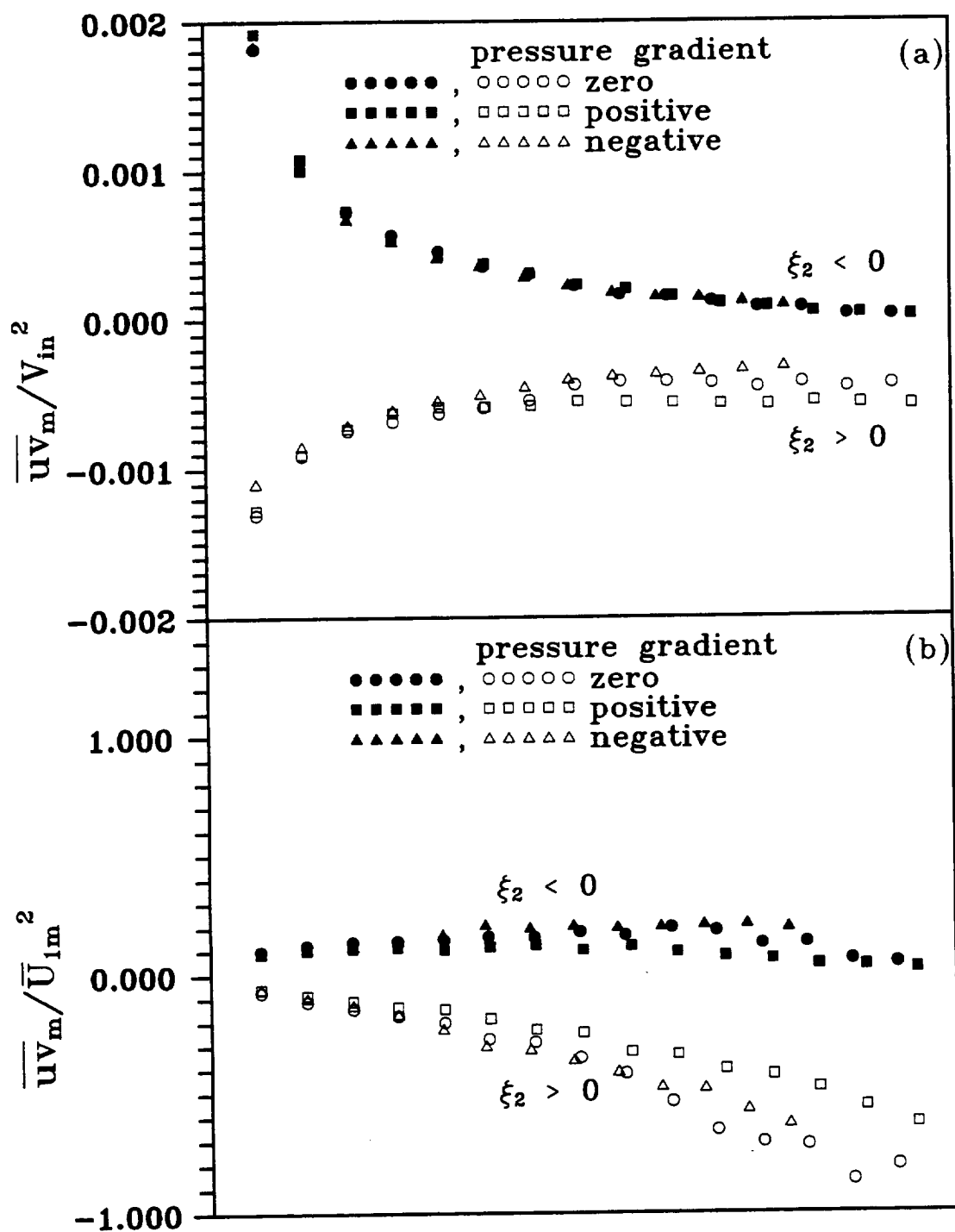
Fig. 74 Streamwise variation of the maximum value of Reynolds shear stress at
zero, positive, and negative streamwise pressure gradients

minimum Reynolds shear stress, occurring at the inner half of the wake, is higher than the maximum value of Reynolds shear stress occurring at the outer half of the wake, except for the two initial measurement locations. In the outer wake, seen in Fig. 74(a), the maximum value of Reynolds shear stress nondimensionalized with the square of average velocity has almost the same value for all three pressure gradients at a particular streamwise location. In the inner half of the wake, the absolute value of minimum Reynolds shear stress nondimensionalized with the square of average velocity, decreases with downstream location at the highest rate for negative pressure gradient and the lowest rate for positive pressure gradient. Figure 74(b) shows that the absolute value of Reynolds shear stress normalized with the square of maximum velocity defect increases with downstream locations for all three pressure gradients. This is the case for both the inner and outer half of the wake, except for the outer half of the wake at positive and zero pressure gradients where the normalized Reynolds shear stress decreases slightly for the last five downstream locations. At a particular streamwise location, the absolute value of normalized shear stress has the highest value for negative pressure gradient and the lowest value for positive pressure gradient. This is similar to Gartshore's (1967) results for a straight wake subjected to adverse pressure gradient. He observed a lower value of normalized Reynolds shear stress compared to the value of normalized Reynolds shear stress for a zero pressure gradient straight wake.

8.3.4. Vorticity, Correlation Coefficient, and Turbulent Kinetic Energy

Figure 75 shows the transverse distribution of normalized vorticity for streamwise locations from $\xi_1/d = 34$ to 244. The mean vorticity is normalized with $\bar{U}_{1m}/b$. Similar to the results of zero pressure gradient straight and curved wakes, the mean vorticity profiles for the present case are almost antisymmetric with respect to the wake center. Therefore, the effect of curvature and pressure gradient on mean vorticity profiles, shown in Fig. 75, can be considered small. The near zero value of vorticity in the region outside the wake suggests that the mean flow is mostly irrotational in that region. As mentioned in section 8.1.4, the calculation of vorticity involves the determination of
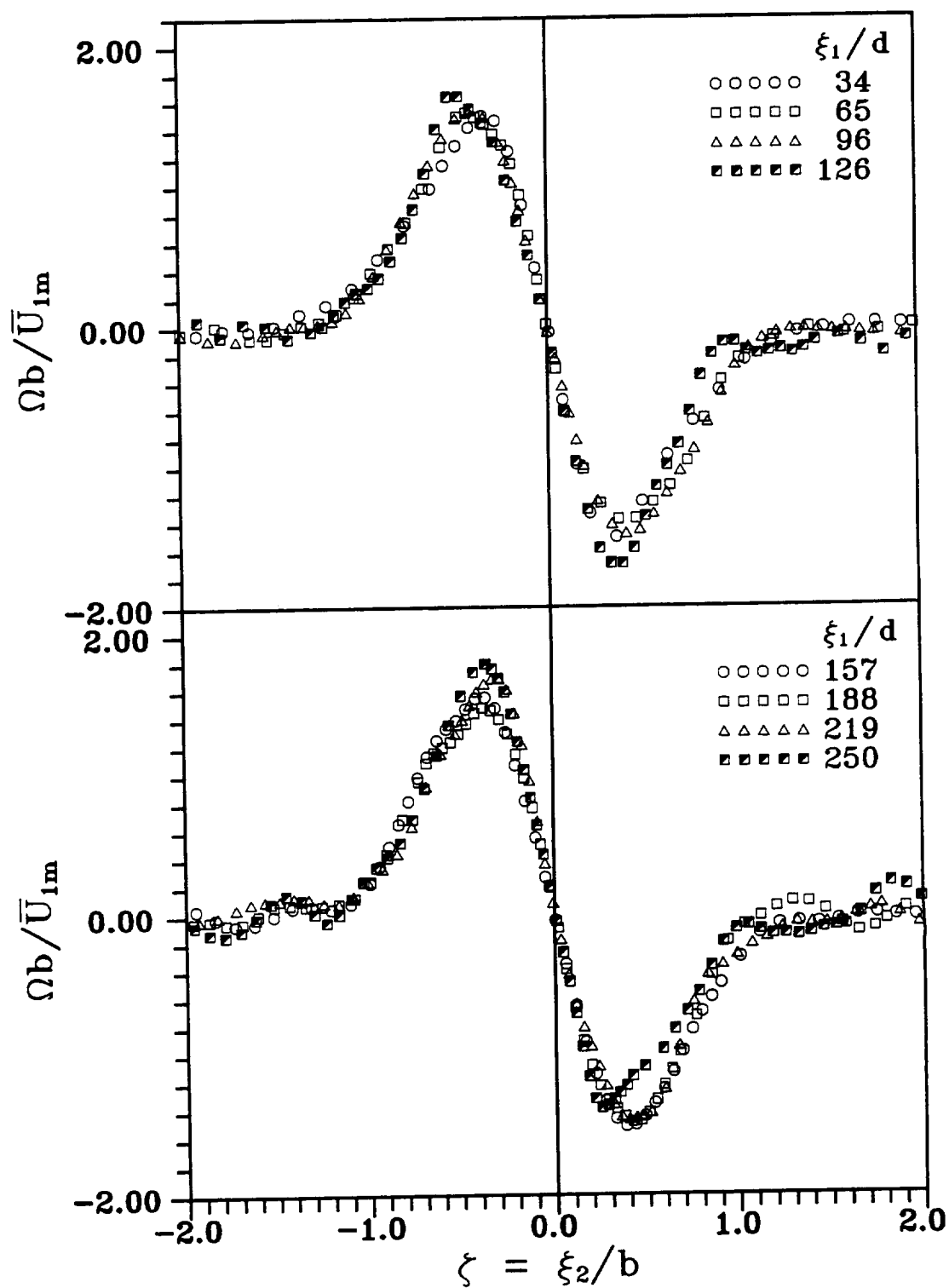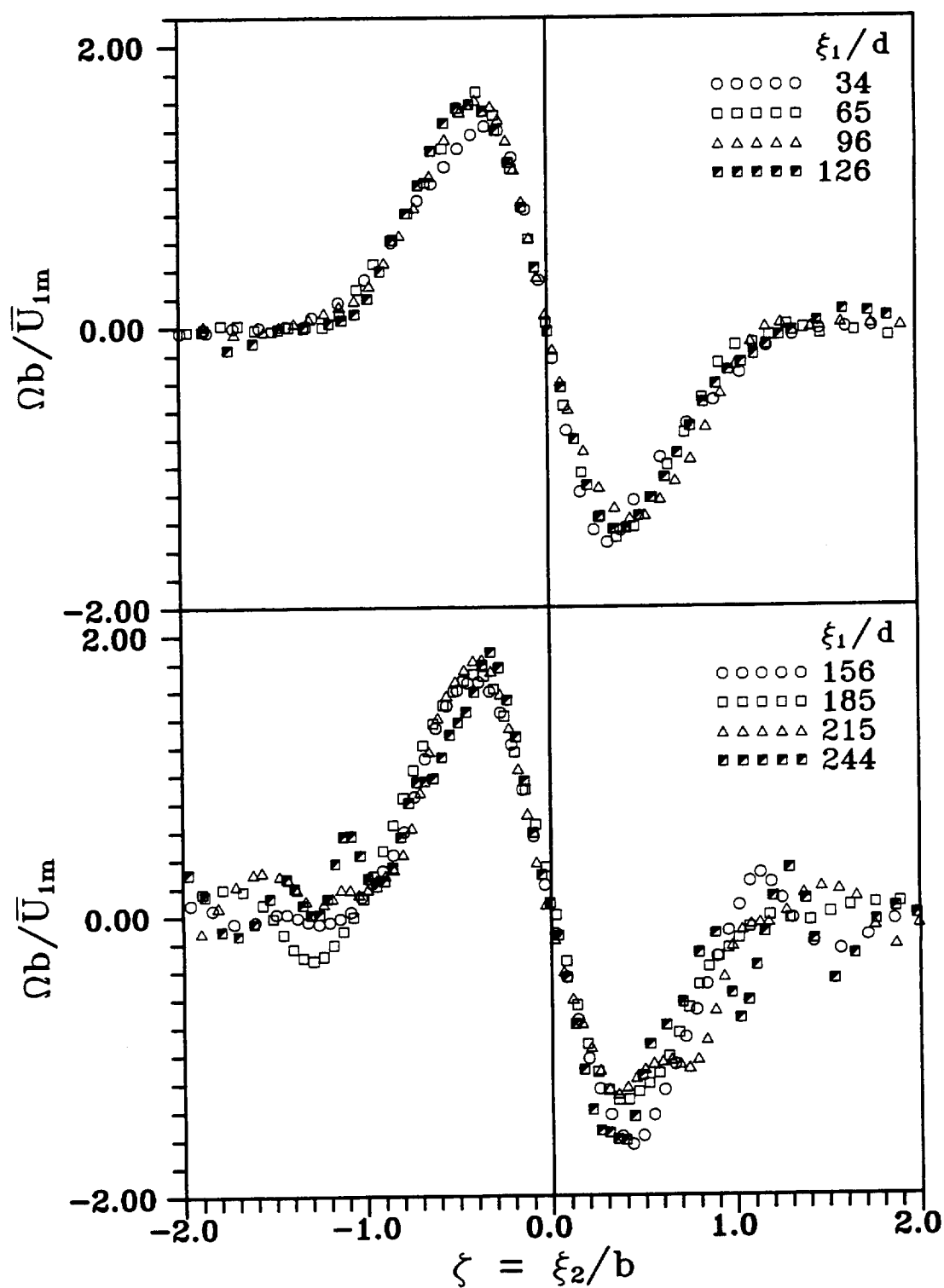
Fig. 75 Transverse distribution of mean vorticity at different streamwise positions and under negative streamwise pressure gradient

transverse gradient of velocity, which introduces scatter in the value of vorticity particularly at higher downstream locations.

Figures 76 and 77 show the transverse distribution of the correlation coefficient at different streamwise locations. The distribution of correlation coefficient is asymmetric with higher absolute values at the inner half of the wake. The maximum absolute value of the correlation coefficient at the inner half of the wake remains constant from ξ_1/d = 96 onwards whereas the maximum absolute value of the correlation coefficient at the outer half of the wake decreases with downstream distance. At a particular streamwise location, the value of correlation coefficient at the outer half of the wake for the negative pressure gradient is slightly higher than the value for zero pressure gradient curved wake. However, for the inner half of the wake, the absolute value of the correlation coefficient has a slightly higher value at zero pressure gradient than at the negative gradient especially at further downstream locations.

Figure 78 shows the transverse distribution of turbulent kinetic energy normalized by the square of the mean velocity defect. The turbulent kinetic energy distribution is asymmetric with respect to the wake center with higher value at the inner half of the wake. The normalized turbulent kinetic energy increases with downstream location. This is because the turbulent kinetic energy decays at a slower rate than that of the mean velocity defect. At locations ξ_1/d > 126, the value of normalized kinetic energy for negative pressure gradient wake is higher than the value for zero pressure gradient wake.

8.4. Unsteady Wake Development at Zero Pressure Gradient

The periodic wakes generated by the cylinders of the rotating wake generator were measured using a stationary X-hot-film probe. The wake generator had three circular cylinders of 1.984 mm dia. fixed at an angle of 120^0 to each other. The periodic wake development was studied for zero streamwise pressure gradient. All the measurements were carried out for an average inlet velocity of about 20 m/s. Measurements were made at five angular positions from $\theta = 0°$ to $40°$ in $10°$ intervals. At each angular
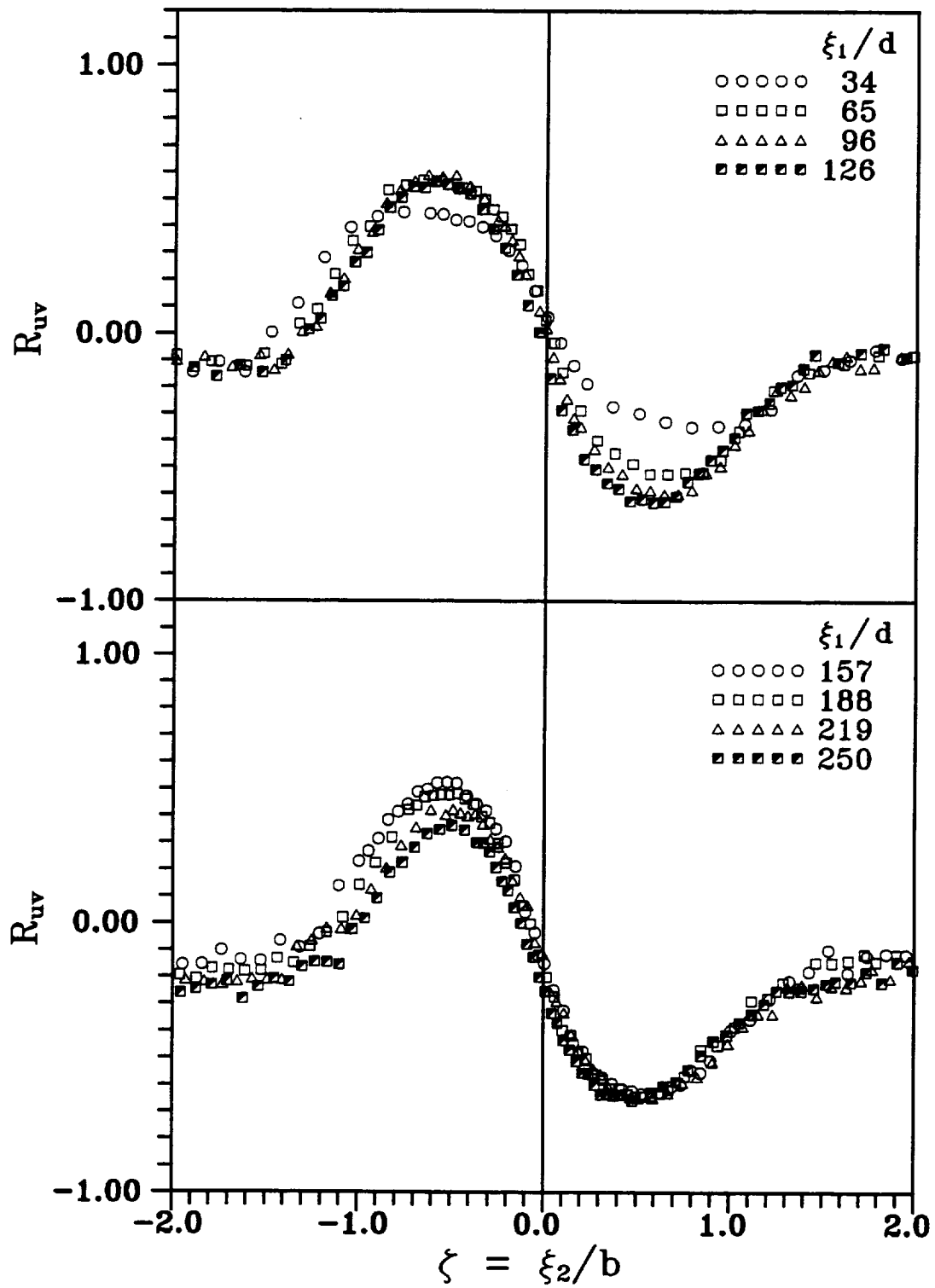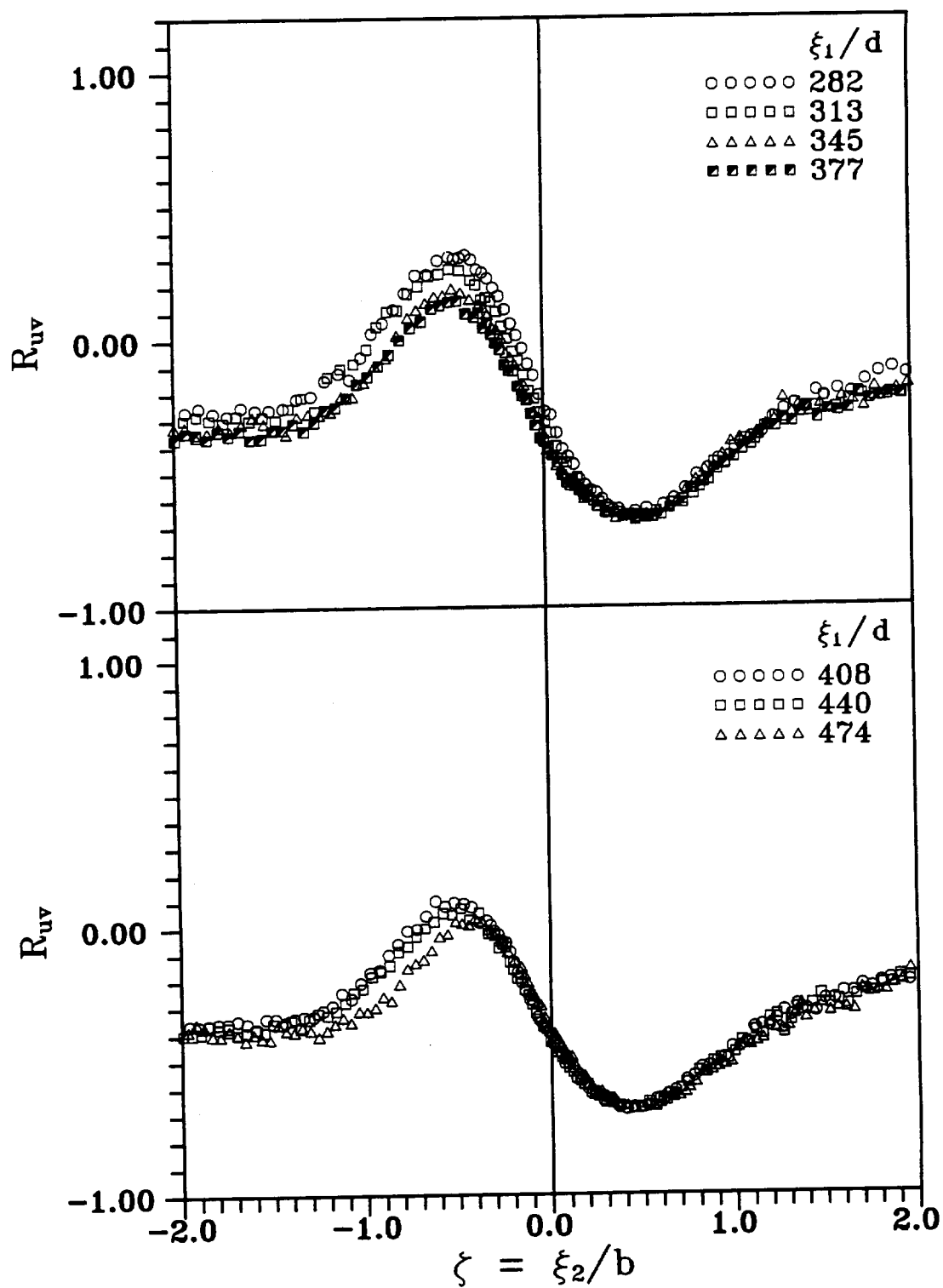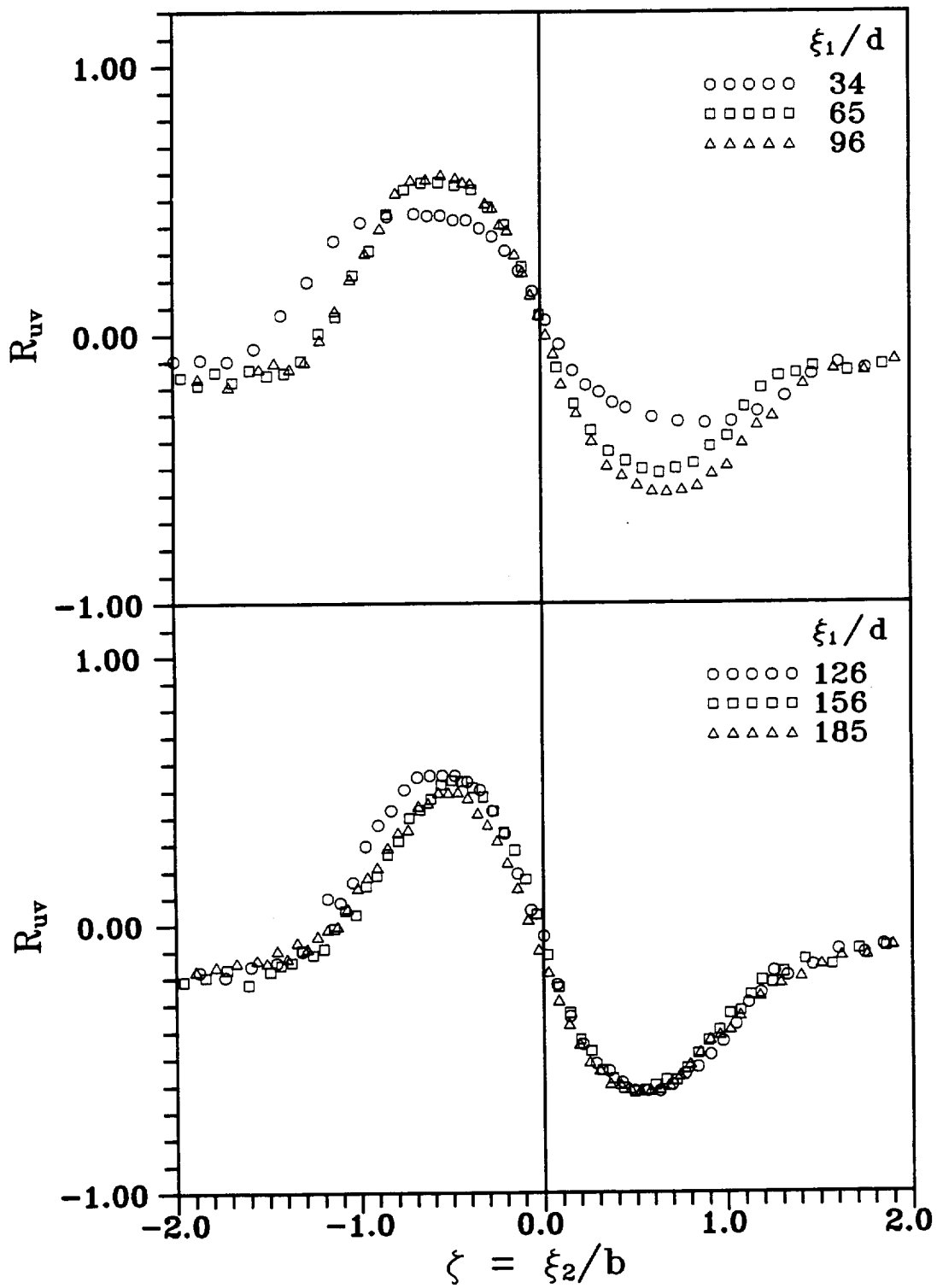
Fig. 76 Transverse distribution of correlation coefficient at different streamwise positions and under negative streamwise pressure gradient, ξ_1/d = 34 to 185
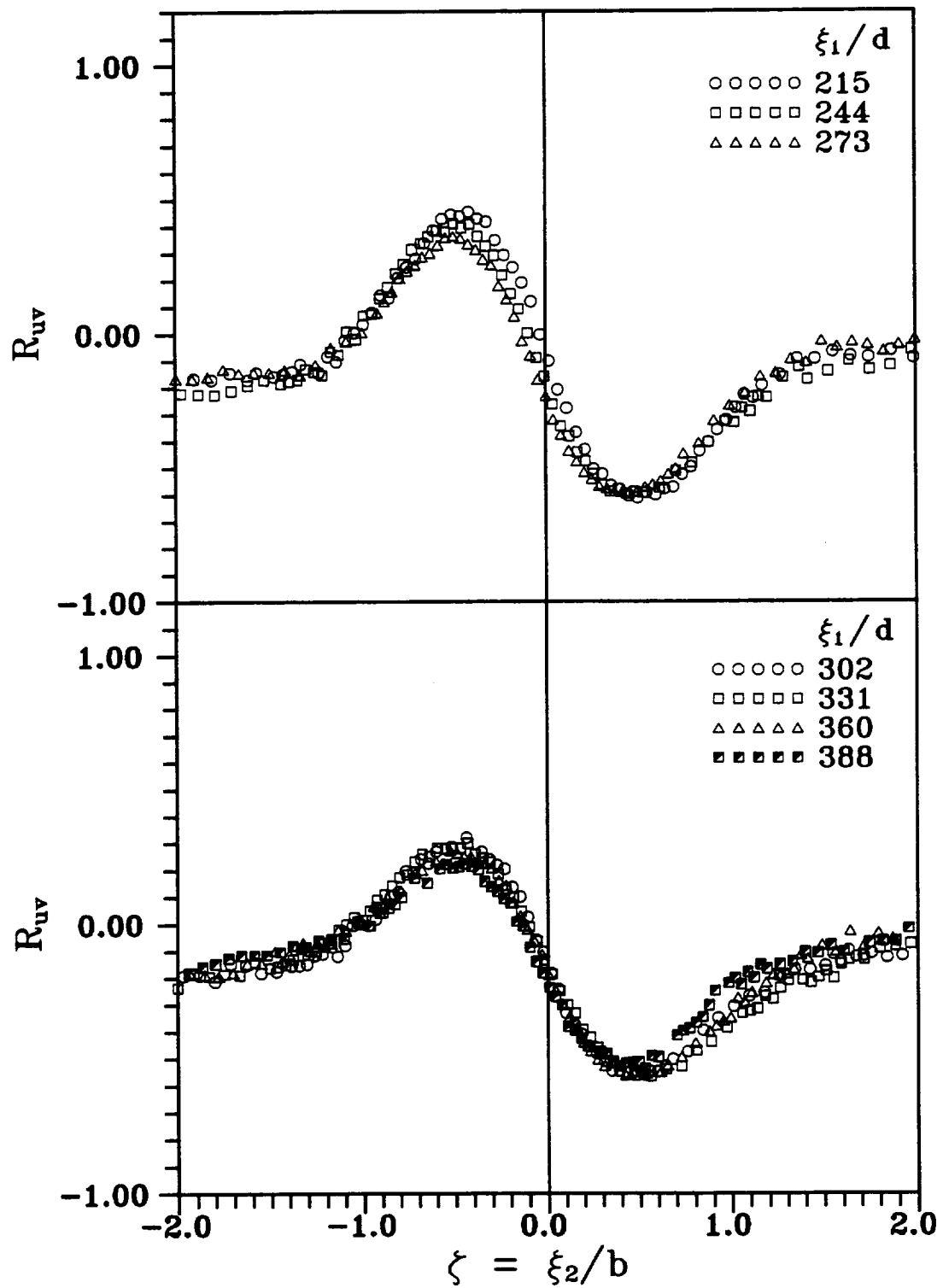
Fig. 77 Transverse distribution of correlation coefficient at different streamwise positions and under negative streamwise pressure gradient, ξ_1/d = 215 to 388
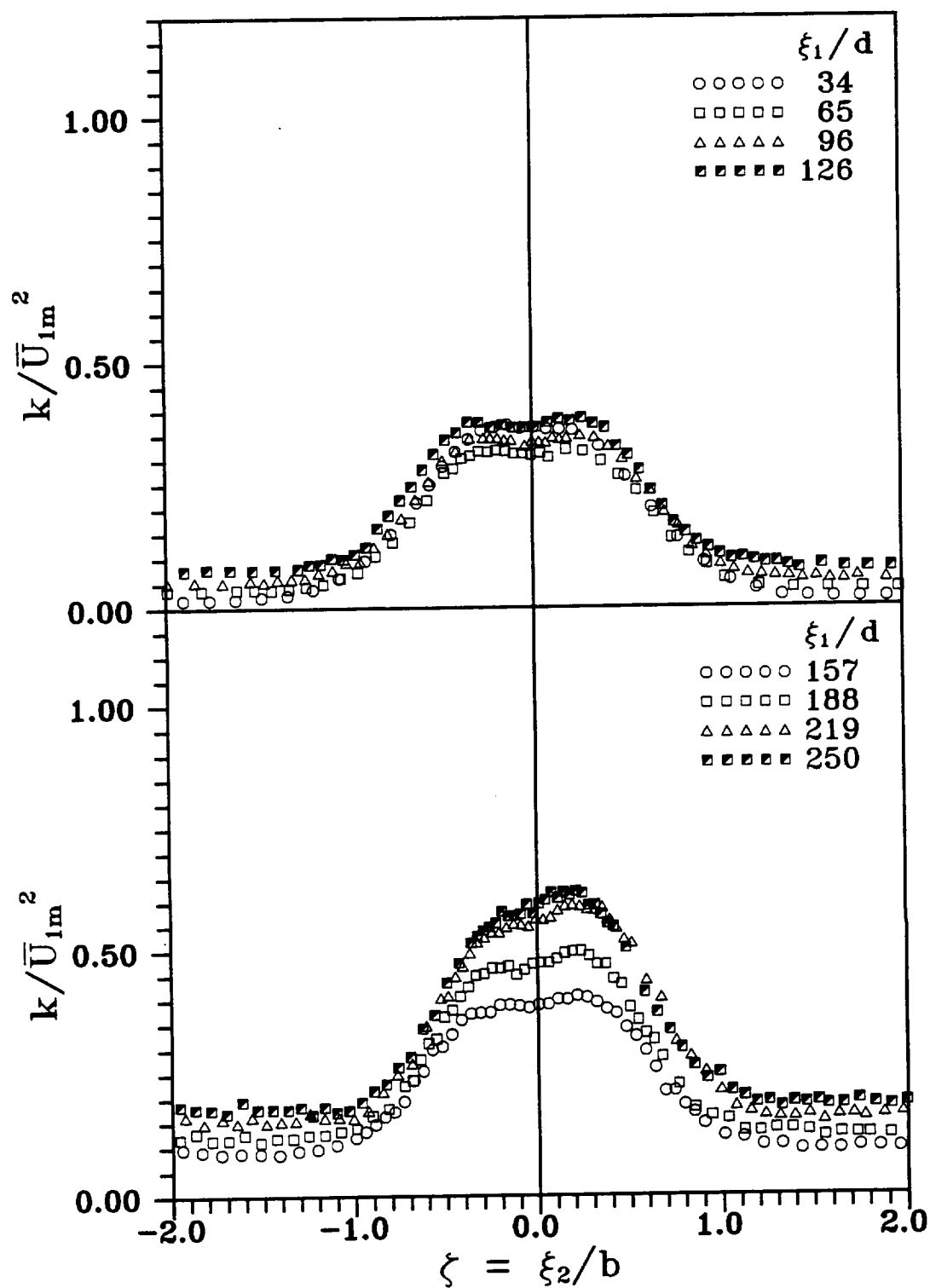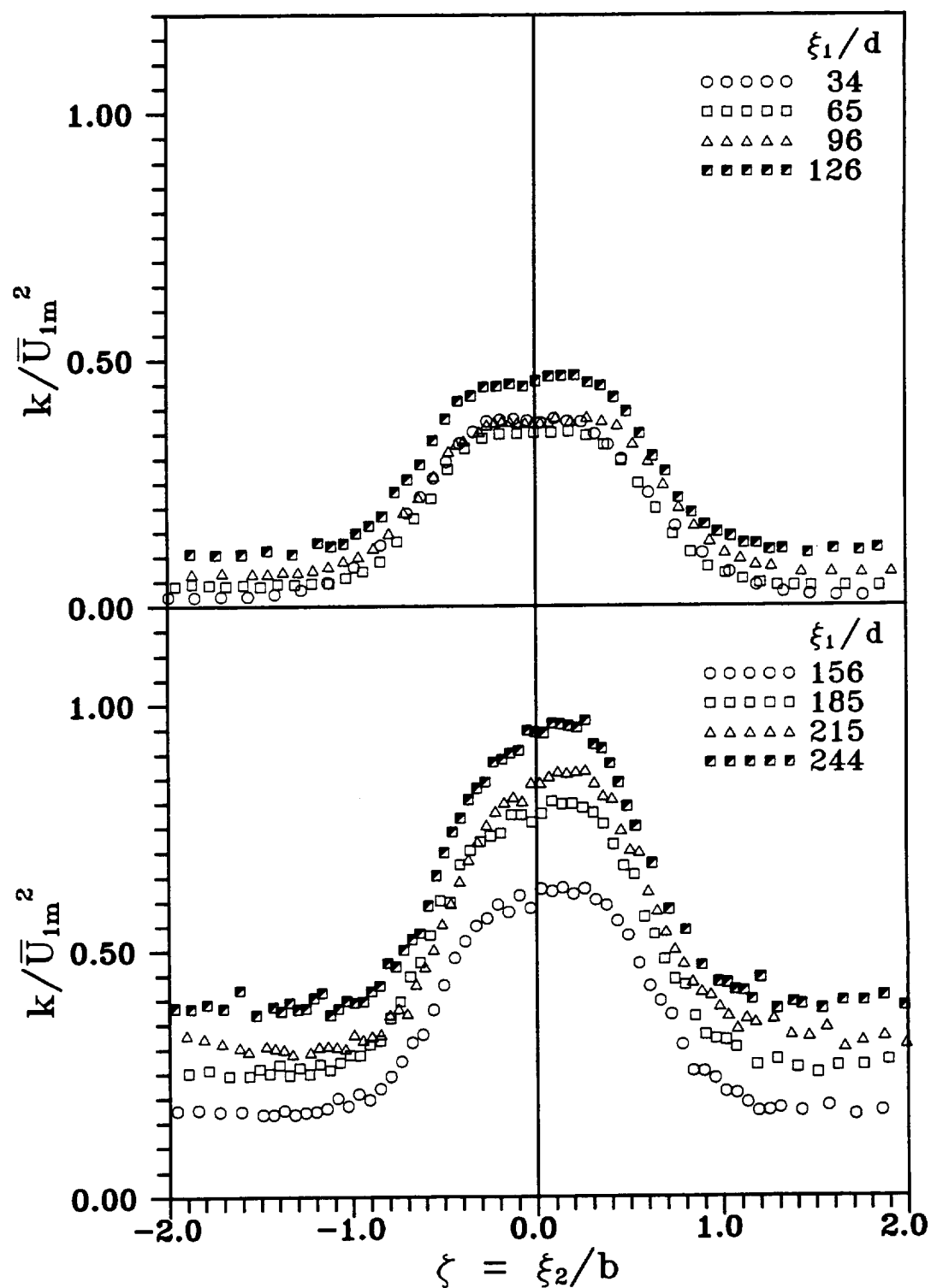
Fig. 78 Transverse distribution of turbulent kinetic energy at different streamwise positions and under negative streamwise pressure gradient

position, measurements were taken at four radial positions. The rotational speed of the wake generator was 300 rpm which corresponds to a Strouhal number, based on the wake passing frequency, equal to 0.0015. Also, measurements were carried out at four different rotational speeds at the inlet ($\theta = 0°$) and at the radial location $r-r_i = 165$ mm.

Instantaneous velocity components obtained in probe coordinates are reduced by phase-averaging. The temporal distribution of phase-averaged velocity and Reynolds stress components in stationary frame of reference and probe coordinates are presented first. It is followed by the distribution of velocity defect, transverse velocity, Reynolds stresses, and third-order correlations, all quantities being represented in the relative frame of reference and similarity coordinates.

8.4.1. Temporal Distribution in Probe Coordinates and Stationary Frame of Reference

Figure 79 shows the phase-averaged tangential component of velocity $<V_t>$ as a function of time at an angular position $\theta = 0°$. The time scale 200 ms corresponds to the time duration for one revolution which is equal to three wake passing periods. The tangential velocity component is in absolute frame of reference and probe coordinates. Measurements were taken at four radial locations, at the center of the channel ($r-r_i = 210$ mm), 70 mm on both sides of the center of the channel ($r-r_i = 140$ and 280 mm), and at a location ($r-r_i = 165$ mm) where the primary wake happens to be exactly in the middle of two secondary wakes. It can be observed that three primary wakes (higher velocity defect) and three secondary wakes (smaller velocity defect) cross a stationary probe during one revolution of the wake generator. Primary wakes are generated during the upward motion of cylinders and secondary wakes are generated during the downward motion of the cylinders. The separation between primary and secondary wakes depends on measurement position (angular and radial), rotational speed, flow velocity, and number of cylinders in the wake generator. From Fig. 79, it appears that the primary and the secondary wake coincide at a radial location between 210 and 280 mm. The phase averaged velocity distribution outside the wake is constant and is equal
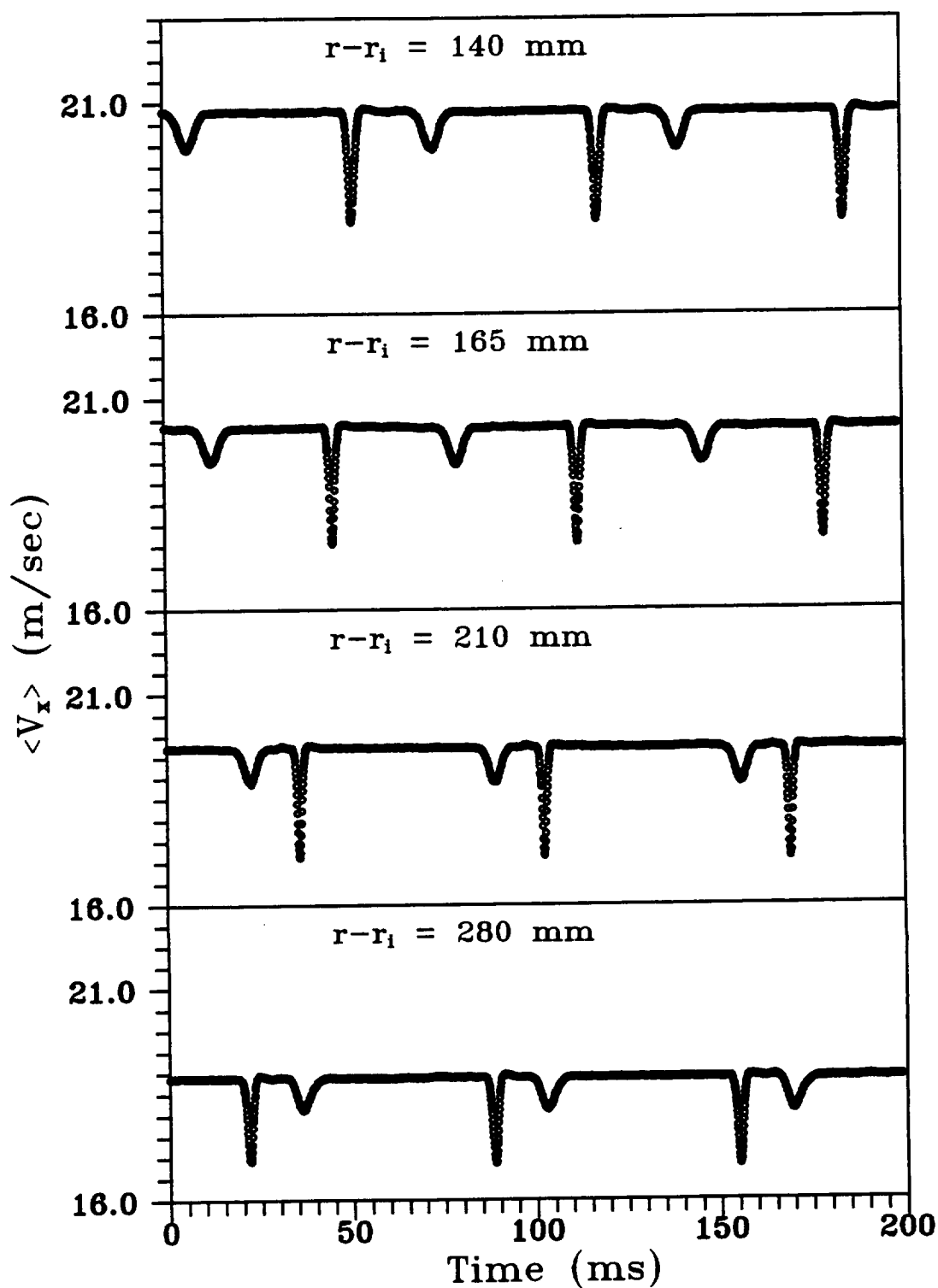
Fig. 79 Phase-averaged velocity $<V_x>$ in stationary frame of reference for the periodic unsteady wake at zero streamwise pressure gradient, $\theta = 0°$, rpm = 300

to the potential velocity (velocity without the wake) at the measurement location. The potential velocity increases towards the convex side of the curved channel, hence the phase averaged tangential velocity distribution has higher value at radial locations nearer to the convex wall. Figures 80-83 shows the phase-averaged tangential velocity distribution for angular positions from $10°$ to $40°$. Distinct primary and secondary wakes can be observed at radial locations except at the radial location r-r_i = 210 mm. At r-r_i = 210 mm, the primary and secondary wakes start to merge together. The secondary wakes are very small by the time they reach an angular position of $40°$.

For further analysis and representation in similarity coordinates, data from selected measurement locations are used. The locations where the primary wakes are situated in the middle of the secondary wakes are selected since they provide data with minimum interference between primary and secondary wakes. At these locations, the phase-averaged velocity components, Reynolds stresses, and turbulence intensity $(Tu = (\sqrt{<v_x^2>}/<V_x>) \times 100)$ are plotted in Figs. 84-89. The tangential and radial component of velocities are plotted in Fig. 84 and 85, respectively. The transverse (radial) velocity distribution is very much different from the distribution obtained behind the stationary cylinder. This is due to the fact that the magnitude of transverse velocity is small which makes the distribution obtained in probe coordinate very much different from the one that would have been obtained in curvilinear coordinate system. As shown later, the distribution of transverse velocity in curvilinear coordinate system and relative frame of reference is similar to the distribution behind the stationary cylinder. The phase averaged turbulence intensity distribution is shown in Fig. 86. The turbulence intensity profiles are asymmetric with respect to the wake center. The maximum value of turbulence intensity which occurs at $\theta = 0°$ is 7.69% and is close to the value obtained at the same angular position for the stationary cylinder, which was 7.93%. When the rotational speed of the wake generator was 600 rpm, the maximum value of phase-averaged turbulence intensity was 7.8% at r - r_i = 165 mm and $\theta = 0°$. The phase-averaged turbulence intensity outside the wake is 1.1%, which is slightly lower than the time averaged turbulence intensity obtained in the case of zero pressure gradient steady wake. In the case of zero pressure gradient steady wake, the location
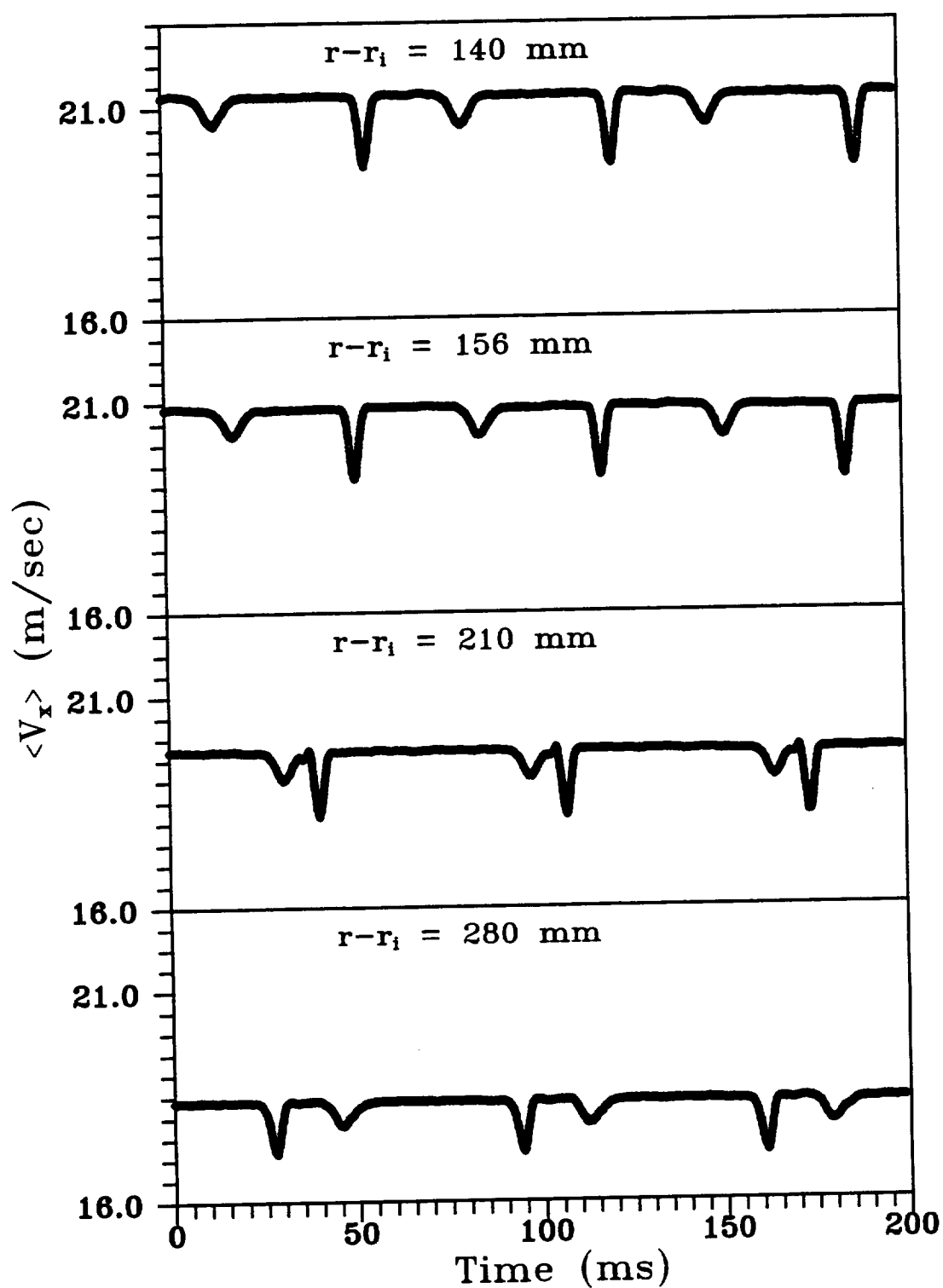
Fig. 80 Phase-averaged velocity $<V_x>$ in stationary frame of reference for the periodic unsteady wake at zero streamwise pressure gradient, $\theta = 10°$, rpm = 300
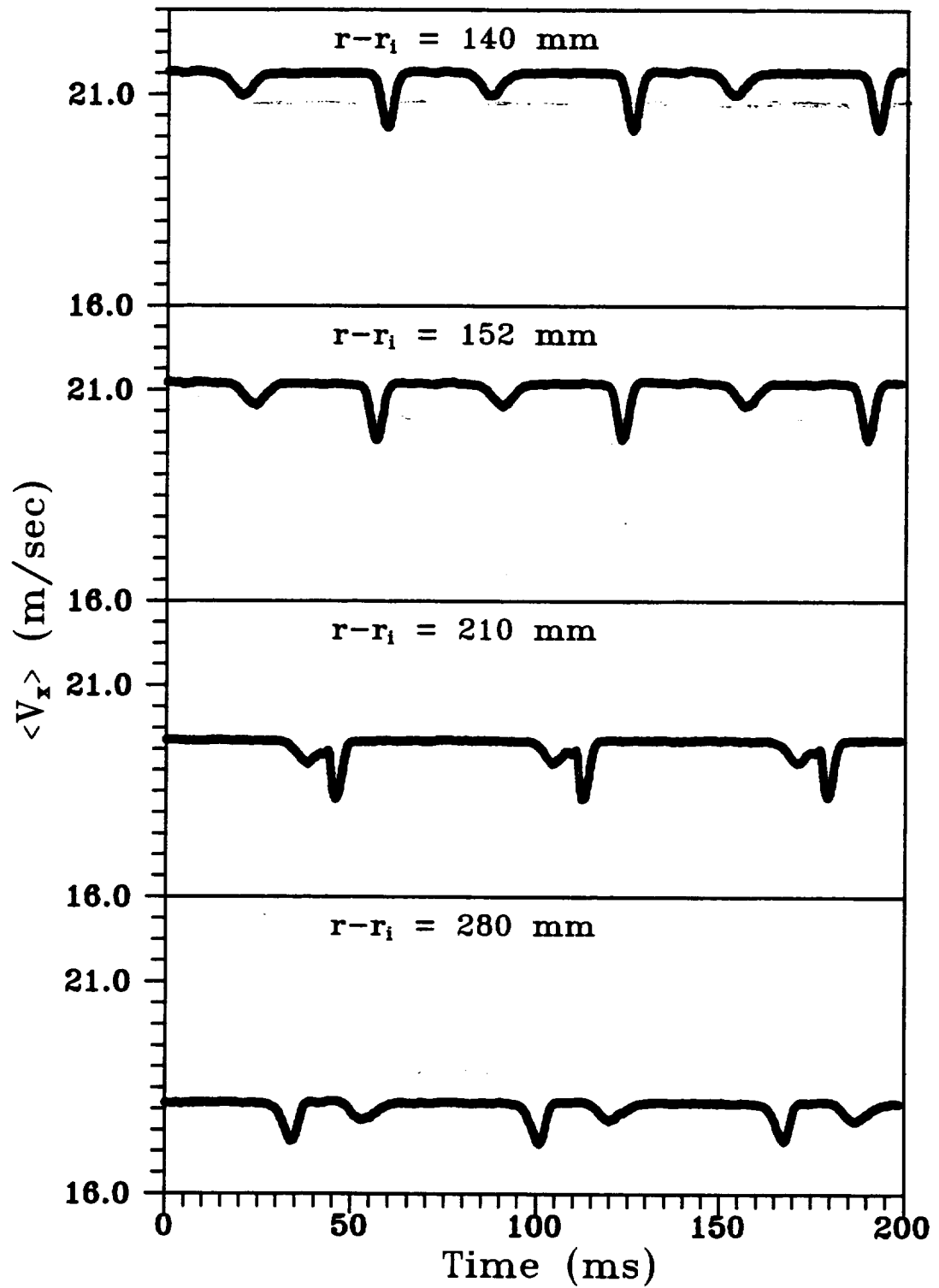
Fig. 81 Phase-averaged velocity $<V_x>$ in stationary frame of reference for the periodic unsteady wake at zero streamwise pressure gradient, $\theta = 20°$, rpm = 300
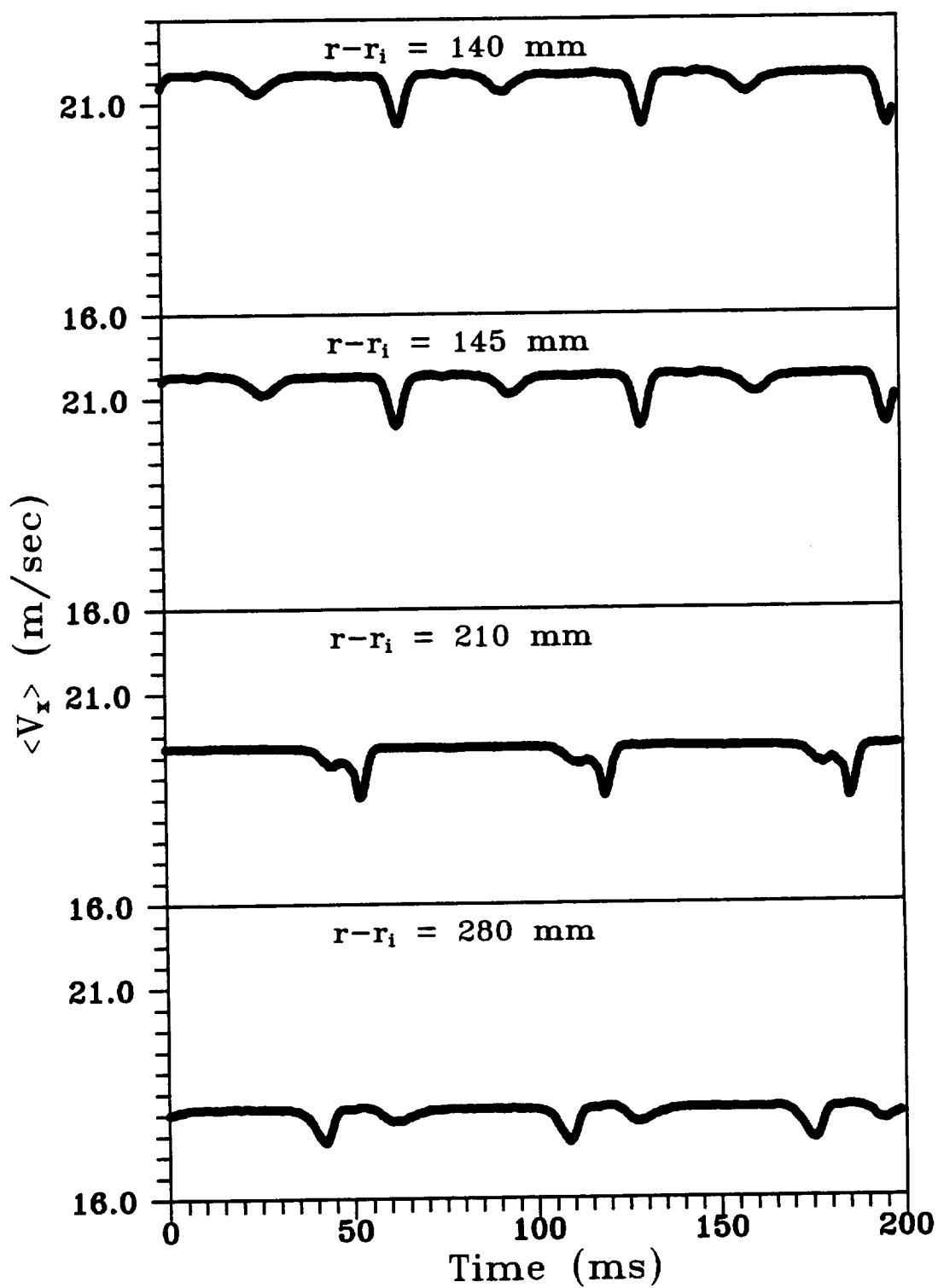
Fig. 82 Phase-averaged velocity $<V_r>$ in stationary frame of reference for the periodic unsteady wake at zero streamwise pressure gradient, $\theta = 30°$, rpm = 300
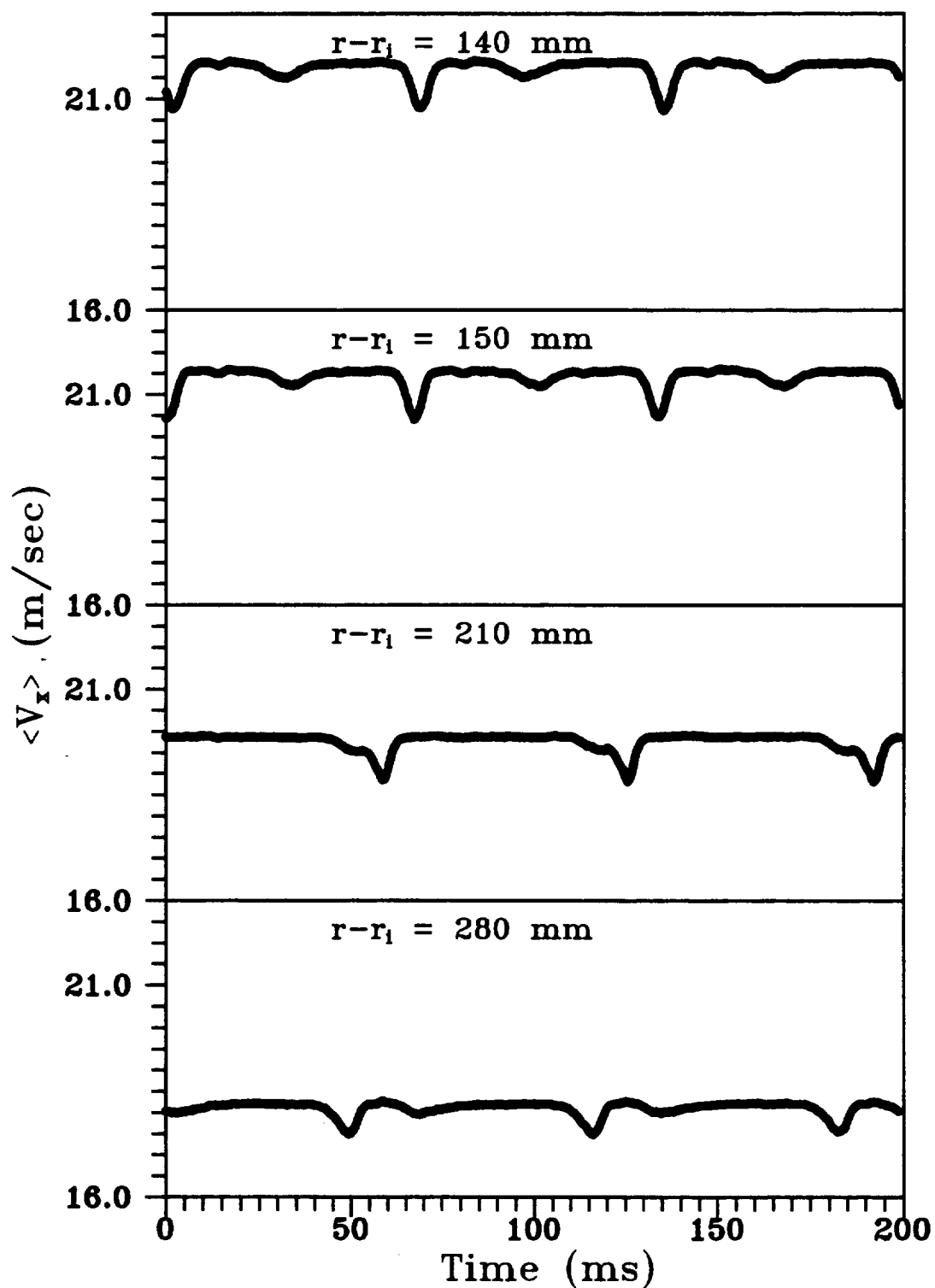
Fig. 83 Phase-averaged velocity $<V_x>$ in stationary frame of reference for the periodic unsteady wake at zero streamwise pressure gradient, $\theta = 40°$, rpm = 300

Fig. 84 Phase-averaged velocity $<V_x>$ in stationary frame of reference for the periodic unsteady wake at zero streamwise pressure gradient, rpm = 300
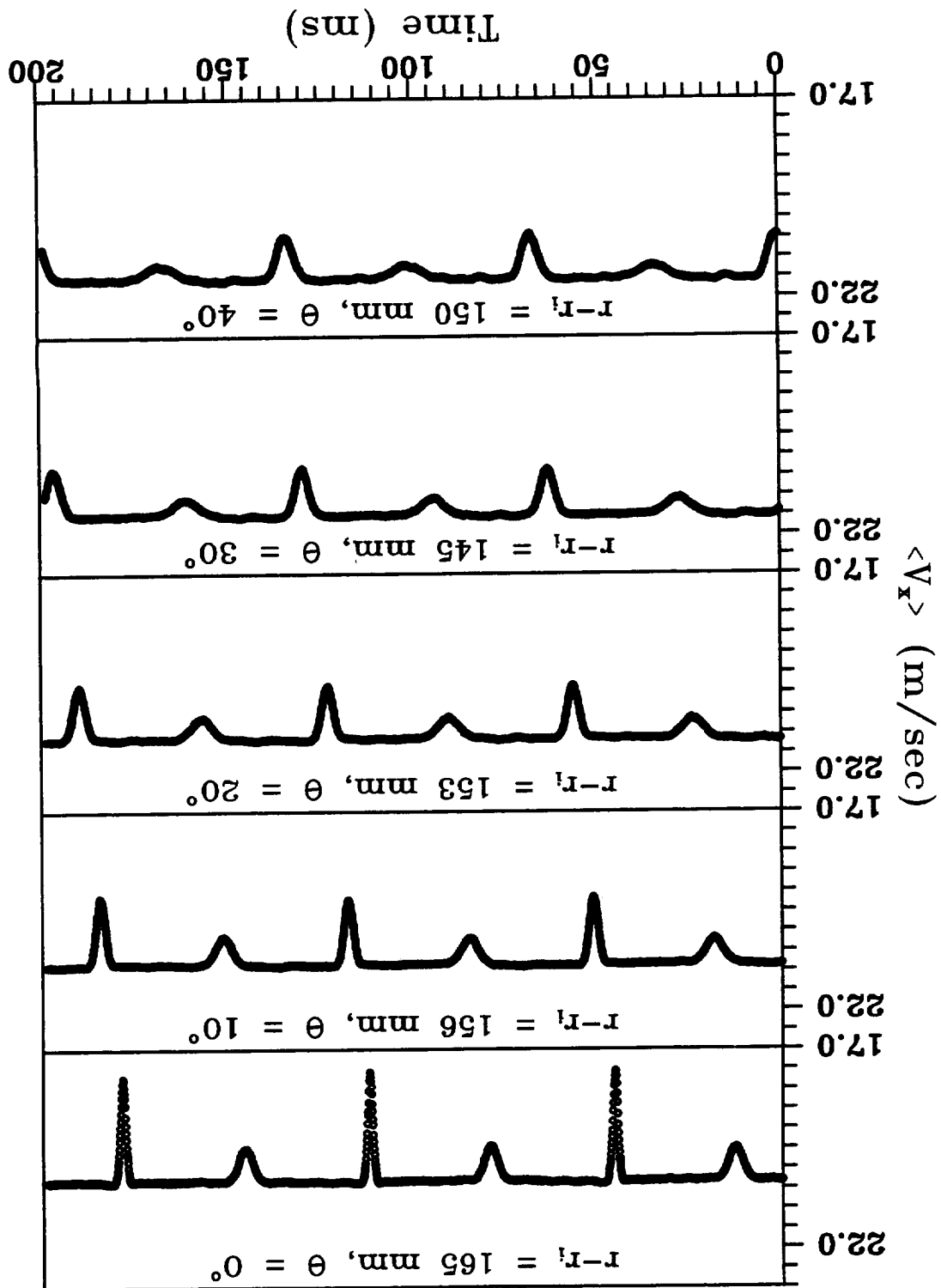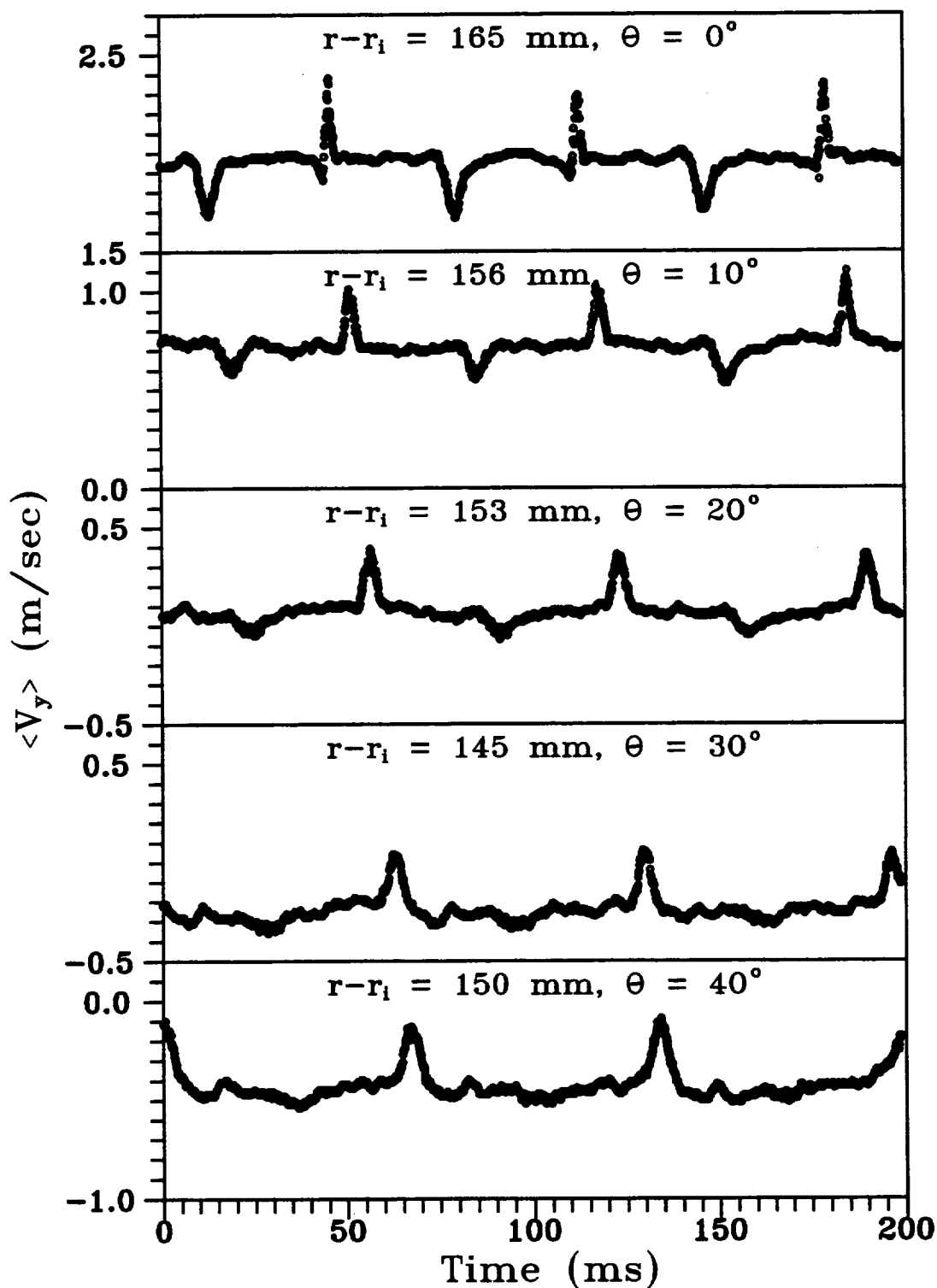
Fig. 85 Phase-averaged velocity $<V_y>$ in stationary frame of reference for the periodic unsteady wake at zero streamwise pressure gradient, rpm = 300
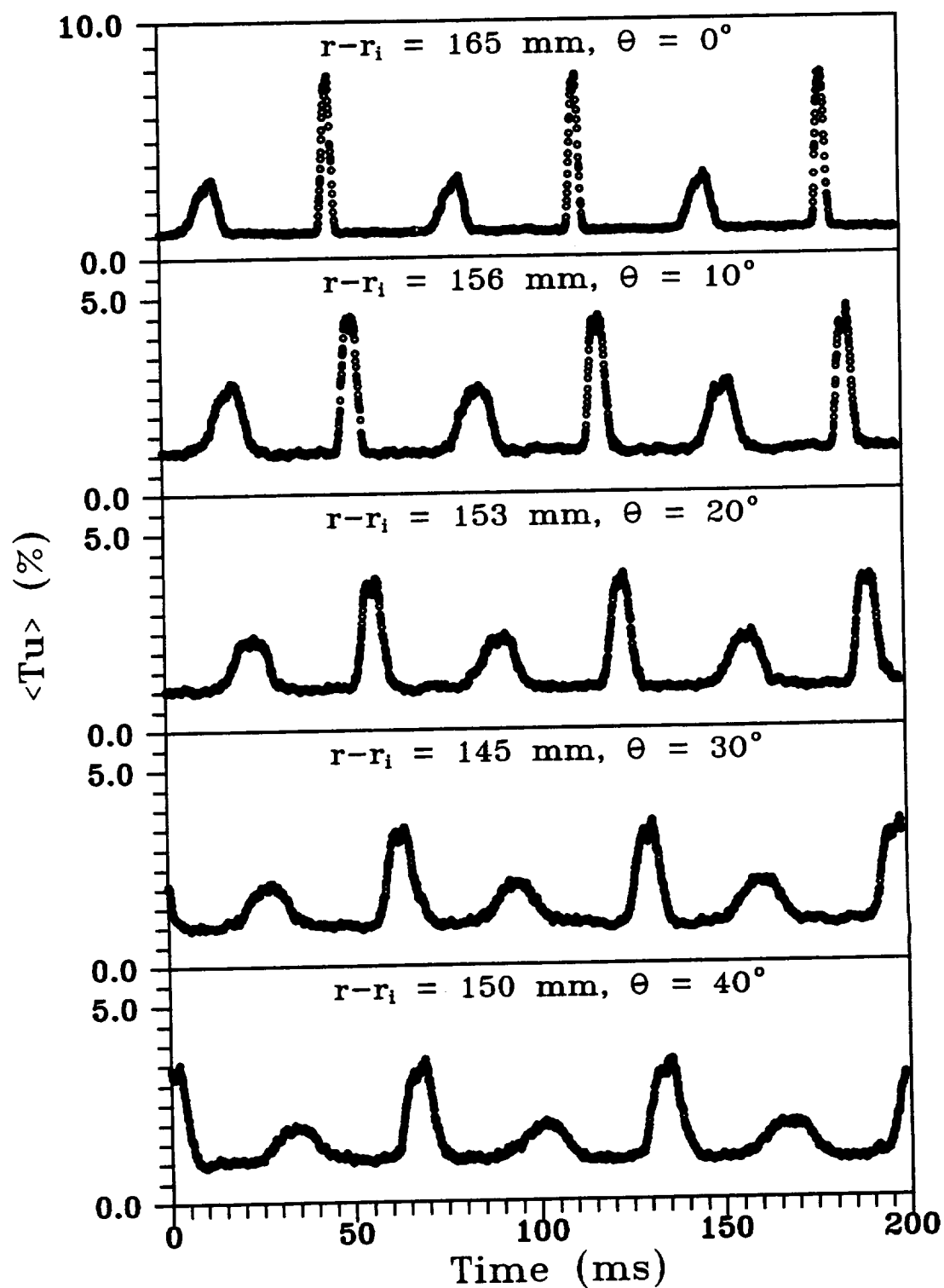
Fig. 86 Phase-averaged turbulence intensity $<Tu>$ in stationary frame of reference for the periodic unsteady wake at zero streamwise pressure gradient, rpm = 300
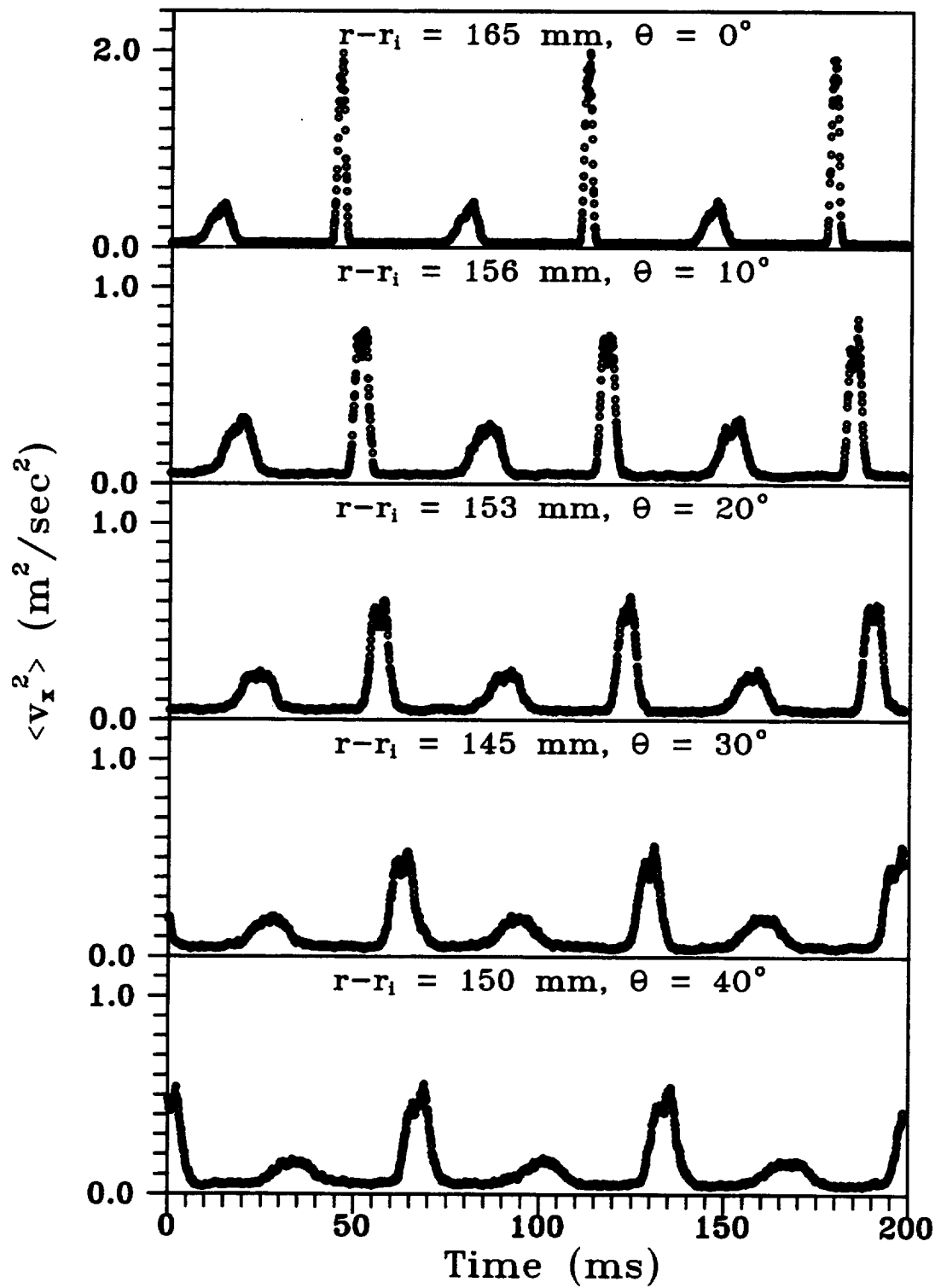
Fig. 87 Phase-averaged Reynolds normal stress $<v_x^2>$ in stationary frame of reference for the periodic unsteady wake at zero streamwise pressure gradient, rpm = 300
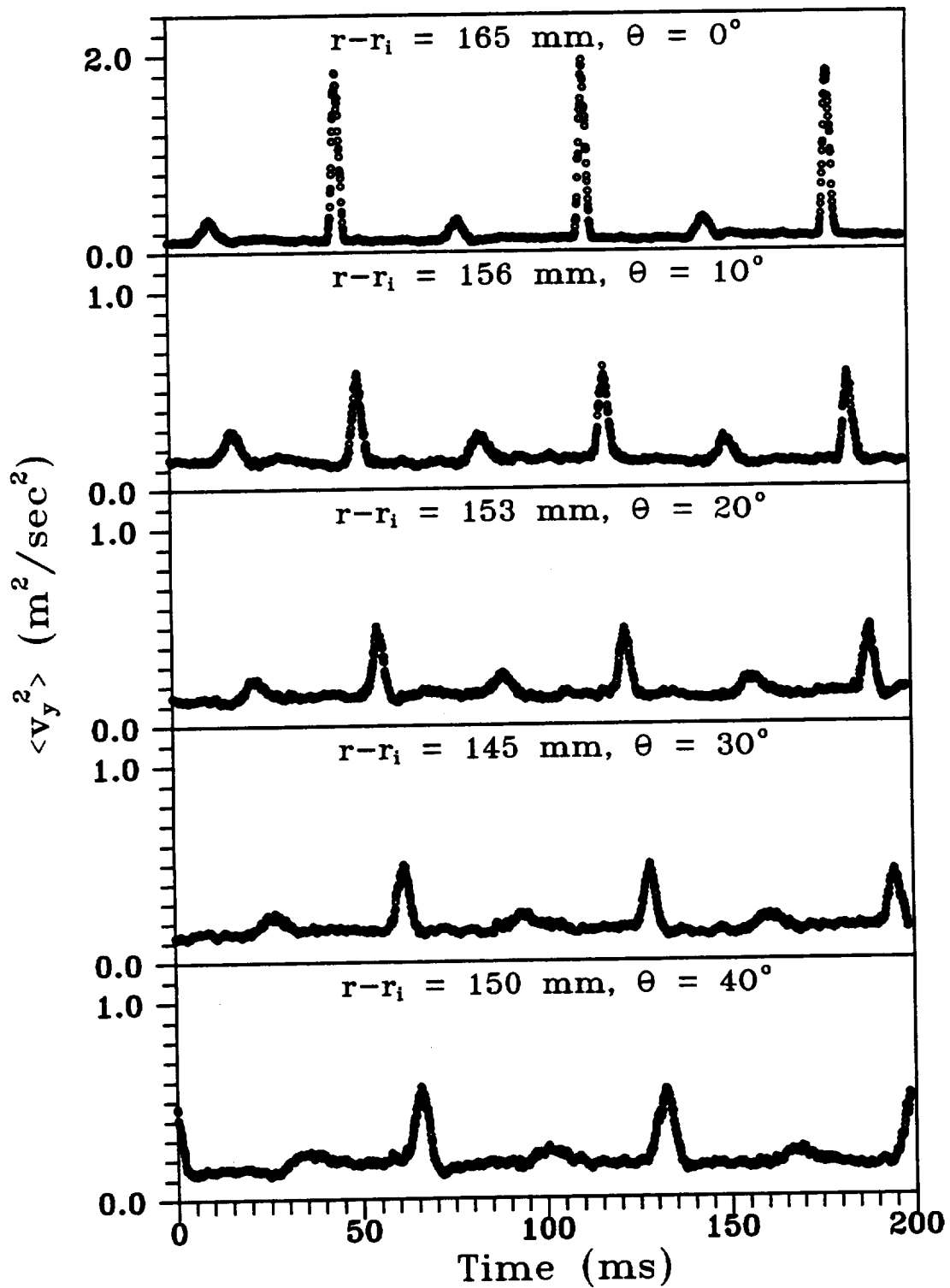
Fig. 88 Phase-averaged Reynolds normal stress $\langle v_y^2 \rangle$ in stationary frame of reference for the periodic unsteady wake at zero streamwise pressure gradient, rpm = 300
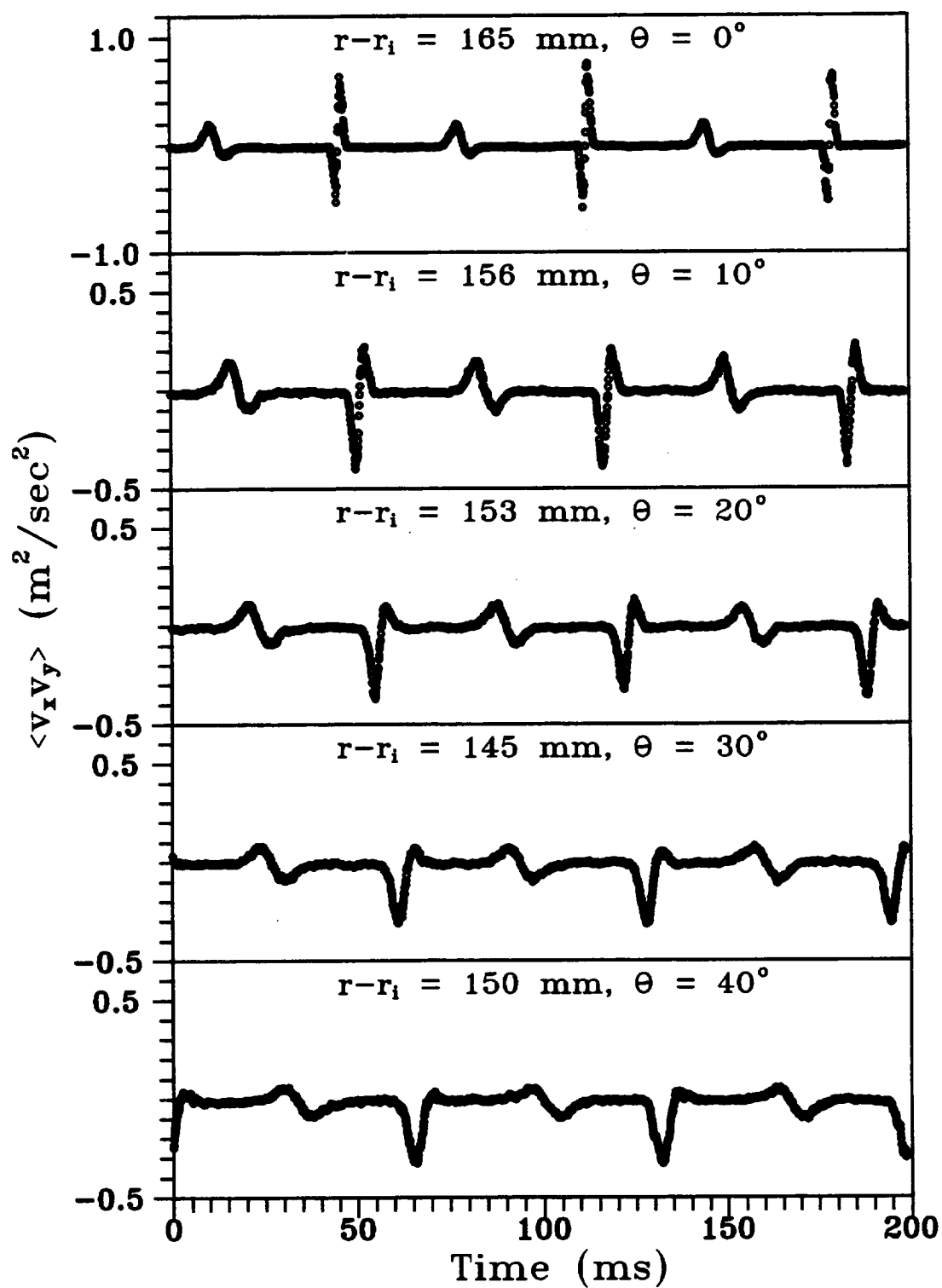
Fig. 89 Phase-averaged Reynolds shear stress $<v_x v_y>$ in stationary frame of reference for the periodic unsteady wake at zero streamwise pressure gradient, rpm = 300

$r - r_i = 165$ mm at $\theta = 0°$ was well outside the wake. The phase-averaged distribution of Reynolds normal stresses are shown in Figs. 87 and 88. Reynolds normal stresses are also asymmetric with respect to the wake center. The phase-averaged Reynolds normal stresses outside the wake increase with downstream location. The secondary wake has a very small value of Reynolds normal stress by the time it reaches the angular position $\theta = 40°$. In fact, the magnitude of the radial component of Reynolds normal stress of the secondary wake at $\theta = 40°$ is comparable to the magnitude of radial component of Reynolds normal stress outside the wake. Temporal distribution of the phase-averaged Reynolds shear stress is plotted in Fig. 89. Similar to the wake of stationary cylinder in the curved channel, the Reynolds shear stress distribution has pronounced asymmetry. The Reynolds shear stress for primary and secondary wakes, shown in Fig. 89, have opposite nature, i.e, in reference to Fig. 89 the left side of the wake has a negative $<v_x v_y>$ for primary wake and positive $<v_x v_y>$ for secondary wake. Conversely, the right side of the wake has a positive $<v_x v_y>$ for primary wake and negative $<v_x v_y>$ for secondary wake. This is because the primary wakes are generated during the upward motion of the cylinder and the secondary wakes are generated during the downward motion of the cylinder. For primary wake, the side of the wake closer to the convex wall, having a negative $<v_x v_y>$, crosses the stationary X-film sensor first. In the case of secondary wake, the side of the wake closer to the concave wall, having a positive $<v_x v_y>$, crosses the stationary X-film sensor first.

Contour plots of phase-averaged turbulence intensity, tangential velocity, and Reynolds stresses are plotted in Figs. 90-94. The time scale t is nondimensionalized with respect to the wake passing period T (≈ 66.66 ms). The tangential velocity is nondimensionalized by average velocity at the wake generator section (≈ 20 m/s) and the Reynolds stresses are nondimensionalized by square of the average velocity at the wake generator section. The contours are plotted in the time-distance plane from the phase-averaged data obtained at five streamwise locations, keeping the probe at a fixed radial location. The upper contour plot at a radial location of $r-r_i = 140$ mm shows distinct primary and secondary wake region. In the lower plot, obtained at the middle of the channel, the primary and secondary wakes seem to be merging together from
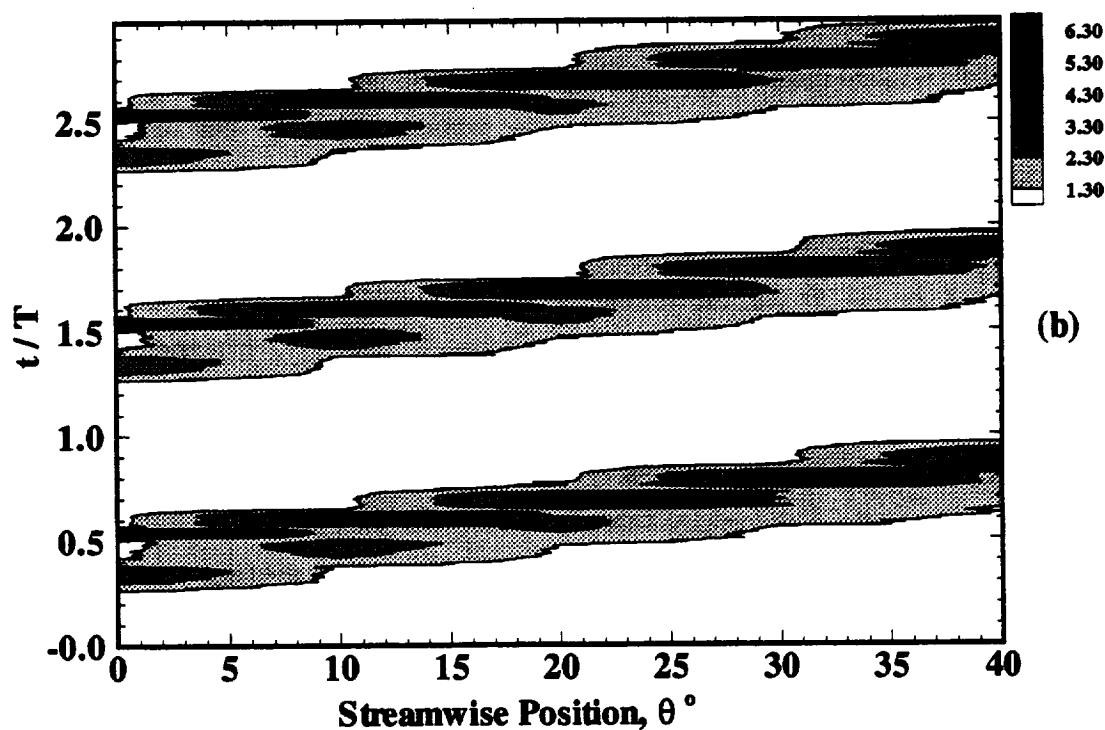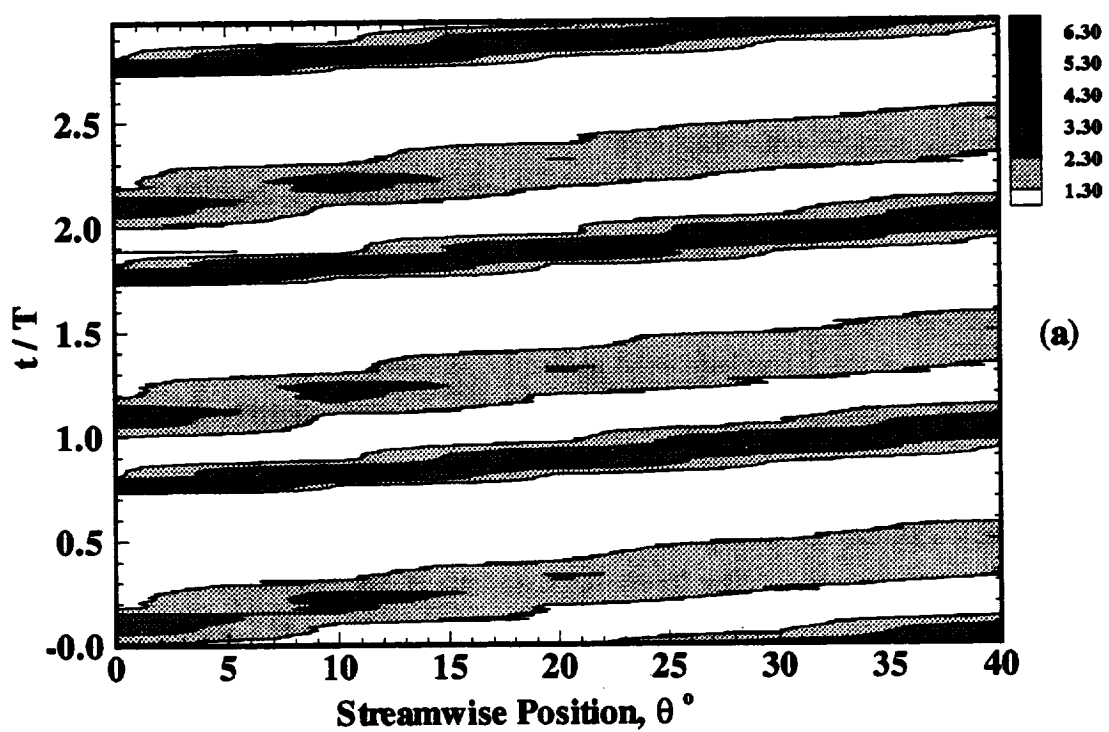
Fig. 90 Contours of phase-averaged turbulence intensity <Tu> [%] for the periodic unsteady wake at zero pressure gradient. (a) r-r_i = 140 mm, (b) r-r_i = 210 mm
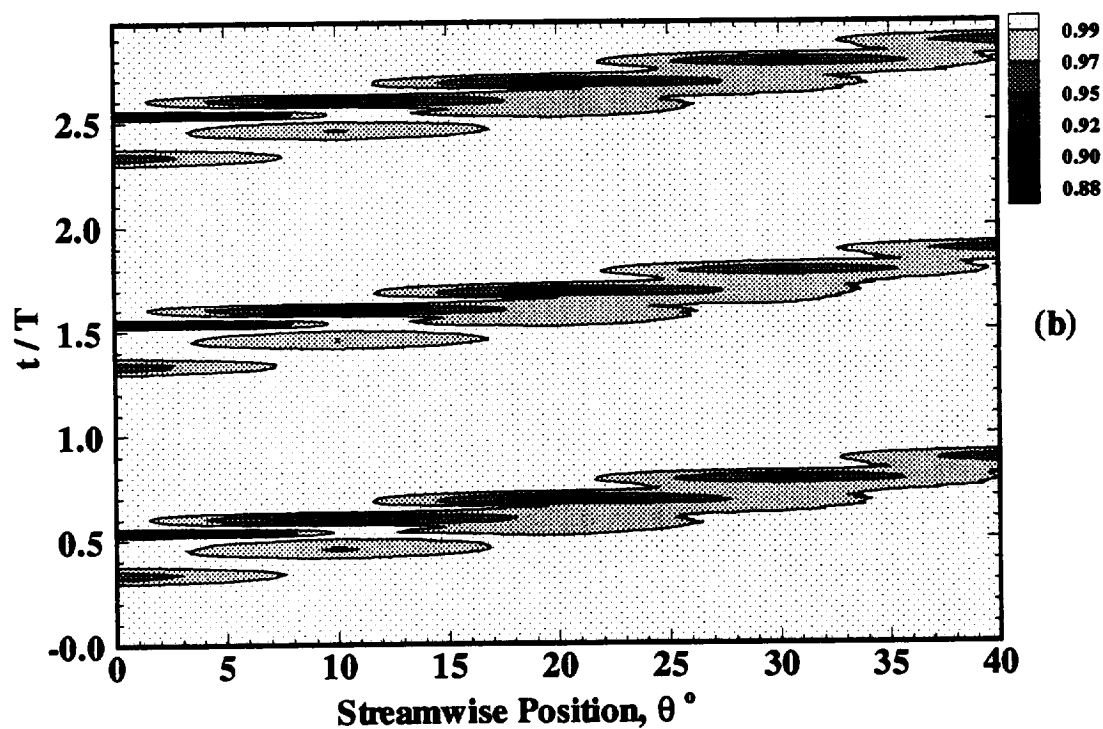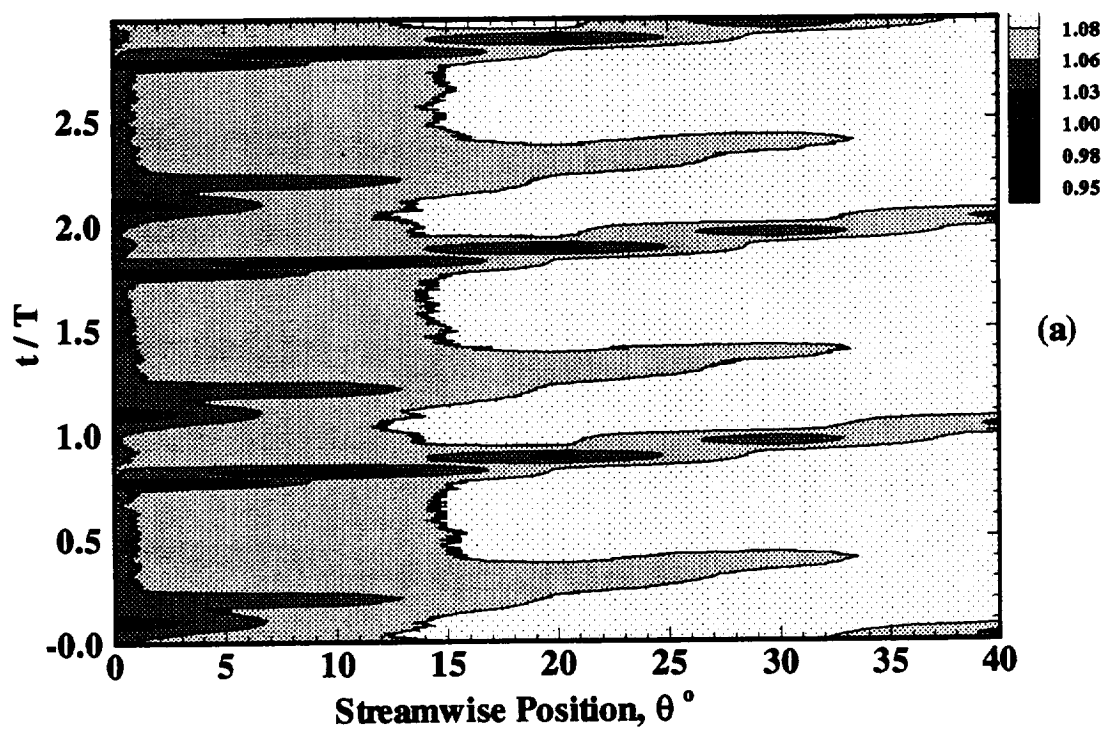
Fig. 91 Contours of phase-averaged velocity $<V_r>/V_{in}$ for the periodic unsteady wake at zero pressure gradient. (a) $r-r_i = 140$ mm, (b) $r-r_i = 210$ mm
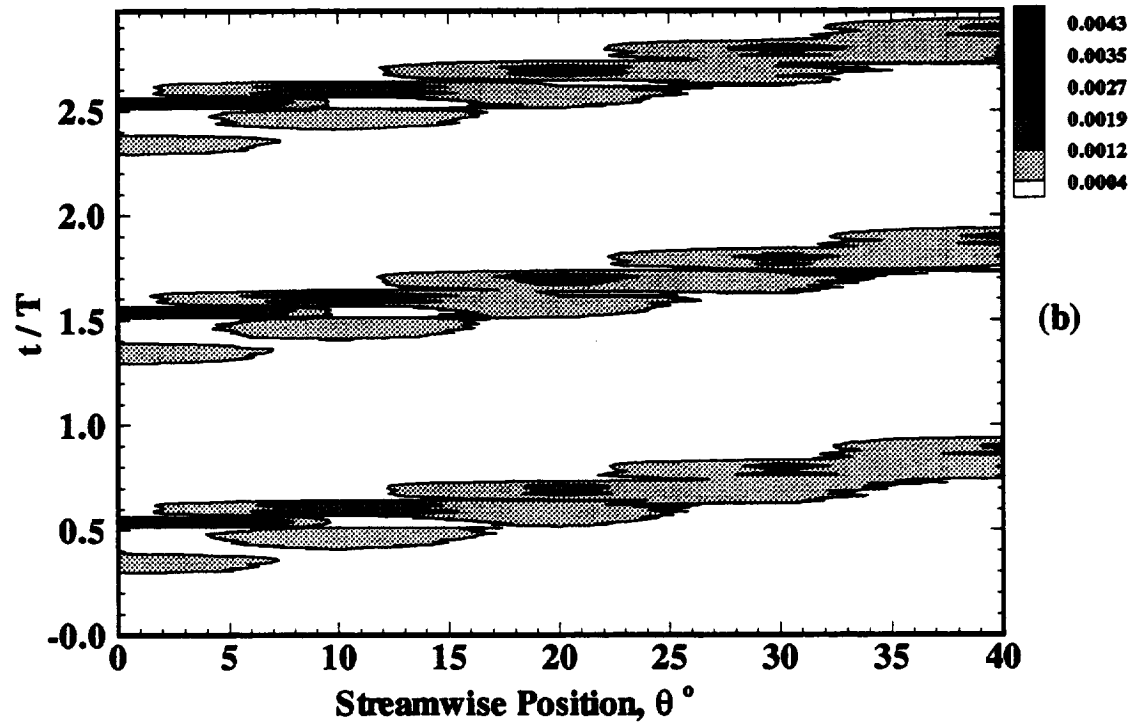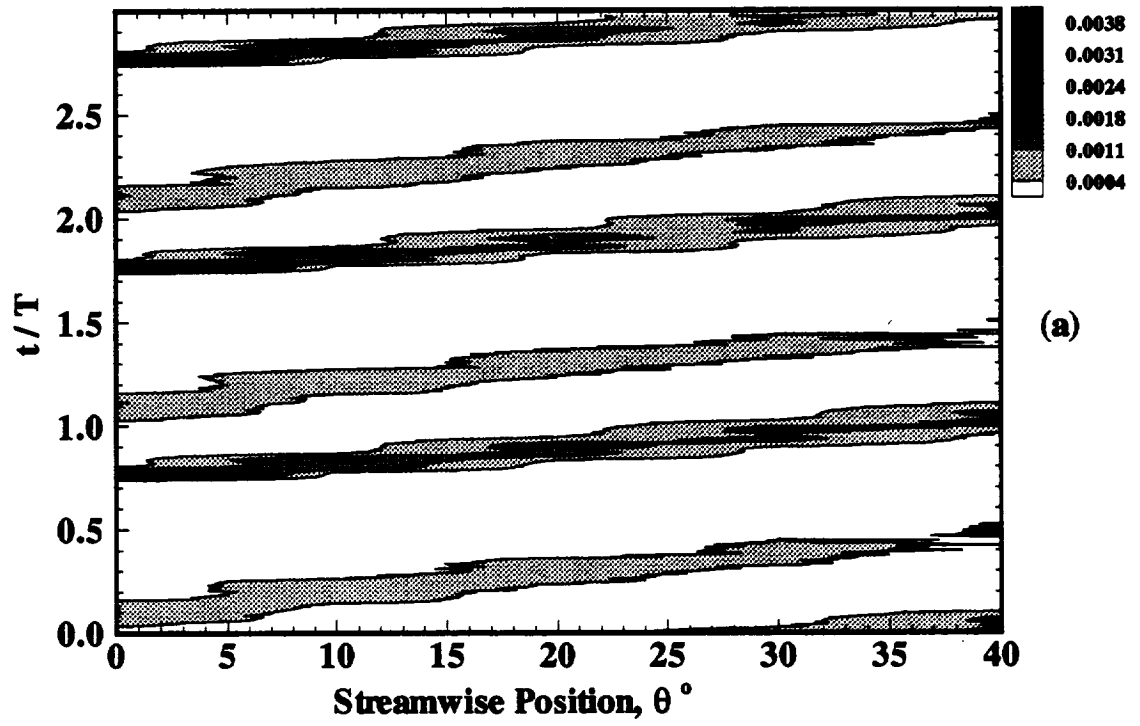
Fig. 92 Contours of phase-averaged Reynolds stress $<v_x^2>/V_{in}^2$ for the periodic unsteady wake at zero pressure gradient. (a) $r-r_i = 140$ mm, (b) $r-r_i = 210$ mm
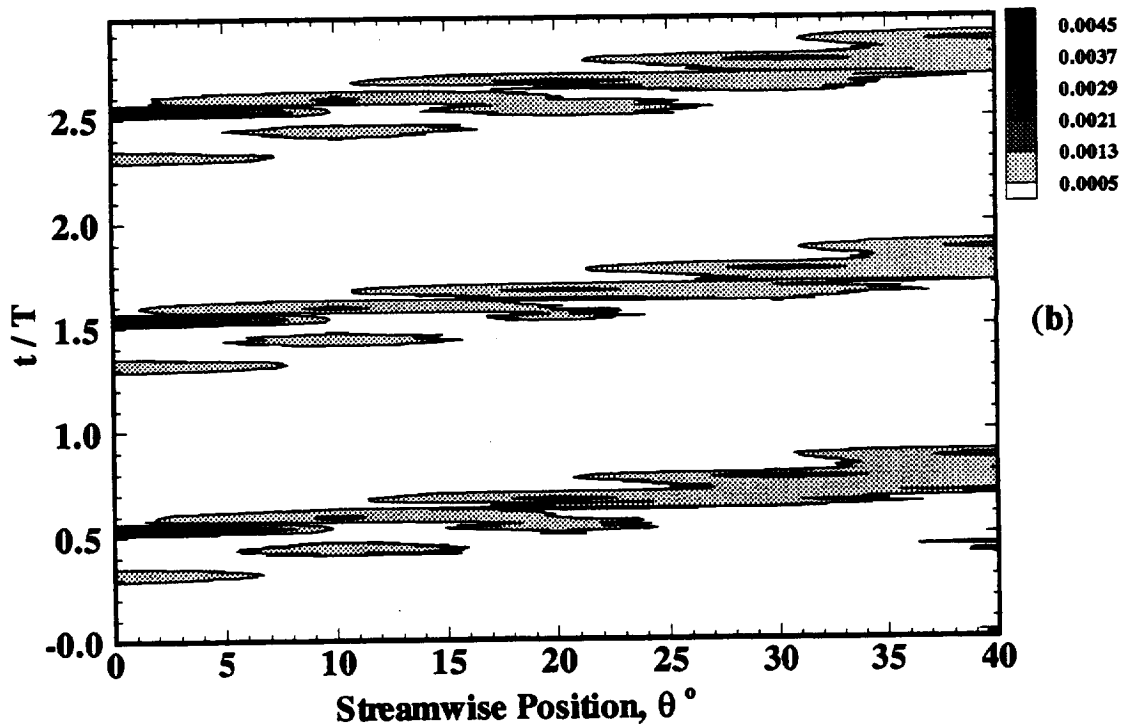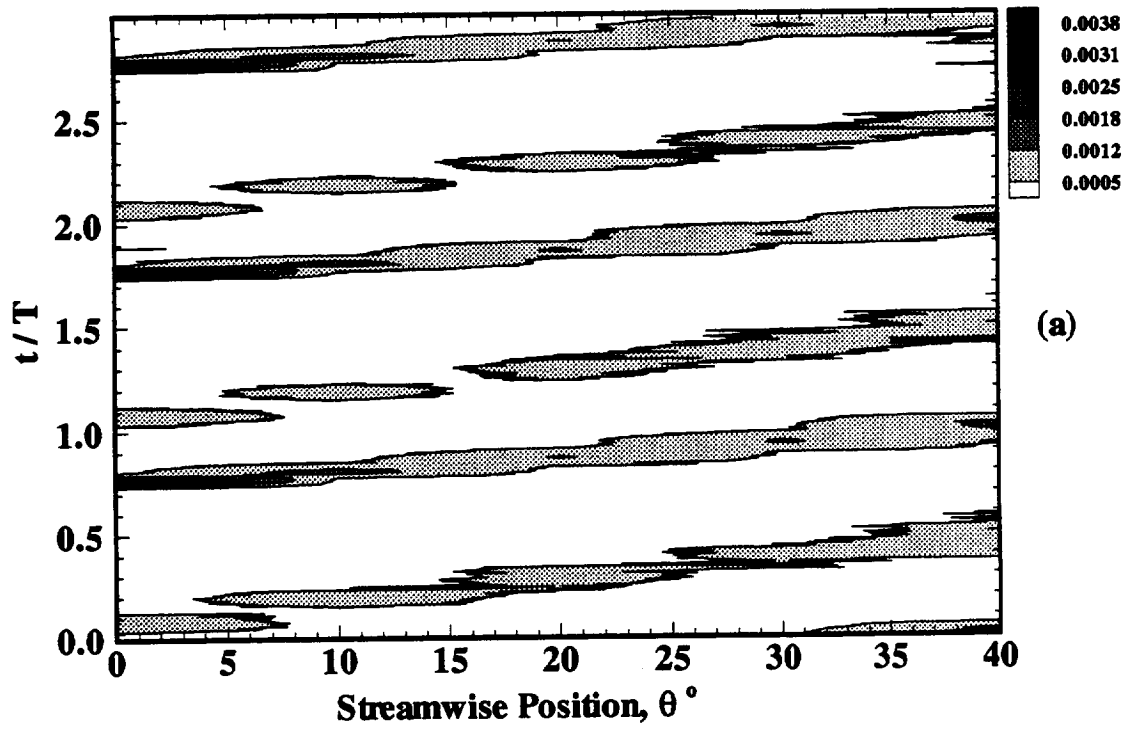
Fig. 93 Contours of phase-averaged Reynolds stress $<v_y^2>/V_{in}^2$ for the periodic unsteady wake at zero pressure gradient. (a) $r\text{-}r_i = 140$ mm, (b) $r\text{-}r_i = 210$ mm
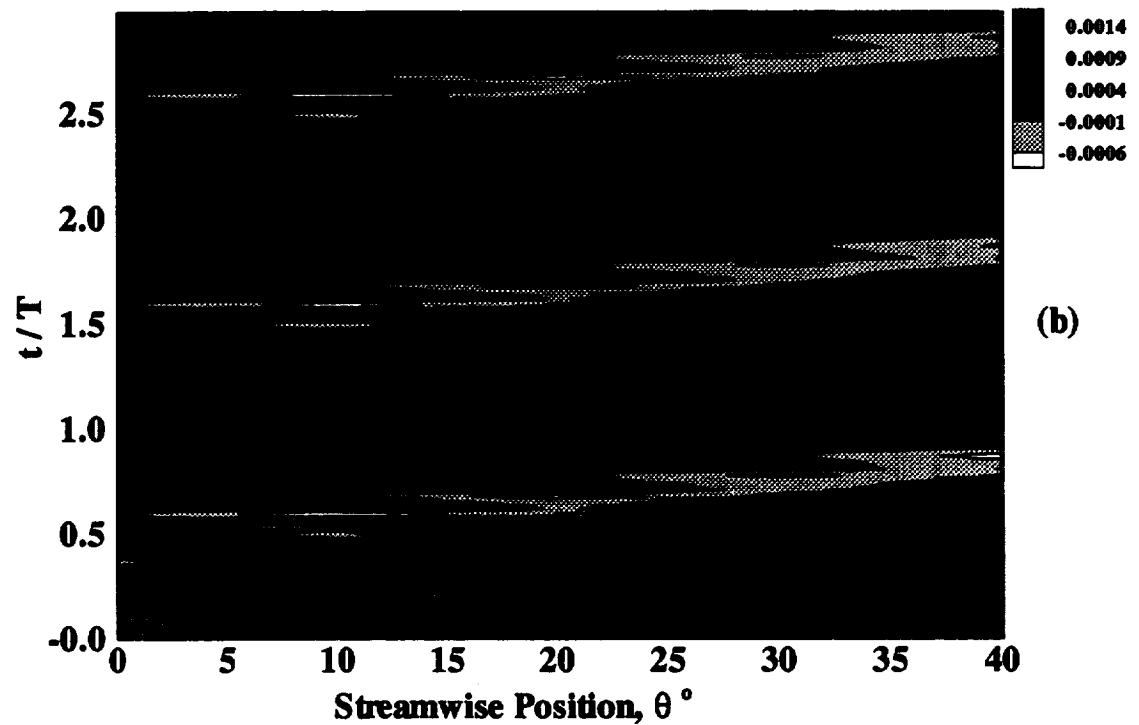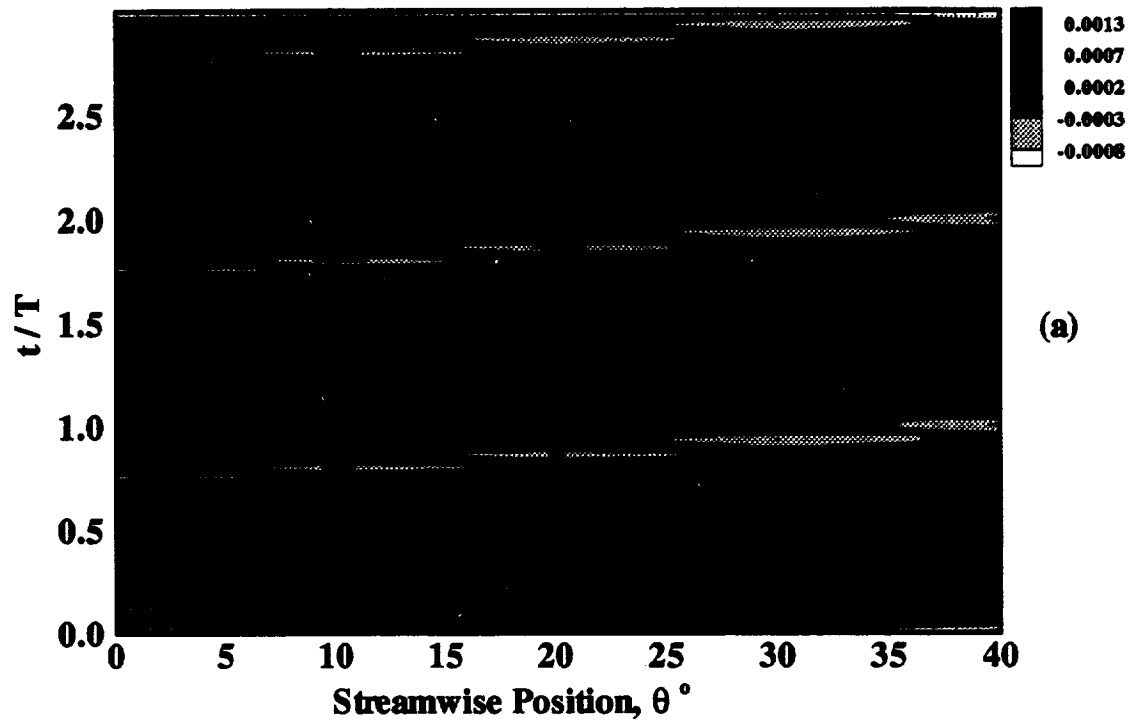
Fig. 94 Contours of phase-averaged Reynolds stress $<v_x v_y>/V_{in}^2$ for the periodic unsteady wake at zero pressure gradient. (a) r-r_i = 140 mm, (b) r-r_i = 210 mm

downstream location 5° onwards. The isolated contours are due to lack of measurement locations. Otherwise, the contour plots exhibit the general behavior of the variation of velocity, Reynolds stresses and turbulence intensity. The phase-averaged turbulence intensity contours in Fig. 90(a) clearly demonstrate the qualitative nature of the primary and secondary wakes. At a particular streamwise position and the center of the wake, the primary wake has higher turbulence intensity than the secondary wake. Also, the primary wake has smaller width than the secondary wake. In Fig. 90(b), the primary and secondary wakes have almost merged together. Figure 91 shows the contours of phase-averaged velocity V_x. The center region of the wake, where the velocity is minimum is shown by darker areas. The contours of phase-averaged Reynolds normal stresses, shown in Figs. 92 and 93, are similar to the contours of turbulence intensity. The phase-averaged Reynolds shear stress contours are given in Fig. 94. The dark region has a positive value of $<v_x v_y>$ and the white region have a negative value of $<v_x v_y>$. The center of the wake and the region outside the wake, have $<v_x v_y>$ value close to zero. This can be clearly seen in Fig. 94(a) for primary wakes up to a streamwise position $\theta = 20°$. In order to get a clean picture, the contour plots of $<v_x v_y>$ has to be plotted in an enlarged scale with high resolution, since there exist a steep transverse gradient of $<v_x v_y>$ at the center of the wake. The contour plots shown in Figs. 90-94, of course, need data at more streamwise positions. However, the contours obtained with limited data, are useful in identifying the primary and secondary wakes and their propagation in the time-distance plane.

8.4.2. Spatial Distribution in Curvilinear Coordinates and Relative Frame of Reference

In order to compare with the stationary wake in zero pressure gradient curved channel, the temporal development of the periodic unsteady wake is transformed to a curvilinear spatial coordinate system relative to the moving cylinder. This transformation is done using the approach described in Section 7. The velocity defect, transverse velocity, Reynolds stresses, and third-order correlations are presented in

similarity coordinates. The results are shown at five downstream locations (angular positions) at a constant rotational speed of 300 rpm. The radial location chosen at each angular position corresponds to the location where the primary wakes are in the middle of the secondary wakes. Also, the results are shown at four different rotational speeds for the measurements taken at the inlet (θ = 0°) and r-r_i = 165 mm.

8.4.2.1. Mean Velocity Distribution

The transverse distribution of mean velocity defect for different streamwise locations are plotted in Fig. 95(a). The mean velocity defect is normalized by its maximum value and the transverse distance by the wake width b. The solid line represents the function φ_{1r}, $\varphi_{1r} = \bar{U}_1/U_{1mr} = e^{-(2)\zeta_r)^2}$, where $\zeta_r = \dfrac{\xi_{2r}}{b}$. The mean velocity defect profiles are symmetric and identical to the steady wake data in the zero pressure gradient curved channel. The profiles of mean velocity defect at different rotational speeds and at a constant measurement location are shown in Fig. 95(b). The mean velocity defect profiles exhibit complete similarity.

The transverse distribution of normalized transverse velocity $\bar{V}_r$ / U_{1mr} for various streamwise locations are plotted in Fig. 96(a). Also, the normalized transverse velocity distribution at four different rotational speeds are shown in Fig. 96(b). The transverse distribution is qualitatively similar to the zero pressure gradient curved wake.

8.4.2.2. Reynolds Stresses

The transverse distribution of the nondimensionalized Reynolds stresses are shown in Figs. 97-99. The Reynolds normal stresses are normalized with respect to its value at the wake center. The values of Reynolds normal stresses at the wake center at different downstream locations are given in Table 9 (Appendix A). The normalized Reynolds stress component in the streamwise direction, are shown in Fig. 97. The results are found to be consistent with measurements obtained behind the stationary
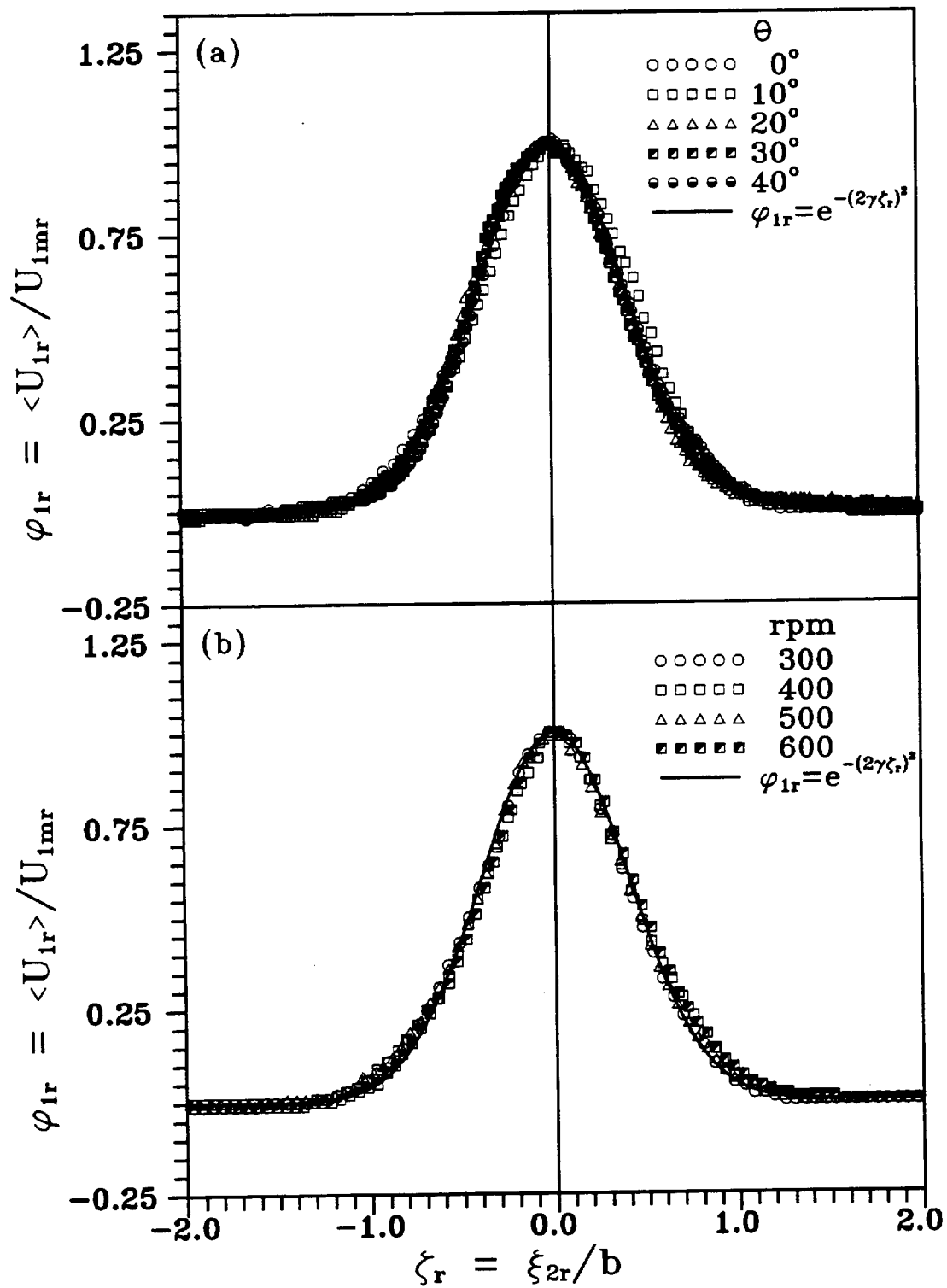
Fig. 95 Transverse distribution of velocity defect for the periodic unsteady wake.
(a) rpm = 300, (b) $\theta = 0°$
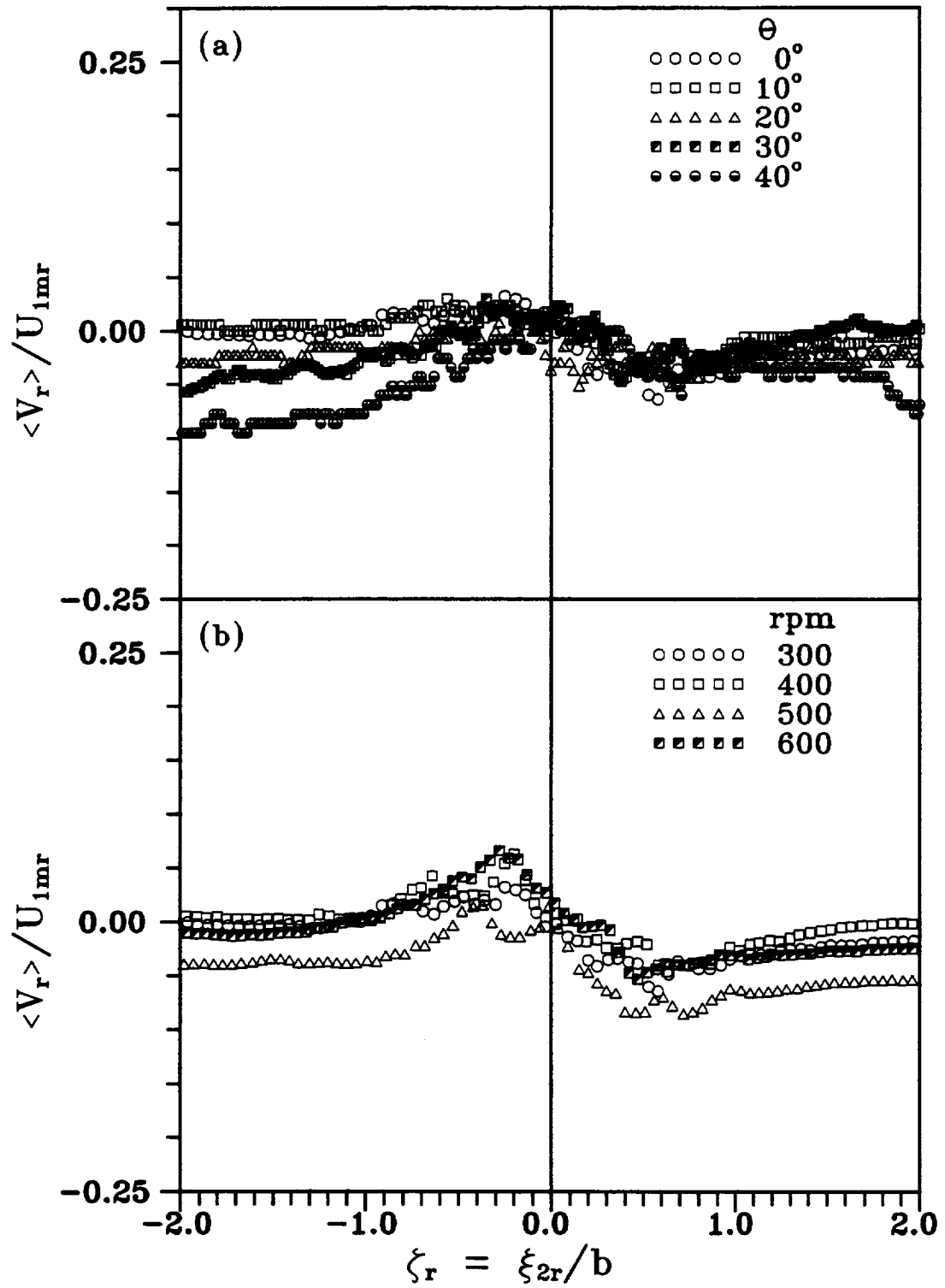
Fig. 96 Transverse distribution of velocity $<V_r>$ for the periodic unsteady wake. (a) rpm = 300, (b) $\theta = 0^\circ$

cylinder in the zero pressure gradient curved channel. The results show asymmetry, with a higher value of Reynolds stress at the inner side than at the outer side of the wake. The effect of rotational speed on the normalized Reynolds stress distribution are small within the range of investigation.

The normalized transverse component of Reynolds stresses are plotted in Fig. 98. Similar to the streamwise component, the maximum value of transverse component of Reynolds stress occurs at the inner half of the wake. The asymmetric feature of the transverse component of Reynolds stress is more than that of the streamwise component.

The transverse distribution of Reynolds shear stress at various streamwise locations are plotted in Fig. 99. The Reynolds shear stress is nondimensionalized by square of the maximum velocity defect. The results are in general agreement with the results of the wake development behind a stationary cylinder in a curved channel. The Reynolds shear stress distribution shows the strong asymmetry due to the curvature. The value of Reynolds shear stress is higher on the inner half of the wake than that on the outer half. It may be observed that the effect of rotational speed on the nondimensional Reynolds stress distribution are small. The Reynolds shear stress at the center of the wake is not equal to zero.

8.4.2.3. Higher Order Correlations

The phase-averaged third-order correlations (triple products) of turbulent fluctuations in relative spatial coordinates are obtained from instantaneous velocity components. Four such correlations, $<u_r^3>$, $<v_r^3>$, $<u_r^2 v_r>$, and $<u_r v_r^2>$, nondimensionalized with respect to the cube of maximum velocity defect U_{Imr} are presented in this section. The conservation equations for turbulent kinetic energy and Reynolds stresses contain terms involving the gradient of the above correlations. The experimental data on the distribution of these correlations can be helpful in modelling these terms in turbulence closure problems.

The transverse distribution of phase-averaged triple product $<u_r^3>/U_{Imr}^3$ at different streamwise locations are shown in Fig. 100(a). The triple product u_r^3 represents the
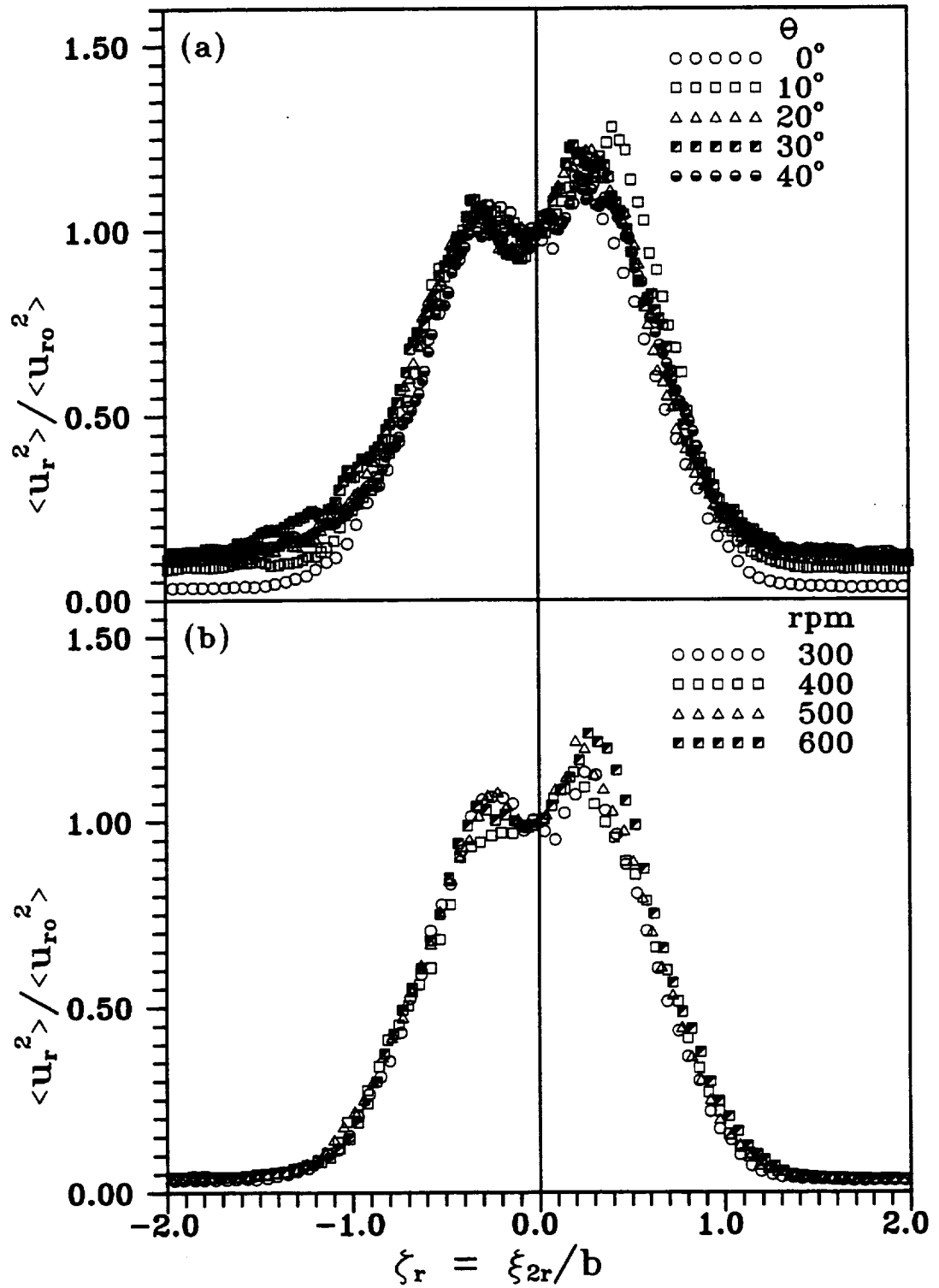
Fig. 97 Transverse distribution Reynolds normal stress $<u_r^2>$ for the periodic unsteady wake. (a) rpm = 300, (b) $\theta = 0°$
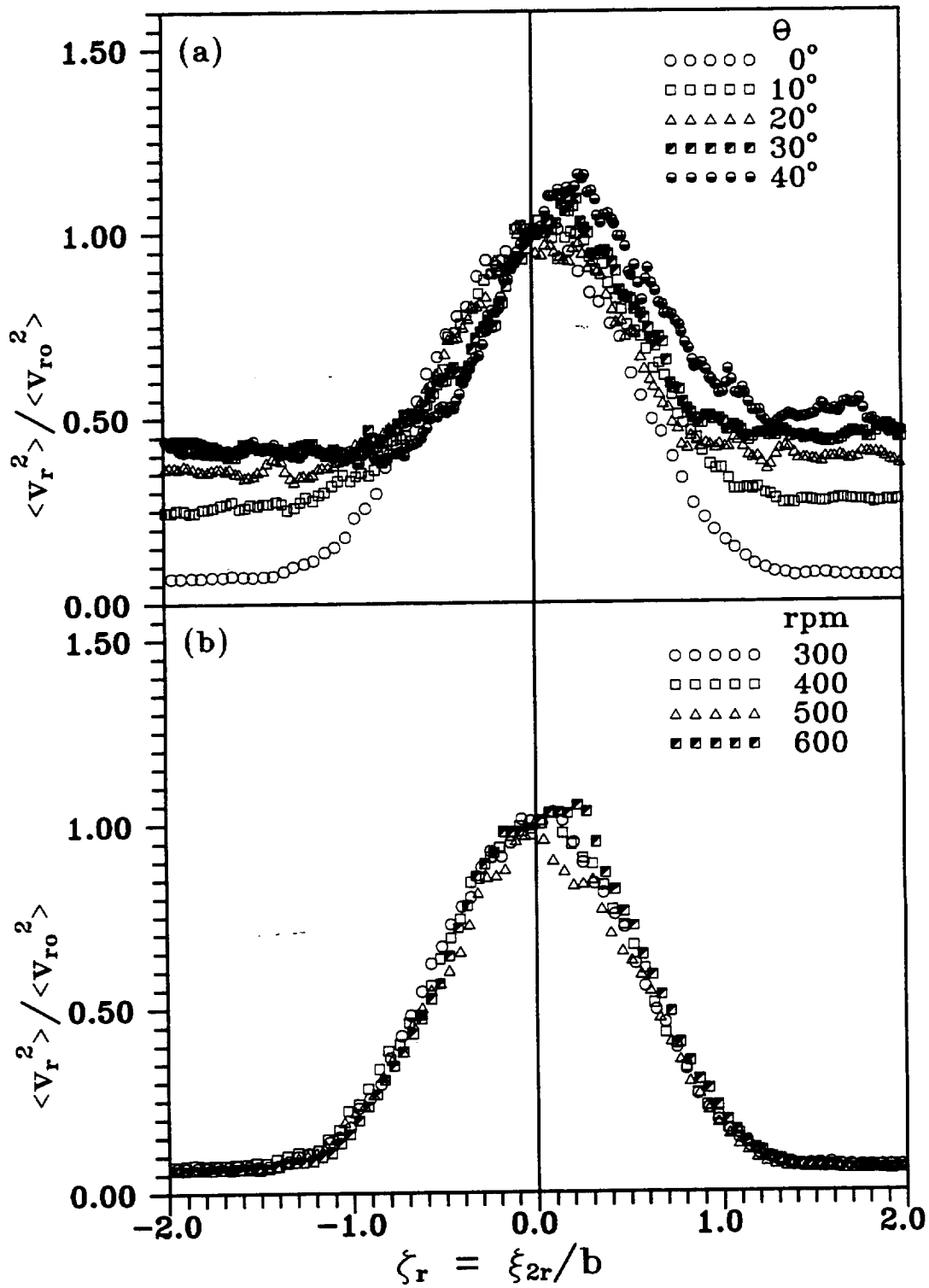
Fig. 98 Transverse distribution Reynolds normal stress $<v_r^2>$ for the periodic unsteady wake. (a) rpm = 300, (b) $\theta = 0°$
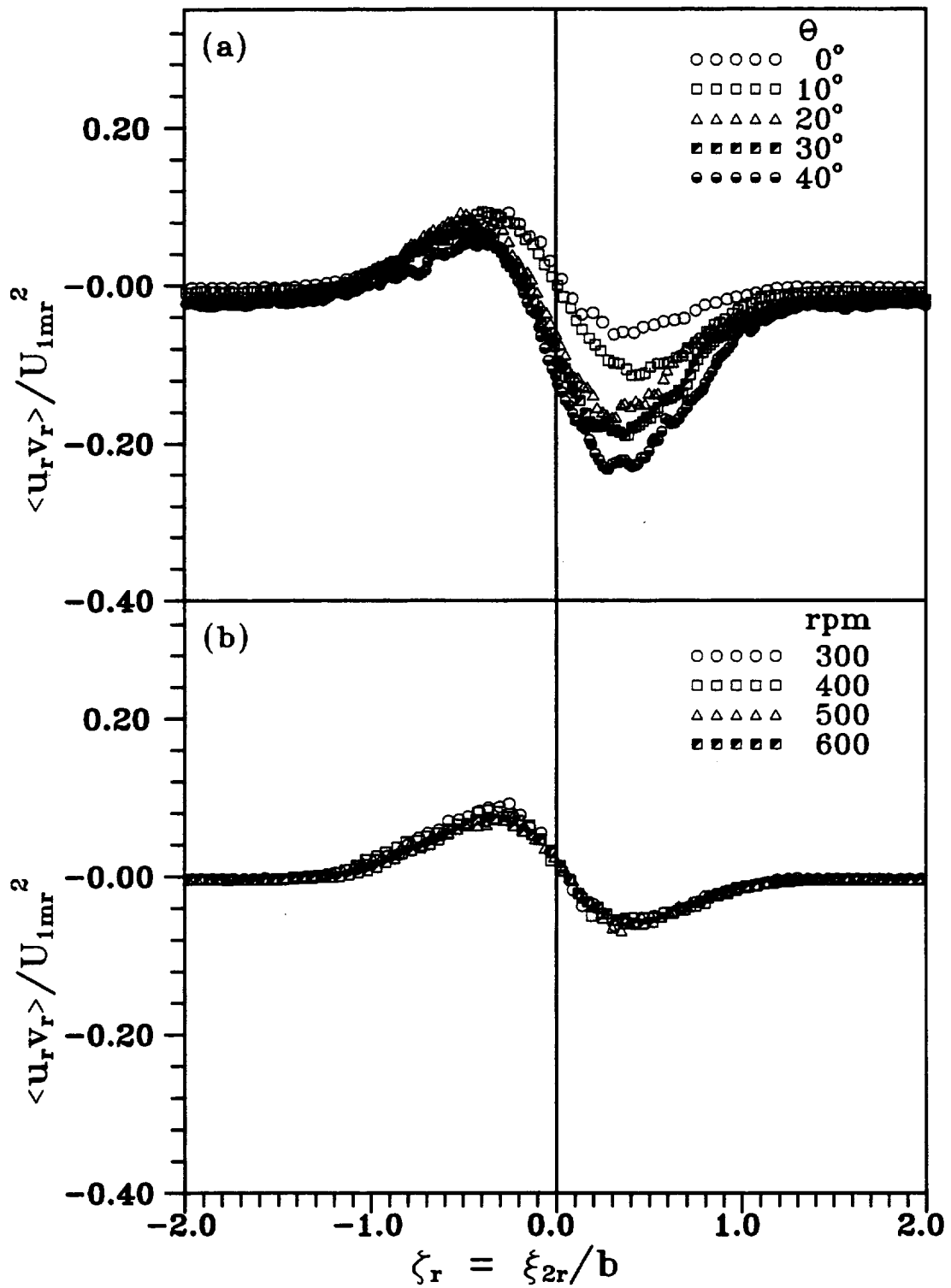
Fig. 99 Transverse distribution of Reynolds shear stress for the periodic unsteady wake. (a) rpm = 300 , (b) θ = 0°

transport of the component of turbulent kinetic energy u_r^2, by the streamwise fluctuation u_r across a unit area normal to the streamwise direction. The distribution $<u_r^3>/U_{1mr}^3$ show asymmetry, with higher value in the inner side of the wake than that in the outer side. In comparison, the straight wake data obtained by Fabris (1983) behind a stationary cylinder is symmetric about the wake center with two negative minima (one on each side of the wake center) and a positive maximum at the wake center. Fig. 100(b) shows the distribution of $<u_r^3>/U_{1mr}^3$ at four rotational speeds at a fixed measurement location. As seen in Fig. 100(b), the effect of rotational speed on the distribution of $<u_r^3>/U_{1mr}^3$ is small.

The transverse distribution of phase-averaged triple product $<v_r^3>/U_{1mr}^3$ at different streamwise locations are shown in Fig. 101(a). The triple product v_r^3 represents the transport of the component of turbulent kinetic energy v_r^2, by the transverse fluctuation v_r across a unit area normal to the transverse direction. The distribution $<v_r^3>/U_{1mr}^3$ show asymmetry, with higher value in the inner side of the wake than that in the outer side. The $<v_r^3>/U_{1mr}^3$ distribution at four rotational speeds shown in Fig. 101(b) is qualitatively similar to the straight wake data obtained by Fabris (1983).

Figures 102(a) and 102(b) show the transverse distribution of $<u_r^2 v_r>/U_{1mr}^3$ at different streamwise positions and rotational speeds, respectively. The triple product $u_r^2 v_r$ represents transport of the component of turbulent kinetic energy u_r^2, by the transverse fluctuation v_r across a unit area normal to the transverse direction. The distribution of $<u_r^2 v_r>/U_{1mr}^3$ shown in Fig. 102(a) has higher values on the inner side of the wake than that on the outer side. The distribution shown in Fig. 102(b) is similar to the straight wake data obtained by Fabris (1983).

Figures 103(a) and 103(b) show the transverse distribution of $<u_r v_r^2>/U_{1mr}^3$ at different streamwise positions and rotational speeds, respectively. The correlation $u_r v_r^2$ represents the transport of the component of turbulent kinetic energy v_r^2, by the streamwise fluctuation u_r across a unit area normal to the streamwise direction. The $<u_r v_r^2>/U_{1mr}^3$ distributions are similar to the distributions of $<u_r^3>/U_{1mr}^3$ shown in Figs. 100(a) and 100(b), but with a lower negative minima.
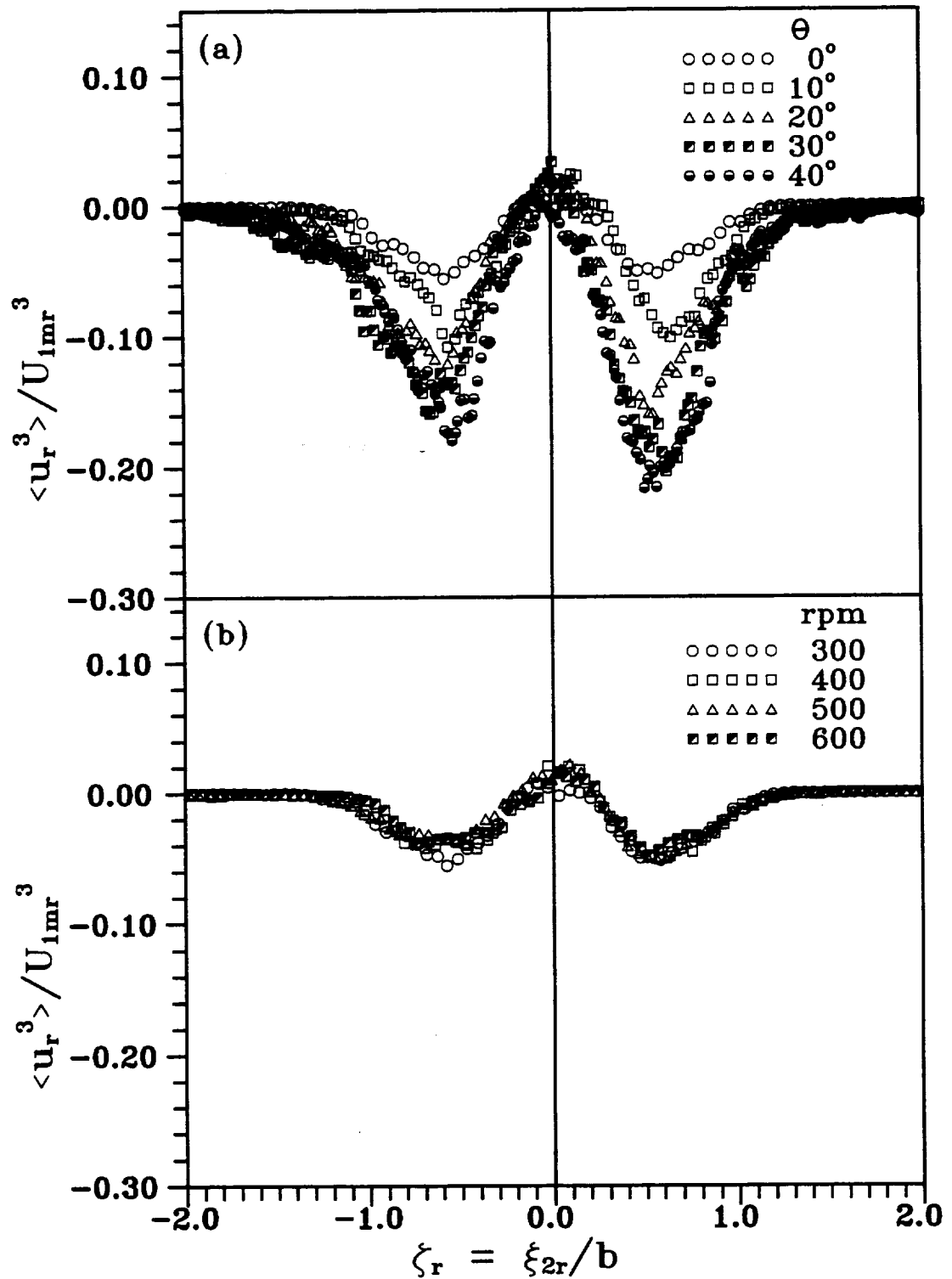
Fig. 100 Transverse distribution of third-order correlation $<u_r^3>$ for the periodic unsteady wake. (a) rpm =300, (b) $\theta = 0°$
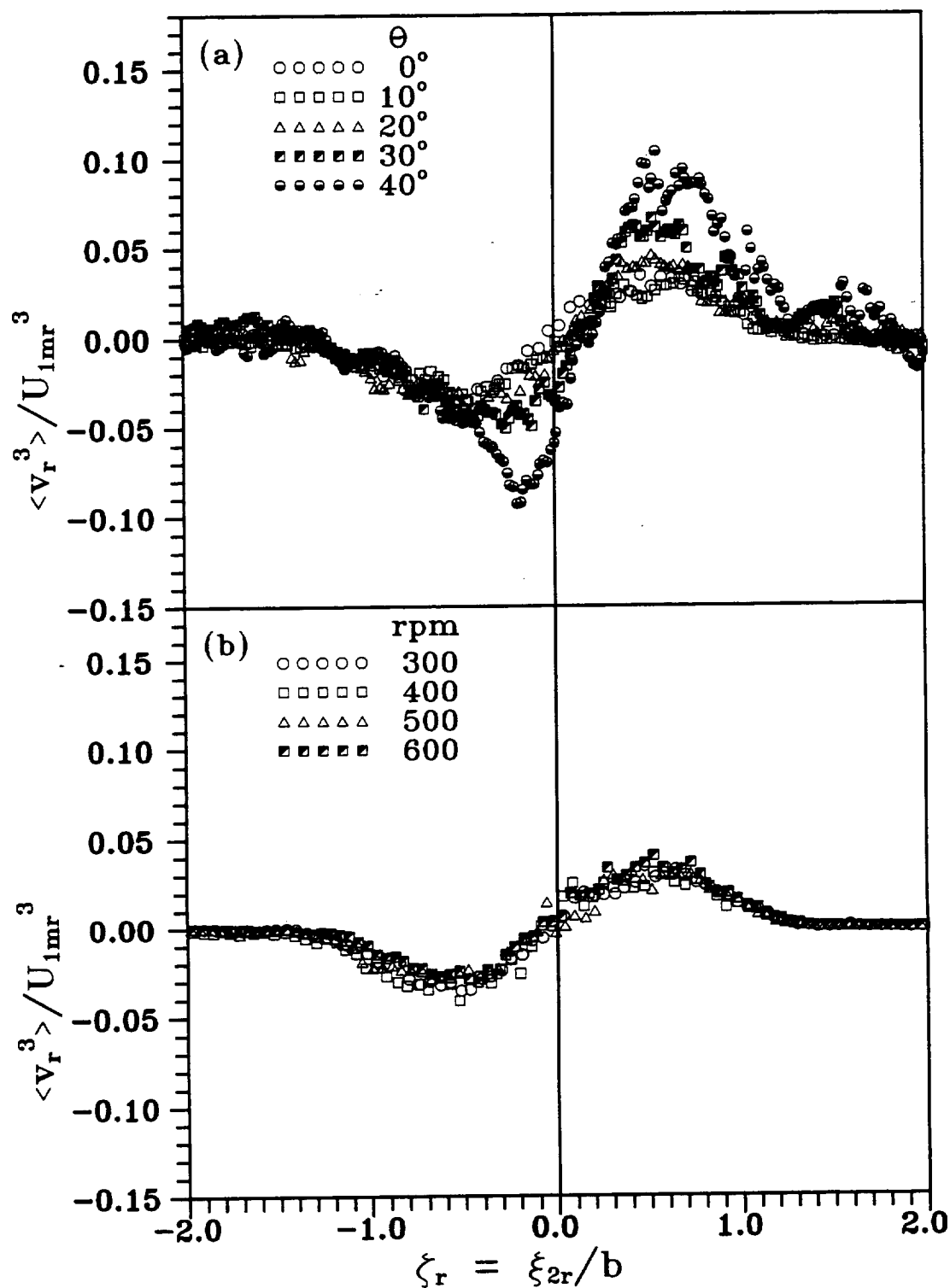
Fig. 101 Transverse distribution of third-order correlation $<v_r^3>$ for the periodic unsteady wake. (a) rpm = 300, (b) $\theta = 0°$
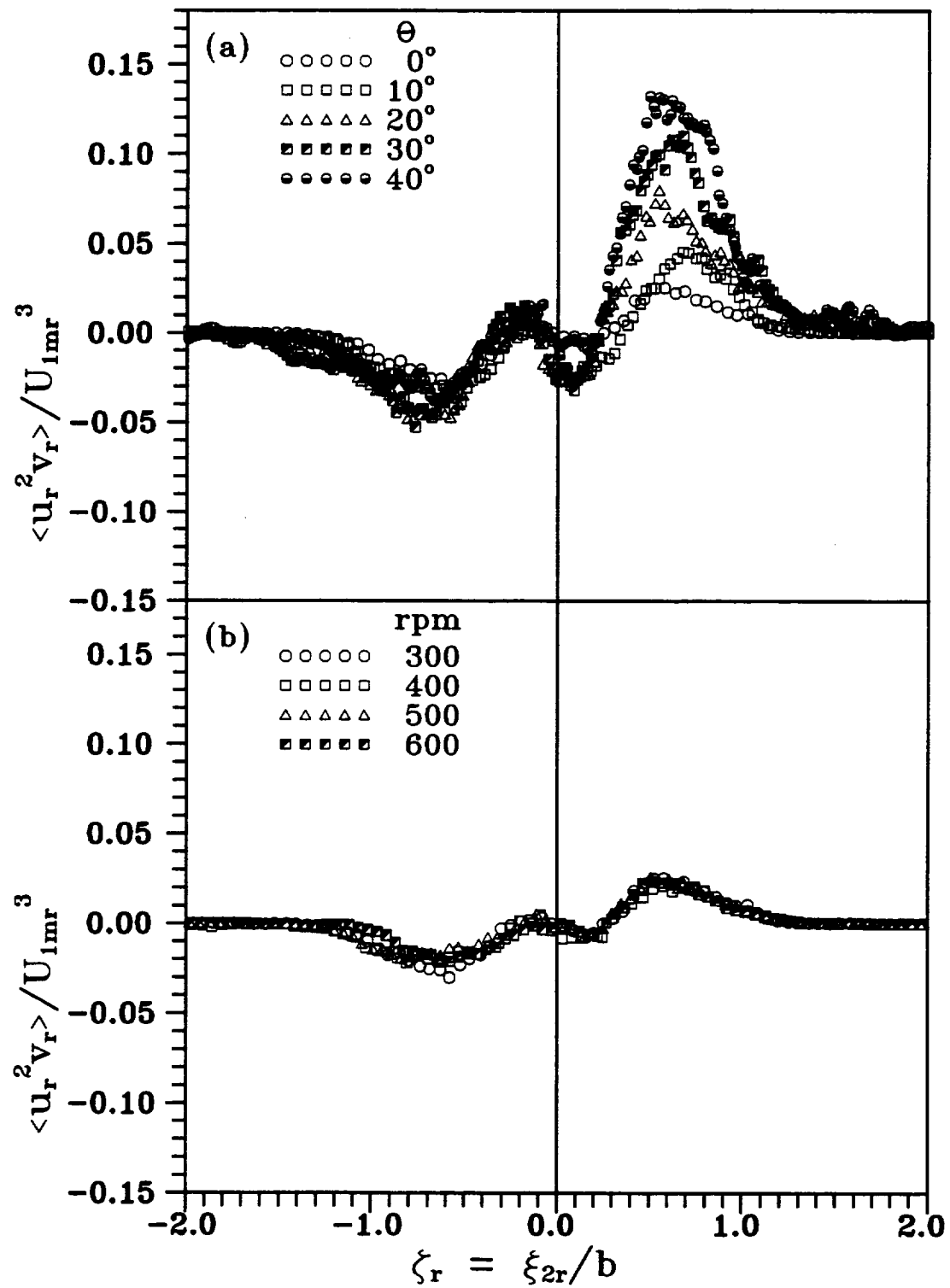
Fig. 102 Transverse distribution of third-order correlation $<u_r^2 v_r>$ for the periodic unsteady wake. (a) rpm = 300, (b) $\theta = 0^\circ$

8.4.2.4. Wake Width, Maximum Velocity Defect, and Integral Parameters

The wake width, maximum velocity defect, potential velocity at the wake center, and wake integral parameters are obtained at different angular positions. The angular and radial positions for data points presented in this section corresponds to the cases described in section 8.4.2 at 300 rpm. The values of maximum velocity defect, wake width, potential velocity at the wake center, and average velocity upstream of the cylinder for above positions are given in Table 9 (Appendix A). The maximum velocity defect and the wake width as a function of angular position are plotted in Figs. 104(a) and 104(b), respectively. The hypothetical potential velocity at the wake center is shown in Fig. 105(a). The slightly increasing value of hypothetical velocity distribution does not imply that the wake is subjected to a negative pressure gradient. This is due to the fact that the radial locations at each angular position was chosen in such a way that the primary wakes were approximately in the middle of the secondary wakes. These radial locations happened to have a potential velocity increasing with downstream location. Figure 105(b) shows the product $U_{1m}b$ at different angular positions. The momentum thickness ratio and shape factor are plotted in Figs. 106(a) and 106(b), respectively. The increasing value of the product $U_{1m}b$ and the momentum thickness ratio can be due to the variation of the pressure along the radial direction. Since the wake generating cylinder is moving upwards, the trajectory of the wake centerline in relative frame of reference is moving towards the concave wall experiencing a higher pressure.
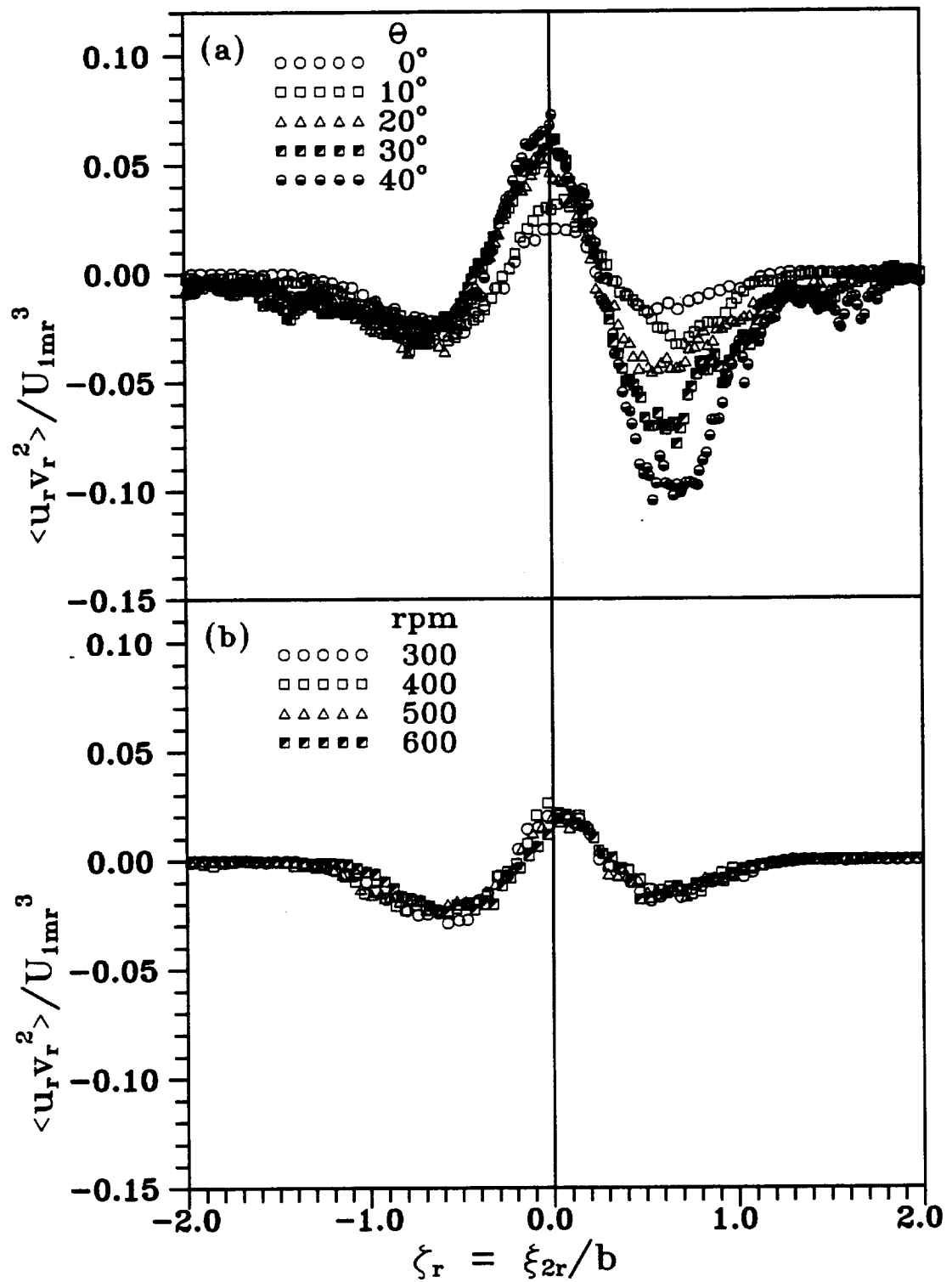
Fig. 103 Transverse distribution of third-order correlation $<u_r v_r^2>$ for the periodic unsteady wake. (a) rpm = 300, (b) $\theta = 0°$
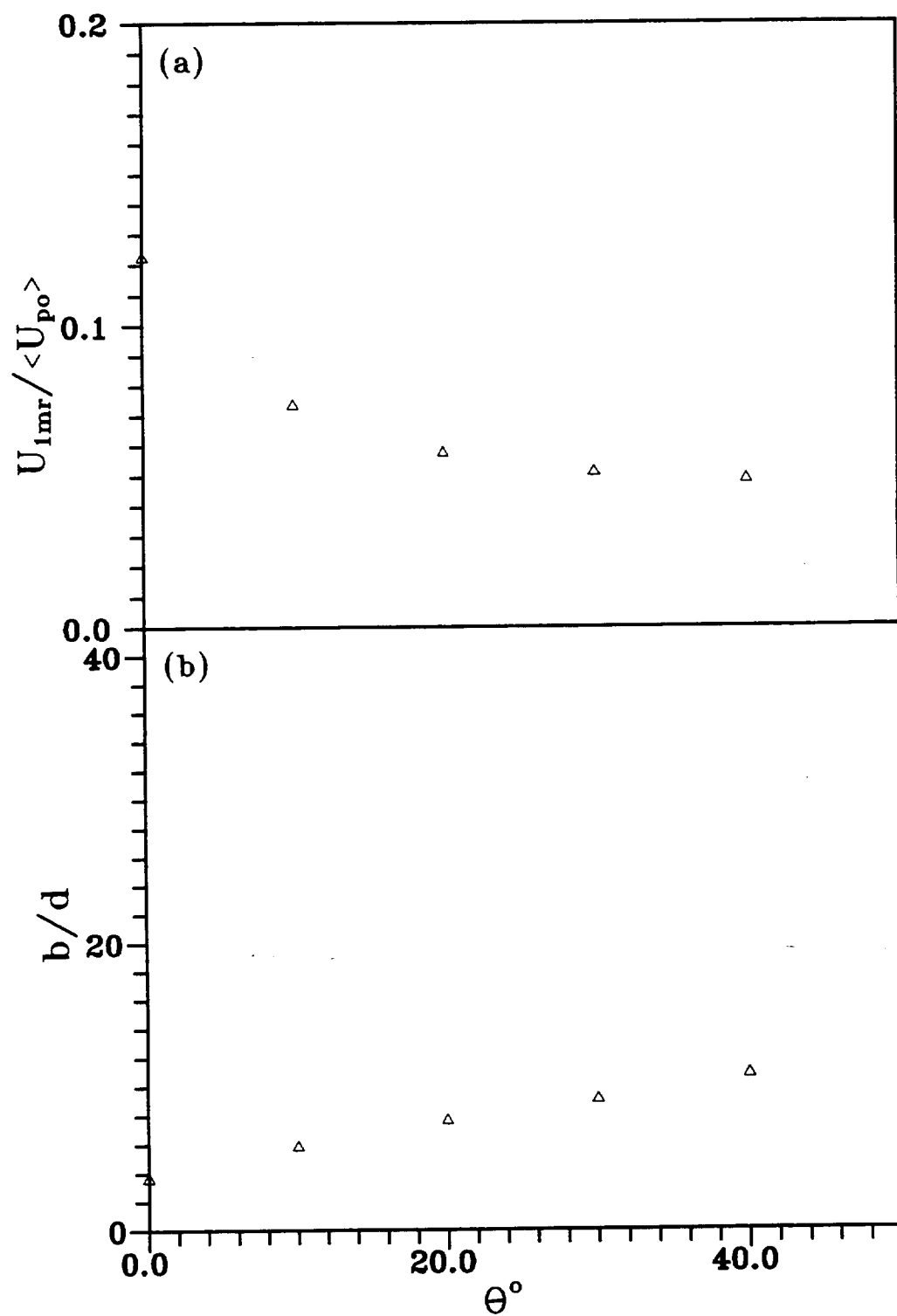
Fig. 104 Decay of maximum velocity defect (a) and growth of wake width (b) as a function of angular position
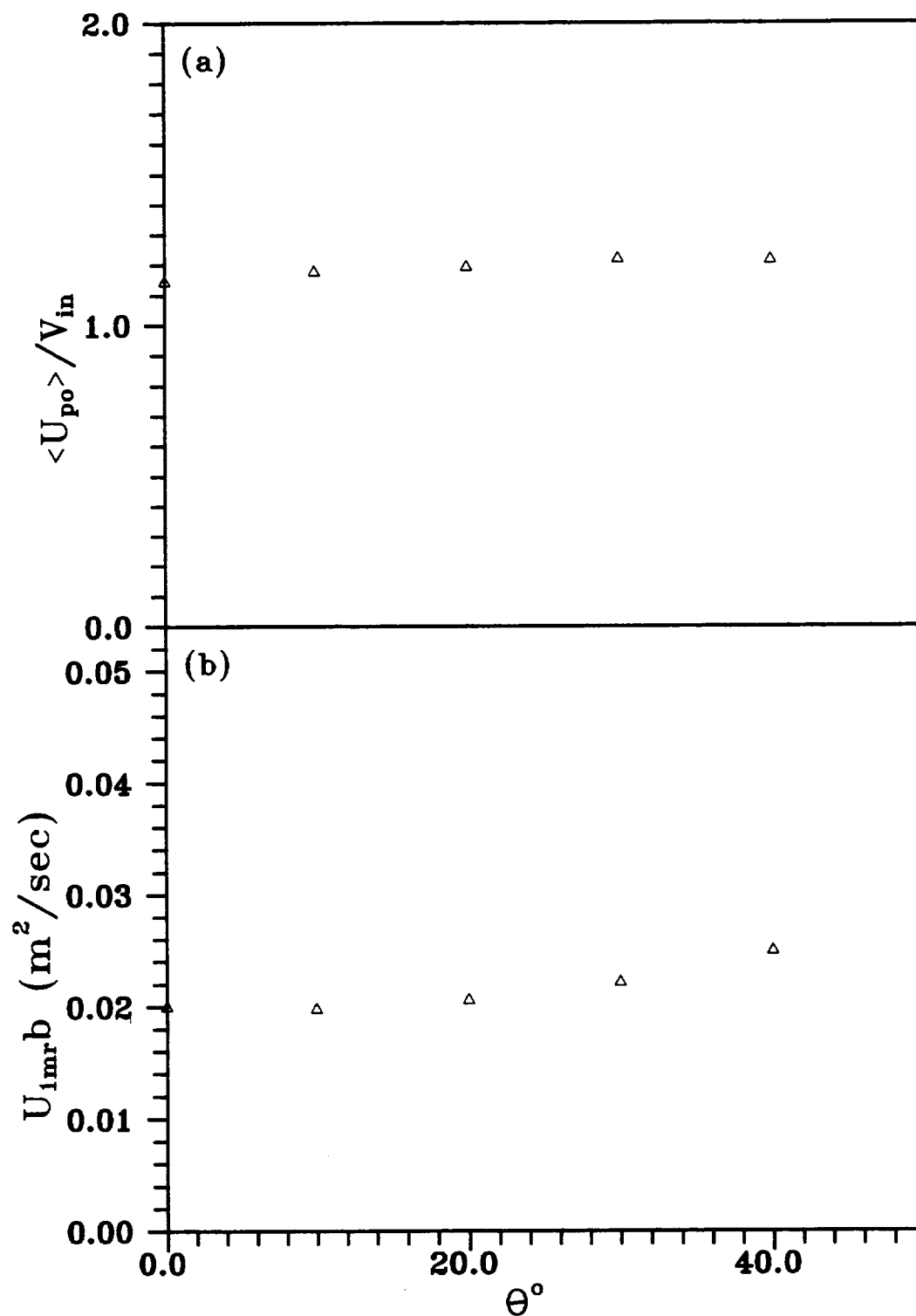
Fig. 105 Variation of potential velocity at wake centre (a) and the integral parameter $U_{lm}b$ (b) as a function of angular position
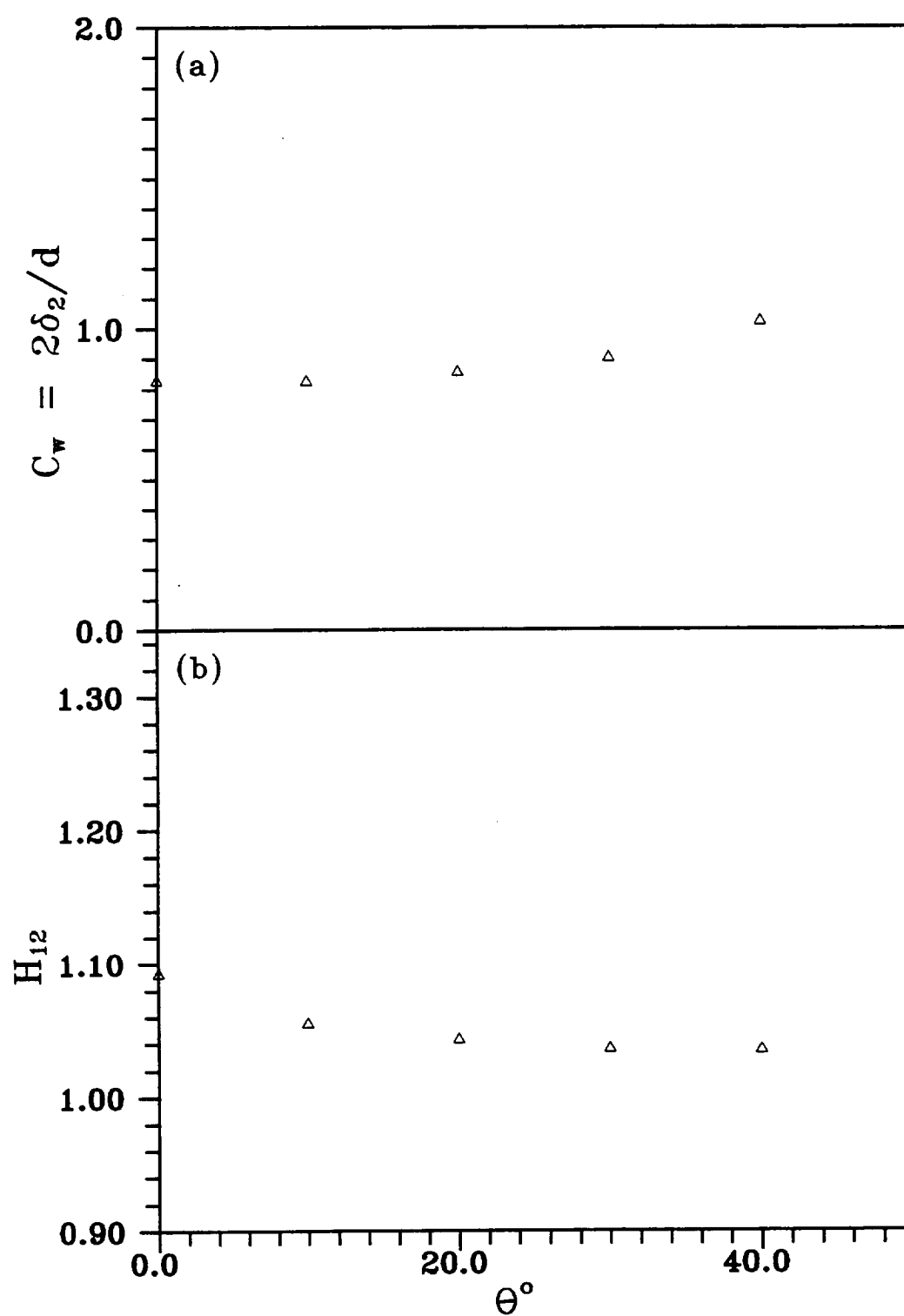
Fig. 106 Momentum thickness ratio (a) and shape factor (b) as a function of angular position

9. CONCLUSIONS

9.1. Wake Development at Positive, Zero, and Negative Pressure Gradients

The wake development behind a stationary cylinder in a curved channel at positive, zero, and negative streamwise pressure gradients was experimentally investigated. The results of the investigation revealed the following aspects of the influence of streamline curvature and streamwise pressure gradient on the development of wakes.

1. The decay of velocity defect and the growth of wake width obtained for the zero pressure gradient curved wake are different from that of a zero pressure gradient straight wake.

2. Comparison of the wake development in the curved channel between the three pressure gradients indicates that the decay of the velocity defect is fastest at negative pressure gradient and slowest at positive pressure gradient. Conversely, the growth of the wake width is fastest at positive pressure gradient and slowest at negative pressure gradient.

3. The momentum thickness ratio as a function of the streamwise distance remains approximately constant at zero pressure gradient, increases at positive pressure gradient, and decreases at negative pressure gradient. The shape factor for all the three pressure gradients decreases with streamwise distance and approaches to unity for far wakes. At a particular streamwise location, the shape factor has the highest value at positive pressure gradient and the lowest value at negative pressure gradient. The momentum thickness ratio and shape factor are well represented by Eq. (8.8) and (8.10), respectively. The product $\bar{U}_{1m}b$ as a function of streamwise location while remaining approximately constant at zero pressure gradient, increases at positive pressure gradient and decreases at negative pressure gradient.

4. The mean velocity defect profiles in similarity coordinates are almost symmetric and follow the Gaussian function for straight wake data. However, small deviations are observed particularly at far downstream locations and at the edges of the wake

where the wake is slightly wider on the inner half. In general, it may be considered that the effect of curvature on mean velocity defect distribution is small.

5. The Reynolds stress distributions in similarity coordinates are strongly influenced by the curvature. Pronounced asymmetric features are observed for all the three components of Reynolds stresses measured. The value of streamwise component of Reynolds stress at the inner half of the of the wake is higher than that of the outer half. The asymmetry in transverse component of Reynolds normal stress is higher than the asymmetry in the streamwise component of Reynolds normal stress. The distribution of transverse component has only one maximum which occurs at the inner side of the wake. The Reynolds shear stress distribution has higher values at the inner half than outer half. The asymmetry of Reynolds stress distribution increases with downstream location. At a particular streamwise location, the absolute value of Reynolds shear stress normalized with the square of the maximum velocity defect, has the highest value for negative pressure gradient and the lowest value for positive pressure gradient.

9.2. Periodic Unsteady Wake Development at Zero Pressure Gradient

The periodic unsteady wake development behind the cylinders of a rotating wake generator in a curved channel at zero streamwise pressure gradient is experimentally investigated employing phase-averaging techniques. The investigation has the following conclusions.

1. The phase-averaging method clearly revealed the propagation of primary and secondary wakes through the curved channel.

2. An approach is made to transform the temporal distribution of velocity and turbulence quantities obtained in stationary frame of reference into a spatial distribution in relative frame of reference.

3. The velocity defect profiles in similarity coordinates are symmetric and follow the Gaussian function for straight wake data.

4. The distribution of phase-averaged Reynolds stresses are consistent with measurements obtained behind the stationary cylinder in the same curved channel. Pronounced asymmetric features are observed for all three components of Reynolds stresses measured. The value of the streamwise component of Reynolds stress at the inner half of the wake is higher than that of the outer half. The asymmetry in the transverse component of Reynolds normal stress is higher than the asymmetry in the streamwise component of Reynolds normal stress. The distribution of the transverse component has only one maximum, which occurs at the inner side of the wake. The Reynolds shear stress distribution has a higher value at the inner half than at the outer half and the asymmetry of Reynolds stress distribution increases with downstream location. The effect of the rotational speed of the wake generator on the Reynolds stress distribution is found to be small for the rotational speeds investigated.

5. The profiles of phase-averaged third-order correlations shows asymmetry with higher values on the inner half of the wake than on the outer half. The effect of rotational speed of the wake generator on the distribution of third-order correlations is small for the rotational speeds investigated.

All the investigations in this report are carried out at the same inlet turbulence. The free-stream turbulence, particularly high levels of free-stream turbulence encountered in actual turbomachines, may influence the characteristics of the wake development. The location of wake generating cylinder with respect to the curved test section may also be an influencing factor in the development of wake. Measurement of all components of Reynolds stress tensor using triple sensor hot-film probe can describe the turbulence structure in detail with a kinetic energy balance estimate. Therefore, more basic and systematic investigations are needed for a better understanding of the wake flows subjected to streamline curvature and streamwise pressure gradient.

REFERENCES

Ashworth, D. A., LaGraff, J. E., Schultz, D.L., 1989, "Unsteady Interaction Effects on a Transitional Turbine Blade Boundary Layer," ASME *Journal Of Turbomachinery*, Vol. 111, pp. 162-168.

Bradshaw, P., 1971, *An Introduction to Turbulence and Its Measurement*, Pergamon Press, Oxford.

Bradshaw, P., 1973, "Effects of Streamline Curvature on Turbulent Flow," *AGARD-AG-*169.

Browne, L. W. B., Antonia, R. A., Chua,L. P., 1989, "Calibration of X-probes for Turbulent Flow Measurements," *Experiments in Fluids*, Vol. 7, pp. 201-208.

Brunn, H. H., Nabhani, N., Al-Kayiem, H. H., Fardad, A. A., Khan, M. A., Hogarth, E., 1990, "Calibration and Analysis of X Hot-wire Probe Signals," *Meas. Sci. Tech.*, Vol. 1, pp. 782-785.

Cantwell, B., Coles, D., 1983, "An Experimental Study of Entrainment and Transport in the Turbulent Near Wake of a Circular Cylinder," *Journal of Fluid Mechanics*, Vol. 136, pp. 321-374.

Castro, I. P., Bradshaw, P., 1976, "The Turbulence Structure of Highly Curved mixing Layer," *Journal of Fluid Mechanics*, Vol. 73, pp. 265-304.

Champagne, F. H., Sleicher, C. A., Wehrmann, O. H., 1967, "Turbulence Measurements with Inclined Hot-wires, Part 1: Heat Transfer Experiments with Inclined Hot-wire," *Journal of Fluid Mechanics*, Vol. 28, pp. 153-175.

Dong, Y., Cumpsty, N. A., 1989a, "Compressor Boundary Layers, Part 1 - Test Facility and Measurements with no Incident Wakes", ASME paper 89-GT-50.

Dong, Y., Cumpsty, N. A., 1989b, "Compressor Boundary Layers, Part 2 Measurements with Incident Wakes", ASME paper 89-GT-51.

Doorly, D. J., Oldfield, M. L. G., 1985, "Simulation of Wake-Passing in a Stationary Turbine Rotor Cascade," *AIAA Journal of Propulsion and Power*, Vol. 1, No. 4, pp. 316-318.

Eifler,J., 1975, "Zur Frage der freien turbulenten Strömungen, insbesondere hinter

ruheneden und bewegten Zylindern," Diss. D-17, Techische Hochschule Darmstadt, Germany.

Eskinazi, S., Yeh, H., 1956, "An Investigation on Fully Developed Turbulent Flows in a Curved Channel," *Journal of Aeronautical Sciences*, Vol. 23, pp. 23-34.

Evans, R. L., 1975, "Turbulence and Unsteadiness Measurements Downstream of a Moving Blade Row", ASME *Journal of Engineering for Power*, January, pp. 131-139.

Fabris, G., 1979, "Conditional Sampling Study of the Turbulent Wake of a Cylinder. Part 1," *Journal of Fluid Mechanics*, Vol. 94, part 4, pp. 673-709.

Fabris, G., 1983, "Third-Order Conditional Transport Correlations in Two-Dimensional Turbulent Wake," *Physics of Fluids*, Vol. 26, No. 2, pp. 422-427.

Gartshore, Ian S., 1967, "Two-Dimensional Turbulent Wakes," *Journal of Fluid Mechanics*, Vol. 30, part 3, pp. 547-560.

Görtler, H., 1940, Über den Einfluß der Wandkümmung auf die Entstehung der Turbulenz," *Zeitschrift für angemandte Mathematik und Mechanik*, Bd. 20, Nr. 3, pp. 138-147. (Translated as "On the Three-dimensional Instability of Laminar Boundary Layers on Concave Walls," *NACA Tech. Memo.* 1375, 1954.).

Hill, P. G., Schaub, U. W., Senoo, Y., 1963, "Turbulent Wakes in Pressure Gradients," *ASME Journal of Applied Mechanics*, pp. 518-524.

Hinze, J. O., 1959, *Turbulence*, McGraw-Hill, New York.

Hoffmann, P. H., Muck, K. C., Bradshaw, P., 1985, "The Effect of Concave Surface on Turbulent Boundary Layers," *Journal of Fluid Mechanics*, Vol. 161, pp. 371-403.

John, J., Schobeiri, T., 1993, "A Simple and Accurate Method of Calibrating X-Probes," ASME *Journal of Fluids Engineering*, Vol. 115, pp. 148-152.

Johnson, F. D., Eckelmann, H., 1984, "A Variable Angle Method of Calibration for X-probes Applied to Wall-bounded Turbulent Shear Flow," *Experiments in Fluids*, Vol. 2, pp. 121-130.

Jorgensen, F. E., 1971, "Directional Sensitivity of Wire and Fiber Film Probes," *DISA Information*, Vol. 11, pp. 31-37.

Koyama, H., 1983,"Effect of Streamline Curvature on Laminar and Turbulent Wakes," *Proc. of Fourth Symp. on Turbulent Shear Flows*, University of Karlsruhe,

Karlsruhe, Germany, pp. 141-155.

Lakshminarayana, B., Poncet, A., 1974, "A Method of Measuring Three-Dimensional Rotating Wakes Behind Turbomachinery Rotors," *ASME Journal of Fluids Engineering*, June, pp. 87-91.

Lekakis, I. C., 1988, "Coherent Structures in Fully Developed Turbulent Pipe Flow," Ph.D. Dissertation, University of Illinois at Urbana Champaign, USA.

Lekakis, I. C., Adrian, R. J., Jones, B. G., 1989, "Measurement of Velocity Vectors with Orthogonal and Non-orthogonal Triple-sensor Probes," *Experiments in Fluids*, Vol. 7, pp. 228-240.

Liu, X., Rodi, W., 1991, "Experiments on Transitional Boundary Layers with Wake-Induced Unsteadiness," *Journal of Fluid Mechanics*, Vol. 231, pp. 229-256.

Liu, X., Rodi, W., 1992, "Measurement of Unsteady Flow and Heat Transfer in a Linear Turbine Cascade," ASME paper 92-GT-323.

Lueptow, R. M., Breuer, K. S., Haritonidis, J. H., 1988, "Computer-aided Calibration of X-probes Using a Look-up Table," *Experiments in Fluids*, Vol. 6, pp. 115-118.

Margolis, D. P., Lumley, J.L., 1965, "Curved Turbulent Mixing Layer", *The Physics of Fluids*, Vol. 8, No. 10, pp. 1775-1784.

Moffat, R.J., 1982, "Contributions to the Theory of Single-Sample Uncertainty Analysis," ASME *Journal of Fluids Engineering*, Vol. 104, pp. 250-260.

Morehouse, K. A., Simoneau, R. J., 1986, "Effect of a Rotor Wake on the Local Heat Transfer on the Forward Half of a Circular Cylinder", *Proceedings, 8th International Heat Transfer Conference*, C. L. Tien et al., eds., Hemisphere Publishing Corp., Washington D.C., Vol. 3, pp. 1249-1256.

Muck, K.C., Hoffmann, P. H., Bradshaw, P., 1985, "The Effect of Convex Surface on Turbulent Boundary Layers," *Journal of Fluid Mechanics*, Vol. 161, pp. 347-369.

Nakayama, A., 1987, "Curvature and Pressure-Gradient Effects on a Small-Defect Wake," *Journal of Fluid Mechanics*, Vol. 175, pp. 215-246.

O' Brien, J.E.,, Simoneau, R. J., LaGraff, J. E., Morehouse, K. A. 1986, "Unsteady Heat Transfer and Direct Comparison to Steady State Measurements in a Rotor-Wake

Experiment", *Proceedings, 8th International Heat Transfer Conference*, C. L. Tien et al., eds., Hemisphere Publishing Corp., Washington D.C., Vol. 3, pp. 1243-1248.

O' Brien, J.E., 1988, "Effects of Wake Passing on Stagnation Region Heat Transfer," ASME HTD-Vol. 103, pp. 17-28.

O' Brien, J.E., Capp, S.P., 1989, "Two-Component Phase-Averaged Turbulent Statistics Downstream of a Rotating Spoked-Wheel Wake Generator," ASME JOURNAL OF TURBOMACHINERY, Vol. 111, No. 4, pp. 475-482.

Orth,U., 1992, "Unsteady Boundary-Layer Transition in Flow Periodically Disturbed by Wakes," ASME paper 92-GT-283.

Pardivala, D., 1991,"Establishment of a Research Facility for Investigating the Effects of Periodic Unsteady Inlet Flow, Pressure Gradient and Curvature on Boundary Layer Development, Wake Development And Heat Transfer," M.S. Thesis, Texas A&M University.

Pfeil, H., Eifler,J., 1975a, "Zur Frage der Schubspannungsverteilung für die ebenen freien turbulenten Strömungen," *Forschung*, Ing.-Wes. 41, Nr. 4, pp. 105-112.

Pfeil, H., Eifler,J., 1975b, "Messungen im turbulenten Nachlauf des Einzelzylinders," *Forschung*, Ing.-Wes. 41, Nr. 5, pp. 137-145.

Pfeil, H., Pache, W., 1977, "Messungen von Strömungsgrenzschichten unter Turbomaschinenbedingungen," *Z Flugwiss. Weltraumforsch*, Vol. 1, pp. 267-277.

Pfeil, H., Schröder, Th., 1981, "Decay of the Wake Behind A Cylinder Crossing Rapidly The Flow," AIAA Paper No. AIAA-81-0209.

Pfeil, H., Herbst,R., Schröder, Th., 1983, "Investigation of the Laminar-Turbulent Transition of Boundary Layers Disturbed by Wakes," ASME *Journal of Engineering for Power*, Vol. 105, pp. 130-137.

Raj, R., Lakshminarayana, B., 1973, "Characteristics of the Wake behind a Cascade of Airfoils," *Journal of Fluid Mechanics*, Vol. 81, part 4, pp. 707-730.

Raj, R., Lakshminarayana, B., 1976, "Three-Dimensional Characteristics of Turbulent Wakes Behind Rotors of Axial Flow Turbomachinery," ASME *Journal of Engineering for Power*, April, pp. 218-228.

Ramjee, V., Neelakandan, D., 1989, "Development of Wake of a Rectangular

Cylinder in a Curved Stream," *Experiments in Fluids, Vol.* 7, pp. 395-399.

Ravindranath, A., Lakshminarayana, B., 1979, "Mean Velocity and Decay Characteristics of the Near and Far Wake of a Compressor Rotor Blade of Moderate Loading", ASME paper No. 79-GT-202.

Ravindranath, A., Lakshminarayana, B., 1980, "Structure and Decay Characteristics of Turbulence in the Near and Far Wake of a Moderately Loaded Compressor Rotor Blade", ASME paper No. 80-GT-95.

Reichardt, H., 1942, "Gesetzmäßigkeiten der freien Turbulenz." *VDI-Forschungsheft,* 414.

Reichardt, H., 1950, "Gesetzmäßigkeiten der freien Turbulenz." *VDI-Forschungsheft,* 412. 2., Auflage Düsseldorf, VDI-Verlag.

Roshko, A., 1953, "On the Development of Turbulent Wakes from Vortex Streets," *N.A.C.A Technical Note* 2913.

Savill, A.M., 1983, "The Turbulent Structure of a Highly Curved Two-Dimensional Wake," *Structure of Complex Turbulent Shear Flow, IUTAM Symposium* 1982 (ed. R.Dumas & L.Fulachier), Springer, New York, pp. 185-197.

Schlichting, H., 1930, "Über das ebene Windschattenproblem." Diss. Göttingen, Ing.-Arch.1, 537-571.

Schlichting, H., 1979, *Boundary Layer Theory*, 7th Ed., McGraw-Hill, New York.

Schobeiri, M. T., 1976, "Näherungslösung der Navier-Stokes'schen Differentialgleichung für eine zweidimensionale stationäre Laminarströmung konstanter Viskosität in konvexen und konkaven Diffusoren und Düsen," *Zeitschrift für angewandte Mathematik und Physik*, Vol. 27, Fasc. 1.

Schobeiri, M. T., 1979, "Theoretische und experimentelle Untersuchungen laminarer und turbulenter Strömungen in Diffusoren," Diss. D-17, Technischen Hochschule Darmstadt, Germany.

Schobeiri, M. T., 1980, "Geschwindigkeits- und Temperaturverteilung in Hamelscher Spiralströmung," *Zeitschrift für angewandte Mathematik und Mechanik*, Vol. 60, pp. 195-200.

Schobeiri, M. T., 1988, "Effects of Periodic Unsteady Flow, Pressure Gradient and

Wall Curvature on Boundary Layer Transition, Wake Development and Heat Transfer," Proposal submitted to NASA-Lewis Research Center.

Schobeiri, T., 1990, "The Influence of Curvature and Pressure Gradient on the Flow Temperature and Velocity Distribution," *International Journal of Mech. Sci.*, Vol. 32, pp. 851-861.

Schobeiri, T., Pardivala, D., 1992, "Establishment of a Research Facility for Investigating the Effects of Periodic Unsteady Inlet Flow, Pressure Gradient and Curvature on Boundary Layer Transition, Wake Development And Heat Transfer," *Rotating Machinery Transport Phenomenon*, Hemisphere Publishing Corp., Washington D.C.

Schobeiri, T., 1992, "Theoretical Study of Wake Development in Curved Channels," Internal Report, Department of Mechanical Engineering, Texas A&M University.

Schobeiri, T., John, J., Pappu, K., 1993, "Development of Two-Dimensional Wakes within Curved Channels under Zero Streamwise Pressure Gradient," under preparation.

Schröder, T., 1985, "Entwicklung des instationären Nachlaufs hinter quer zur Strömungsrichtung bewegten Zylindern und dessen Einfluß auf das Umschlagverhalten von ebenen Grenzschichten stromabwärts angeordneter Versuchskörper," Diss. D-17, Technische Hochschule Darmstadt, Germany.

Townsend, A. A., 1947, "Measurements in the Turbulent Wake of a Cylinder," *Proc. Roy. Soc. Lond.*, A190, pp. 551-561.

Townsend, A. A., 1949a, "Momentum and Energy Diffusion in the Turbulent Wake of a Cylinder," *Proc. Roy. Soc. Lond.*, A197, pp. 124-140.

Townsend, A. A., 1949b, "The Fully Developed Turbulent Wake of a Circular Cylinder," *Aust. J. Sci. Res.* 2, pp. 451-468.

Townsend, A. A., 1956, *Structure of Turbulent Shear Flows*, 1 st ed., Cambridge University Press, London.

Uberoi, M. S., Freymuth, P. 1969, "Spectra of Turbulence in Wakes behind Circular Cylinders," *The Physics of Fluids*, Vol. 12, No. 7, pp. 1359-1363.

Wattendorf, F. L., 1935, "A Study of the Effect of Curvature on Fully Developed Turbulent Flow," *Proc. Roy. Soc. Lond.*, Vol. 148, pp. 565-598.

Webster, C. A. G., 1962, "A Note on the Sensitivity to Yaw of a Hot-wire Anemometer," *Journal of Fluid Mechanics*, Vol. 13, pp. 307-312.

Willmarth, W. W., Bogar, T. J., 1977, "Survey and New Measurements of Turbulent Structure Near the Wall," *Physics of Fluids*, Vol. 20, pp. S9-S21.

Yavuzkurt, S., 1984, "A Guide to Uncertainty Analysis of Hot-wire Data," ASME *Journal of Fluids Engineering*, Vol. 106, pp. 181-186.

APPENDIX A

TABLE OF REFERENCE QUANTITIES

Table 6 Values of selected quantities of the steady wake at zero streamwise pressure gradient

θ (o)	ξ_1/d	$\bar{U}_{1m}$ (m/s)	b (mm)	$\bar{U}_{po}$ (m/s)	$\overline{u_o^2}$ (m²/s²)	$\overline{v_o^2}$ (m²/s²)	$\bar{V}_{in}$ (m/s)
0	34	2.598	7.44	20.02	1.862	2.004	19.31
5	65	1.734	11.27	20.07	0.880	0.727	19.29
10	96	1.392	13.78	20.12	0.629	0.476	19.30
15	126	1.217	16.76	20.51	0.531	0.401	19.35
20	157	1.084	19.88	20.57	0.470	0.357	19.32
25	187	0.905	22.88	20.60	0.419	0.343	19.32
30	218	0.846	26.13	20.38	0.375	0.322	19.33
35	248	0.686	27.34	18.77	0.300	0.280	19.37
40	278	0.611	33.88	19.11	0.273	0.299	19.34
45	309	0.540	36.92	19.11	0.263	0.289	19.33
50	339	0.494	33.96	19.49	0.253	0.305	19.32
55	370	0.491	39.87	20.03	0.245	0.326	19.33
60	400	0.469	45.91	19.59	0.225	0.326	19.31
65	431	0.445	49.21	20.26	0.229	0.350	19.37
70	461	0.453	47.70	20.31	0.218	0.352	19.39

Table 7 Values of selected quantities of the steady wake at positive streamwise pressure gradient

θ (o)	ξ_1/d	$\bar{U}_{1m}$ (m/s)	b (mm)	$\bar{U}_{po}$ (m/s)	$\overline{u_o^2}$ (m²/s²)	$\overline{v_o^2}$ (m²/s²)	$\bar{V}_{in}$ (m/s)
0	34	2.793	7.06	19.27	1.833	1.965	19.10
5	65	1.952	10.56	19.17	0.876	0.704	19.10
10	96	1.550	13.30	18.85	0.631	0.444	19.09
15	126	1.311	16.13	18.00	0.510	0.333	19.20
20	157	1.216	18.97	17.76	0.470	0.294	19.07
25	188	1.075	22.77	17.68	0.446	0.279	19.06
30	219	0.954	25.00	17.37	0.419	0.262	19.08
35	250	0.898	29.76	16.94	0.380	0.258	18.94
40	282	0.780	33.17	17.02	0.374	0.267	18.92
45	313	0.778	35.28	16.63	0.361	0.273	19.07
50	345	0.716	41.37	16.33	0.346	0.285	18.99
55	377	0.698	43.03	16.34	0.334	0.297	18.99
60	408	0.649	48.58	15.61	0.303	0.288	19.08
65	440	0.609	51.27	15.66	0.297	0.301	19.08
70	474	0.578	56.68	15.64	0.279	0.303	19.09

Table 8 Values of selected quantities of the steady wake at negative streamwise
pressure gradient

θ (o)	ξ_1/d	$\bar{U}_{1m}$ (m/s)	b (mm)	$\bar{U}_{po}$ (m/s)	$\overline{u_o^2}$ (m²/s²)	$\overline{v_o^2}$ (m²/s²)	$\bar{V}_{in}$ (m/s)
0	34	2.710	6.92	20.23	1.777	1.924	19.36
5	65	1.826	10.76	20.78	0.846	0.720	19.35
10	96	1.447	12.15	21.44	0.573	0.469	19.36
15	126	1.173	14.38	22.15	0.458	0.377	19.34
20	156	0.946	17.16	22.82	0.391	0.335	19.33
25	185	0.795	18.22	23.56	0.338	0.317	19.34
30	215	0.733	20.79	24.19	0.300	0.300	19.34
35	244	0.648	22.40	23.78	0.248	0.278	19.41
40	273	0.588	24.04	24.63	0.227	0.283	19.40
45	302	0.538	24.18	25.37	0.210	0.292	19.41
50	331	0.522	24.22	26.06	0.199	0.300	19.43
55	360	0.471	26.30	26.65	0.183	0.304	19.44
60	388	0.435	28.78	27.29	0.180	0.316	19.44

Table 9 Values of selected quantities of the unsteady wake at zero streamwise pressure gradient

θ (o)	U_{1mr} (m/s)	b (mm)	$<U_{po}>$ (m/s)	$<u_{ro}^2>$ (m²/s²)	$<v_{ro}^2>$ (m²/s²)	$\bar{V}_{in}$ (m/s)
0	2.732	7.35	22.25	1.642	1.761	19.74
10	1.693	11.77	22.91	0.653	0.478	19.75
20	1.351	15.36	23.30	0.542	0.372	19.75
30	1.226	18.17	23.86	0.479	0.347	19.78
40	1.160	21.61	23.74	0.507	0.361	19.75

APPENDIX B

PROGRAMS FOR DATA ACQUISITION, REDUCTION, AND ANALYSIS

The programs listed in this appendix contain several calls to assembly and FORTRAN language subroutines. All of the assembly and some of the FORTRAN subroutines are not listed in this appendix. However, they are available from the principal investigator.

B.1. Calibration Programs

```
************************************************************************
1. Program to calibrate pressure transducers, thermocouples etc.
************************************************************************
* This program calibrates the output of any channel of RC Electronic A/D
* board against a known quantity applied to the sensor connected to the
* corresponding A/D channel to achieve the highest possible accuracy of
* the system.
* The program samples data from all 1,2,4,8,or 16 channels, and displays
* the voltages, which are then compared to known  inputs like voltage,
* pressure,temperature etc. To run this program, you must have a
* reliable voltmeter,pressure calibrator, thermocouple calibrator etc.
* An output file 'cal16.cal' is generated, which gives the coefficients
* of the best (least-squares) polynomial fit for the channel. The order
* of the polynomial is given by npol and the number of coefficients by
* npol+1.  A second output file 'cal16.out' is also generated, which
* simply keeps a record of the known input values(read from voltmeter,
* pressure calibrator, thermocouple calibrator) and values obtained from
* sampling. Output file 'cal16.cal' is designed to be used by copying
* it to the calibration coefficient files like 'pres.cal' which are used
* by actual data acquisition programs like ADRDTR4.FOR, AUTO4.FOR etc.
* The sampling is done in 1-shot mode. This is the easiest way to
* configure the RC ISC-16, which is used to fill one data buffer(<32K)
* and then stop.  This is also the best way to take short (< 32K), fast
* (up to .5MHz aggregate sample rate ) bursts of data.  Data more than
* 32K is sampled in discontinuous blocks with each block of 32K size.
* External assembly routines: AD0S, AD1S, RD1S - all in  AD10LIB.LIB
* External fortran routines:
* LSFIT (subroutine for finding the coefficients of a polynomial of any
* order by least-squares fit), IVER
************************************************************************
        program CAL
        parameter (max=33000)
        integer*4    npol,ks,inc,index,nsapch
        integer*2    idat(max)
        integer*4    nch, itime, ierr, size, isize, delay, idisk
        real*4       avg(50,16),sumsq(16),rms(16)
        real*4       rmst(16),avgt(50,16),x(50),y(50)
        real*8       coeff(20),a(20),var(20)
        character*32 file
        logical*1 IVER,ldisk,lscr
```

```
      data idisk/0/
      data iout,iout3 /10,12/

c  Read the ADC input parameters
      write(6,*)'Select the A/D channel number to calibrate?'
      read(*,*)ichn
      nch=1
      if (ichn.gt. 1) nch=2
      if (ichn.gt. 2) nch=4
      if (ichn.gt. 4) nch=8
      if (ichn.gt. 8) nch=16
      write(*,110)
      read(*,*)itime
      write(*,115)
      read(*,*)delay
      write(*,120)
      read(*,*)size
      isize=2**(size+8)
      write(*,*)'Number of blocks'
      read(*,*) nbl
      nsapch=isize/nch
      open(unit=iout,file='cal.out')
c  Write data to sreen or disk?
      ldisk=.false.
      lscr=.false.
      if(IVER(' write to disk')) ldisk=.true.
      if(IVER('0print array?')) lscr=.true.
      inc=0
  200 continue
      inc = inc + 1
      write(*,14)
      read(*,*) y(inc)
      write(iout,*) y(inc)
      write(*,*) '    '
      do 250 j=1,nch
        Avgt(inc,j) = 0.0
        RMSt(j) = 0.0
  250 continue
      do 800 iav = 1,nbl
c  Set up the RC board, and go on keyboard prompt
      call AD0S(nch, itime, size)
      call AD1S(delay)
c  Read idat
      call RD1S(idat, isize, ierr, idisk)
c Inspect ierr flag
      write(*,130)ierr
c Write array to screen?
      if(lscr) write(*,160)(idat(i),i=1,isize)
c Option to save data on disk
      if(ldisk) then
   40    write(*,180)
         read(*,140)file
         open(unit=2,file=file,form='binary',err=40,status='unknown')
         write(2)isize,nch,itime,delay
         write(2)(idat(i),i=1,isize)
         close(unit=2)
         write(*,*)'ok'
      endif
      write(6,15) iav,isize
c Now calculate averages and RMS fluctuation levels
      do 300 j=1,nch
        sumsq(j) = 0.
```

```
300   Avg(inc,j) = 0.
      do 450 i=1,nsapch
        do 400 j=1,nch
          index  = (i-1)*nch + j
          Avg(inc,j)=avg(inc,j)+(idat(index)-2048.)*.004882812
400       continue
450     continue
      do 500 j=1,nch
        Avg(inc,j) = avg(inc,j)/nsapch
        avgt(inc,j) = avgt(inc,j) + avg(inc,j)
500   continue
c  rms calculations
c
      do 600 i=1,nsapch
        do 600 j=1,nch
          index = (i-1)*nch + j
          del=avg(inc,j)-(float(idat(index))-2048.0)*.004882812
          Sumsq(j) = sumsq(j) + del*del
600   continue
      do 700 j=1,nch
        rms(j)  = sqrt(sumsq(j)/nsapch)
        rmst(j) = rmst(j) + rms(j)
700   continue
800 continue
      write(*,*) '  sampling has finished'
      do 850 j=1,nch
        avg(inc,j) = avgt(inc,j)/nbl
        rms(j) = rmst(j)/nbl
850 continue
c  Now write the averaged results to screen and to disk.
c
      write(*,22)
      do 900 ich=1,nch
        if(avg(inc,ich).ne.0) then
          write(*,23) ich,Avg(inc,ich),rms(ich),
     $    rms(ich)/avg(inc,ich)*100.
          write(iout,23) ich,Avg(inc,ich),rms(ich),
     $    rms(ich)/avg(inc,ich)*100.
        else
          write(*,23) ich,Avg(inc,ich),rms(ich)
          write(iout,23) ich,avg(inc,ich),rms(ich)
        endif
900   continue
      write(*,13) inc
      write(*,2)
      read(*,*) isamp
      if(isamp.eq.0) then
        if(inc.lt.3) then
          write(*,*) 'The no. of data only',inc
          write(*,*) 'Hence  this session is terminated. Bye '
          go to 2000
        end if
        go to 1000
      end if
c  Now loop back to do more sampling at a new voltage.
c
      go to 200
1000 continue
c  Sampling is now complete for several tests.
c  Now open the calibration output file cal16.cal and perform
c  the least squares fits.
      open(unit=iout3,file='cal16.CAL')
```

```
      write(6,*)'Enter the order of the polynomial?'
      read(5,*) npol
      write(*,*) ' Performing least squares fits :'
      do 1050 i=1,inc
        x(i)=avg(i,ichn)
 1050 continue
      call LSFIT(inc,x,y,npol,a,var,coeff,ks)
      write(6,*) (coeff(ipol),ipol=1,npol+1)
      write(iout3,*) (coeff(ipol),ipol=1,npol+1)
      write(iout3,*) 'calibration constants; ch# ',ichn
      do  i=1,inc
        write(iout3,*) x(i),y(i)
      end do
      close(unit=iout3)
 2000 continue
      close(unit=iout)
c
c Formats
    2 format(' Enter your response here : ')
    5 format(/,' Exiting program CAL.FOR')
   13 format(//,' You have now tested', i3,' points. ',/,
     $          ' (A minimum of ten points are recommended',
     $          ' for a good calibration)',//,
     $          ' Do you want to test at another point? : ',/,
     $      5x,'(0) no ',/,
     $      5x,'(1) yes')
   14 format(//,' Enter the dependent variable like voltage, pressure,
     $temperature etc.?')
   15 format(' Sampled block number',i3,2x,i5,' size')
   22 format(//,' Averaged results of A/D conversions :',/,
     $            5x,' Channel',6x,'X (DC)',
     $            8x,'X (RMS)',5x,'RMS (%)')
   23 format(' ',7x,i3,3F14.5)
  110 format(' itime [usec, 1-65384]:'\)
  115 format(' delay [usec, 0-65535]:'\)
  120 format(' -- select buffer size --'/' SIZE     BUFFER'/
     $' 0         256'/' 1          512'/' 2         1024'/
     $' 3        2048'/' 4         4096'/' 5         8192'/
     $' 6       16384'/' 7        32768'/' enter SIZE:'\)
  130 format(' ierr = ',i1)
  140 format(a)
  160 format(16i5)
  180 format(/' disk filename:'\)
      end
```

****
2. Program to obtain calibration coefficients of single sensor hot-wire/film probe
****

```
*  This program analyze the data stored during single sensor hot-
*  film/hot-wire calibration. The calibration is done using the program
*  ADRDTR.  The hot-wire is placed with proper orientation in low
*  turbulence, uniform velocity jet of the calibration nozzle.  The hot-
*  wire output from the signal conditioner is taken against a reference
*  velocity obtained from the differential pressure across the nozzle.
*  A fourth order polynomial curve fitting is used to get the calibration
*  coefficients.
*     External  assembly  routines: RDFILS, RDBLK,  RDFILC  -  all  in
AD10LIB.LIB
*  Fortran routines: LSFIT (curve fitting using least square polynomial
*  fit), IVER
```

```
*   FILES:   master.fil: contains the path of the root.fil
*       root .fil: input file containing the names of the
*       names of document file, data file and output file.
*       .dat -data files       (input)
*       .doc -document files   (input)
*       .out - output files.   (output)
*   CTA.CAL     : The output file containing the calibration constant and
*   the average temperature during the calibration.
*   CTA.OUT     : The output file generated by this program contains
*   hot-wire output, temperature compensated output and the velocity.
*   Signal connection:
*   Ch1 : Hotwire    Ch3: Thermocouple
*   Ch2 : Hotwire    Ch4: Pressure transducer
***********************************************************************
      program CTAN
      parameter (max=33000)
      integer*2  idat(max)
      integer*4  n, nch, itime, size, isize, delay
      integer*4  ierr,nsapch
      integer*4  npol,ks,inc
      real*8 coeff(15),a(40),var(15)
      real*4 sumsq(16),rms(16),rmst(16),avg(16),avgt(16)
      real*4 pc(5),tc(5),vel(300),hw(300),t(300),hwc(300)
      character*25 fili,filo,fild,filp
      logical*1 IVER,lscr
      data afac/1.0019/
c  Write data to sreen or disk?
      lscr=.false.
      if(IVER('0print array?')) lscr=.true.
      Write(6,*)'Sensor temperature in "C"?'
      read(5,*) tsens
c  open the file containing pressure calibration coefficients.
      open(unit=8,file='pres.cal')
      read(8,*)(pc(i), i=1,3)
      close(8)
c  open the file containing calibration coefficients for thermocouple.
      open(unit=8,file='temp.cal')
      read(8,*)(tc(i), i=1,3)
      close(8)
c
      open(unit=8,file='master.fil')
      read(8,*) ntest
      read(8,'(a25)') filp
      close(8)
      tsavg=0.0
      inc=0
c  open the file containing the filenames and number of files
10    open(unit=8,file=filp)
      read (8,*)nf
      inc=inc+1
      do 15 i=1,inc
15    read(8,175) fili,fild,filo
      close(8)
      open(unit=8,file=fild)
      read(8,*) pstat,patm
      close(8)
c  open the ADC data file and read the header
      call RDFILS(fili,n, nch, itime, delay, ierr)
      write(*,110)n,nch,itime,delay,ierr
c  select a block size
      if(inc.eq.1) then
         write(*,120)
```

```fortran
      read(*,*)size
      endif
      isize=2**(size+8)
      nblock=n/isize
      nsapch=isize/nch
      write(6,*)'Reading the data file: ',fili
      write(*,130)nblock,isize
      do 250 j=1,nch
         Avgt(j) = 0.0
         RMSt(j) = 0.0
  250 continue
      do 800  nb = 1,nblock
         call RDBLK(idat, nb, isize, ierr)
c  Inspect IERR flag
         write(*,150)ierr
c  Write array to screen?
         write(6,80) nb,isize
         if(lscr) then
            if(IVER(' Show this block?')) write(6,170)(idat(i),i=1,isize)
         endif
c  Now calculate averages and RMS fluctuation levels
         do 300 j=1,nch
            Sumsq(j) = 0.
  300    Avg(j) = 0.
         do 450 i=1,nsapch
            do 400 j=1,nch
               index  = (i-1)*nch + j
               Avg(j)=Avg(j)+(idat(index)-2048.)*.004882812
  400       continue
  450    continue
         do 500 j=1,nch
            Avg(j) = Avg(j)/nsapch
            write(6,*)'channel#', j,'        Average value= ',Avg(j)
            Avgt(j) = Avgt(j) + Avg(j)
  500    continue
c        RMS calculations
c
         do 600 i=1,nsapch
            do 600 j=1,nch
               index = (i-1)*nch + j
               Del=Avg(j)-(FLOAT(idat(index))-2048.0)*.004882812
               Sumsq(j) = Sumsq(j) + Del*Del
  600    continue
         do 700 j=1,nch
            RMS(j)  = SQRT(Sumsq(j)/nsapch)
            write(6,*)'channel#', j,'        RMS value= ',RMS(j)
            RMSt(j) = RMSt(j) + RMS(j)
  700    continue
  800 continue
      call RDFILC(ierr)
      do 850 j=1,nch
         Avg(j) = Avgt(j)/nblock
         RMS(j) = RMSt(j)/nblock
  850 continue
c  Now write the averaged results to screen and to disk.
      temp=avg(3)**2.0*tc(3) +avg(3)*tc(2) +tc(1)
      pavg=(avg(4)**2.0*pc(3) +avg(4)*pc(2) +pc(1))*25.4*9.81
      rho=(patm*13.6+pstat)*.0348432/(temp+273.15)
      if (pavg.lt.0.0) pavg=0.0
      velpn=sqrt(2.0*pavg/rho)*afac
      tstat=temp
      tsavg=tsavg+tstat
```

```fortran
      tavg=tsavg/inc
      write(6,*)'rho=',rho
      write(*,85)
c  Write to the output file
      open(unit=9,file=filo)
      do 900 ich=1,nch
         write(6,90) ich,Avg(ich),RMS(ich)
         write(9,90) ich,Avg(ich),RMS(ich)
  900 continue
      write(6,95)avg(1),velpn,temp,tstat
      write(9,95)avg(1),velpn,temp,tstat
      close(9)
      t(inc)=tstat
      hw(inc)=avg(1)
      vel(inc)=velpn
c  Repeat processing the next file ?
      if (inc.lt.nf) go to 10
c  Temperature compensation  of hotwire output for variation in fluid
c  temperature
      do 910 j=1,nf
  910 hwc(j)=hw(j)*sqrt((tsens-tavg)/(tsens -t(j)))
      call CLS
c  Write the results of velocity Vs hot-wire output
      open(unit=9,file='CTA.OUT')
      write(6,*) '      VOLTAGE      T.C. VOLTAGE        VELOCITY'
      do 920 j=1,nf
         write(9,*) hw(j),hwc(j),vel(j)
  920 write(6,*) hw(j),hwc(j),vel(j)
c  Performing the least square fit for a polynomial of order 4
      npol=4
      call LSFIT(inc,hwc,vel,npol,a,var,coeff,ks)
      Write(6,*)'CALIBRATION CONSTANTS AT  TEMPERATURE  ', tavg
      write(6,*)(coeff(ipol),ipol=1,npol+1)
c Write calibration coefficients to CAL.OUT
      open(unit=9,file='CTA.CAL')
      write(9,*)(coeff(ipol),ipol=1,npol+1)
      write(9,*)'Average temperature=',tavg
      close(9)
c  Formats
   80 format(' Calculated block number',i3,2x,i5,' size')
   85 format(//,' Averaged results of A/D conversions :',/,
     $          5x,' Channel',6x,'X (DC)',
     $          8x,'X (RMS)')
   90 format(' ',7x,i3,2F14.5)
   95 format(' hotwire voltage ',10x, 'velocity ',10x, 'total temp.'
     $,'static temp'/,f10.4,15x,f10.4,12x,f8.3,10x,f8.3)
  100 format(/' ADC filename:'\)
  101 format(a)
  110 format(' n:',i6,' nch:',i2,' itime:',i5,' delay:',i5,'ierr',i2)
  120 format(' -- select block size --'/' SIZE    BUFFER'/
     *' 0        256'/' 1        512'/' 2        1024'/
     *' 3       2048'/' 4       4096'/' 5        8192'/
     *' 6      16384'/' 7      32768'/' enter SIZE:'\)
  130 format(' There are ',i3,' blocks of ',i5,' words..')
  140 format(/' read block#:'\)
  150 format(' ierr:',i2)
  170 format(16i5)
  175 format(a,2x,a,2x,a)
      end
```

```
****************************************************************************
3. Program to calibrate X-hot-film/wire probe
****************************************************************************
*  This program calibrate a cross wire/film probe. Velocity calibration
*  of both wires and simultaneous angle calibration are done one after
*  another. The probe has to rotated for desired flow angle.
*  Program write blocks of data continuously to disk. The file size is
*  is limited only by disk space, although here MAXBLOCK = 32 to give
*  a 3MB upper limit.Select a block size between 512 and 32768 words.
*
*  Assembly routines called: ADFILS,ADHALT,ADC0,ADC1,RDBUF,ADFILC
*  FORTRAN  routines: IVER,FGEN,SRDDSKB,RESULT
*  FILES:     .dat,.fil,.doc -output
****************************************************************************
      program XCAL
      integer*4 n, nch, itime, delay, size, isize
      parameter (max=32768, maxblock=32)
      integer*2 idat(max), ierr(maxblock)
      integer*4 idisk, jerr
      logical*1 IVER,ishow,iangle,itype
      character*80 sent
      character*25 fild(300),fili(300),filo(300),filp,filnam
      character*25 root
      data idisk/1/
      write(6,*)'Enter the root file name (without extension)?'
      read(*,500) root
      ntest=0
      in=1
      do while(root(in:in).ne.' ')
        filp(in:in)=root(in:in)
        in=in+1
      end do
      filp(in:in+3)='.fil'
c  Open the master.fil and write the file name
      open(unit=9,file='master.fil')
      write(9,'(a)')filp
      close(9)
c  Read the ADC input parameter
      write(*,100)
      read(*,*)nch
      write(*,110)
      read(*,*)itime
      write(*,115)
      read(*,*)delay
      write(*,120)
      read(*,*)size
      isize=2**(size+8)
      write(*,130)
      read(*,*)nblock
      n=isize*nblock
   10 call CLS
      itype=.true.
      Write(6,600)
c  iw =1(velocity  calibration wire 1), 2(velocity calibration wire 2),
c  iw = 3(angle calibration for both wires)
      if(IVER('0Velocity Calibration?')) then
        iangle=.false.
        write(6,*)'Wire 1 or 2?'
        read(5,*)iw
      else
        if(IVER('0Angle Calibration ?')) iangle=.true.
        iw=3
```

```
          endif
          inc=0
          ishow=.false.
          if(IVER('0Show data or results?')) ishow=.true.
c  Generate the file names for .dat, .doc and .out files
   40   ntest=ntest+1
          call FGEN(root,ntest,fili,fild,filo)
          call CLS
          filnam=fili(ntest)
          write(6,300) filnam
          pause 'Please [ENTER] to start'
c  Open data file, write file header, initialize RC board
          call ADFILS(filnam,n, nch, itime, delay, jerr)
          call ADHALT()
          call ADC0(nch, itime, size)
          write(*,*)'sampling data..'
          call ADC1(delay)
c  Read NBLOCK blocks of data from RC A/D and write to file

          do i=1,nblock
            call RDBUF(idat, isize, ierr(i), idisk)
          enddo
c  Stop the ADCs, close the data file
          call ADHALT()
          call ADFILC(jerr)

c  Inspect IERR array for error flags
          write(*,140)(i,ierr(i),i=1,nblock)

C Input test parameters
          If(itype) then
            write(6,*)' Static pressure in "mm" of water?'
            read(5,*) PSTAT
            write(6,*)' Barometric pressure in "mm" of Hg ?'
            read(5,*)patm
            write(6,*)'Any other parameters to document? (max. one line)'
            read(5,'(a80)')sent
            itype=.false.
          endif
          if(iangle) then
            Write(6,*)'Write Flow Angle ALPHA with respect to wire 1'
            read(5,*)alpha
          else
            if(iw.eq.1) alpha=45.
            if(iw.eq.2) alpha=-45.
          endif

c  Get time and date
          call GETTIM(ihr,imin,isec,i100)
          call GETDAT(iyr,imon,iday)
c  Document this test
          open(unit=8,file=fild(ntest))
          write(8,*)pstat,patm,alpha,iw
          write(8,*)fili(ntest)
          write(8,*)sent
          write(8,450)imon,iday,ihr,imin
          close(8)
c Update .fil; later used by data analysis software
          open(unit=8,file=filp)
          write(8,*)ntest
          do j=1,ntest
            write(8,400)fili(j),fild(j),filo(j)
```

```
         enddo
         close(8)
c   reads data from disk and show results?
         if(ishow) then
            if(IVER('0read  data from disk?')) Call SRDDSKB(fili)
            inc=inc+1
            if(IVER('0Show results?')) Call RESULT(inc)
         endif

c   Repeat acquiring new data for different velocity or angle?
         if(IVER('0Continue?'))
         $goto 40
c   Move to new location
         if(IVER('0Continue Velocity or Angle Calibration ?'))goto 10
         write(6,*)'terminating the program at your request'
         stop 'bye'
c  formats

 100   format(/' nch [1,2,4,8,16]:'\)
 110   format(' itime [usec, 1-65384]:'\)
 115   format(' delay [usec, 0-65535]:'\)
 120   format(' -- select buffer size --'/' SIZE     BUFFER'/
       *'  0         256'/' 1         512'/' 2         1024'/
       *'  3        2048'/' 4        4096'/' 5         8192'/
       *'  6       16384'/' 7       32768'/' enter SIZE:'\)
 130   format(' nblock:'\)
 140   format(' block#',i3,'  ierr = ',i1)
 280   format(a30)
 300   format( ' Complete sampled data will be stored in ',a)
 400   format(a,2x,a,2x,a)
 450   format(' DATE: ',i2,'/',i2,5x,'TIME:  ',i2,'-',i2)
 500   format(a)
 600   format(' X-WIRE CALIBRATION.'//' This has two steps. Velocity Cali
       $bration of each wires and Angle Calibration.'//' During Velocity
       $calibration keep the wire normal to flow at all velocities.'//' Ang
       $le calibration is done by changing the flow angle by turning the
       $probe.')
       end


 ********************************************************************
 4. Program to obtain the velocity calibration coefficients of each of the
 sensor of the X-probe from a calibration using XCAL.FOR and keeping the
 sensor normal to flow.
 ********************************************************************

 *   This program process the data files generated during cross wire *
 calibration using XCAL.FOR. This generates an output file XCALP.OUT
 *   containing the angle ,voltage output and velocity.
 *   The velocity calibration coefficients will be stored in PX1.CAL and
 *   PX2.CAL for sensor 1 and 2 respectively.
 *   The X-wire is calibrated in a in a low turbulence, uniform velocity
 *   profile.The hot-wire output from the signal conditioner is taken
 *   against a reference velocity obtained from the pressure drop across
 *   the nozzle.
 *   A fourth order polynomial curve fitting is used to get the velocity
 *   calibration coefficients.
 *   Routines called: LSFIT: least squares polynomial fit
 *   FILES:   Master.fil: contains the path of the root.fil
 *            root .FIL : input file containing the information on
 *            the number of data points and the names of
 *            document file, data file and output file.
```

```
*   .dat -data files        (input)
*   .doc -document files.(input)
*   .out - output files.  (output)
*   PX1.CAL              : The file containing the calibration coefficients
*   PX2.CAL                and the average temperature during the calibration.
*   XCALP.OUT     : The output file generated by this program contains
*   anemometer output, temperature compensated output, the velocity,
*   angle, and type of calibration (1-wire1, 2-wire2, 3-angle calibration)
*
*   Signal connection:
*    Ch1 : X1 Hotwire    Ch3: Thermocouple
*    Ch2 : X2 Hotwire    Ch4: Differential pressure transducer
*****************************************************************************
      program XCALP
      parameter (max=33000)
      integer*2 idat(max),iwm(300)
      integer*4 n, nch, itime, size, isize, delay
      integer*4 ierr,nsapch
      integer*4 npol,ks,inc
      real*8 Coeff(15),A(40),Var(15)
      real*4 Sumsq(16),RMS(16),RMST(16),Avg(16),Avgt(16)
      real*4 pc(5),tc(5),vel(300),hw1(300),t(300),hwc1(300)
      real*4 hw2(300),hwc2(300),alpm(300),x(300),y(300)
      character*25 fili,filo,fild,filp
      data afac/1.0019/
*   afac -area ratio factor for computing the nozzle exit velocity
*   afac=1/sqrt(1-(d2/d1)**4)
c   Write data to sreen or disk?
      Write(6,*)'Sensor temperature in "C"?'
      read(5,*) tsens

c   open the file containing calibration constants for pressure
c   transducer.
      open(unit=8,file='pres.cal')
      read(8,*)(pc(i), i=1,3)
      close(8)
c   open the file containing calibration constants for thermocouple.
      open(unit=8,file='temp.cal')
      read(8,*)(tc(i), i=1,3)
      close(8)
c
      open(unit=8,file='master.fil')
      read(8,'(a25)') filp
      close(8)
      tsavg=0.0
      inc=0
c   open the file containing the filenames and number of files
 10   inc=inc+1
      open(unit=8,file=filp)
      read (8,*)nf
      do  i=1,inc
        read( 8,175) fili,fild,filo
      enddo
      close( 8)
      write(6,*)'Reading the doc. file: inc=',inc
      open(unit=8,file=fild)
      read(8,*) pstat,patm,alpha,iw
      close(8)
      do 250 j=1,nch
        Avgt(j) = 0.0
        RMSt(j) = 0.0
 250  continue
```

```
c   select a block size
        if(inc.eq.1) then
            call RDFILS(fili,n, nch, itime, delay, ierr)
            write(*,110)n,nch,itime,delay,ierr
            write(*,120)
            read(*,*)size
            isize=2**(size+8)
            nblock=n/isize
            nsapch=isize/nch
            write(*,130)nblock,isize
            call RDFILC(ierr)
        endif
        write(6,*)'Reading the data file: ',fili
        do 800  nb = 1,nblock
c   open the ADC data file and read the header
            call RDFILS(fili,n, nch, itime, delay, ierr)
c   Read the  data
            call RDBLK(idat, nb, isize, ierr)
c   Inspect IERR flag
            write(*,150)ierr
            write(6,80) nb,isize
c close data file
            call RDFILC(ierr)

c  Now calculate averages and RMS fluctuation levels
            do 300 j=1,nch
                Sumsq(j) = 0.
  300       Avg(j) = 0.
            do 450 i=1,nsapch
                do 400 j=1,nch
                    index = (i-1)*nch + j
                    Avg(j)=Avg(j)+(idat(index)-2048.)*.004882812
  400           continue
  450       continue
            do 500 j=1,nch
                Avg(j) = Avg(j)/nsapch
                write(6,*)'channel#', j,'        Average value= ',Avg(j)
                Avgt(j) = Avgt(j) + Avg(j)
  500       continue
c   RMS calculations
c
            do 600 i=1,nsapch
                do 600 j=1,nch
                    index = (i-1)*nch + j
                    Del=Avg(j)-(FLOAT(idat(index))-2048.0)*.004882812
                    Sumsq(j) = Sumsq(j) + Del*Del
  600       continue
            do 700 j=1,nch
                RMS(j)  = SQRT(Sumsq(j)/nsapch)
                write(6,*)'channel#', j,'        RMS value= ',RMS(j)
                RMSt(j) = RMSt(j) + RMS(j)
  700       continue
  800   continue
        do 850 j=1,nch
            Avg(j) = Avgt(j)/nblock
            RMS(j) = RMSt(j)/nblock
  850   continue
c   Now write the averaged results to screen and to disk.
        temp=avg(3)**2.0*tc(3) +avg(3)*tc(2) +tc(1)
        pavg=(avg(4)**2.0*pc(3) +avg(4)*pc(2) +pc(1))*25.4*9.81
        rho=(patm*13.6+pstat)*.0348432/(temp+273.15)
c   The next line prevents the blowing up of the program at zero velocity
```

```
c   where the pressure transducer can indicate slight -ve reading.
      if (pavg.lt.0.0) pavg=0.0
      velpn=sqrt(2.0*pavg/rho)*afac
      tstat=temp
      tsavg=tsavg+tstat
      tavg=tsavg/inc
      write(6,*)'Writing to output file:  inc=',inc
      write(*,85)
c   Write to the output file
      open(unit=10,file=filo)
      write(6,*)'nch=',nch
      do 900 ich=1,nch
      write(6,90) ich,Avg(ich),RMS(ich)
        write(10,90) ich,Avg(ich),RMS(ich)
  900 continue
      write(6,95)avg(1),avg(2),velpn,temp
      write(10,95)avg(1),avg(2),velpn,temp
      close(10)
      t(inc)=tstat
      hw1(inc)=avg(1)
      hw2(inc)=avg(2)
      vel(inc)=velpn
      iwm(inc)=iw
      alpm(inc)=alpha

c   Repeat processing the next file ?
      if (inc.lt.nf) go to 10
c  Temperature compensation  of hotwire output for variation in fluid
c  temperature
      do 910 j=1,nf
        hwc1(j)=hw1(j)*sqrt((tsens-tavg)/(tsens -t(j)))
  910 hwc2(j)=hw2(j)*sqrt((tsens-tavg)/(tsens -t(j)))
      call CLS
c  Write the results of velocity Vs hot-wire output
      open(unit=9,file='XCALP.OUT')
      write(6,*) 'TYPE     ANGLE      X1      X1C      X2      X2C     VELOCITY  '
      write(9,*) 'TYPE     ANGLE      X1      X1C      X2      X2C     VELOCITY  '
      do 920 j=1,nf
        write(9,180)iwm(j),alpm(j),hw1(j),hwc1(j),hw2(j),hwc2(j),vel(j)
  920   write(6,180)iwm(j),alpm(j),hw1(j),hwc1(j),hw2(j),hwc2(j),vel(j)
      write(9,'(a,f5.2)')'Average temperature=',tavg
      close(9)
      Write(6,*)'You may edit XCALP.OUT for zero velocity reading'
      Write(6,*)'To edit type COMMAND . When finished type EXIT'
      Pause
c  Performing the least square fit for a polynomial of order 4
      npol=4
      Write(6,*)'CALIBRATION CONSTANTS AT  TEMPERATURE  ', tavg
      do i=1,2
        n=0
        open(unit=8,file='XCALP.OUT')
        read(8,*)
        do  j=1,nf
          read(8,180)iwm(j),alpm(j),hw1(j),hwc1(j),hw2(j),hwc2(j),vel(j)
          if(iwm(j).eq.i) then
            n=n+1
            if(i.eq.1) x(n)=hwc1(j)
            if(i.eq.2) x(n)=hwc2(j)
            y(n)=vel(j)
          endif
        enddo
        call LSFIT(n,x,y,npol,a,var,coeff,ks)
```

```
      if(i.eq.1) then
        write(6,*)'Wire 1'
        open(unit=9,file='PX1.CAL')
      endif
      if(i.eq.2) then
        write(6,*)'Wire 2'
        open(unit=9,file='PX2.CAL')
      endif
      write(6,*)(coeff(ipol),ipol=1,npol+1)
c  Write calibration coefficients
      write(9,*)(coeff(ipol),ipol=1,npol+1)
      write(9,*)'Average temperature=',tavg
      close(9)
      close(8)
    enddo
c  Formats
  80  format(' Calculated block number',i3,2x,i5,' size')
  85  format(//,' Averaged results of A/D conversions :',/,
     $           5x,' Channel',6x,'X (DC)',
     $           8x,'X (RMS)')
  90  format(' ',7x,i3,2F14.5)
  95  format('    X1 volts         ',10x, ' X2 volts ',10x, 'Velocity m/s.'
     $,'      Temp C'/,f10.4,15x,f10.4,12x,f8.3,10x,f8.3)
 100  format(/' ADC filename:'\)
 101  format(a)
 110  format(' n:',i6,' nch:',i2,' itime:',i5,' delay:',i5,'ierr',i2)
 120  format(' -- select block size --'/' SIZE    BUFFER'/
     *'  0          256'/' 1          512'/' 2         1024'/
     *'  3         2048'/' 4         4096'/' 5         8192'/
     *'  6        16384'/' 7        32768'/' enter SIZE:'\)
 130  format(' There are ',i3,' blocks of ',i5,' words..')
 140  format(/' read block#:'\)
 150  format(' ierr:',i2)
 170  format(16i5)
 175  format(a,2x,a,2x,a)
 180  format(1x,i1,5x,f5.1,4(5x,f6.4),5x,f6.3)
      end
```

```
*************************************************************************
5. Program to determine Yaw calibration coefficients
*************************************************************************
* This program determines the yaw calibration functions alpha id, H, H*
*  and fit alpha id Vs alpha & alpha id Vs H* using fifth order
*  polynomial. The coefficients of the polynomial are written to AL.CAL
*  and H.CAL
*  Input calibration files: PRES.CAL, TEMP.CAL
*                           PX1.CAL, PX2.CAL (velocity calibration
*  obtained by keeping the wires normal to flow. Generated by XCALP.FOR)
*
*  Routines called    : LSFIT (least square fit program)
*  FILES: filp         : input file containing the information on the
*  number of data points and the names of document file, data file and
*  output file.
*                .dat -data files  of angle calibration(input)
*                .doc -document files.(input)
*                .out - output files.  (output)
*
*  XCALF.OUT    : output file with alpha, alphaid, Ve1, Ve2 etc.
*
*  Signal connection:
*  Ch1 : Hotwire   X1       Ch3: Thermocouple
```

```
*  Ch2 : Hotwire   X2      Ch4: Differential pressure transducer
****************************************************************************
        program XCALF
        parameter (max=33000)
        integer*2 idat(max)
        integer*4 n, nch, itime, size, isize, delay,inc
        integer*4 ierr,nsapch
        real*4 Avg(8),Avgt(8)
        real*4 hwvel(8),hwvelt(8)
        real*4 pc(5),tc(5),x1c(5),x2c(5)
        real*4 hvoltt(16),hvolttt(16)
        real*4 hh(200),AL(200),ALI(200)
        real*8 ac(15),hc(15),A(40),Var(15)
        character*25 fili,filo,fild,filp
        character*80 sent
        data afac/1.0019/
        Write(6,*)'Sensor temperature in "C"?'
        read(5,*) tsens

c   open the file containing velocity calibration constants for hot-wire
        open(unit=8,file='PX1.cal')
        read(8,*)(x1c(i), i=1,5)
        read(8,5)fili,tcal
        write(6,*)'tcal',tcal
        close(8)
        open(unit=8,file='PX2.cal')
        read(8,*)(x2c(i), i=1,5)
        read(8,5)fili,tcal
        write(6,*)'tcal',tcal
        close(8)

c   open the file containing calibration constants for pressure
c   transducer.
        open(unit=8,file='pres.cal')
        read(8,*)(pc(i), i=1,3)
        close(8)
c   open the file containing calibration constants for thermocouple.
        open(unit=8,file='temp.cal')
        read(8,*)(tc(i), i=1,3)
        close(8)
c   open the master file
        open(unit=8,file='master.fil')
        read(8,*) ntest
        read(8,'(a)') filp
        close(8)
        inc=0
c   open the file containing the filenames and number of files
        write(6,*) filp
   10   open(unit=8,blocksize=3096,file=filp)
        read (8,*)nf
        inc=inc+1
        do 15 i=1,inc
   15   read(8,175) fili,fild,filo
        close(8)
        write(6,*)'reading doc.',inc
        open(unit=8,file=fild)
        read(8,*) pstat,patm,alpha,iw
        close(8)
        do 250 j=1,nch
          Avgt(j) = 0.0
          hwvelt(j)=0.0
          hvolttt(j)=0.
```

```fortran
 250 continue
     tempt=0.0
     pavgt=0.0
     velpnt=0.
     if(inc.eq.1) then
        call RDFILS(fili,n, nch, itime, delay, ierr)
        write(*,110)n,nch,itime,delay,ierr
        write(*,120)
        read(*,*)size
        isize=2**(size+8)
        nblock=n/isize
        nsapch=isize/nch
        write(*,130)nblock,isize
        call RDFILC(ierr)
     endif
     write(6,*)'Reading the data file: ',fili
     open(unit=9,file=filo)
     do 800  nb = 1,nblock
c  open the ADC data file and read the header
        call RDFILS(fili,n, nch, itime, delay, ierr)
C  Read the  data
        call RDBLK(idat, nb, isize, ierr)
c  Inspect IERR flag
        write(*,150)ierr
        write(6,80) nb,isize
c close data file
        call RDFILC(ierr)
c  Now calculate averages and RMS fluctuation levels
        do 300 j=1,nch
           hwvel(j)=0.
           hvoltt(j)=0.0
 300    Avg(j) = 0.0
        do 450 i=1,nsapch
          do 400 j=1,nch
             index  = (i-1)*nch + j
             Avg(j)=Avg(j)+(idat(index)-2048.)*.004882812
 400      continue
 450    continue
        do 500 j=1,nch
          Avg(j) = Avg(j)/nsapch
          write(6,*)'channel#', j,'         Average value= ',Avg(j)
          Avgt(j) = Avgt(j) + Avg(j)
 500    continue

        temp=(avg(3)**2.0*tc(3) +avg(3)*tc(2) +tc(1))
      pavg=(avg(4)**2.0*pc(3) +avg(4)*pc(2) +pc(1))*25.4*9.81
        rho=(patm*13.6+pstat)*.0348432/(temp+273.15)
        if(pavg.lt.0.0) pavg=0.
        velpn=sqrt(2.0*pavg/rho)*afac
        do 510 i=1,nsapch
          do 510 j=1,2
             index=(i-1)*nch +j
             hvolt=(idat(index)-2048.)*.004882812
             hvolt=hvolt*sqrt((tsens-tcal)/(tsens -temp))
             hvoltt(j)=hvoltt(j)+hvolt
             if(j.eq.1) then
                hwvel(j)=hwvel(j)+(x1c(1)+x1c(2)*hvolt+x1c(3)*hvolt**2.
     $          +x1c(4)*hvolt**3.0 +x1c(5)*hvolt**4.)
             else
                hwvel(j)=hwvel(j)+(x2c(1)+x2c(2)*hvolt+x2c(3)*hvolt**2.
     $          +x2c(4)*hvolt**3.0 +x2c(5)*hvolt**4.)
             endif
```

```
  510    continue
         do 525 j=1,2
           hwvel(j)=hwvel(j)/nsapch
           hvoltt(j)=hvoltt(j)/nsapch
           hwvelt(j) = hwvelt(j) + hwvel(j)
           hvolttt(j)=hvolttt(j)+hvoltt(j)
  525    continue
         tempt=tempt+temp
         pavgt=pavgt+pavg
         velpnt=velpnt+velpn
         write(6,*)'ALPHA      X1       X1C      X2       X2C     PRESS      TEMP
      $  VEL.PN    Veff1    Veff2'
         if(nb.eq.1) then
           write(9,*)'ALPHA      X1       X1C      X2       X2C     PRESS      TEMP
      $    VEL.PN    Veff1    Veff2'
         endif
         write(6,85) alpha,avg(1),hvoltt(1),avg(2),hvoltt(2),pavg/9.81,
      $  temp,velpn,hwvel(1),hwvel(2)
         write(9,85) alpha,avg(1),hvoltt(1),avg(2),hvoltt(2),pavg/9.81,
      $  temp,velpn,hwvel(1),hwvel(2)
  800 continue
         do  850 j=1,nch
           Avg(j) = Avgt(j)/nblock
  850 continue
         do 875 j=1,2
           hwvel(j)= hwvelt(j)/nblock
           hvoltt(j)=hvolttt(j)/nblock
  875 continue
         temp=tempt/nblock
         pavg=pavgt/nblock
         velpn=velpnt/nblock
c  Now write the final results to screen and to disk.
c  Write to the output file
         Write(6,*)'Final Averaged Results'
         Write(9,*)'Final Averaged Results'
         write(6,85) alpha,avg(1),hvoltt(1),avg(2),hvoltt(2),pavg/9.81,
      $temp,velpn,hwvel(1),hwvel(2)
         write(9,85) alpha,avg(1),hvoltt(1),avg(2),hvoltt(2),pavg/9.81,
      $temp,velpn,hwvel(1),hwvel(2)
         close(9)
c  CALCULATE H and AlPHAid
         alid=(atan(hwvel(1)/hwvel(2)))*57.29578-45.0
         H1 =velpn*velpn/(hwvel(1)*hwvel(1)+hwvel(2)*hwvel(2))
         H2 =sqrt(h1)
         H3 =sqrt(h1)*cos(alid/57.29578)
         H4 =sqrt(h1)*cos(alpha/57.29578)
         if (inc.eq.1) then
           open(unit=7,file='XCALF.OUT')
           write(7,*)'ANGLE Veff1 m/s Veff2 m/s V  m/s     ALPHAid    H       H2
      $  H3     H* '
         endif
         write(7,70)alpha,hwvel(1),hwvel(2),velpn,ALID,H1,H2,H3,H4
         write(6,*)'ANGLE Veff1 m/s Veff2 m/s V  m/s     ALPHAid    H       H2
      $  H3     H* '
         write(6,70)alpha,hwvel(1),hwvel(2),velpn,ALID,H1,H2,H3,H4
c  Repeat processing the next file ?
         if (inc.lt.nf) go to 10
         rewind (7)
         read(7,'(a)')sent
         write(6,*)sent
         do  j=1,nf
           read (7,70)al(j),hwvel(1),hwvel(2),velpn,ALI(j),H1,H2,H3,HH(j)
```

```
      write(6,70)al(j),hwvel(1),hwvel(2),velpn,ALI(j),H1,H2,H3,HH(j)
      enddo
      close(7)
c   calculate AL.CAL and H.CAL files
      npol=5
      call LSFIT(nf,ali,al,npol,a,var,ac,ks)
      call LSFIT(nf,ali,hh,npol,a,var,hc,ks)
      open(unit=9,file='H.CAL')
      write(6,*)'H.CAL'
      write(9,*)(HC(ipol),ipol=1,6)
      write(6,*)(HC(ipol),ipol=1,6)
      close(9)
      open(unit=9,file='AL.CAL')
      write(6,*)'AL.CAL'
      write(9,*)(AC(ipol),ipol=1,6)
      write(6,*)(AC(ipol),ipol=1,6)
      close(9)

c   Formats
  5   format(a26,f9.6)
 70   format(1x,f5.1,3(2x,f7.4),3x,f6.2,4(2x,f5.3))
 80   format(' Calculated block number',i3,2x,i5,' size')
 85   format(1x,f5.1,4(2x,F6.4),2x,f6.2,2x,f5.2,3(2x,f6.3))
 90   format(' ',7x,i3,2F14.5)
 95   format(' hotwire voltage ',10x, 'velocity ',10x, 'temperature'
     $,/,f10.4,15x,f10.4,12x,f8.3)
100   format(/' ADC filename:'\)
101   format(a)
110   format(' n:',i6,' nch:',i2,' itime:',i5,' delay:',i5,'ierr:',i2)
120   format(' -- select block size --'/' SIZE     BUFFER'/
     *' 0         256'/' 1         512'/' 2         1024'/
     *' 3         2048'/' 4         4096'/' 5         8192'/
     *' 6         16384'/' 7         32768'/' enter SIZE:'\)
130   format(' There are ',i3,' blocks of ',i5,' words..')
140   format(/' read block#:'\)
150   format(' ierr:',i2)
170   format(16i5)
175   format(a25,2x,a25,2x,a25)
      end
```

```
****************************************************************************
```
6.Program to obtain the velocity calibration coefficients of each of the sensor of the X-probe from a calibration using XCAL.FOR and keeping the sensors at 45° to flow.
```
****************************************************************************
*   This program process the data files generated during X-probe
*   calibration at alpha=0(i.e. both sensors at 45deg to flow)using
*   XCAL.FOR. This generates an output file VEFF.OUT containing voltage
*   output and effective velocity.  The velocity calibration coefficients
*   will be stored in X1.CAL and X2.CAL for sensor 1 and 2 respectively.
*   The X-probe is calibrated in a in a low turbulence, uniform velocity
*   jet.  A fourth order polynomial curve fitting is used to get the
*   velocity calibration coefficients.
*
*   Routines called: LSFIT: least square polynomial fit
*                     AHC  : ALPHAid and H for a given ALPHA
*   FILES:  Master.fil: contains the path of the root.fil
*   root .FIL : data file containing the information on
*   the number of data points and the names of document file, data file
*   and output file.
*   .dat -data files        (input)
```

```
*   .doc -document files.(input)
*   .out - output files.  (output)
*   X1.CAL   : The file containing the calibration constant and
*   X2.CAL(output) the average temperature during the calibration.
*
*   VEFF.OUT    : The output file generated by this program contains
*   (output)       hot-wire output,temperature compensated output,
*                  the velocity ,angle
*
*   Signal connection:
*   Ch1 : X1 Hotwire        Ch3: Thermocouple
*   Ch2 : X2 Hotwire        Ch4: Differential pressure transducer
*****************************************************************************
        program VEFF
        integer*2 idat(33000)
        integer*4 n, nch, itime, size, isize, delay
        integer*4 ierr,nsapch
        integer*4 npol,ks,inc
        real*8 Coeff(15),A(40),Var(15)
        real*4 Sumsq(8),RMS(8),RMST(8),Avg(8),Avgt(8)
        real*4 pc(5),tc(5),vel(300),hw1(300),t(300),hwc1(300)
        real*4 hw2(300),hwc2(300),alpm(300),x(300),y(300)
        real*4 ve1(300),ve2(300)
        character*25 fili,filo,fild,filp
        data afac/1.0019/
c  afac -area ratio factor for computing the nozzle exit velocity
c  afac=1/sqrt(1-(d2/d1)**4)
c  Write data to sreen or disk?
        Write(6,*)'Sensor temperature in "C"?'
        read(5,*) tsens
c  Get the ALPHAid and H for a given alpha
        write(6,*)'Enter the angle alpha?'
        read(5,*)AL
        call AHC(AL,ALI,H)
        write(6,*)'alphaid= ',ali, 'h= ',h
        RK2=Cos(AL/57.29578)/(H*(sqrt(TAN((ALI+45.)/57.29578)*TAN((ALI
        $+45.)/57.29578)+1.)))
        RK1=RK2*TAN((ALI+45.)/57.29578)
        write(6,*)'Rk1=',rk1,'RK2=',rk2

c  open the file containing calibration constants for pressure
c  transducer.
        open(unit=8,file='pres.cal')
        read(8,*)(pc(i), i=1,3)
        close(8)
c  open the file containing calibration constants for thermocouple.
        open(unit=8,file='temp.cal')
        read(8,*)(tc(i), i=1,3)
        close(8)
c
        open(unit=8,file='master.fil')
        read(8,'(a25)') filp
        close(8)
        tsavg=0.0
        inc=0
c  open the file containing the filenames and number of files
   10   inc=inc+1
        open(unit=8,file=filp)
        read (8,*)nf
        do  i=1,inc
          read( 8,175) fili,fild,filo
        enddo
```

```
          close( 8)
          write(6,*)'Reading the doc. file: inc=',inc
          open(unit=8,file=fild)
          read(8,*) pstat,patm,alpha,iw
          close(8)
          do 250 j=1,nch
            Avgt(j) = 0.0
            RMSt(j) = 0.0
  250 continue
c  select a block size
          if(inc.eq.1) then
            call RDFILS(fili,n, nch, itime, delay, ierr)
            write(*,110)n,nch,itime,delay,ierr
            write(*,120)
            read(*,*)size
            isize=2**(size+8)
            nblock=n/isize
            nsapch=isize/nch
            write(*,130)nblock,isize
            call RDFILC(ierr)
          endif
          write(6,*)'Reading the data file: ',fili
          do 800  nb = 1,nblock
c  open the ADC data file and read the header
          call RDFILS(fili,n, nch, itime, delay, ierr)
c  Read the  data
          call RDBLK(idat, nb, isize, ierr)
c  Inspect IERR flag
          write(*,150)ierr
          write(6,80) nb,isize
c  close data file
          call RDFILC(ierr)

c  Now calculate averages and RMS fluctuation levels
          do 300 j=1,nch
            Sumsq(j) = 0.
  300     Avg(j) = 0.
          do 450 i=1,nsapch
            do 400 j=1,nch
              index  = (i-1)*nch + j
              Avg(j)=Avg(j)+(idat(index)-2048.)*.004882812
  400     continue
  450     continue
          do 500 j=1,nch
            Avg(j) = Avg(j)/nsapch
            write(6,*)'channel#', j,'         Average value= ',Avg(j)
            Avgt(j) = Avgt(j) + Avg(j)
  500     continue
c
c     RMS calculations
c
          do 600 i=1,nsapch
            do 600 j=1,nch
              index = (i-1)*nch + j
              Del=Avg(j)-(FLOAT(idat(index))-2048.0)*.004882812
              Sumsq(j) = Sumsq(j) + Del*Del
  600     continue
          do 700 j=1,nch
            RMS(j)   = SQRT(Sumsq(j)/nsapch)
            write(6,*)'channel#', j,'              RMS value= ',RMS(j)
            RMSt(j) = RMSt(j) + RMS(j)
  700     continue
```

```
      800 continue
          do 850 j=1,nch
            Avg(j) = Avgt(j)/nblock
            RMS(j) = RMSt(j)/nblock
      850 continue
c  Now write the averaged results to screen and to disk.
          temp=avg(3)**2.0*tc(3) +avg(3)*tc(2) +tc(1)
          pavg=(avg(4)**2.0*pc(3) +avg(4)*pc(2) +pc(1))*25.4*9.81
          rho=(patm*13.6+pstat)*.0348432/(temp+273.15)
c The next line prevents the blowing up of the program at zero velocity
c where the pressure transducer can indicate slight -ve reading.
          if (pavg.lt.0.0) pavg=0.0
          velpn=sqrt(2.0*pavg/rho)*afac
          tstat=temp
          tsavg=tsavg+tstat
          tavg=tsavg/inc
          write(6,*)'Writing to output file:  inc=',inc
          write(*,85)
c  Write to the output file
          open(unit=10,file=filo)
          write(6,*)'nch=',nch
          do 900 ich=1,nch
            write(6,90) ich,Avg(ich),RMS(ich)
            write(10,90) ich,Avg(ich),RMS(ich)
      900 continue
          write(6,95)avg(1),avg(2),velpn,temp
          write(10,95)avg(1),avg(2),velpn,temp
          close(10)
          t(inc)=tstat
          hw1(inc)=avg(1)
          hw2(inc)=avg(2)
          vel(inc)=velpn
          alpm(inc)=alpha
c  Repeat processing the next file ?
          if (inc.lt.nf) go to 10
c  Temperature compensation  of hotwire output for variation in fluid
c  temperature
          do 910 j=1,nf
            hwc1(j)=hw1(j)*sqrt((tsens-tavg)/(tsens -t(j)))
            hwc2(j)=hw2(j)*sqrt((tsens-tavg)/(tsens -t(j)))
            Vel(j)=RK1*vel(j)
      910 ve2(j)=RK2*vel(j)
          call CLS
c Write the results of velocity Vs hot-wire output
          open(unit=9,file='VEFF.OUT')
          write(6,*) 'ANGLE    X1    X1C    X2    X2C    VEL   Vel   Ve2'
          write(9,*) 'ANGLE    X1    X1C    X2    X2C    VEL   Vel   Ve2'
          do 920 j=1,nf
            write(9,180)alpm(j),hw1(j),hwc1(j),hw2(j),hwc2(j),vel(j),Vel(j),
        $ Ve2(j)
      920 write(6,180)alpm(j),hw1(j),hwc1(j),hw2(j),hwc2(j),vel(j),Vel(j),
          $Ve2(j)
          write(9,'(a,f5.2)')'Average temperature=',tavg
          close(9)
          Write(6,*)'You may edit VEFF.OUT for zero velocity reading'
          Write(6,*)'To edit type COMMAND . When finished type EXIT'
          Pause
c Performing the least square fit for a polynomial of order 4
          npol=4
          Write(6,*)'CALIBRATION CONSTANTS AT  TEMPERATURE  ', tavg
          open(unit=8,file='VEFF.OUT')
          read(8,*)
```

```
      do j=1,nf
        read(8,180)alpm(j),hw1(j),hwc1(j),hw2(j),hwc2(j),vel(j),ve1(j),
     $  Ve2(j)
        x(j)=hwc1(j)
        y(j)=vel(j)
      enddo
      close(8)
      call LSFIT(nf,x,y,npol,a,var,coeff,ks)
      write(6,*)'Wire 1'
      open(unit=9,file='x1.CAL')
      write(6,*)(coeff(ipol),ipol=1,npol+1)
c Write calibration coefficients
      write(9,*)(coeff(ipol),ipol=1,npol+1)
      write(9,*)'Average temperature=',tavg
      close(9)
      do  j=1,nf
        x(j)=hwc2(j)
        y(j)=ve2(j)
      enddo
      call LSFIT(nf,x,y,npol,a,var,coeff,ks)
      write(6,*)'Wire 2'
      open(unit=9,file='x2.CAL')
      write(6,*)(coeff(ipol),ipol=1,npol+1)
c Write calibration coefficients
      write(9,*)(coeff(ipol),ipol=1,npol+1)
      write(9,*)'Average temperature=',tavg
      close(9)
c  Formats
  80  format(' Calculated block number',i3,2x,i5,' size')
  85  format(//,' Averaged results of A/D conversions :',/,
     $          5x,' Channel',6x,'X (DC)',
     $          8x,'X (RMS)')
  90  format(' ',7x,i3,2F14.5)
  95  format('   X1 volts          ',10x, ' X2 volts ',10x, 'Velocity m/s.'
     $,'     Temp C'/,f10.4,15x,f10.4,12x,f8.3,10x,f8.3)
 100  format(/' ADC filename:'\)
 101  format(a)
 110  format(' n:',i6,' nch:',i2,' itime:',i5,' delay:',i5,'ierr',i2)
 120  format(' -- select block size --'/' SIZE    BUFFER'/
     *' 0         256'/' 1         512'/' 2         1024'/
     *' 3        2048'/' 4        4096'/' 5         8192'/
     *' 6       16384'/' 7       32768'/' enter SIZE:'\)
 130  format(' There are ',i3,' blocks of ',i5,' words..')
 140  format(/' read block#:'\)
 150  format(' ierr:',i2)
 170  format(16i5)
 175  format(a,2x,a,2x,a)
 180  format(1x,f5.1,4(4x,f6.4),3(4x,f6.3))
      end
```

B.2. Data Acquisition Programs

```
*******************************************************************
1. Data acquisition program for measurements using single sensor hot-
film/wire probe
*******************************************************************
*   This program is used to acquire single sensor data at various
*   radial locations by moving the probe to  successive
*   points in auto mode. This is done by calling the TRAV routine.
*   The locations to move are read from coord.dat file
*   Features:
*   Write blocks of data continuously to disk. The file size is
*   is limited only by disk space, although here MAXBLOCK = 32 to give
*   a 3MB upper limit.
*   select a block size between 512 and 32768 words and read any
*   single block into the IDAT data array.
*   EXTERNAL CALLS: RDFILO, RDBLK & RDFILC, all in ADCLIB.
*                 : TRAV (for moving the unislide), FGEN(generate
*                   file names), PVT(read pressure and temperature)
*                   RESULT, SRDDSKB(read and display data)
*   Data files    : Coord.dat (contains the current location,over
*                   travel limits,location to move)

*-----------------------------------------------------------------
      program AUTO4.FOR
      integer*4 n, nch, itime, delay, size, isize
      parameter (max=32768, maxblock=32)
      integer*2 idat(max), ierr(maxblock)
      integer*4 idisk, jerr
      logical*1 IVER,ishow,itrav
      character*80 ch,sent
      character*25 fild(300),fili(300),filo(300),filp,filnam
      character*25  root
      double precision y(300),xn,xo
      data idisk/1/

* Move the probe position
      ntest=0
      ith=0
      inc=0
      ishow=.false.
      if(IVER('0Show data or results?')) ishow=.true.
      itrav=.false.
      if(IVER('0Traverse the probe during this test?')) then
        itrav=.true.
      else
        np=0
        xo=0.
        go to 1
      endif
      open(Unit=8,file='coord.dat')
      read(8,*)ch
      read(8,*)np
      read(8,*)(y(I), i=1,np)
      close(8)
      write(6,*)'Data will be taken at the following points'
      write(6,*)(Y(i),i=1,np)
  4   ith=ith+1
      xn=Y(ith)
  c   write(6,*) xn,ith
```

```
      call TRAV(ith,xo,xn)
      if(ith.gt.1) go to 6
* read the ADC input parameter
 1    write(*,100)
      read(*,*)nch
      write(*,110)
      read(*,*)itime
      write(*,115)
      read(*,*)delay
      write(*,120)
      read(*,*)size
      isize=2**(size+8)
      write(*,130)
      read(*,*)nblock
      n=isize*nblock
      write(6,*)'enter the root file name(without extension)?'
      read(*,500) root
      in=1
      do while(root(in:in).ne.' ')
        filp(in:in)=root(in:in)
        in=in+1
      end do
      filp(in:in+3)='.fil'
 6    ntest=ntest+1
      if(ntest.eq.1) then
        open(unit=9,file='master.fil')
        write(9,*) ntest
        write(9,'(a)')filp
        close(9)
      endif
      call FGEN(root,ntest,fili,fild,filo)
      call CLS
      filnam=fili(ntest)
      write(6,300) filnam
c  Reading temperature and pressure in one shot mode
      call PVT(temp,pres)
c     pause 'Please [ENTER] to start'
*  open data file, write file header, initialize RC board
      call ADFILS(filnam,n, nch, itime, delay, jerr)
      call ADHALT()
      call ADC0(nch, itime, size)
      write(*,*)'sampling hot-wire data..'
      call ADC1(delay)
*  read NBLOCK blocks of data from RC A/D and write to file

      do 10 i=1,nblock
 10   call RDBUF(idat, isize, ierr(i), idisk)
*  stop the ADCs, close the data file
      call ADHALT()
      call ADFILC(jerr)
* inspect IERR array for error flags
      write(*,140)(i,ierr(i),i=1,nblock)
C Input test parameters
      If(ntest.eq.1) then
        write(6,*)' Static pressure in "mm" of water?'
        read(5,*) PSTAT
        write(6,*)' Barometric pressure in "mm" of Hg ?'
        read(5,*)patm
        write(6,*)'Any other parameters to document? (max. one line)'
        read(5,'(a80)')sent
      endif
c get time and date
```

```
      call GETTIM(ihr,imin,isec,i100)
      call GETDAT(iyr,imon,iday)
c document this test
      open(unit=8,file=fild(ntest))
      write(8,*)temp,pres,pstat,patm,-xo
      write(8,*)fili(ntest)
      write(8,*)sent
      write(8,450)imon,iday,ihr,imin
      close(8)
c update .fil; later used by data analysis software
      open(unit=8,file=filp)
      write(8,*)ntest
      do 20 j=1,ntest
  20  write(8,400)fili(j),fild(j),filo(j)
      close(8)
* repeat?
      if(itrav.eqv..false.) then
        if(IVER('0repeat acquiring new data at this location?')) goto 6
      endif
* reads data from disk and show results?
      if(ishow) then
        if(IVER('0read  data from disk?')) Call SRDDSKB(fili)
        inc=inc+1
        if(IVER('0Show results?')) Call RESULT(inc)
      else
        go to 90
      endif
*  repeat acquiring new data?
      if(IVER('0repeat acquiring new data?')) goto 1
* Move to new location
  90  if(ith.lt.NP) go to 4
      write(6,*)'terminating the program at your request'
      stop 'bye'

* formats

 100  format(/' nch [1,2,4,8,16]:'\)
 110  format(' itime [usec, 1-65384]:'\)
 115  format(' delay [usec, 0-65535]:'\)
 120  format(' -- select buffer size --'/' SIZE     BUFFER'/
     *' 0         256'/' 1         512'/' 2         1024'/
     *' 3        2048'/' 4        4096'/' 5         8192'/
     *' 6       16384'/' 7       32768'/' enter SIZE:'\)
 130  format(' nblock:'\)
 140  format(' block#',i3,'  ierr = ',i1)
 280  format(a30)
 300  format( ' HOT-WIRE data will be stored in ',a,/,' SAMPLING FOR
     * PRESSURE AND TEMPERATURE..')
 400  format(a25,2x,a25,2x,a25)
 450  format(' DATE: ',i2,'/',i2,5x,'TIME: ',i2,'-',i2)
 500  format(a)
      end
```

```
*********************************************************************
2. Data acquisition program for measurements using X-hot-film/wire probe
*********************************************************************
*  This program is used acquire data from X-probe by traversing the probe
*  to different locations in auto mode.
*  This is done by calling the TRAV routine. The locations to move are
*  read from coord.dat file
*  Features:
```

```
*  Write blocks of data continuously and then read it. The file size is
*  is limited only by disk space, although here MAXBLOCK = 32 to give
*  a 3MB upper limit.
*  Select a block size between 512 and 32768 words and read any
*  single block into the IDAT data array.
*  External routines required:
*      ADFILS, ADC0, ADC1, RDBUF, ADHALT & ADFILC, RDFILO, RDBLK &
*      RDFILC, all in ADCLIB.
*      Fortran subroutines:
*      IVER    : asks for confirmation [Y/N]
*      FGEN    : generates file name with appropriate extension No.
*      LAG     : make a given delay between next line of execution
*      SPVT8   : subroutine to get the average pressure,temp, etc.
*      SRDDSKB : subroutine to read and display the raw data
*      SXRES   : for showing the result for a given point
*      ATRAV   : for moving the unislide
*      Data files : Coord.dat (contains the locations to move)
*  Signal connection:
*  Ch1 : Hotwire    X1      Ch3: Thermocouple
*  Ch2 : Hotwire    X2      Ch4: Differential pressure
*                               transducer(0-10mm),PR1
*  Ch5 : Differential pressure transducer(0-100mm),PR2
********************************************************************
        program XAUTO
        integer*4 n, nch, itime, delay, size, isize
        parameter (max=32768, maxblock=32)
        integer*2 idat(max), ierr(maxblock)
        integer*4 idisk, jerr
        logical*1 IVER,itrav
        character*80 ch,sent
        character*25 fild(300),fili(300),filo(300),filp,filnam
        character*25  root
        double precision y(300),xn,xo
        data idisk/1/

*  Move the probe position
        ntest=0
        ith=0
        inc=0
        ishow=.false.
        write(6,*)'Enter the delay in seconds for acquiring data after the
      * probe movement'
        read(*,*)ilag
        if(IVER('0Show data or results?')) ishow=.true.
        itrav=.false.
        if(IVER('0Traverse the probe during this test?')) then
          itrav=.true.
        else
          np=0
          xo=0.
          go to 1
        endif
        open(Unit=8,file='coord.dat')
        read(8,*)ch
        read(8,*)np
        read(8,*)(y(I), i=1,np)
        close(8)
        write(6,*)'Data will be taken at the following points'
        write(6,*)(Y(i),i=1,np)
4       ith=ith+1
        xn=Y(ith)
c       write(6,*) xn,ith
```

```fortran
      call ATRAV(ith,xo,xn)
      if(ith.gt.1) go to 6
* read the ADC input parameter
 1    write(*,100)
      read(*,*)nch
      write(*,110)
      read(*,*)itime
      write(*,115)
      read(*,*)delay
      write(*,120)
      read(*,*)size
      isize=2**(size+8)
      write(*,130)
      read(*,*)nblock
      n=isize*nblock
      write(6,*)'enter the root file name(without extension)?'
      read(*,500) root
      in=1
      do while(root(in:in).ne.' ')
         filp(in:in)=root(in:in)
         in=in+1
      end do
      filp(in:in+3)='.fil'
 6    ntest=ntest+1
      if(ntest.eq.1) then
         open(unit=9,file='master.fil')
         write(9,*) ntest
         write(9,'(a)')filp
         close(9)
      endif
      call FGEN(root,ntest,fili,fild,filo)
      call CLS
      filnam=fili(ntest)
      write(6,290) ilag
      call LAG(ilag)
      write(6,300) filnam
c     pause 'Please [ENTER] to start'
* open data file, write file header, initialize RC board
      call ADFILS(filnam,n, nch, itime, delay, jerr)
      call ADHALT()
      call ADC0(nch, itime, size)
      write(*,*)'sampling hot-wire data..'
      call ADC1(delay)
* read NBLOCK blocks of data from RC A/D and write to file
      do 10 i=1,nblock
 10   call RDBUF(idat, isize, ierr(i), idisk)
* stop the ADCs, close the data file
      call ADHALT()
      call ADFILC(jerr)
* inspect IERR array for error flags
      write(*,140)(i,ierr(i),i=1,nblock)
      write(6,350)
c acquiring  temperature and pressure in one shot mode
      call SPVT8(temp,pr1,pr2)
C Input test parameters
      If(ntest.eq.1) then
         write(6,*)' Static pressure in "mm" of water?'
         read(5,*) PSTAT
         write(6,*)' Barometric pressure in "mm" of Hg ?'
         read(5,*)patm
         write(6,*)'Any other parameters to document? (max. one line)'
         read(5,'(a80)')sent
```

```fortran
      endif
c get time and date
      call GETTIM(ihr,imin,isec,i100)
      call GETDAT(iyr,imon,iday)
c document this test
      open(unit=8,file=fild(ntest))
      write(8,*)temp,pr1,pr2,pstat,patm,-xo
      write(8,*)fili(ntest)
      write(8,*)sent
      write(8,450)imon,iday,ihr,imin
      close(8)
c update .fil; later used by data analysis software
      open(unit=8,file=filp)
      write(8,*)ntest
      do 20 j=1,ntest
   20 write(8,400)fili(j)
      close(8)
* repeat?
      if(itrav.eqv..false.) then
        if(IVER('0repeat acquiring new data at this location?')) goto 6
      endif
* reads data from disk and show results?
      if(ishow) then
        if(IVER('0read  data from disk?')) Call SRDDSKB(fili(ntest))
        inc=inc+1
        if(IVER('0Show results?')) Call SXRES(inc)
      else
        go to 90
      endif

* repeat acquiring new data?

      if(IVER('0repeat acquiring new data?')) goto 1
* Move to new location
   90 if(ith.lt.NP) go to 4
      write(6,*)'terminating the program at your request'
      stop 'bye'

* formats

  100 format(/' nch [1,2,4,8,16]:'\)
  110 format(' itime [usec, 1-65384]:'\)
  115 format(' delay [usec, 0-65535]:'\)
  120 format(' -- select buffer size --'/' SIZE     BUFFER'/
     *' 0             256'/' 1           512'/' 2          1024'/
     *' 3            2048'/' 4          4096'/' 5          8192'/
     *' 6           16384'/' 7         32768'/' enter SIZE:'\)
  130 format(' nblock:'\)
  140 format(' block#',i3,'  ierr = ',i1)
  280 format(a30)
  290 format(' Waiting for the specified delay',I3,' Sec')
  300 format(' HOT-WIRE data will be stored in ',a)
  350 format(' SAMPLING FOR PRESSURE AND TEMPERATURE..')
  400 format(a25)
  450 format(' DATE: ',i2,'/',i2,5x,'TIME: ',i2,'-',i2)
  500 format(a)
      end
```

```
************************************************************************
```
3. Data acquisition program for phase-averaged measurements using X-hot-film/wire probe
```
************************************************************************
*   This program is used acquire data from X-probe by traversing the probe
*    to different locations in auto mode.   A/D board is externally
triggered
*   by once in a revolution per signal from fiber optic proximity sensor.
*   The locations to move are read from coord.dat file
*   Feature: Data acquisition of A/D board in one-shot mode.
*   External routines required:
*       ADOS, AD1S, RD1S, ADFILO, ADFILC - all in AD10LIB.LIB
*       Fortran subroutines:
*       IVER     : asks for confirmation [Y/N]
*       FGEN     : generates file name with appropriate extension No.
*       LAG      : make a given delay between next line of execution
*       SPVT8    : subroutine to get the average pressure,temp, etc.
*       SRDDSKB  : subroutine to read and display the raw data
*       SXRES    : for showing the result for a given point
*       TRAV     : for moving the unislide
*       SRPM     : get rpm of wake generator
*       Data files : Coord.dat (contains the locations to move)
*   Signal connection:
*   Ch1 : Hotwire    X1        Ch3: Thermocouple
*   Ch2 : Hotwire    X2        Ch4: Differential pressure
*                                   transducer(0-10mm),PR1
*   Ch5 : Differential pressure transducer(0-100mm),PR2
************************************************************************
        program UXAUTO
        parameter (max=32768)
        integer*2 idat(max)
        integer*4 n, nch, nrev, itime, delay, size, isize,idisk
        integer*4 ierr,ierrf
        logical*1 IVER,itrav
        character*80 ch,sent
        character*25 fild(300),fili(300),filo(300),filp,filnam
        character*25  root
        double precision y(300),xn,xo
        data idisk,nrev/1,1/

*   Move the probe position
        ntest=0
        ith=0
        inc=0
        write(6,*)'Enter the delay in seconds for acquiring data after the
     *   probe movement'
        read(*,*)ilag
        write(6,*)'Enter the approximate rpm ? (Exact value will be found
     $later)'
        read(*,*)rpm
        itrav=.false.
        if(IVER('0Traverse the probe during this test?')) then
          itrav=.true.
        else
          np=0
          xo=0.
          go to 12
        endif
        open(Unit=8,file='coord.dat')
        read(8,*)ch
        read(8,*)np
        read(8,*)(y(I), i=1,np)
```

```
        close(8)
        write(6,*)'Data will be taken at the following points'
        write(6,*)(Y(i),i=1,np)
  4     ith=ith+1
        xn=Y(ith)
c       write(6,*) xn,ith
        call TRAV(ith,xo,xn)
c  Get the rpm
 12     call SRPM(rpm)
        if(ith.gt.1) go to 6
* read the ADC input parameter
        write(*,100)
        read(*,*)nch
        write(*,115)
        read(*,*)delay
        write(6,*)'Buffer Size is the total number of samples taken during
       $ one revolution.'
        write(*,120)
        read(*,*)size
        isize=2**(size+8)
        itime= 60000000*nch/(rpm*isize)
        Write(6,*)'Based on the revolution of',rpm,' rpm and given buffer
       $size the sampling interval  is :',itime,' micro sec'
        write(6,*)'You may change the rpm now.'
        if(IVER('0Did you change the rpm?')) go to 12
        write(6,*)'Total Number of revolution for sampling?'
        read(*,*)nrev
        write(6,*)'Total Number of rods?'
  _     read(*,*)nrod
        n=isize*nrev
        write(6,*)'enter the root file name(without extension)?'
        read(*,500) root
        in=1
        do while(root(in:in).ne.' ')
          filp(in:in)=root(in:in)
          in=in+1
        end do
        filp(in:in+3)='.fil'
  6     ntest=ntest+1
        if(ntest.eq.1) then
          open(unit=9,file='master.fil')
          write(9,*) ntest
          write(9,'(a)')filp
          close(9)
        endif
        call FGEN(root,ntest,fili,fild,filo)
        call CLS
        filnam=fili(ntest)
        write(6,290) ilag
        call LAG(ilag)
        write(6,300) filnam
c       pause 'Please [ENTER] to start

* open data file, write file header
        call ADFILS(filnam,n, nch, itime, delay, ierr)
        write(*,*)'sampling hot-wire data..'

* initialize RC board, and go on keyboard prompt
        do 10 j=1,nrev
          call ADOS(nch, itime, size)
* Waiting for external trigger
          call TRIGO()
```

```
* read from RC ISC-16 -> IDAT -> disk, and inspect IERR flag
        call RD1S(idat, isize, ierr, idisk)
        write(*,*)j, ' ierr = ',ierr
 10     continue

* close the file when done
        call ADFILC(ierrf)

c  Reading temperature and pressure in one shot mode
        call SPVT8(temp,pr1,pr2)
C Input test parameters
        If(ntest.eq.1) then
          write(6,*)' Static pressure in "mm" of water?'
          read(5,*) PSTAT
          write(6,*)' Barometric pressure in "mm" of Hg ?'
          read(5,*)patm
          write(6,*)'Any other parameters to document? (max. one line)'
          read(5,'(a80)')sent
        endif
c get time and date
        call GETTIM(ihr,imin,isec,i100)
        call GETDAT(iyr,imon,iday)
c document this test
        open(unit=8,file=fild(ntest))
        write(8,*)temp,pr1,pr2,pstat,patm,-xo
        write(8,*)rpm,nrod,nrev
        write(8,*)fili(ntest)
        write(8,*)sent
        write(8,450)imon,iday,ihr,imin
        close(8)
c update .fil; later used by data analysis software
        open(unit=8,file=filp)
        write(8,*)ntest
        do 20 j=1,ntest
 20     write(8,400)fili(j)
        close(8)
* repeat?
        if(itrav.eqv..false.) then
          if(IVER('0repeat acquiring new data at this location?')) goto 6
        endif
* Move to new location
 90     if(ith.lt.NP) go to 4
        stop

* formats

100    format(/' nch [1,2,4,8,16]:'\)
110    format(' itime [usec, 1-65384]:'\)
115    format(' delay [usec, 0-65535]:'\)
120    format(' -- select buffer size --'/' SIZE     BUFFER'/
      *' 0          256 '/' 1          512'/' 2          1024'/
      *' 3         2048'/' 4         4096'/' 5         8192'/
      *' 6        16384'/' 7        32768'/' enter SIZE:'\)
130    format(' nblock:'\)
140    format(' block#',i3,'  ierr = ',i1)
280    format(a30)
290    format(' Waiting for the specified delay',I3,' Sec')
300    format(' HOT-WIRE data will be stored in ',a)
350    format(' SAMPLING FOR PRESSURE AND TEMPERATURE..')
400    format(a25)
450    format(' DATE: ',i2,'/',i2,5x,'TIME: ',i2,':',i2)
500    format(a)
```

end

B.3. Data Reduction and Analysis Programs

```
************************************************************************
1. Data reduction program for processing the data obtained by single
   sensor hot-film/wire measurements
************************************************************************
*   This program reduces the data generated by programs like ADRDTR4,
*   AUTO4, etc.  The data file is opened as a random access file and
*   addressed similar to RDDSKB, but all from FORTRAN
*   Routines called: IVER
*   FILES: PROCESS.PAR : data file containing the information on
*               (input)    the number of data points and the names of
*                          document file, data file and output file.
*   .dat -data files       (input)
*   .doc -document files.(input)
*   .out - output files.  (output)
*   CTA.CAL     : The file containing the calibration constant and
*   (input)        the average temperature during the calibration.
*   Signal connection:
*   Ch1 : Hotwire                   Ch3: Thermocouple
*   Ch2 : Reserved for hotwire      Ch4: Differential pressure transducer
************************************************************************
      program BPRO
      parameter (max=33000)
      integer*2 idat(max)
      integer*4 n, nch, itime,isize, delay,inc
      integer*4 ierr,nsapch
      real*4 Sumsq(8),RMS(8),RMST(8),Avg(8),Avgt(8),turb(8)
      real*4 vrms(8),vrmst(8),hwvel(8),hwvelt(8),hwvsq(8)
      real*4 turbt(8)
      real*4 ctc(5),hvoltt(16),hvolttt(16)
      character*25 fili,filo,fild,filp
      character*80 sent
c  tsens = Sensor temperature in "C"
c  yzero = Multiplication factor to change the sign of co-ordinate
c          ( -1.0 or 1.0 )
      open(unit=8,file='bpro.par')
      read(8,*)tsens,yzero,isize
      close(8)
c  open the file containing calibration constants for hot-wire
      open(unit=8,file='cta.cal')
      read(8,*)(ctc(i), i=1,5)
      read(8,5)fili,tcal
      close(8)
c  open the master file
      ntes=0
    3 open(unit=8,file='master.fil')
      ntes=ntes+1
      read(8,*) ntest
      do 7 i=1,ntes
    7 read(8,'(a)') filp
      close(8)
      inc=0
c  open the file containing the filenames and number of files
      write(6,*) filp
   10 open(unit=8,file=filp)
      read (8,*)nf
      inc=inc+1
      do 15 i=1,inc
   15 read(8,175) fili,fild,filo
```

```
      close(8)
      write(6,*) fild
      open(unit=8,file=fild)
      read(8,*)temp,pres,pstat,patm,posit
      posit=posit*yzero
      close(8)

c  open the ADC data file and read the header
      call RDFILS(fili,n, nch, itime, delay, ierr)
      write(*,110)n,nch,itime,delay,ierr
c  select a block size

      nblock=n/isize
      nsapch=isize/nch
c        call CLS
      write(6,*)'Reading the data file: ',fili
      write(*,130)nblock,isize

      do 250 j=1,nch
        Avgt(j) = 0.0
        RMSt(j) = 0.0
        hwvelt(j)=0.0
        vrmst(j)=0.0
        hvoltt(j)=0.
        turbt(j)=0.
  250 continue
      open(unit=9,file=filo)
      do 800  nb = 1,nblock
        call RDBLK(idat, nb, isize, ierr)
c  Inspect IERR flag
        write(*,150)ierr
c  Write array to screen?
        write(6,80) nb,isize
c        if(lscr) then
c        if(IVER(' Show this block?')) write(6,170)(idat(i),i=1,isize)
c        endif
c   Now calculate averages and RMS fluctuation levels
        do 300 j=1,nch
          Sumsq(j) = 0.
          hwvel(j)=0.
          hwvsq(j)=0.0
          vrms(j)=0.
          hvoltt(j)=0.0
  300   Avg(j) = 0.0
        do 450 i=1,nsapch
          do 400 j=1,nch
            index  = (i-1)*nch + j
            Avg(j)=Avg(j)+(idat(index)-2048.)*.004882812
  400     continue
  450     continue
        do 500 j=1,nch
          Avg(j) = Avg(j)/nsapch
          write(6,*)'channel#', j,'          Average value= ',Avg(j)
          Avgt(j) = Avgt(j) + Avg(j)
  500   continue
c  Calculate density and velocity at the pneumatic probe
        rho=(patm*13.6+pstat)*.0348432/(temp+273.15)
        if(pres.lt.0.0) pres=0.
        velpn=sqrt(2.0*pres*9.81/rho)

        do 510 i=1,nsapch
          do 510 j=1,1
```

```
               index=(i-1)*nch +j
               hvolt=(idat(index)-2048.)*.004882812
               hvolt=hvolt*sqrt((tsens-tcal)/(tsens -temp))
               hvoltt(j)=hvoltt(j)+hvolt
               hwvel(j)=hwvel(j) + (ctc(1)+ctc(2)*hvolt+ctc(3)*hvolt**2.
     $         +ctc(4)*hvolt**3.0 +ctc(5)*hvolt**4.)
  510    continue

         do 525 j=1,1
            hwvel(j)=hwvel(j)/nsapch
            hvoltt(j)=hvoltt(j)/nsapch
c           write(6,*)'channel#', j,'          hvoltt= ',hvoltt(j)
c           write(6,*)'channel#', j,'          Average velocity= ',hwvel(j)
            hwvelt(j) = hwvelt(j) + hwvel(j)
            hvoltt(j)=hvolttt(j)+hvoltt(j)
  525    continue

c     RMS calculations
c
         do 600 i=1,nsapch
            do 620 j=1,nch
               index = (i-1)*nch + j
               Del=Avg(j)-(FLOAT(idat(index))-2048.0)*.004882812
               Sumsq(j) = Sumsq(j) + Del*Del
  620       continue
            do 625 j=1,1
               index=(i-1)*nch + j
               hvolt=(idat(index)-2048.)*.004882812
               hvolt=hvolt*sqrt((tsens-tcal)/(tsens -temp))
               hvel=   (ctc(1)+ctc(2)*hvolt+ctc(3)*hvolt**2.
     $         +ctc(4)*hvolt**3.0 +ctc(5)*hvolt**4.)
               del=hwvel(j)-hvel
               hwvsq(j)=hwvsq(j)+del*del
  625       continue
  600    continue
         do 700 j=1,nch
            RMS(j)  = SQRT(Sumsq(j)/nsapch)
            write(6,*)'channel#', j,'              RMS value= ',RMS(j)
            RMSt(j) = RMSt(j) + RMS(j)
  700    continue
         do 725 j=1,1
            vrms(j)=SQRT(hwvsq(j)/nsapch)
            turb(j)= (vrms(j)/hwvel(j))*100.0
c           write(6,*)'channel#', j,'              RMS velocity= ',VRMS(1)
            VRMSt(j) = VRMSt(j) + VRMS(j)
            turbt(j)=turbt(j)+turb(j)
  725    continue

         write(6,*)'POSITION  VOLTAGE  VOLT.C   PRESS     TEMP      VEL.PN
     $   VEL.ANE  VEL.RMS  TURB.'
         if(nb.eq.1) then
            write(9,*)'POSITION  VOLTAGE  VOLT.C   PRESS     TEMP      VEL.PN
     $   VEL.ANE  VEL.RMS  TURB.'
         endif

         write(6,70)posit,avg(1),hvoltt(1),pres,temp,velpn
     $   ,hwvel(1),vrms(1),turb(1)
         write(9,70) posit,avg(1),hvoltt(1),pres,temp,velpn
     $   ,hwvel(1),vrms(1),turb(1)
  800 continue
c  close the file
         call RDFILC(ierr)
```

```
      do  850 j=1,nch
        Avg(j) = Avgt(j)/nblock
        RMS(j) = RMSt(j)/nblock
  850 continue
      do 875 j=1,2
        hwvel(j)= hwvelt(j)/nblock
        VRMS(j) = VRMSt(j)/nblock
        turb(j)= turbt(j)/nblock
        hvoltt(j)=hvolttt(j)/nblock
  875 continue
c Now write the averaged results to screen and to disk.
      write(*,85)
c Write to the output file

      Write(9,*)'Averaged Results'
      write(6,70) posit,avg(1),hvoltt(1),pres,temp,velpn
     $,hwvel(1),vrms(1),turb(1)
        write(9,70) posit,avg(1),hvoltt(1),pres,temp,velpn
     $,hwvel(1),vrms(1),turb(1)
      close(9)
      if (inc.eq.1) then
c Create the output filename for velocity,turb. etc.
        in=1
        do while(filp(in:in).ne.'.')
          filo(in:in)=filp(in:in)
          in=in+1
        end do
        filo(in:in+3)='.out'
c Write the results of velocity and turbulence
        open(unit=7,file=filo)
        write(7,*)'POSITION  VOLTAGE  VOLT.C   PRESS     TEMP      VEL.PN
     $ VEL.ANE  VEL.RMS  TURB.'
       endif
      write(7,70)posit,avg(1),hvoltt(1),pres,temp,velpn
     $,hwvel(1),vrms(1),turb(1)

c Repeat processing the next file ?
        if (inc.lt.nf) go to 10
      rewind (7)
      read(7,'(a)')sent
      write(6,*)sent
      do  j=1,nf
        read(7,70) posit,avg(1),hvoltt(1),pres,temp,velpn
     $   ,hwvel(1),vrms(1),turb(1)
        write(6,70) posit,avg(1),hvoltt(1),pres,temp,velpn
     $   ,hwvel(1),vrms(1),turb(1)
       enddo
       if(ntes.lt.ntest) go to 3
c Formats
   5 format(a26,f9.6)
  70 format(f9.4,2(2x,f7.3),4(2x,f7.2),2x,f5.3,2x,f5.2)
  80 format(' Calculated block number',i3,2x,i5,' size')
  85 format(//,' Averaged results of A/D conversions :',/,
     $          5x,' Channel',6x,'X (DC)',
     $          8x,'X (RMS)')
  90 format(' ',7x,i3,2F14.5)
  95 format(' hotwire voltage ',10x, 'velocity ',10x, 'temperature'
     $,/,f10.4,15x,f10.4,12x,f8.3)
 100  format(/' ADC filename:'\)
 101  format(a)
 110  format(' n:',i6,' nch:',i2,' itime:',i5,' delay:',i5,'ierr:',i2)
 120  format(' -- select block size --'/' SIZE    BUFFER'/
```

```
            *' 0          256'/' 1        512'/' 2        1024'/
            *' 3         2048'/' 4       4096'/' 5        8192'/
            *' 6        16384'/' 7      32768'/' enter SIZE:'\)
     130   format(' There are ',i3,' blocks of ',i5,' words..')
     140   format(/' read block#:'\)
     150   format(' ierr:',i2)
     170   format(16i5)
     175   format(a25,2x,a25,2x,a25)
           end


*****************************************************************
2. Data reduction program for processing the data obtained X-hot-
   film/wire measurements
*****************************************************************
*   This program reduces the data generated by programs like XACQUIR,
*   XAUTO, etc.  The data file is opened as a random access file and
*   addressed similar to RDDSKB, but all from FORTRAN
*   The program calculates the velocity components, turbulence
*   intensities and Reynolds stresses for the data sets.
*   Similar to XPROCESS but used for processing for a number of different
*   test sets using batch file mode and using entirely fortran routines
*   Yaw calibration function
*   H=H4=Cos(alpha)*sqrt(V**2./(Ve1**2.+Ve2**2.))
*   FILES: filp (input) - data file containing the information on
*           the number of data points and the names of document file, data
*           file and output file.
*            .dat -data files       (input)
*            .doc -document files.(input)
*            .out - output files.  (output)
*   X1.CAL, X2.CAL (input)        : velocity calibration file
*   AL.CAL, H.CAL  (input)        : yaw angle calibration file
*   Signal connection:
*   Ch1 : Hotwire   X1      Ch3: Thermocouple
*   Ch2 : Hotwire   X2      Ch4: Differential pressure
*                               transducer(0-10mm),PR1
*   Ch5 : Differential pressure transducer(0-100mm),PR2
*****************************************************************
       program BXPRO
       parameter (max=33000)
       integer*2 idat(max)
       integer*4 n, nch, itime,  isize, delay,inc
       integer*4 ierr,nsapch,irecl,ir0
       real*4 Avg(4),Avgt(4)
       real*4 rmst(4),sumsq(4),rms(4)
       real*4 vrms(4),vrmst(4),turbt(4),hwvel(4),vet(4)
       real*4 u(4),ve(4),ut(4),hwvsq(4),turb(4)
       real*4 x1c(5),x2c(5)
       real*4 ac(6),hc(6)
       real*4 hvoltt(4),hvolttt(4)
       character*25 fili(300)
       character*25 filp,fo1,fo2,fild,filo
       character*80 sent
c      data bitf/.004882812/
       data irecl/1/
       bitf=.004882812
c  bitf= bit factor of A/D board  1bit = bitf volts
       open(unit=8,file='BXPRO.PAR')
       read(8,*) tsens,isize
       close(8)
c  open the file containing velocity calibration constants for hot-wire
       open(unit=8,file='X1.cal')
```

```fortran
      read(8,*)(x1c(i), i=1,5)
      write(6,*)(x1c(i), i=1,5)
      read(8,5)filp,tcal
      write(6,*)'tcal=',tcal
      close(8)
      open(unit=8,file='X2.cal')
      read(8,*)(x2c(i), i=1,5)
      write(6,*)(x2c(i), i=1,5)
      read(8,5)filp,tcal
      write(6,*)'tcal=',tcal
      close(8)
c  Open the angle calibration coefficients of X-wire
      open(unit=8,file='H.cal')
      read(8,*)(hc(i), i=1,6)
      write(6,*)'H.CAL coefficients',(hc(i), i=1,6)
      close(8)
      open(unit=8,file='AL.cal')
      read(8,*)(ac(i), i=1,6)

      write(6,*)'AL.cal coefficients',(ac(i),i=1,6)
      close(8)
c  open the master file
      open(unit=8,file='master.fil')
      read(8,*) ntest
      read(8,'(a)') filp
      close(8)
      inc=0
c  open the file containing the filenames and number of files
      write(6,*) filp
      open(unit=8,file=filp)
      read (8,*)nf
      do 15 i=1,nf
   15 read(8,175) fili(i)
      close(8)
   10 inc=inc+1
      call FILDO(fili(inc),fild,filo)
      write(6,*)'reading doc. file', fild
      open(unit=8,file=fild)
      read(8,*)temp,pr1,pr2,pstat,patm,xo
      close(8)
      do 250 j=1,nch
        Avgt(j) = 0.0
        RMSt(j) = 0.0
        vrmst(j)=0.0
        hvolttt(j)=0.
        turbt(j)=0.
        ut(j)=0.
        vet(j)=0.
  250 continue
   20 rst1=0.
      rst2=0.
      rst3=0.
      open(unit=9,file=filo)
*  select a block size
      if(inc.eq.1) then
        open(unit=2,file=fili(inc),form='binary',access='direct',
     $  recl=irecl,status='old',err=20)
        read(2,rec=1)n,nch,itime,delay
        write(*,110)n,nch,itime,delay
        nblock=n/isize
        nsapch=isize/nch
        write(6,*)'Reading the data file: ',fili(inc)
```

```
              write(*,130)nblock,isize
              close(unit=2)
           endif

           do 800  nb = 1,nblock
c   open the ADC data file and read the header
C   Read the  data
           open(unit=2,file=fili(inc),form='binary',access='direct',
     $     recl=irecl,status='old',err=20)
           read(2,rec=1)n,nch,itime,delay
           ir0=((nb-1)*isize*2)+16-isize
           read(2,rec=ir0+i,iostat=ierr)(idat(i),i=1,isize)
c   Inspect IERR flag
           write(*,150)ierr
           write(6,80) nb,isize
c   close data file
c         call RDFILC(ierr)
           close(unit=2)
c   Now calculate averages and RMS fluctuation levels
           do 300 j=1,nch
             Sumsq(j) = 0.
             hwvel(j)=0.
             hwvsq(j)=0.0
             vrms(j)=0.
             hvoltt(j)=0.0
             u(j)=0.0
             ve(j)=0.
             Avg(j) = 0.0
 300       continue
           rs3=0.
           do 450 i=1,nsapch
             do 400 j=1,nch
               index  = (i-1)*nch + j
               Avg(j)=Avg(j)+(idat(index)-2048.)*bitf
 400       continue
 450       continue
           do 500 j=1,nch
             Avg(j) = Avg(j)/nsapch
             Avgt(j) = Avgt(j) + Avg(j)
 500       continue
           rho=(patm*13.6+pstat)*.0348432/(temp+273.15)

           do 510 i=1,nsapch
             do  j=1,2
               index=(i-1)*nch +j
               hvolt=(idat(index)-2048.)*bitf
               hvolt=hvolt*sqrt((tsens-tcal)/(tsens -temp))
               hvoltt(j)=hvoltt(j)+hvolt
               if(j.eq.1) then
                 hwvel(j)=hvolt*(hvolt*(hvolt*(hvolt*x1c(5)+x1c(4))+
     $           x1c(3))+x1c(2))+x1c(1)
                 else
                 hwvel(j)=hvolt*(hvolt*(hvolt*(hvolt*x2c(5)+x2c(4))+
     $           x2c(3))+x2c(2))+x2c(1)
                 endif
               ve(j)=ve(j)+hwvel(j)
             enddo
             ali=(atan(hwvel(1)/hwvel(2)))*57.29578-45.0
             al=ali*(ali*(ali*(ali*(ali*ac(6)+ac(5))+ac(4))+ac(3))+ac(2)
     $       )+ac(1)
             h=ali*(ali*(ali*(ali*(ali*hc(6)+hc(5))+hc(4))+hc(3))+hc(2)
     $       )+hc(1)
```

```
                VTP=H*sqrt(hwvel(1)*hwvel(1)+hwvel(2)*hwvel(2))
                U(1)=U(1)+VTP
                u(2)=u(2)+VTP*tan(al/57.29578)
        510     continue

                do 525 j=1,2
                  ve(j)=ve(j)/nsapch
                  hvoltt(j)=hvoltt(j)/nsapch
                  U(j)=U(j)/nsapch
                  vet(j) = vet(j) + ve(j)
                  hvolttt(j)=hvolttt(j)+hvoltt(j)
                  ut(j)=ut(j)+u(j)
        525     continue

      c   RMS and Turbulence of U and V components.

                do 600 i=1,nsapch
                  do  j=1,2
                    index=(i-1)*nch +j
                    Del=Avg(j)-(FLOAT(idat(index))-2048.0)*bitf
                    Sumsq(j) = Sumsq(j) + Del*Del
                    hvolt=(idat(index)-2048.)*bitf
                    hvolt=hvolt*sqrt((tsens-tcal)/(tsens -temp))
                    if(j.eq.1) then
                      hwvel(j)=hvolt*(hvolt*(hvolt*(hvolt*x1c(5)+x1c(4))+
             $        x1c(3))+x1c(2))+x1c(1)
                    else
                      hwvel(j)=hvolt*(hvolt*(hvolt*(hvolt*x2c(5)+x2c(4))+
             $        x2c(3))+x2c(2))+x2c(1)
                    endif
                  enddo
                  ali=(atan(hwvel(1)/hwvel(2)))*57.29578-45.0
                  al=ali*(ali*(ali*(ali*(ali*ac(6)+ac(5))+ac(4))+ac(3))+ac(2)
             $    )+ac(1)
                  h=ali*(ali*(ali*(ali*(ali*hc(6)+hc(5))+hc(4))+hc(3))+hc(2)
             $    )+hc(1)
                  VTP=H*sqrt(hwvel(1)*hwvel(1)+hwvel(2)*hwvel(2))
                  do  j=1,2
                    if(j.eq.1) del=u(j)-VTP
                    if(j.eq.2) del=u(j)-VTP*tan(al/57.29578)
                    hwvsq(j)=hwvsq(j)+del*del
                  enddo
      c   Reynolds Stress uv
                  rs3=rs3+(u(1)-VTP)*(u(2)-VTP*tan(al/57.29578))
        600     continue
                rs1=hwvsq(1)/nsapch
                rs2=hwvsq(2)/nsapch
                rs3=rs3/nsapch
                do 725 j=1,2
                  RMS(j)  = SQRT(Sumsq(j)/nsapch)
                  vrms(j)=SQRT(hwvsq(j)/nsapch)
                  turb(j)= (vrms(j)/U(1))*100.0
                  VRMSt(j) = VRMSt(j) + VRMS(j)
                  RMSt(j) = RMSt(j) + RMS(j)
                  turbt(j)=turbt(j)+turb(j)
        725     continue
                rst1=rst1+rs1
                rst2=rst2+rs2
                rst3=rst3+rs3
                write(6,*)'rho=',rho
                write(9,*)'  POS     X1    X1C    X2    X2C   VE1 VE2  PR1
             $  PR2   TEMP  RMS1  RMS2'
```

```
            write(6,*)' POS      X1     X1C    X2     X2C    VE1  VE2    PR1
     $  PR2  TEMP  RMS1  RMS2'
            write(6,70)xo,avg(1),hvoltt(1),avg(2),hvoltt(2),ve(1),ve(2),pr1,
     $  pr2,temp,rms(1),rms(2)
            write(9,70)xo,avg(1),hvoltt(1),avg(2),hvoltt(2),ve(1),ve(2),pr1,
     $  pr2,temp,rms(1),rms(2)
            write(9,*) ' POS mm  U m/s  V m/s  Urms  Vrms Utur% Vtur%    RS1
     $  RS2       RS3    '
            write(9,75)xo,u(1),u(2),vrms(1),vrms(2),turb(1),turb(2),rs1,rs2,
     $  rs3
            write(6,*) ' POS mm  U m/s  V m/s  Urms  Vrms Utur% Vtur%    RS1
     $  RS2       RS3    '
            write(6,75)xo,u(1),u(2),vrms(1),vrms(2),turb(1),turb(2),rs1,rs2,
     $  rs3
 800  continue
        do  850  j=1,nch
          Avg(j)  = Avgt(j)/nblock
          RMS(j)  = RMSt(j)/nblock
 850  continue
        do 875 j=1,2
          ve(j)= vet(j)/nblock
          VRMS(j)  =   VRMSt(j)/nblock
          turb(j)= turbt(j)/nblock
          hvoltt(j)=hvolttt(j)/nblock
          u(j)=ut(j)/nblock
 875  continue
        rs1=rst1/nblock
        rs2=rst2/nblock
        rs3=rst3/nblock
c  Now write the final results to screen and to disk.
c  Write to the output file
        Write(6,*)'Final Averaged Results'
        Write(9,*)'Final Averaged Results'
        write(6,70)xo,avg(1),hvoltt(1),avg(2),hvoltt(2),ve(1),ve(2),pr1,
     $ pr2,temp,rms(1),rms(2)
        write(9,70)xo,avg(1),hvoltt(1),avg(2),hvoltt(2),ve(1),ve(2),pr1,
     $ pr2,temp,rms(1),rms(2)
         write(6,75)xo,u(1),u(2),vrms(1),vrms(2),turb(1),turb(2),rs1,rs2,
     $ rs3
         write(9,75)xo,u(1),u(2),vrms(1),vrms(2),turb(1),turb(2),rs1,rs2,
     $ rs3
         close(9)
         if(inc.eq.1) then
c  Create the output filenames
          in=1
          do while(filp(in:in).ne.'.')
            fo1(in:in)=filp(in:in)
            fo2(in:in)=filp(in:in)
            in=in+1
          end do
          fo1(in:in+4)='a.out'
          fo2(in:in+4)='b.out'
          open(unit=7,file=fo1)
          open(unit=11,file=fo2)
          write(7,*)' POS      X1     X1C    X2     X2C    VE1  VE2    PR1
     $   PR2  TEMP  RMS1  RMS2'
          write(11,*)' POS mm  U m/s  V m/s  Urms  Vrms Utur% Vtur%    RS1
     $      RS2       RS3    '
         endif
         write(7,70)xo,avg(1),hvoltt(1),avg(2),hvoltt(2),ve(1),ve(2),pr1,
     $ pr2,temp,rms(1),rms(2)
         write(11,75)xo,u(1),u(2),vrms(1),vrms(2),turb(1),turb(2),rs1,rs2,
```

```
      $  rs3
c   Repeat processing the next file ?
         if (inc.lt.nf) go to 10
         rewind (11)
         read(11,'(a)')sent
         write(6,*)sent
         do   j=1,nf
           read (11,75)xo,u(1),u(2),vrms(1),vrms(2),turb(1),turb(2),rs1,rs2,
      $   rs3
           write(6,75)xo,u(1),u(2),vrms(1),vrms(2),turb(1),turb(2),rs1,rs2,
      $   rs3
         enddo
         close(11)
c   Formats
    5    format(a26,f9.6)
    70   format(f7.2,4(1x,f6.3),2(1x,f5.2),2(1x,f6.3),1x,f5.2,2(1x,f5.3))
    75   format(1x,f7.2,2(1x,f6.2),2(1x,f5.3),2(1x,f5.2),3(2x,f8.3))
    80   format(' Calculated block number',i3,2x,i5,' size')
    90   format(' ',7x,i3,2F14.5)
    95   format(' hotwire voltage ',10x, 'velocity ',10x, 'temperature'
      $,/,f10.4,15x,f10.4,12x,f8.3)
   100   format(/' ADC filename:'\)
   101   format(a)
   110   format(' n:',i6,' nch:',i2,' itime:',i5,' delay:',i5)
   130   format(' There are ',i3,' blocks of ',i5,' words..')
   140   format(/' read block#:'\)
   150   format(' ierr:',i2)
   170   format(16i5)
   175   format(a25,2x,a25,2x,a25)
         stop
         end
****************************************************************************
         Subroutine FILDO(fi,fild,filo)
         character*25 fi,fild,filo
         in=1
         do while(fi(in:in).ne.'.')
           fild(in:in)=fi(in:in)
           filo(in:in)=fi(in:in)
           in=in+1
         end do
         fild(in:in+3)='.doc'
         filo(in:in+3)='.out'
         return
         end
```

****
3. Data reduction program employing ensemble averaging or phase-averaging for processing the data obtained X-hot-film/wire measurements
****
```
*   This program reduces the data generated by programs like UXACQUIR,
*   UXAUTO, etc.  The data file is opened as a random access file and
*   addressed similar to RDDSKB, but all from FORTRAN
*   The program calculates the ensemble averaged velocity components,
*   turbulence intensity, Reynolds stresses and triple correlations for
*   the data sets.
*   Similar to BXPRO but used for  ensemble averaging .
*   The program uses   entirely fortran routines
*   Yaw calibration function H=H4=Cos(alpha)*sqrt(V**2/(Vel**2+Ve2**2))
*   FILES: filp (input) - data file containing the information on
*          the number of data points and the names of document file, data
```

```
*          file and output file.
*             .dat -data files      (input)
*             .doc -document files.(input)
*             .out - output files.  (output)
*   X1.CAL, X2.CAL (input)        : velocity.calibration file
*   AL.CAL, H.CAL   (input)       : yaw angle calibration file
*   Signal connection:
*   Ch1 : Hotwire    X1      Ch3: Thermocouple
*   Ch2 : Hotwire    X2      Ch4: Differential pressure
*                                 transducer(0-10mm),PR1
*   Ch5 : Differential pressure transducer(0-100mm),PR2
*************************************************************************
       program BUXPRO
       parameter (max=4096)
       integer*2 idat(max)
       integer*4 n, nch, itime,  isize, delay,inc
       integer*4 ierr,nsapch,irecl,ir0
       real*4 hwvel(4)
       real*4 x1c(5),x2c(5)
       real*4 ac(6),hc(6)
       real*4 u(2048),v(2048),dt(2048),dx(2048),du(2048),dv(2048)
       real*4 rs1(2048),rs2(2048),rs3(2048),tur1(2048)
       real*4 uuu(2048),vvv(2048),uuv(2048),vvu(2048)
       character*25 fili(300)
       character*25 filp,fild,filo,fo1
c  bitf= bit factor of A/D board  1bit = bitf volts
       data bitf/.004882812/
       data irecl/1/
c  rad= radius of the wake generator
       data rad/0.151/
       open(unit=8,file='BUXPRO.PAR')
c  tsens=sensor operating temperature
       read(8,*) tsens
       close(8)
c  open the file containing velocity calibration constants for hot-wire
       open(unit=8,file='X1.cal')
       read(8,*)(x1c(i), i=1,5)
       write(6,*)(x1c(i), i=1,5)
       read(8,5)filp,tcal
       write(6,*)'tcal=',tcal
       close(8)
       open(unit=8,file='X2.cal')
       read(8,*)(x2c(i), i=1,5)
       write(6,*)(x2c(i), i=1,5)
       read(8,5)filp,tcal
       write(6,*)'tcal=',tcal
       close(8)
c  Open the angle calibration coefficients of X-wire
       open(unit=8,file='H.cal')
       read(8,*)(hc(i), i=1,6)

       write(6,*)'H.CAL coefficients',(hc(i), i=1,6)
       close(8)
       open(unit=8,file='AL.cal')
       read(8,*)(ac(i), i=1,6)

       write(6,*)'AL.cal coefficients',(ac(i),i=1,6)
       close(8)
c  open the master file
       open(unit=8,file='master.fil')
       read(8,*) ntest
       read(8,'(a)') filp
```

```
      close(8)
      inc=0
c  open the file containing the filenames and number of files
      write(6,*) filp
      open(unit=8,file=filp)
      read (8,*)nf
      do 15 i=1,nf
 15   read(8,175) fili(i)
      close(8)
 10   inc=inc+1
      call FILDO(fili(inc),fild,filo)
c Create the output filenames
      in=1
      do while(filo(in:in).ne.'.')
        fol(in:in)=filo(in:in)
        in=in+1
      end do
      fol(in:in+4)='a.out'
      write(6,*)'reading doc. file', fild
      open(unit=8,file=fild)
      read(8,*)temp,pr1,pr2,pstat,patm,xo
      read(8,*)rpm,nrod,nrev
c nrod=number of rods, nrev=number of revolution
      close(8)
c  select a block size
 20   if(inc.eq.1) then
        open(unit=2,file=fili(inc),form='binary',access='direct',
     $  recl=irecl,status='old',err=20)
        read(2,rec=1)n,nch,itime,delay
        write(*,110)n,nch,itime,delay
        isize=n/nrev
        nsapch=isize/nch
        write(6,*)'Reading the data file: ',fili(inc)
        write(*,130)nrev,isize
        close(unit=2)
      endif
 30      do i=1,nsapch
        u(i)=0.
        v(i)=0.
        rs1(i)=0.
        rs2(i)=0.
        rs3(i)=0.
        uuu(i)=0.
        vvv(i)=0.
        uuv(i)=0.
        vvu(i)=0.
      enddo
      do 800  nb = 1,nrev
        open(unit=2,file=fili(inc),form='binary',access='direct',
     $  recl=irecl,status='old',err=30)
        read(2,rec=1)n,nch,itime,delay
        ir0=((nb-1)*isize*2)+16-isize
        read(2,rec=ir0+i,iostat=ierr)(idat(i),i=1,isize)
c  Inspect IERR flag
        write(*,150)ierr
        write(6,80) nb,isize
c  close data file
        close(unit=2)
        open (unit=15,file='d:\u00\uu.dat')
        do 510 i=1,nsapch
          do  j=1,2
            index=(i-1)*nch +j
```

```fortran
            hvolt=(idat(index)-2048.)*bitf
            hvolt=hvolt*sqrt((tsens-tcal)/(tsens -temp))
            if(j.eq.1) then
               hwvel(j)=hvolt*(hvolt*(hvolt*(hvolt*x1c(5)+x1c(4))+
     $         x1c(3))+x1c(2))+x1c(1)
            else
               hwvel(j)=hvolt*(hvolt*(hvolt*(hvolt*x2c(5)+x2c(4))+
     $         x2c(3))+x2c(2))+x2c(1)
            endif
c           ve(j)=ve(j)+hwvel(j)
         enddo
         ali=(atan(hwvel(1)/hwvel(2)))*57.29578-45.0
         al=ali*(ali*(ali*(ali*(ali*ac(6)+ac(5))+ac(4))+ac(3))+ac(2)
     $   )+ac(1)
         h=ali*(ali*(ali*(ali*(ali*hc(6)+hc(5))+hc(4))+hc(3))+hc(2)
     $   )+hc(1)
         VTP=H*sqrt(hwvel(1)*hwvel(1)+hwvel(2)*hwvel(2))
*  Calculate the sum for the ensemble average of U and V velocities
         U(i)=U(i)+VTP
         V(i)=V(i)+VTP*tan(al/57.29578)
         write(15,'(3(1x,f5.2))')VTP,VTP*tan(al/57.29578),
     $   VTP*VTP*tan(al/57.29578)
 510     continue
         close(15)
         pause
 800  continue
      do i=1,nsapch
        u(i)=u(i)/nrev
        v(i)=v(i)/nrev
      enddo
c
c  Calculate the ensemble RMS AND SHEAR STRESS and Triple correlation
 60   write(6,*)'Opening the data file'
      do 900 nb=1,nrev
         open(unit=2,file=fili(inc),form='binary',access='direct',
     $   recl=irecl,status='old',err=60)
         read(2,rec=1)n,nch,itime,delay
         ir0=((nb-1)*isize*2)+16-isize
         read(2,rec=ir0+i,iostat=ierr)(idat(i),i=1,isize)
c  Inspect IERR flag
         write(*,150)ierr
         write(6,80) nb,isize
c  close data file
         close(unit=2)

         do 600 i=1,nsapch
           do j=1,2
             index=(i-1)*nch +j
             hvolt=(idat(index)-2048.)*bitf
             hvolt=hvolt*sqrt((tsens-tcal)/(tsens -temp))
             if(j.eq.1) then
                hwvel(j)=hvolt*(hvolt*(hvolt*(hvolt*x1c(5)+x1c(4))+
     $          x1c(3))+x1c(2))+x1c(1)
             else
                hwvel(j)=hvolt*(hvolt*(hvolt*(hvolt*x2c(5)+x2c(4))+
     $          x2c(3))+x2c(2))+x2c(1)
             endif
           enddo
           ali=(atan(hwvel(1)/hwvel(2)))*57.29578-45.0
           al=ali*(ali*(ali*(ali*(ali*ac(6)+ac(5))+ac(4))+ac(3))+ac(2)
     $     )+ac(1)
           h=ali*(ali*(ali*(ali*(ali*hc(6)+hc(5))+hc(4))+hc(3))+hc(2)
```

```fortran
      $     )+hc(1)
            VTP=H*sqrt(hwvel(1)*hwvel(1)+hwvel(2)*hwvel(2))
            du(i)=VTP-u(i)
            dv(i)=VTP*tan(al/57.29578)-v(i)
c  Reynolds Normal stress
            rs1(i)=rs1(i)+du(i)*du(i)
            rs2(i)=rs2(i)+dv(i)*dv(i)
c  Reynolds Shear Stress uv
            rs3(i)=rs3(i)+du(i)*dv(i)
c  Triple correlations
            uuu(i)=uuu(i)+du(i)*du(i)*du(i)
            vvv(i)=vvv(i)+dv(i)*dv(i)*dv(i)
            uuv(i)=uuv(i)+du(i)*du(i)*dv(i)
            vvu(i)=vvu(i)+dv(i)*dv(i)*du(i)
  600     continue
  900 continue
          delt=itime/1000.
c  dx=v.dt=r*omega.dt=r*2*pi*rpm/60 .dt; 2*pi/60=0.104719755
          delx=rad*0.104719755*rpm*delt
          do i=1,nsapch
            rs1(i)=rs1(i)/nrev
            rs2(i)=rs2(i)/nrev
            rs3(i)=rs3(i)/nrev
            tur1(i)=sqrt(rs1(i))*100./u(i)
            dt(i)=(i-1)*delt
            dx(i)=(i-1)*delx
            uuu(i)=uuu(i)/nrev
            vvv(i)=vvv(i)/nrev
            uuv(i)=uuv(i)/nrev
            vvu(i)=vvu(i)/nrev
          enddo
c  Write to the output file
          open(unit=9,file=fo1)
          write(9,*)' DT ms  DY mm U m/s V m/s  Utur%  RS1    RS2    RS3
      $uuu   vvv     uuv    vvu '
          write(6,*)' DT ms  DY mm U m/s V m/s  Utur%  RS1    RS2    RS3
      $uuu   vvv     uuv    vvu '
          do i=1,nsapch
            write(6,75)dt(i),dx(i),u(i),v(i),tur1(i),rs1(i),rs2(i)
      $    ,rs3(i),uuu(i),vvv(i),uuv(i),vvu(i)
            write(9,75)dt(i),dx(i),u(i),v(i),tur1(i),rs1(i),rs2(i)
      $    ,rs3(i),uuu(i),vvv(i),uuv(i),vvu(i)
          enddo
          close(9)
c  Repeat processing the next file ?
          if (inc.lt.nf) go to 10
c  Formats
    5 format(a26,f9.6)
   75 format(f7.3,1x,f5.1,1x,f5.2,1x,f6.3,1x,f5.2,2(1x,f5.3),1x,f6.3
      $,1x,f7.4,3(1x,f6.3))
   80 format('+Revolution no: ',i3,2x,i5,' size')
   90 format(' ',7x,i3,2F14.5)
   95 format(' hotwire voltage ',10x, 'velocity ',10x, 'temperature'
      $,/,f10.4,15x,f10.4,12x,f8.3)
  100 format(/' ADC filename:'\)
  101 format(a)
  110 format(' n:',i7,' nch:',i2,' itime:',i5,' delay:',i5)
  130 format(' There are ',i3,' blocks of ',i5,' words..')
  140 format(/' read block#:'\)
  150 format('+ierr:',i2)
  170 format(16i5)
  175 format(a25,2x,a25,2x,a25)
```

```
          stop
          end


***************************************************************
4. Data analysis program for steady wake
***************************************************************
* This program calculates the following quantities from the output files
* generated by program  XPROCESS.FOR, BXPRO.FOR, etc.
*   u1m    = maximum of wake defect velocity
*   u1/u1m = wake defect velocity/maximum wake defect velocity
*   yc     = location of wake centerline
*   b      = inegral(u1/u1m) / u1m
*   theta  = momentum thickness
*   pr1    = static pressure
*   uv     = average of instantaneous velocity correlation
*   External Subroutines.
*   csakm - Gives the spline coefficients of the data points.
*   CSSCV - Gives the spline coefficients of the data points by smoothing
*   CSITG - Uses the spline coeffs. to calculate the integral.
*   IWKIN - Assigns larger workspace for the program.
*   CSVAL - Gives interpolated values using the spline coeffs.
*   LSFIT - Fits the potential flow with a first order polynomial.
***************************************************************
          program SN100
          real*8 acoeff(100),var(20),coeff(20)
          real*4 x(140),y(140),pr(140)
          common /worksp/ rwksp
          real rwksp(70000)
          dimension break0(140)
          dimension ccoef0(4,140)
          dimension yo(150),u(150),v(150),urms(150),vrms(150),utur(150)
          dimension vtur(150),rs1(150),rs2(150),rs3(150),pr1(150),pr2(150)
          dimension temp(150),f2(150),uv(150),u1(150),cuv(150),uo(150)
          character*30 fi1,fi2,fi3,fo1,fo2,fd1
          external csakm,IWKIN,CSITG,CSVAL,LSFIT
          call IWKIN(90000)
*
*         Read the angle of the traversing axis from inlet.
          write(*,*) 'Enter the angle of traversing axis (Inlet is 0deg) ?'
          read(5,*) ag
*   Read the input file name fi1
          write(*,*) 'Input the name of the file to analyze ....A.DAT'
          read(5,'(a)') fi1
*   Generate the second input file name fi2, related document file fd1 and
*   output files fo1 and fo2
          in=1
          do while(fi1(in:in).ne.'.')
             fi2(in:in)=fi1(in:in)
             fi3(in:in)=fi1(in:in)
             fd1(in:in)=fi1(in:in)
             fo1(in:in)=fi1(in:in)
             fo2(in:in)=fi1(in:in)
             in=in+1
          end do
          fi2(in-1:in+5)='b.dat'
          fi3(in-1:in+6)='b1.dat'
          fd1(in-1:in+7)='001.doc'
          fo1(in-1:in+5)='c.out'
          fo2(in-1:in+5)='d.out'
          write(6,100)fi1,fi2,fd1,fo1,fo2
          pause 'Press return to continue'
```

```
*   Open and read the data in the document file "fd1"
        open(unit=8,file=fd1)
        read(8,*)te,p1,p2,pstat,patm
        write(6,*)te,p1,p2,pstat,patm
        close(8)

*   Open and read the data inthe first input file "fi1"(...a.dat)
        open(unit=8,file=fi1)
        i=1
        do while(.not.eof(8))
          read(8,70)yo(i),avg,hvoltt,avg,hvoltt,ve,ve,pr1(i),
     $    pr2(i),temp(i),rms,rms
c         write(6,70)yo(i),avg,hvoltt,avg,hvoltt,ve,ve,pr1(i),
c    $    pr2(i),temp(i),rms,rms
          i=i+1
        end do
        close(8)
*   Read the direction of resultant velocity vector from "fi3"(...b.dat)
        open(unit=8,file=fi3)
        read(8,*)alpha
        write(6,*)'alpha= ',alpha
        eta=alpha/57.2957
        close(8)
*   Open and read the data in the second input file "fi2"(...b.dat)
        open(unit=8,file=fi2)
        i=1
        do while(.not.eof(8))
          read(8,*)yo(i),uo(i),v(i),urms(i),vrms(i),utur(i),vtur(i),
     $    rs1(i),rs2(i),rs3(i)
*   Convert the u velocity in s-direction
          u(i)=uo(i)*cos(eta)+v(i)*sin(eta)
*         write(6,75)yo(i),uo(i),v(i),urms(i),vrms(i),utur(i),vtur(i),
*    $    rs1(i),rs2(i),rs3(i)
          i=i+1
        end do
        n=i-1
        close(8)
*
*   Input the boundary coordinates for fitting the potential flow and
*   arrange them in ascending order, y4>y3>y2>y1
        write(6,*)'Input Y-coord boundaries for fitting potential flow (mm
     *.): '
        write(6,*)'First Y-coord for convex side?'
        read(5,*)y1
        yt=y1
        write(6,*)'Second Y-coord for convex side?'
        read(5,*)y2
        if(y2.lt.y1) then
          y1=y2
          y2=yt
        endif
        write(6,*)'First Y-coord for concave side?'
        read(5,*)y3
        yt=y3
        write(6,*)'Second Y-coord for concave side?'
        read(5,*)y4
        if(y4.lt.y3)then
          y3=y4
          y4=yt
        endif
        Write(6,*) 'y1=',y1,'mm y2=',y2,'mm y3=',y3,'mm y4=',y4,'mm'
*   Calculation of the potential flow fit. The data points for the
```

```
potential
* flow will be stored in x(j),y(j)
      j=0
      do i=1,n
         if((yo(i).ge.y1).and.(yo(i).le.y2)) then
           j=j+1
           x(j)= yo(i)
           y(j)= u(i)
           pr(j)=pr2(i)
         endif
         if((yo(i).ge.y3).and.(yo(i).le.y4)) then
           j=j+1
           x(j)= yo(i)
           y(j)= u(i)
           pr(j)=pr2(i)
         endif
      enddo
      np=j

* Fitting the potential flow, npol=degree of polynomial
* np=number of data points for potential flow fit
      Write(6,*)'Degree of polynomial for potential flow? 1, .....,5'
      read(5,*) npol
      call LSFIT(np,x,y,npol,acoeff,var,coeff,ks)
      do i=npol+2,11
         coeff(i)=0.0
      enddo
      Write(6,*)'Polynomial coefficients for potential flow:',(coeff(i),
     $ i=1,npol+1)
* Fit the u velocity data with cubic spline
      Write(6,*)'Enter your choice of interpolation: (1)Cubic spline
     $(2)Cubic spline with smoothing'
      read(5,*)ii
      if(ii.eq.1) then
        call CSAKM(n,yo,u,break0,ccoef0)
      else
         iequal=0
         if(n.lt.20) iequal=2
         call CSSCV(n,yo,u,iequal,break0,ccoef0)
      endif
* Locate the wake centerline at the maximum of u1 (u1=Up-u). Also u1m.
      Write(6,*)'Enter your choice of locating u1m: (1) through program
     $(2)manual input from u1m curve'
      read(5,*)ii
      if(ii.eq.1) then
         call WCENT(n,coeff,break0,ccoef0,y2,y3,yc,u1m)
      else
        Write(6,*)'u1m from the curve?'
        read(5,*)u1m
        write(6,*)'u1m location radially from convex wall?'
        read(5,*)yc
      endif
* Locate the wake center as the point where uv=0.
      Write(6,*)'Want to locate wake center from total pressure? (1) Yes
     $  (2) No'
      read(5,*)ip
      if(ip.eq.1) then
         call PTCENT(yc,x,pr,yo,pr2,n,np,ryc)
      endif
c     write(6,*) yc,ryc,u1m
* Calculate u1 and f2(function for momentum thickness)
* at measuring locations.
```

```
      do i=1,n
        up=yo(i)*(yo(i)*(yo(i)*(yo(i)*(yo(i)*coeff(6)+coeff(5))+coeff(4)
     $   )+coeff(3))+coeff(2))+coeff(1)
        xt=yo(i)
c         u1(i)=up-CSVAL(xt,n-1,break0,ccoef0)
        u1(i)=up-u(i)
        f2(i)=u(i)*u1(i)
      enddo
      upc=yc*(yc*(yc*(yc*(yc*coeff(6)+coeff(5))+coeff(4)
     $   )+coeff(3))+coeff(2))+coeff(1)
*
*   Locating the wake width from Total pressure  profile
      derr1=.01
      derr2=.01
      npol1=1
 50   call WLOC(y1,y2,y3,y4,yc,x,pr,yo,pr2,n,np,ylr,yur,derr1,derr2,
     $npol1)
*      calculate momentum thickness and b

      call BTHETA(ylr,yc,yur,f2,coeff,break0,ccoef0,bl,bu,br,thel,theu,
     $ther,ulm,n,yo,npol)
      write(6,*)'yl        yu        w         b         theta'
      write(6,'(5(1x,f7.3))')ylr,yur,yur-ylr,br,ther
      write(6,*)'The present convergence factors for locating the edge
o
     $f wake from Ptot were: convex side-',derr1,', concave side-',derr2
      Write(6,350)
      read(5,*)ii
      if(ii.eq.1) then
        write(6,*)'Enter the new convergence factors'
        read(5, *) derr1,derr2
        go to 50
      endif

*   calculate the wake width from u-profile
      derr1=.01
      derr2=.01
 60   call WLOC(y1,y2,y3,y4,yc,x,y,yo,u,n,np,yl,yu,derr1,derr2,npol)
*   calculate momentum thickness and b
      call BTHETA(yl,yc,yu,f2,coeff,break0,ccoef0,bl,bu,b,thel,theu,
     $theta,ulm,n,yo,npol)
      write(6,*)' ylr       yur       wr        br        thetar'
      write(6,'(5(1x,f7.3))')ylr,yur,yur-ylr,br,ther
      write(6,*)' yl        yu        w         b         theta'
      write(6,'(5(1x,f7.3))')yl,yu,yu-yl,b,theta
      write(6,*)'The present convergence factors for locating the edge
     $of wake from u were: convex side- ',derr1,', concave side- ',derr2
      Write(6,350)
      read(5,*)ii
      if(ii.eq.1) then
        write(6,*)'Enter the new convergence factors'
        read(5, *) derr1,derr2
        go to 60
      endif
      w=yu-yl
      wl=yc-yl
      wu=yu-yc

*   Calculate static pressure distribution at measuring location
      rho=(patm*13.55+pstat)*.0348432/(te+273.15)
      write(6,*)'rho=',rho
      do i=1,n
```

```
          pr2(i)=pr2(i)-(0.5*rho*(uo(i)*uo(i)+v(i)*v(i)))/(9.81*13.55)
       enddo
*
*  Calculate total impulse =Uaverage.Vaverage+(u'v')bar
       do i=1,n
         uv(i) = uo(i)*v(i)+rs3(i)
       enddo
*
*  Calculate correlation coefficient (u'v')bar/(urms.vrms)
       do i=1,n
         cuv(i) = -rs3(i)/(urms(i)*vrms(i))
       enddo
*
* Open the output files
       open(unit=9,file=fo1,status='unknown')
       Write(6,*)'ANG    yc       ulm    upc   ulm.b  ulm.b/upc  bl     bu
     $ b      thel  theu  the'
       Write(9,*)'ANG    yc       ulm    upc   ulm.b  ulm.b/upc  bl     bu
     $ b      thel  theu  the'
       write(6,150)ag,yc,ulm,upc,ulm*b,ulm*b/upc,bl,bu,b,thel,theu,theta
       write(9,150)ag,yc,ulm,upc,ulm*b,ulm*b/upc,bl,bu,b,thel,theu,theta
       Write(6,*)'ANG    ryc       wl      wu     w'
       Write(9,*)'ANG    ryc       wl      wu     w'
       write(6,250)ag,ryc,wl,wu,w
       if(ip.eq.1) write(9,250)ag,ryc,wl,wu,w
       close(9)
       pause'Press Enter to continue'
       open(unit=10,file=fo2,status='unknown')
       write(6,*)'POS.mm   (Yc-Y)/b  ul  ul/ulm pstat    UV      Corr.'
       write(10,*)'POS.mm   (Yc-Y)/b  ul  ul/ulm pstat    UV      Corr.'
       do i=1,n
         write(6,300)yo(i),(yc-yo(i))/b,ul(i),ul(i)/ulm,pr2(i),uv(i),
     $ cuv(i)
         write(10,300)yo(i),(yc-yo(i))/b,ul(i),ul(i)/ulm,pr2(i),uv(i),
     $ cuv(i)
       enddo
       close(10)

* Formats
  70   format(f7.2,4(1x,f6.3),2(1x,f5.2),2(1x,f6.3),1x,f5.2,2(1x,f5.3))
  75   format(1x,f7.2,2(1x,f6.2),2(1x,f5.3),2(1x,f5.2),3(2x,f8.3))
 100   format(' Input data files     : ',a25,2x,a25,
     *        /,' Input document files : ',a25,
     *        /,' Output files         : ',a25,2x,a25,
     *      /,' WARNING :   Input files should exist.',//)
 150   format(1x,f3.0,1x,f7.3,1x,f5.3,1x,f5.2,2(1x,f6.3),3(1x,f6.2),
     $3(1x,f5.3))
 250   format(1x,f3.0,1x,f7.3,3(1x,f6.2))
 300   format(2(1x,f7.3),2(1x,f5.3),1x,f6.3,1x,f7.3,1x,f6.3)
 350   format(' Enter (1): To repeat with another convergence factor',/,'
     $         (2):  To continue')
       stop
       end

********************************************************************
       subroutine WCENT(n,coeff,break0,ccoef0,y2,y3,yc,ulm)
*  This subroutine determines the center of the wake, defined as the
*  location where ul is maximum.
*  Input Arguments :
*    n      = number of data points
*    coeff = coefficient of the polynomial fit for potential flow
*    break0= break points for the piecewise cubic splines
```

```
*     ccoef0= local coefficient of the cubic pieces
*     y2,y3 = yc,the wake center is located in between y2 and y3
*   Output Arguments:
*     yc    = wake center
*     ulm   = maximum value of wake defect velocity, ul=Up-u
***************************************************************************
      real*8 coeff(20)
      dimension break0(150)
      dimension ccoef0(4,150)
      y=y2
      ulm=.0
      do while (abs(y-y3).gt..025)
        y=y+0.05
        up=y*(y*(y*(y*(y*coeff(6)+coeff(5))+coeff(4))+
     $  coeff(3))+coeff(2))+coeff(1)
        vu=up-CSVAL(y,n-1,break0,ccoef0)
        if(vu.gt.ulm) then
          ulm=vu
          yc=y
        endif
      enddo
      write(6,*)'Wake center=',yc,'mm','  Max. wake defect=',ulm,'m/s'
      return
      end

***************************************************************************
      subroutine PTCENT(yc,x,pr,yo,pr2,n,np,ryc)
*  This subroutine determines the center of the wake, defined as the
*  location of minimum total pressure
*  Input Arguments :
*     n     = number of data points
*     np    = number of data points in the potential flow region
*     yo,pr2= coordinates of data (position,Ptotal)
*     x,pr  = coordinates of data (position,Ptotal)in the potential flow
*             region
*     yc    = wake center defined by ulm location
*  Output Arguments:
*     ryc   = wake center defined by the point where total pressure is
*             minimum
***************************************************************************
      dimension yo(150),pr2(150),break1(150)
      dimension ccoef1(4,150)
      real*4 x(150),pr(150)
      real*8 acoeff(100),var(20),coefp(20)

*  Do line fit through the potential flow region
      Write(6,*)'Degree of polynomial for total pressure in  potential
     $flow region? 1, .....,3'
      read(5,*) npol
      call LSFIT(np,x,pr,npol,acoeff,var,coefp,ks)
      do i=npol+2,11
        coefp(i)=0.0
      enddo

*  Do a cubic spline smoothing fit through the total pressure data
      iequal=0
      if(n.lt.20) iequal=2
      write(6,*)'Cubic Spline smoothing of total pressure data...'
      call CSSCV(n,yo,pr2,iequal,break1,ccoef1)
      y=yc-10.
      y3=yc+10.
      plm=0.
```

```
      do while (abs(y-y3).gt..025)
        y=y+0.05
        up=y*(y*(y*coefp(4)+coefp(3))+coefp(2))+coefp(1)
        vu=up-CSVAL(y,n-1,break1,ccoef1)
        if(vu.gt.plm) then
          plm=vu
          ryc=y
        endif
      enddo
      write(6,*)'Wake center from total pressure=',ryc,'mm'
      return
      end
*****************************************************************
      subroutine WLOC(y1,y2,y3,y4,yc,x,urm,yo,urms,n,np,ylr,yur,derr1,
     $derr2,npol)
*  This subroutine locates the edge of the wake
      dimension break2(150)
      dimension ccoef2(4,150)
      dimension yo(150),urms(150)
      real*8 acoeff(100),var(20),cf(20)
      real*4 x(150),urm(150)
      logical*1 itype
      call LSFIT(np,x,urm,npol,acoeff,var,cf,ks)
      do i=npol+2,11
        cf(i)=0.0
      enddo
*  Fit the measured urms data with cubic spline
      call CSAKM(n,yo,urms,break2,ccoef2)
      write(6,*)'Calculating the edge of the wake .....'
      do j=1,2
        itype=.true.
        if(j.eq.1)then
          high=yc
c          rlow   = (y1+y2)*.5
          rlow = y2-5.
          derr=derr1
        else
          rlow   = yc
c          high = (y3+y4)*.5
          high = y3+5.
          derr=derr2
        endif
        i=0
        do while (itype)
          i=i+1
          if(j.eq.1) rlow=rlow+.05
          if(j.eq.2) high=high-.05
*  Area under u from rlow to high
          au=CSITG(rlow,high,n-1,break2,ccoef2)
*  Area under potential velocity up from rlow to high =aup2-aup1
          aup1=asum(rlow,cf,npol)
          aup2=asum(high,cf,npol)
          aup = aup2-aup1
          df=abs(aup-au)
          if(i.eq.1) df2=df
          if(abs(1-df/df2).gt.derr) itype=.false.
        enddo
        if(j.eq.1) ylr=rlow
        if(j.eq.2) yur=high
      enddo
      return
      end
```

```
********************************************************************
      subroutine BTHETA(yl,yc,yu,f2,coeff,break0,ccoef0,bl,bu,b,thel,
     $theu,theta,ulm,n,yo,npol)
*  This subroutine calculate momentum thickness theta and b
*  theta=((integral(ul*u.dy ))/upc**2.);b=bl+bu (b=(integral(udy)/ulm
      real*8 coeff(20)
      dimension break0(150),break3(150),f2(150),yo(150)
      dimension ccoef0(4,150),ccoef3(4,150)
      upc=yc*(yc*(yc*(yc*(yc*coeff(6)+coeff(5))+coeff(4))+
     $ coeff(3))+coeff(2))+coeff(1)
      aup1=asum(yl,coeff,npol)
      aup2=asum(yc,coeff,npol)
      aup3=asum(yu,coeff,npol)
      aupl=aup2-aup1
      aul = CSITG(yl,yc,n-1,break0,ccoef0)
      aull= aupl-aul
      aupu=aup3-aup2
      auu = CSITG(yc,yu,n-1,break0,ccoef0)
      aulu= aupu-auu
      aul = aulu+aull
      bl  = aull/ulm
      bu  = aulu/ulm
      b   = bl+bu
*      write(6,*)'bl=',bl,'mm bu=',bu,'mm b=',b,'mm'
*  Momentum thickness ; Integral of f2 /upc*upc
      call CSAKM(n,yo,f2,break3,ccoef3)
      thel=CSITG(yl,yc,n-1,break3,ccoef3)
      thel=thel/(upc*upc)
      theu=CSITG(yc,yu,n-1,break3,ccoef3)
      theu=theu/(upc*upc)
      theta=thel+theu
*      write(6,*)'thel=',thel,'mm theu=',theu,'mm theta=',theta
*      $,'mm'
      return
      end


********************************************************************
      Function asum(x,cff,npol)
*  asum is the value of the integral at x of a polynomial of degree npol
      real*8 cff(20)
      do i=npol+2,11
        cff(i)=0.0
      enddo
      asum=x*(x*(x*(x*(x*(x*cff(6)/6.+cff(5)/5.)+cff(4)/4.)+cff(3)/3.)+
     $cff(2)/2.)+cff(1))
      return
      end


********************************************************************
```

5. Data analysis program to obtain the quantities in curvilinear coordinate system for steady wake

```
********************************************************************
* This program calculates the velocities and Reynolds stresses in S-N
* coordinates.  The S direction is along the line passing through ulm.
*  ulm    = maximum of wake defect velocity
*  ul/ulm = wake defect velocity/maximum wake defect velocity
*  yc     = location of wake centerline
*  b      = inegral(ul/ulm) / ulm
*  theta  = momentum thickness
*  prl    = static pressure
*  uv     = average of instantaneous velocity correlation
```

```
*
*    External Subroutines.
*    CSAKM - Gives the spline coefficients of the data points.
*    CSSCV - Gives the spline coefficients of the data points by smoothing
*    CSITG - Uses the spline coeffs. to calculate the integral.
*    IWKIN - Assigns larger workspace for the program.
*    CSVAL - Gives interpolated values using the spline coeffs.
******************************************************************************
      program SN120
      common /worksp/ rwksp
      real rwksp(70000)
      dimension yo(150),u(150),v(150),urms(150),vrms(150),utur(150)
      dimension vtur(150),rs1(150),rs2(150),rs3(150),pr1(150),pr2(150)
      dimension temp(150),uv(150),u1(150),cuv(150)
      dimension us(150),vs(150),u1s(150),rs1s(150),rs2s(150),rs3s(150)
      character*30 fi1,fi2,fi3,fi5,fo1,fo2,fo3,fd1,fi6
*    The locus of ulm is curve fitted w.r.t this coordinate.
      external CSAKM,IWKIN,CSITG,CSVAL,LSFIT
      call IWKIN(70000)
*    Read the input file name fi1
      write(*,*) 'Input the name of the file to analyze ....A.DAT'
      read(5,'(a)') fi1
c      write(6,*) 'Input the name of file containing ulm locations'
c      read(5,'(a)') fi4

*    Generate the second input file name fi2, related document file fd1 and
*    output files fo1 and fo2
      in=1
      do while(fi1(in:in).ne.'.')
         fi2(in:in)=fi1(in:in)
         fi3(in:in)=fi1(in:in)
         fi5(in:in)=fi1(in:in)
         fi6(in:in)=fi1(in:in)
         fd1(in:in)=fi1(in:in)
         fo1(in:in)=fi1(in:in)
         fo2(in:in)=fi1(in:in)
         fo3(in:in)=fi1(in:in)
         in=in+1
      end do
      fi2(in-1:in+5)='b.dat'
      fi3(in-1:in+5)='d.dat'
      fi5(in-1:in+5)='c.dat'
      fi6(in-1:in+5)='b1.dat'
      fd1(in-1:in+7)='001.doc'
      fo1(in-1:in+5)='e.out'
      fo2(in-1:in+5)='f.out'
      fo3(in-1:in+5)='g.out'
      write(6,100)fi1,fi2,fd1,fo1,fo2,fo3
      pause 'Press return to continue'
* Open and read the data in the document file "fd1"
      open(unit=8,file=fd1)
      read(8,*)te,p1,p2,pstat,patm
      write(6,*)te,p1,p2,pstat,patm
      close(8)

*    Open and read the data inthe first input file "fi1"(...a.dat)
      open(unit=8,file=fi1)
      i=1
      do while(.not.eof(8))
         read(8,*)yo(i),avg,hvoltt,avg,hvoltt,ve,ve,pr1(i),
     $   pr2(i),temp(i),rms,rms
         write(6,70)yo(i),avg,hvoltt,avg,hvoltt,ve,ve,pr1(i),
```

```fortran
      $  pr2(i),temp(i),rms,rms
         i=i+1
      end do
      close(8)
* Open and read the data in the second input file "fi2"(...b.dat)
      open(unit=8,file=fi2)
      i=1
      do while(.not.eof(8))
         read(8,*)yo(i),u(i),v(i),urms(i),vrms(i),utur(i),vtur(i),
      $  rs1(i),rs2(i),rs3(i)
*        write(6,75)yo(i),u(i),v(i),urms(i),vrms(i),utur(i),vtur(i),
*     $ rs1(i),rs2(i),rs3(i)
         i=i+1
      end do
      n=i-1
      close(8)
*  Open and read the data in the  input file "fi3"(...d.dat)
      open(unit=8,file=fi3)
      i=1
      do while(.not.eof(8))
         read(8,*)yo(i),aaa,u1(i),bbb,bob,ccc,ddd
         write(6,110)yo(i),aaa,u1(i),bbb,bob,ccc,ddd
         i=i+1
      end do
      n=i-1
      close(8)
*  Open and read the data in the input file "fi5" containing ulm etc for
*  the present location
      open(unit=8,file=fi5)
      read(8,*)agp,ycp,ulmp,upcp,ulmbp,ulmbcp,blp,bup,bp,thelp,theup,
      $ thetap
      write(6,120)agp,ycp,ulmp,upcp,ulmbp,ulmbcp,blp,bup,bp,thelp,
      $theup,thetap
      close(8)
* Read the direction of resultant velocity vector from "fi3"(...b1.dat)
      open(unit=8,file=fi6)
      read(8,*)eta
      write(6,*)'eta= ',eta
      eta=eta/57.2957
      close(8)
c       pause'Enter to continue...'
*
      PAUSE'PRESS ENTER TO CONTINUE'
      do i=1,n
         us(i)=u(i)*cos(eta)+v(i)*sin(eta)
         vs(i)=v(i)*cos(eta)-u(i)*sin(eta)
         u1s(i)=u1(i)*cos(eta)
         rs1s(i)=rs1(i)*cos(eta)*cos(eta)+rs2(i)*sin(eta)*
      $  sin(eta)+rs3(i)*sin(2.*eta)
         rs2s(i)=rs1(i)*sin(eta)*sin(eta)+rs2(i)*cos(eta)*
      $  cos(eta)-rs3(i)*sin(2.*eta)
         rs3s(i)=(rs2(i)-rs1(i))*.5*sin(2.*eta)+rs3(i)*cos(2.*eta)
         uv(i) = us(i)*vs(i)+rs3s(i)
      enddo
      b   = ulmbp/ulmp
      ulm=ulmp
      ulm2=ulm*ulm
      upc=upcp
      bl= blp
      bu= bup
      thel=thelp
      theu=theup
```

```
        theta=thetap
*    Calculate static pressure distribution at measuring location
        rho=(patm*13.55+pstat)*.0348432/(te+273.15)
        write(6,*)'rho=',rho
        do i=1,n
          pr2(i)=pr2(i)-(0.5*rho*(u(i)*u(i)+v(i)*v(i)))/(9.81*13.55)
        enddo
*    Calculate correlation coefficient (u'v')bar/(urms.vrms)
        do i=1,n
          cuv(i)=(-1.*rs3s(i))/(sqrt(rs1s(i)*rs2s(i)))
        enddo
*
        pause'Press Enter to continue'
*    Open the output files
*    Output the quantities in the dimensional form to "...f.out"
        open(unit=10,file=fo2)
        write(6,*)'POS.mm       u       v       u1     pstat  rs1    rs2    rs3
     $    UV      Corr.  ANGLE'
        write(10,*)'POS.mm       u       v       u1     pstat  rs1    rs2    rs3
     $    UV      Corr.  ANGLE'
        do i=1,n
          write(6,300)yo(i),us(i),vs(i),u1s(i),pr2(i),rs1s(i),rs2s(i),
     $    rs3s(i),uv(i),cuv(i),eta*57.2958
          write(10,300)yo(i),us(i),vs(i),u1s(i),pr2(i),rs1s(i),rs2s(i),
     $    rs3s(i),uv(i),cuv(i),eta*57.2958
        enddo
        close(10)
*
        write(6,*)"Subtract base line values from rs1 ? Yes:(1) No:
     $(2)"
        read(5,*)is
*    Subtract the Base line Values from rs1s (SBVRS)
        if(is.eq.1) then
          write(6,*)'Subtracting base line values from rs1....'
          call SBVRS(yo,rs1s,n)
        endif
*
        write(6,*)"Subtract base line values from rs2 ? Yes:(1) No:
     $(2)"
        read(5,*)is
*    Subtract the Base line Values from rs2s (SBVRS)
        if(is.eq.1) then
          write(6,*)'Subtracting base line values from rs2....'
          call SBVRS(yo,rs2s,n)
        endif
*
        write(6,*)"Subtract base line values from rs3 ? Yes:(1) No:
     $(2)"
        read(5,*)is
*    Subtract the Base line Values from rs3s (SBVRS)
        if(is.eq.1) then
          write(6,*)'Subtracting base line values from rs3....'
          call SBVRS(yo,rs3s,n)
        endif

*    Locate the maximum of rs1s and rs2s
        Write(6,*)'Locating the  rs1 at wake center...'
        call RSMAX(yo,rs1s,n,rs1m,ycp)
        Write(6,*)'Locating the  rs2 at wake center... '
        call RSMAX(yo,rs2s,n,rs2m,ycp)

* Output the mean quantities at each stream wise location to "...e.out"
```

```
      open(unit=9,file=fo1,status='unknown')
      Write(6,*)'ANG    yc    eta1  u1m    upc   u1m.b u1m.b/upc b    the1
     $ theu  the rs1mn rs2mn'
      Write(9,*)'ANG    yc    eta1  u1m    upc   u1m.b u1m.b/upc b    the1
     $ theu  the rs1mn rs2mn'
      write(6,150)agp,ycp,eta*57.2957,u1m,upc,u1m*b,u1m*b/upc,b,the1,
     $theu,theta,rs1m/u1m2,rs2m/u1m2
      write(9,150)agp,ycp,eta*57.2957,u1m,upc,u1m*b,u1m*b/upc,b,the1,
     $theu,theta,rs1m/u1m2,rs2m/u1m2
      close(9)
*
      pause'Enter to continue...'
*  Output the quantities in nondimensionalized form
      open(unit=10,file=fo3)
      write(6,*)'POS.mm (Yc-Y)/b  u1/u1m  v/u1m  rs1N     rs2N     rs3N
     $ UVN   UaVaN'
      write(10,*)'POS.mm (Yc-Y)/b  u1/u1m  v/u1m  rs1N     rs2N     rs3N
     $ UVN   UaVaN'
      do i=1,n
        write(6,320)yo(i),(ycp-yo(i))/b,u1s(i)/u1m,vs(i)/u1m,rs1s(i)/
     $ rs1m,rs2s(i)/rs2m,rs3s(i)/u1m2,uv(i)/u1m2,us(i)*vs(i)/u1m2
        write(10,320)yo(i),(ycp-yo(i))/b,u1s(i)/u1m,vs(i)/u1m,rs1s(i)/
     $ rs1m,rs2s(i)/rs2m,rs3s(i)/u1m2,uv(i)/u1m2,us(i)*vs(i)/u1m2
      enddo
      close(10)

*  Formats
  70  format(f7.2,4(1x,f6.3),2(1x,f5.2),2(1x,f6.3),1x,f5.2,2(1x,f5.3))
  75  format(1x,f7.2,2(1x,f6.2),2(1x,f5.3),2(1x,f5.2),3(2x,f8.3))
 100  format(' Input data files    : ',a25,2x,a25,
     *        /,' Input document files : ',a25,
     *        /,' Output files         : ',/,1x,a25,1x,a25,1x,a25,
     *      /,' WARNING :  Input files should exist.',//)
 110  format(2(1x,f7.3),2(1x,f5.3),1x,f6.3,1x,f7.3,1x,f6.3)
 120  format(1x,f3.0,1x,f7.3,1x,f5.3,1x,f5.2,2(1x,f6.3),3(1x,f6.2),
     $3(1x,f5.2))
 150  format(1x,f3.0,1x,f6.2,1x,f6.3,1x,f5.3,2(1x,f6.3),1x,f6.3,
     $1x,f5.2,2(1x,f4.2),1x,f5.3,2(1x,f5.3))
 300  format(1x,f7.3,4(1x,f6.3),2(1x,f5.3),1x,f6.3,1x,f7.3,1x,f8.5,1x,
     $f6.2)
 320  format(2(1x,f7.3),1x,f5.3,1x,f6.3,3(1x,f7.4),1x,f8.3,1x,f8.3)
 350  format(' Enter (1): To repeat with another convergence factor',/,'
     $         (2):  To continue')
      stop
      end


**************************************************************************
      subroutine RSMAX(rx,ry,n,rmax,rxc)
*  This subroutine find the maximum from a set of data points after
*  subjected to cubic spline smoothing
*  rx&ry- data sets, n-number of data sets          (input )
*  rmax - maximum of rx                  (output)
*  rxc  - center of the wake where the value of ry = rmax(input)
      dimension rx(150),ry(150)
      dimension break0(150)
      dimension ccoef0(4,150)
      iequal=0
      if(n.lt.20) iequal=2
      call CSSCV(n,rx,ry,iequal,break0,ccoef0)
      rmax =CSVAL(rxc,n-1,break0,ccoef0)
      return
      end
```

```
****************************************************************************
      subroutine SBVRS(yo,rs,n)
*  This subroutine subtract the base value from all rs(i)
*  The base line value is found from the polynomial fit.
*  yo(i) : independent variable eg:radial position     (input)
*  rs(i) : dependent variable   eg:Reynolds stress      (input/output)
*  n       : number of data points                      (input)
****************************************************************************
      integer*4 npol,ks,np
      real*8 acoeff(40),var(12),coeff(12)
      real*4 x(100),y(100)
      dimension yo(150),rs(150)
*  Input the boundary coordinates for base line fit and arrange
*  them in ascending order, y4>y3>y2>y1
      write(6,*)'Input Y-coord boundaries for the base line fit (mm):'
      write(6,*)'First Y-coord for convex side?'
      read(5,*)y1
      yt=y1
      write(6,*)'Second Y-coord for convex side?'
      read(5,*)y2
      if(y2.lt.y1) then
        y1=y2
        y2=yt
      endif
      write(6,*)'First Y-coord for concave side?'
      read(5,*)y3
      yt=y3
      write(6,*)'Second Y-coord for concave side?'
      read(5,*)y4
      if(y4.lt.y3)then
        y3=y4
        y4=yt
      endif
      Write(6,*) 'y1=',y1,'mm y2=',y2,'mm y3=',y3,'mm y4=',y4,'mm'
* Calculation of base line fit fit. The data points for the base line
* fit will be stored in x(j),y(j)
      j=0
      do i=1,n
        if((yo(i).ge.y1).and.(yo(i).le.y2)) then
          j=j+1
          x(j)= yo(i)
          y(j)= rs(i)
        endif
        if((yo(i).ge.y3).and.(yo(i).le.y4)) then
          j=j+1
          x(j)= yo(i)
          y(j)= rs(i)
        endif
      enddo
      np=j
* Fitting the base line fit, npol=degree of polynomial
* np=number of data points for base line fit
      Write(6,*)'Degree of polynomial for base line fit flow? 1, ...,5'
      read(5,*) npol
      call LSFIT(np,x,y,npol,acoeff,var,coeff,ks)
      do i=npol+2,11
        coeff(i)=0.0
      enddo
      Write(6,*)'Polynomial coefficients for base line fit:',(coeff(i),
     $ i=1,npol+1)
      do i=1,n
        rs(i)=rs(i)-(yo(i)*(yo(i)*(yo(i)*(yo(i)*(yo(i)*coeff(6)+coeff(5))
```

```
$  +coeff(4))+coeff(3))+coeff(2))+coeff(1))
 enddo
 return
 end
```

1. AGENCY USE ONLY (Leave blank)	2. REPORT DATE January 1996	3. REPORT TYPE AND DATES COVERED Final Contractor Report

4. TITLE AND SUBTITLE	5. FUNDING NUMBERS
A Study of the Development of Steady and Periodic Unsteady Turbulent Wakes Through Curved Channels at Positive, Zero, and Negative Streamwise Pressure Gradients, Part I	WU–505–90–52 G–NAG3–1256

6. AUTHOR(S)

M.T. Schobeiri and J. John

7. PERFORMING ORGANIZATION NAME(S) AND ADDRESS(ES)	8. PERFORMING ORGANIZATION REPORT NUMBER
Texas A&M University Department of Mechanical Engineering College Station, Texas 77843	E–10097

9. SPONSORING/MONITORING AGENCY NAME(S) AND ADDRESS(ES)	10. SPONSORING/MONITORING AGENCY REPORT NUMBER
National Aeronautics and Space Administration Lewis Research Center Cleveland, Ohio 44135–3191	NASA CR–198448

11. SUPPLEMENTARY NOTES

Project Manager, Barbara L. Lucci, Internal Fluid Mechanics Division, NASA Lewis Research Center, organization code 2630, (216) 433–5902.

12a. DISTRIBUTION/AVAILABILITY STATEMENT	12b. DISTRIBUTION CODE
Unclassified - Unlimited Subject Category 34 This publication is available from the NASA Center for Aerospace Information, (301) 621–0390.	

13. ABSTRACT (Maximum 200 words)

The turbomachinery wake flow development is largely influenced by streamline curvature and streamwise pressure gradient. The objective of this investigation is to study the development of the wake under the influence of streamline curvature and streamwise pressure gradient. The experimental investigation is carried out in two phases. The first phase involves the study of the wake behind a stationary circular cylinder (steady wake) in curved channels at positive, zero, and negative streamwise pressure gradients. The mean velocity and Reynolds stress components are measured using a X-hot-film probe. The measured quantities obtained in probe coordinates are transformed to a curvilinear coordinate system along the wake centerline and are presented in similarity coordinates. The results of the steady wakes suggest strong asymmetry in velocity and Reynolds stress components. However, the velocity defect profiles in similarity coordinates are almost symmetrical and follow the same distribution as the zero pressure gradient straight wake. The results of Reynolds stress distributions show higher values on the inner side of the wake than the outer side. Other quantities, including the decay of maximum velocity defect, growth of wake width, and wake integral parameters, are also presented for the three different pressure gradient cases of steady wake. The decay rate of velocity defect is fastest for the negative streamwise pressure gradient case and slowest for the positive pressure gradient case. Conversely, the growth of the wake width is fastest for the positive streamwise pressure gradient case and slowest for the negative streamwise pressure gradient. The second phase studies the development of periodic unsteady wakes generated by the circular cylinders of the rotating wake generator in a curved channel at zero streamwise pressure gradient. Instantaneous velocity components of the periodic unsteady wakes, measured with a stationary X-hot-film probe, are analyzed by the phase averaging techniques. The temporal distribution of velocity and Reynolds stress components obtained in a stationary frame of reference are transformed to a spatial distribution in a relative frame of reference. Profiles of phase-averaged velocity and Reynolds stress distributions in the relative frame of reference and similarity coordinates are presented. The velocity defect and Reynolds stress distributions agree with the results of the wake development behind a stationary cylinder in the curved channel at zero streamwise pressure gradient. The phase-averaged third-order correlations, presented in the relative frame of reference and similarity coordinates, show pronounced asymmetric features.

14. SUBJECT TERMS			15. NUMBER OF PAGES 272
Wake flow; Curvature; Pressure gradient			16. PRICE CODE A12

17. SECURITY CLASSIFICATION OF REPORT Unclassified	18. SECURITY CLASSIFICATION OF THIS PAGE Unclassified	19. SECURITY CLASSIFICATION OF ABSTRACT Unclassified	20. LIMITATION OF ABSTRACT

National Aeronautics and
Space Administration

Lewis Research Center
21000 Brookpark Rd.
Cleveland, OH 44135-3191

Official Business
Penalty for Private Use $300

POSTMASTER: If Undeliverable — Do Not Return